INFORMATION TO USERS

This manuscript has been reproduced from the microfilm master. UMI films the text directly from the original or copy submitted. Thus, some thesis and dissertation copies are in typewriter face, while others may be from any type of computer printer.

The quality of this reproduction is dependent upon the quality of the copy submitted. Broken or indistinct print, colored or poor quality illustrations and photographs, print bleedthrough, substandard margins, and improper alignment can adversely affect reproduction.

In the unlikely event that the author did not send UMI a complete manuscript and there are missing pages, these will be noted. Also, if unauthorized copyright material had to be removed, a note will indicate the deletion.

Oversize materials (e.g., maps, drawings, charts) are reproduced by sectioning the original, beginning at the upper left-hand corner and continuing from left to right in equal sections with small overlaps. Each original is also photographed in one exposure and is included in reduced form at the back of the book.

Photographs included in the original manuscript have been reproduced xerographically in this copy. Higher quality 6" x 9" black and white photographic prints are available for any photographs or illustrations appearing in this copy for an additional charge. Contact UMI directly to order.

UMI

A Bell & Howell Information Company
300 North Zeeb Road, Ann Arbor MI 48106-1346 USA
313/761-4700 800/521-0600

MODIFICATION AND EVALUATION OF A WATER SURFACE SAMPLER TO INVESTIGATE THE DRY DEPOSITION AND AIR WATER EXCHANGE OF POLYCHLORINATED BIPHENYLS (PCBs)

BY

YUCEL TASDEMIR

Submitted in partial fulfillment of the
requirements for the degree of
Doctor of Philosophy in Environmental Engineering
in the Graduate College of the
Illinois Institute of Technology

Approved _____
Adviser

Chicago, Illinois
December 1997

ACKNOWLEDGMENT

I want to thank my research advisor, Dr. Thomas M. Holsen, for his wonderful guidance, support, and easy-going but determined nature. He has provided me with knowledge and perspective on many subjects. His patient and encouragements are always appreciated. In addition to my work at IIT, Dr. Holsen's connections provided the chance for a variety of collaborative studies with some outside research groups.

I wish to thank Drs. Nasrin K. Khalili and Kenneth E. Noll for their help during the experimental set-up design and discussions on the subject. I must emphasise Dr. Khalili's friendly and supportive encouragements for all occasions. Her help and trust are always remembered. I wish to thank my other dissertation committee members, Dr. Dimitri J. Moschandreas and Dr. Walt Eisenberg, for their review and comments on this study and serving on my dissertation committee.

I would like to thank Dr. Thomas J. Murphy for allowing me to run my samples in his laboratory. Dr. Murphy's total cooperation and supplement of warm working environment in his laboratory are deeply appreciated. His knowledge and commitment to excellence are very inspirational.

I want to thank Dr. Terry F. Bidleman for his invitation to his laboratory in Canada and his friendly attitude. His excellent literature works on distribution of organic contaminant in the atmosphere gave me some sights on this research. I want to thank Thomas Harner for his full collaboration whenever it was needed. I would like to thank Dr. Thomas P. Franz for his generousity in sending me all the experimental details and other supplementary documents. He was always ready to help and give insights from his experiences.

I want to extent my thanks to my fellow graduate students who have been always kind and helpful during my study at IIT and I wish them well in their future. I thank my colleagues Mustafa, Nedim, Aysun and Wut for their help and cooperation during the every step of sampling and analysis. I want to also thank Halil, Ali and Usama for their discussion on data interpretation and softwares.

I would like to extent my great appreciation to the Republic of Turkey (Uludag Universitesi) for giving me oppurtunity to complete my Ph.D. study through its financial support.

Finally, I thank my family for giving me a lifetime of love, support and encouregement. This study cannot be achieved without my mother and father's patience and understanding.

TABLE OF CONTENTS

CHAPTER Page

LIST OF TABLES

LIST OF FIGURES

Figure Page

ABSTRACT

Dry deposition is an effective removal mechanism for polychlorinated biphenyls (PCBs) from the atmosphere. In this study a new analytical technique was developed to characterize the transport and deposition of PCBs in the environment. This technique featured a modified water surface sampler (WSS) in conjuction with greased surrogate surfaces and traditional high-volume sampler.

Ambient air samples were collected with a high-volume sampler in Chicago, IL from June to October 1995 to determine concentrations and gas/particle partitionings of PCBs. The total PCB concentration was about 1.9 ng/m^3 and on average 95% of the total PCB concentration was in the vapor phase.

The partitioning between gas and particulate phase was modeled using the Junge-Pankow model. The measured particle phase concentration for low molecular weight (MW) PCBs was lower than those predicted by Junge-Pankow model while the opposite case was observed for the high MW PCBs.

PCB dry deposition fluxes were measured with knife-edge surrogate surfaces and a modified water surface sampler (WSS). The knife-edge surface measured particulate phase deposition and the WSS measured both particulate and gas phase deposition. The average flux to the WSS and plate were about 1200 and 240 ng/m^2-d, respectively. In general, medium molecular weight PCBs were dominant.

Average dry deposition velocities, calculated by dividing the fluxes by the concentrations, for both the particle and gas phases were calculated to be 6.5 cm/s and 0.7 cm/s, respectively. The difference between the dry deposition velocities is due to the different deposition phenomena affecting the particulate and gas phases. A modified two-film gas-exchange model which depends on wind speed, water temperature, and properties of PCBs was used to predict the overall gas phase mass transfer coefficient compared well with the measured values.

CHAPTER I

INTRODUCTION

The interest in atmospheric deposition (both dry and wet) by the scientific community has increased a great deal over the past decade because of their significant contribution to the pollution budget of many natural waters (Murphy et al., 1977, Bidleman, 1981, Holsen et al., 1991, Hornbuckle et al., 1994). The Great Lakes are good examples of water bodies which can be significantly impacted by atmospheric deposition due to their huge surface area and proximity to major pollution sources such as cities, industrial complexes, coal-fired power plants, and agricultural lands. For instance, more than 50% of Lakes Superior, Michigan and Huron's current PCBs loadings come from atmospheric deposition (Colborn et al., 1990). The effects of deposited material can even influence remote areas like the Arctic (Daelemans et al., 1992). However, unlike wet deposition, there is still no acceptable collection and analytical method for dry deposition.

Dry particles and gases in the air may settle onto a surface at a rate which is a function of their physical and chemical characteristics, meteorological conditions, and surface characteristics. Many researchers used different kinds of surrogate surfaces to measure dry deposition such as Teflon plates, petri dishes, filters, and buckets (Davidson et al., 1985, Davidson and Wu, 1990, Dolske and Gatz, 1985). In this study greased strips on the top of the knife-edge plate were used for measurement of PCB particle phase dry deposition. This surrogate surface (Noll et al., 1988) has some disadvantages for measuring the dry deposition of semivolatile organic compounds (PCBs) including 1)

separation between grease and analyte is difficult, 2) the grease may capture the PCB gas phases.

A water surface sampler (WSS) was developed in order to minimize these disadvantages as well as capture gas phase dry deposition. The sampler surface is water which was continuously replenished to maintain a constant water level and residence time thereby minimizing the effects of water evaporation losses. Eventually, deposited PCBs (gas and particle) were captured by either a filter or XAD-2 resin. Evaluation of this system is very important because it is a natural surface (i.e. water) rather than grease or filter. PCBs are dissolved into water based on Henry's law which is a well defined constant rather than grease partitioning which is not well known. In addition, PCBs associated with particles do not bounce off. This system enables the calculation of the magnitude and direction of PCBs fluxes.

In this study, ambient air samples were collected using a high volume sampler in order to determine the PCB concentration and distribution between the particle and vapor phases. Dry deposition samples were gathered using the water surface sampler (WSS) and plates (greased strips) with a sharp leading edge.

PCB mass transfer coefficients to water will be measured for the first time. In the two-film gas exchange model, the overall gas phase mass transfer coefficient ($^2K_{A1}$) equals to the dry deposition velocity of the gas phase. These results will then be compared with the available models in order to determine how well the WSS works.

This thesis contains seven chapters. Chapter I presents an overview and the objectives of this study. Chapter II briefly reviews related literature. Chapter III states the materials and methods used in this study. Chapter IV gives a detailed QA/QC of this study. Chapter V contains the results and their discussion. Chapter VI summarizes the major conclusions from this study. Chapter VII details the future work and is followed by an appendix and a list of references.

The overall objectives are summarized as follows:

1. Modify and evaluate a water surface sampler to directly measure the PCB flux,

2. Measure and characterize the atmospheric PCB dry deposition (flux) to water and plates,

3. Develop techniques to analyze the collected data under strict QA/QC requirements and to compare the measured and modeled dry deposition flux of PCBs,

4. Evaluate the gas/particle partitioning of PCBs.

CHAPTER II

LITERATURE REVIEW

In this study a water surface sampler (WSS) was used to measure dry deposition and air-water exchange of PCBs in the ambient air. In this chapter information about PCBs including emission sources, bioaccumulation and regulations, ambient concentrations, gas/particle phase distribution, dry deposition flux and velocity, and mass transfer coefficients are reviewed.

2.1. An Overview of Polychlorinated Biphenyls (PCBs)

Polychlorinated biphenyls (PCBs) consist of 209 compounds with the structure $C_{12}H_xCl_y$ where x=0-9 and y=10-x (Alford-Stevens, 1986). PCBs have two benzene rings connected by a single bond. They are obtained by substituting from 2 to 10 Cl atoms into the bipheyl aromatic structure (Manahan, 1991). Strictly speaking, the monochlorobiphenyls are not PCBs. However, they included into the PCBs because they are the members of this chemical class.

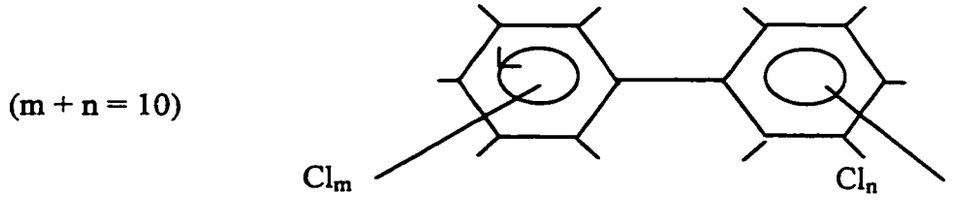

Figure 2.1. PCB Structure

The term congener is applied to any one of the 209 PCBs (Sawyer et. al., 1994) and isomer refers to PCBs that have the same number of chlorine atoms but different arrangements of the chlorines on the biphenyl rings. Ballschmiter and Zell constructed a system that assigns to each compound a number from 1 to 209. This system was adopted by the International Union of Pure and Applied Chemists, the numbers are, therefore, also called IUPAC numbers (Sawyer et. al., 1994).

PCBs were produced and sold largely in the US by Monsanto Chemical Co. from 1929 to 1975 (LaGrega, 1994).This company sold them under the Aroclor trademark (Alford-Stevens, 1986). Aroclor is a term used to refer commercial PCB formulations. Each Aroclor has a four-digit number. The first two numbers indicate the existing carbons in the phenyl ring, and the last two numbers refer to the weight percent of chlorine (Alford-Stevens, 1986). The exception to this code is Aroclor 1016 that contains mono-through hexachlorinated homologs with an average chlorine content of 41% (TPFP, 1993). Table 2.1. summarizes some important characteristics of selected Aroclors.

PCBs are stable compounds which have low vapor pressure, low water solubility, and high dielectric constants (Sawyer et. al., 1994). In addition, they are resistant to acids and bases, compatible with organic materials, resistant to oxidation and reduction, excellent electrical insulator, thermally stable, and nonflammable (Mullin et al., 1984). They were used as coolants and dielectric fluids in transformers and capacitors, as heat transfer fluids, as coatings to reduce the flammability of wood products, as plasticizers, as additives to some epoxy paints, inks, dust control agents, carbonless paper and pesticides

Table 2.1. Some Physical and Chemical Properties of Selected Aroclors (Adopted from TPFP, 1993)

Property	Aroclor 1232	Aroclor 1248	Aroclor 1262
Molecular weight	232.2	299.5	389
Color	Clear	Clear	No data
Physical state	Oil	Oil	No data
Boiling point	290-325 °C	340-375 °C	390-425 °C
Density, g/cm^3 at 25 °C	1.26	1.44	1.64
Water Solubility, mg/L	No data	0.054; 0.06(24 °C)	0.052 (24 °C)
Partition coefficient			
-LogK_{ow}	5.1	6.2	No data
-LogK_{oc}	No data	No data	No data
Vapor pressure mmHg at 25°C	4.06 E-3	4.94 E-4	No data
Henry's law constant atm.m^3/mol at 25C	No data	2.8 E-3	No data
Flashpoint, °C	152-154	193-196	No data
Flammability limits	328 °C	None to B.P.	None to B.P.
Conversion factors Air (25 °C)	1 mg/m^3= 0.105 ppm	1 mg/m^3= 0.08 ppm	1 mg/m^3= 0.061 ppm

(Alford-Stevens, 1986). The lipophilic nature and persistence of PCBs in the environment increase their bioaccumulation potential in higher levels in the food chain (Mullin et al., 1984).

PCBs manufacture, processing, distribution and use were banned except in totally enclosed systems in the USA by regulations issued under the authority of the "Toxic Substances Control Act (TSCA - Section 6)" passed in 1976 (Manahan, 1991). Their disposal has been strictly controlled.

PCBs degrade slowly and tend to bioaccumulate and some PCBs interfere with animal reproduction (TPFP, 1993, Hornbuckle et al, 1994). Experimentally determined ratios of concentration in the organism over the concentration in water (BCF) values for various Aroclors are very high for aquatic species such as fish, shrimp, oyster. The BCF value ranges between 26,000 to 660,000 and it will generally increase as the degree of chlorination of Aroclor increases (TPFP, 1993).

PCB concentrations have declined since 1977 in many animal tissues, gull eggs, and sediment cores from some lakes (Panshin and Hites, 1994a). On the other hand, atmospheric PCB concentrations have not changed appreciably especially over the Great Lakes (Hornbuckle et. al., 1993 and Panshin and Hites, 1994a). Panshin and Hites (1994a and 1994b) stated two possible reasons for this 1) the PCB concentration has remained steady or 2) the decreased PCB concentration has not been detected due to poor analysis methods.

Adsorption of PCBs to sediments or other organic matter is an important fate process in the aqueous environment. It was determined that PCB concentrations are bigger in sediments and suspended matter than in the water column (Colborn et al., 1990). When the chlorine amount in PCB congeners decreases, sorption decreases because of their increasing water solubility and decreasing octanol-water partition coefficients.

Polychlorinated biphenyls (PCBs) have been emitted into the environment from anthropogenic activities. They can be transported long distances and deposited at remote areas where there is no emission source. PCBs are found in the Arctic snowpack and food chain and in the Antarctic (Baker et. al., 1993, Aguilar et al., 1994, Picer and Picer, 1995, Stow, 1995). These results indicate that PCBs transportation and deposition are global pathways. Some researchers call this cycle "global distillation". Table 2.2. presents some PCB concentrations found in different environments.

2.2. PCB Sources in the Environment

There are no PCB point source emissions from industries into the air in the US except unreported fugitive emissions. Some concentrated PCB wastes (> 50 ppm) are transferred off-site for destruction by incineration which has a regulation efficiency of at least 99.9%. Therefore, some release is possible from incinerators even those that are specifically designed for PCB destruction.

Table 2.2.. PCBs Concentrations in Different Environments (Adopted fromTPFP, 1993)

Location	Concentration range
Indoor (School and Office)	230 - 460 ng/m^3
Outdoor	
Urban	1-10 ng/m^3
Rural	0.05-1 ng/m^3
Airborne Particulates	~5 - 30 μg/g
Great Lakes Water	0.5-3.3 ng/L (17 ng/L, max)
Groundwater	60-1270 ng/L (in New Jersey)
Soil	10-40 μg/kg
Rainwater	
Urban	10 - 250 ng/m^3
Rural	1 - 50 ng/m^3
Freshwater fish	0.5 μg/g.
Municipal refuse and sewage incinerators	300 - 3000 ng/m^3
Workplace - PCB disposal facility	0.85 - 40 μg/m^3

One of the major sources of PCB release to the air is the redistribution of the compounds present in soil, and natural waters. Other possible PCB sources are release from disposal sites containing transformers, capacitors, and other PCB wastes; incomplete combustion of PCB containing wastes; failure of transformers containing PCBs and improper disposal of PCBs. Landfills can be considered as a continuous source of PCB release into the air because while carbon dioxide and methane are released, they can carry PCBs and other

VOCs into the air (TPFP, 1993). Erickson (1992) mentioned that municipal water chlorination and incineration of other chlorinated organics may cause production of some lower chlorinated PCBs. The total worldwide PCBs production through 1980 is estimated to be approximately 1.1×10^9 kg (Erickson, 1992).

The PCB sources in the past to natural waters could be from the manufacture of carbonless copy papers; iron, steel, and aluminum foundries; effluents from pulp and paper mills; and electrical industries due to accidental loss of capacitor and transformer liquids (Manahan, 1991, Alford-Stevens, 1986, Erickson, 1992). At the present time, the main source of PCBs to surface waters is the environmental cycling process, which involves volatilization of PCBs from soil and surface waters into the atmosphere and then PCBs return to earth via washout/fallout (Murphy et al., 1981; Holsen et al., 1991).

In the past, PCB containing wastes were disposed of in landfills. PCBs may enter the groundwater through leaching of soils containing low organic matter or soils from some hazardous waste sites. Currently, the PCB sources to soil are the disposal of low levels of PCB wastes (<50 ppm) and/or wastes from accidental leaks or spillage from older electrical transformers (TPFP, 1993). Again, the major source of PCBs in soil may come from the environmental cycling process.

2.3. Potential Pathways and Exposed Populations

PCBs, which were discovered as an environmental pollutant in 1966 (Manahan, 1991), are widely found in the environment (in air, water, soil, and wildlife) (Hippelein et al.,

1996, Asplund et al., 1994, Norstrom et al., 1994). The detection of PCBs in blood, and breast milk from the people demonstrates the widespread exposure of PCBs (Dahle et al., 1995). The general population may be exposed to PCBs by inhalation of contaminated air, and ingestion of contaminated water or contaminated food. In the past, the major body burden for PCBs was food consumption; however, at the present time, both inhalation of indoor air and consumption of fish are considered as major sources of human exposures (Colborn et al., 1990; Asplund et al., 1994).

Populations close to PCB containing hazardous waste sites may be exposed to PCBs mainly by inhalation and consuming contaminated water and fish from local waters. People who are working inside these sites may be exposed to additional PCBs by dermal touch. Occupational exposure to PCBs would be several orders of magnitude higher than general population exposure. Other workplace exposures to PCBs can occur during repair and maintenance of PCB transformers, accidents, fires, or spills involving PCB transformers, and disposal of PCB materials (TPFP, 1993).

2.4. Bioaccumulation, Health and Regulations

PCBs are of concern because of the wide variety of human health and environmental problems that are linked to their presence. Among these are several types of cancer, central nervous system disorders, adverse productive outcomes, and some organ disorders (LaGrega et al. 1994).

PCBs can bioaccumulate and biomagnify through the food web. A water flea in Great Lakes (GLs) may collect 400 times more PCB concentration than exists in the water. The PCB concentrations in the eggs of a gull, which is at the highest level of the food web in the GLs, was determined to be 25 million times higher than in the water (Colborn et al., 1990). Since PCBs are able to bioaccumulate in fish tissue, PCBs can be found at elevated concentrations in humans who regularly eat PCB contaminated fish. It was concluded that fish from the Baltic Sea is a major source of exposure of PCBs to Swedes (Asplund et al., 1994). Swain stated that "In term of exposure potential, it is possible to breathe the air in the rural Lake Michigan basin and drink its water for a lifetime before achieving the same effective exposure that one would receive from eating a single one pound fish meal of Lake Michigan lake trout." Swain's (1982) speculation also supports the main pathway idea of contaminated fish consumption.

PCBs are classified as a B2 carcinogen (probable human carcinogen) by US EPA. This classification was based on the evidence of hepatocellular carcinomas in three strains of rats and two strains mice (IRIS, 1994). Although human carcinogenicity data is inadequate, yet there is suggestive evidence of risk of liver cancer in humans; moreover, there is sufficient animal carcinogenicity data for this classification (TPFP, 1993; IRIS, 1994). When chlorine number increases, the toxicity in general increases yet LaGrega et al., (1994) reported that the most toxic class of congeners is pentachlorobiphenyls. Some US government agencies have made recommendations about PCB exposure to protect human health. A summary is presented in Table 2.3.

Table 2.3. Some Maximum Allowable PCB Levels Recommended by US Agencies (Adopted from TPFP, 1993).

Agency	Where	Level
Environmental Protection Agency (EPA)	Drinking water	4 μg /L for adults 1 μg /L for children
Food and Drug Administration (FDA)	Egg, milk, dairy products, fish, shellfish, poultry	0.3, 1.5, 1.5, 2, 2, 3 ppm, respectively.
National Institute or Occupational Safety and Health (NIOSH)	Workplace	1.0 mg/m^3 for 10 hrs/day (of 40 hour workweeek)
Occupational Safety and Health Administration (OSHA)	Workplace	0.5 mg/m^3 (54% chlorine) 1.0 mg/m^3 (42% chlorine) for 8-hour workday

Even though there is no specific PCB concentration targets in Clean Air Act, there are acceptable air level (AAL) values recommended in some states (Table 2.4.).

Table 2.4. Acceptable Ambient Air Levels (AAL) for Some States (Adopted from TPFP, 1993)

State	PCB Type	AAL, $\mu g/m^3$
Kansas	Total PCBs	0.0083 (Annual)
Massachusetts	Total PCBs	0.0081 (24-hr average)
South Caroline	Total PCBs	2.5 (24-hr average)
Virginia	Total PCBs	8.0 (24-hr average)

2.5. Degradation of PCBs

Since PCBs are widespreaded throughout the world, they can be found in the different matrixes in the nature (Van Bavel et al., 1996, Hammond and Patterson, 1993, Daskalakis and O'Connor, 1995, Hippelein et al., 1996, Asplund et al., 1994, Norstrom et al., 1994) ; thus, their movement (fate), interactions, transport and degradation rates differ from one matrix to another. Since they are persistent, their removal from the environment is very slow.

PCBs are chemically inert when contacted with other materials under the normal conditions. However, PCBs may be hydrolyzed to oxibiphenyls under extreme conditions of high temperature (300 - 400 °C) and high pressure with the existence of sodium hydroxide solution (Liu, 1991). Moreover, strong sunlight may degrade PCBs and phenolic materials and polychlorinated dibenzofurans may form (Pracer, 1995).

PCBs can be degraded biologically at slow rates (Bedard and May, 1996). Dehalogenation of PCBs is more rapid with cultures using inocula prepared from PCB contaminated sites in which the bacteria had the opportunity to develop strains to biodegrade the wastes (Haluska et al., 1995). However, the different number of chlorine atoms in each PCB congener makes biodegradation pathways complex because anaerobic bacteria are more effective when PCBs have 5 or more Cl's yet aerobic bacteria prefers PCBs containing 4 or less Cl atoms per molecule (Manahan, 1990). It should also be noted that it is not only the number of substituents but also their orientations which influence degradation rates (Neilson, 1994).

The ultimate PCB removal technology is incineration. Based on TSCA rules (1979), PCBs (>50 ppm) must be burned in high-efficiency incinerators which have to have 99.9% combustion efficiency and meet some specific operating conditions such as combustion temperature, retention time, and stack oxygen concentration (Rickman, 1991).

2.6. Airborne Concentrations

Measured PCB concentrations from some places in the USA are given in Table 2.5. Urban area PCB concentrations are much higher than those measured in remote and rural areas. In general atmospheric concentrations of PCBs are higher in the summer than the winter because amount of PCBs in the atmosphere is determined by volatilization of PCB congeners from the soil or other sorbents on the earth surface (Kaupp et al., 1996). However, some researchers have also found no seasonal variations in PCB concentrations (Hornbuckle et al., 1995; Sugita, et al., 1994; Ngabe, 1992).

Indoor air concentrations are higher than typical ambient outdoor air. The normal indoor air PCB concentrations were at least one order of magnitude higher than those detected in the surrounding outdoor air (TPFP, 1993). This increased concentration is due to leakages from appliances and devices which contains PCBs.

Table 2.5. Some Measured Total PCB Concentrations in the USA

Location	Concentration range, ng/m^3	Date	Reference
Urban (for USA)	0.5 - 30		TPFP
Chicago, IL	7.55 - 20.26	May & June'90	Holsen et. al.
Chicago, IL	0.30 - 9.9	Feb.'88	Cotham et.al.
Chicago ,IL		May-July, 1994 and Jan. 1995	Simcik et al.
- Lake	0.13 - 1.14		
- Urban	0.09 - 14.2		
Bloomington, IN	0.65 - 2.53	April to June'93	Panshin & Hites
Columbia, SC	4.4	Summer'78	Bidleman.
Columbia, SC	2.3	Summer'85	Foreman et al.
Green Bay	0.1 - 0.3	1988 - 1990	Sweet and Basu
Lakes Superior	0.01 - 0.02	Jan. - Feb. 1991	Basu et al.
& Ontario	0.3 - 0.5	May - June 1991	

Table 2.6. gives some ambient air concentrations measured in different countries. In some cases the concentration levels are extremely high (Wanatabe et al., 1996) even for concentrations measured near PCB storage sites.

Table 2.6. Some Measured PCB Concentrations in the World

Location	Concentration range, ng/m^3	Reference
Bangkok, Thailand (near a storage site)	820	Wanatabe et al., 1996
Southern Taiwan		Chen et al., 1996
- rural	2.50	
- urban	4.51	
- industrial	5.91	
Southern Taiwan		Lee et al., 1996
- rural	2.61	
- urban	4.75	
- petroleum refinery	5.02	
Canadian Arctic	0.01 to 0.26	Patton et al., 1989
Rome, Italy	0.11 - 14	Turri-Baldassarri et al., 1994
Sweden	0.07 - 0.38	Bidleman et al., 1987
Japan (Tokyo)	20	Kimbrough, 1980
Canadian Arctic	0.009 - 0.026	Patton et al., 1989
UK	0.48 - 2.47	Halsall et al., 1993

2.7. Gas - Particle Partitioning

PCB partitioning between the gas and particle phases affects the transport, fate, residence time and removal processes of PCBs in the atmospheric environment (Baker et.al., 1993). Gas - particle partitioning is a function of both gas and particle concentrations, compositions, characteristics, and atmosphere temperature. Sampling artifacts, including

adsorption of gas phase PCBs onto particles on the filter and onto the filter itself and blow-off of PCB gases from the particles collected on the filter complicate gas - particle partitioning measurements. The best way to minimize these artifacts is to keep sampling times as short as possible which minimizes fluctuations in the temperature, humidity and atmospheric concentrations (Baker et. al., 1993; Cotham et al., 1992).

Table 2.7. summarizes measured airborne PCB partitioning between the particle and gas phase. As seen from this table, PCBs in the air exist mainly in the gas phase and there is a wide range of reported values on the gas and particle distribution percentages. Partitioning varies with temperature. For example, a study in Bloomington, IN showed that the gas phase contained 99% and 90% of the total PCBs in the summer and winter periods, respectively.

The relationship between the particle-bound PCB concentration and the measured particle mass concentration varies significantly because the partitioning will differ extensively depending on site, meteorological conditions and particle characteristics (Falconer and Bidleman, 1995, Baker et al., 1993). Similarly particle-associated PCB concentrations cannot be estimated from particle mass concentrations only. Table 2.8. summarizes some literature values of particle-bound PCB concentrations.

Table 2.7. PCB Partition Values Between Gas and Particle Phases

Location	Gas (%)	Particle (%)	Reference
Chicago, IL	96	4	Murphy and Rzeszutko, 1977
Lake Michigan (Chicago)	87	13	Murphy and Rzeszutko, 1977
Toronto, Ontario	57 - 86	14 - 43	Gilbertson, 1976
Hamilton, Ontario	82 - 95	5 - 18	Gilbertson, 1976
Columbia, SC	92	8	Bidleman, 1979
Lake Superior	95 - 100	0 - 5	Eisenreich et al., 1981
Bloomington, IN			
- in the summer	99	1	Hermanson, 1989
- in the winter	90	10	Hermanson, 1989
Southern Taiwan- urban	60.9	39.1	Chen et al., 1996
Green Bay	95-99	1-5	Sweet and Basu, 1993

The size distribution of PCBs are not presented very well in the literature. A recent study stated that the particle size distribution of total PCBs was bimodal and the industrial particles were dominant in the fine particle mode (d_p<2.5 μm), while urban site particles were dominant in the coarse particle mode (d_p>2.5 μm) (Chen et. al., 1996). Moreover, Holsen et al. (1991) concluded that urban areas contained a significant amount of PCBs associated with coarse particles.

Table 2.8. Particle-bound PCB Concentrations

Location	Value, μg/g	Reference
Bloomington, IN	0.1 - 9.6	Hermanson, 1989
Chicago, IL	30 - 50	Holsen et al., 1991
Southern Taiwan		Chen et al., 1996
- rural	10.3	
- urban	13.9	
- industrial	9.24	

The size distribution of PCBs are not presented very well in the literature. A recent study stated that the particle size distribution of total PCBs was bimodal and the industrial particles were dominant in the fine particle mode (d_p<2.5 μm), while urban site particles were dominant in the coarse particle mode (d_p>2.5 μm) (Chen et. al., 1996). Moreover, Holsen et al. (1991) concluded that urban areas contained a significant amount of PCBs associated with coarse particles.

The Junge-Pankow model was developed to predict the reversible adsorption of gases to aerosols (Pankow et al., 1993 and 1994; Falconer and Bidleman, 1995). The basis of the model is a linear Langmuir isotherm with compound adsorption expressed by the relation between aerosol surface area available for adsorption (θ, cm^2/cm^3 air) and the saturation

subcooled liquid vapor phase (p°_L ,Pa) (Cotham and Bidleman, 1992 and 1995). The calculation of ϕ is shown below:

$$\phi = c\theta / (p^{\circ}_L + c\theta) \qquad (2.1)$$

where ϕ is the fraction of total atmospheric concentration adsorbed to the aerosol and c, (17.2 Pa cm) depends on the thermodynamics of the adsorption process, sorbate molecular weight and the surface properties of the aerosol (Cotham and Bidleman, 1992; Falconer et al., 1995). Although p°_L values are well established, c and θ are not well known (Bidleman, 1984: Hinckley et al., 1990). Bidleman suggested the values of θ based on Whitby's size distribution of accumulation mode aerosols: urban air = 1.1E-5, average continental background air = 1.5 E-6, clean continental background air = 4.2 E-7. The particulate fraction can also be defined by using high-volume collectors and expressed in terms of C_p ,C_g and K_p as follows;

$$\phi = C_p / [C_g + C_p] \qquad (2.2)$$

$$\phi = 1 / [1 + C_g/C_p] \qquad (2.3)$$

where C_p is the contaminant concentration associated with aerosols (ng/ m^3), C_g is the gas-phase contaminant concentration (ng/m^3) and TSP is the total suspended particle concentration ($\mu g/m^3$) (Falconer et al., 1995).

The combination of above equations would give the particle/gas partition coefficient K_p [$=C_p/TSP)/C_g$];

$$\log K_p = \log [(C_p/TSP)/C_g] = \log c\theta/TSP - \log p^\circ_L \quad (2.4)$$

$$\log K_p = \log [(C_p/TSP)/C_g] = b_r - m_r \log p^\circ_L \quad (2.5)$$

Table 2.9., adopted from Falconer et al., 1995, is the summary of the K_p values for some PCB congeners for Chicago samples.

Table 2.9. Particle / Gas Partition Coefficients (K_p) at 25 °C

Congener Number	Total Chlorines	$\log p^\circ_L$	C_g (ng/m^3) range	log (avg K_p)
37	3	-1.90	183-1100	-5.03
49	4	-1.77	19-382	-5.33
101	5	-2.47	39-1890	-4.70
138	6	-3.29	15-18	-3.94
171	7	-3.73	71-95	-3.64

A linear regression of log K_p versus log p_L° will give a slope of m_r and an intercept of b_r which is related to the specific surface area of the particle when there are no artifacts. Based on the theory (Equations 2.7.4. and 2.7.5.), $m_r = -1$ but in real life it fluctuates due

to variability in c among compounds, changes in temperature, atmospheric concentration of contaminants, TSP values, and filtration artifacts (Pankow and Bidleman, 1992 and Falconer et al., 1995). Table 2.10. gives some theoretical values from the studies of Falconer et al. (1995) and Cotham and Bidleman (1995).

Table 2.10. m_r and b_r Values of Regression Equations ($\log K_p = b_r - m_r \log p_L$)

PCB Type	m_r	b_r	Reference
Multi-ortho	-0.848	-6.583	Falconer et al., 1995
Mono-ortho	-0.832	-6.354	Falconer et al., 1995
Non-ortho	-0.821	-6.134	Falconer et al., 1995
All congeners	-0.864	-6.507	Falconer et al., 1995
All congeners	-0.726	-5.18	Cotham and Bidleman, 1995

2.8. Deposition

It is now known that pollutants which are emitted into the atmosphere are transported for various distances and may then deposit on an aquatic or terrestrial surface. As the control on industrial point sources increases, atmospheric deposition may be responsible for a bigger burden of contaminations to large water bodies. Therefore, it should be realized that water quality goals cannot be reached unless air quality objectives are achieved (Baker et al., 1993).

Atmospheric deposition is considered to be one of the major source of PCBs in the Great Lakes (Murphy et al., 1981; Eisenreich, 1981; Strachan et. al., 1988). Although PCB production was banned in the USA in the late 1970s, PCB levels are high in the Great Lakes fish due to atmospheric inputs and internal exchanges (DAPGL, 1994).

Atmospheric deposition and removal (volatilization) processes are very important processes on the Great Lakes PCB burden calculations (Strachan and Eisenreich, 1988)(Table 2.11.)

Table 2.11. Results of Input and Output Calculations for PCBs to the GLs

Lake	Input, kg/yr	% Atmospheric input	Output, kg/yr	% Volatilization
Superior	606	90	190	86
Michigan	685	58	7550	68
Huron	636	63	2760	75
Erie	2520	20	2390	46
Ontario	2540	13	1320	53

There have been scientific studies of atmospheric deposition for more than 10 years. Some relatively simple models considering physical and chemical processes have been developed to estimate deposition. However, this phenomena is much more complex. An overall understanding of deposition process for a single contaminant will depend on not only emission rates, transport and fate characteristics of a pollutant, but also aerosol behavior, absorption, volatilization, and bioavability of contaminants (Murphy et al.,

1981; Baker et al., 1993). There are two main atmospheric deposition processes, and both wet and dry will be discussed in detail in the following sections. Figure 2.2. summarizes the deposition phenomena in a simplistic way.

2.8.1. Dry Deposition. Atmospheric dry deposition results from the transport and accumulation of gas or/and particle contaminants onto a surface during the periods of no precipitation. The dry deposition phenomena is fairly complex and assumed an irreversible process: it is affected both by gas transfer and sorption onto the surface. The amount of dry deposition is a function of contaminant concentration and characteristics, atmosphere conditions and the receptor surface (Hoff et al., 1996; Zannetti, 1990; Holsen et al., 1991; Murphy et al., 1981). Dry deposition is measured by the deposition velocity V_d which is the ratio between contaminant deposition flux, F (ng/m^2-d) and contaminant concentrations, c (ng/m^3) and shown as follows;

$$V_d = F / c \tag{2.6}$$

V_d is not a real velocity yet an "effective" one (Zannetti, 1990). V_d is referred as a velocity because of its units. Gravitational settling has an important effect for the large particle deposition; therefore, it might be acceptable to call V_d a real velocity for these particles. For very small particles (d_p less than 0.1 μm), Brownian movement dominates the deposition velocity; however, motion of large particles (d_p bigger than 1 μm) is controlled by sedimentation effects that increases with the particle size (Holsen et al.,

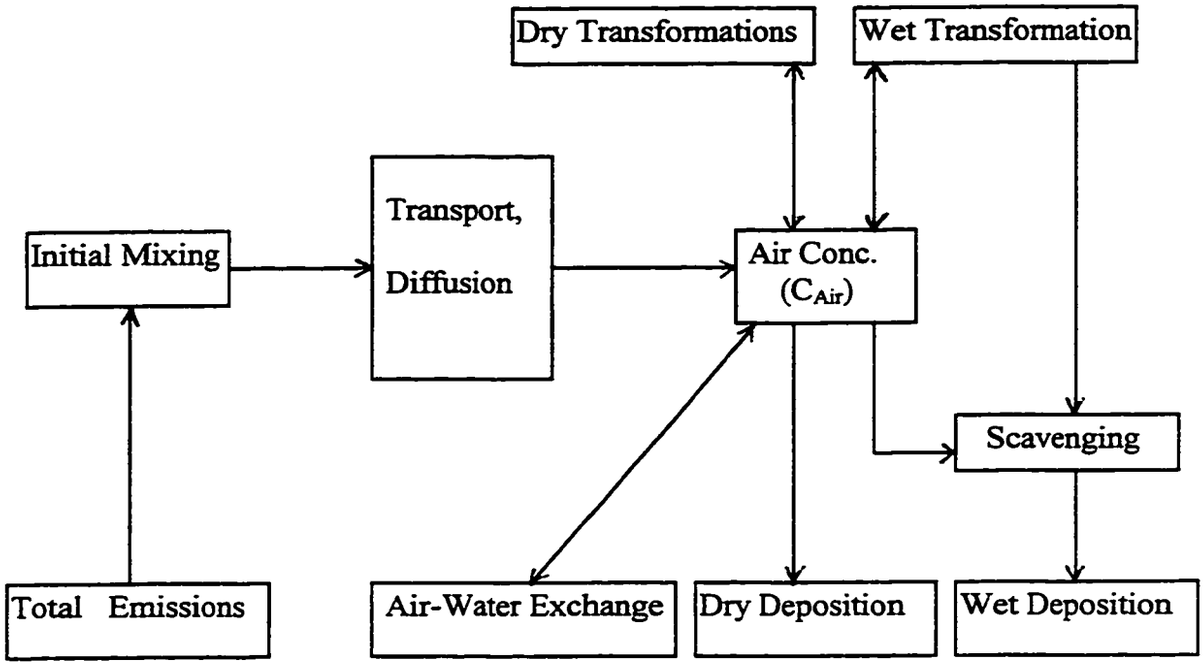

Figure 2.2. Schematic Illustration of Deposition Phenomena

1991; Zannetti, 1990). Intermediate size particles (0.1 μm < d_p < 1 μm) on the other hand, are under the effects of impaction and interception, which are not easy to quantify accurately. Particles in intermediate range have lowest predicted deposition velocities because of the relative weakness of Brownian motion and gravitational settling effects (Zannetti, 1990; Seinfeld, 1986). Dry deposition of gases is governed by their chemical interactions with the surface but it should be noted that physical conditions have a strong effect on this mechanisms (i.e. when wind speed increases, individual air-phase mass transfer coefficient (k_a) and water-phase individual mass transfer coefficient (k_w) values increases as a result resistances decrease; therefore, flux increases).

Meteorological, chemical, physical and maybe biological resistances may have important effects on dry deposition velocity (V_d) (Finlayson-Pitts and Pitts, 1986). Because of this, a wide variety of dry deposition velocities are reported. These authors mention that dry deposition velocities for the same components increased when the surface was wet rather than dry or during day time rather than night time. The wide range in dry deposition velocities could be caused by experimental uncertainties as well as meteorological conditions, surface type, and diurnal variations (Finlayson-Pitts, and Pitts, 1986).

The dry deposition phenomena from the atmosphere to the surface can be described with a three step transport process which takes place in planetary, quasi-laminar, and surface layers (Seinfeld, 1986; Finlayson -Pitts and Pitts, 1986).

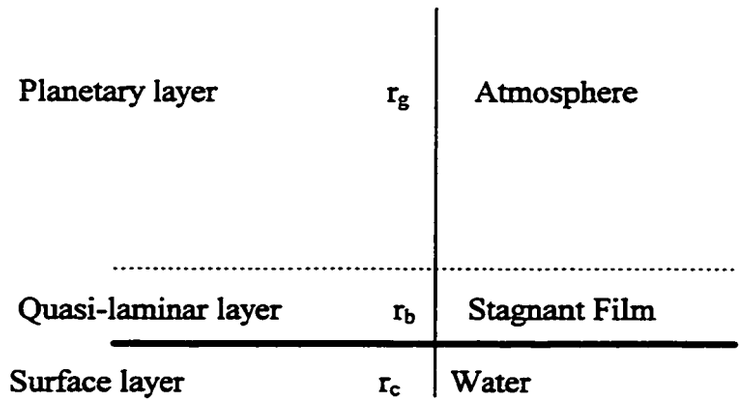

Figure 2.3. Atmospheric Deposition Phenomena in Terms of Boundary Layers

Dry deposition can be determined either by direct measurements or calculations (models and mass balances). Mitzel et al. (1993) developed a model for PCBs. The results from this study suggests that PCB deposition has a seasonal trend, with higher deposition rates in spring and early summer. Another conclusion from this study is that low molecular weight congeners dominate the PCB deposition to the Lakes Michigan, Superior and Ontario.

The flux of PCBs in Bloomington, IN was calculated with two different approaches by Panshin and Hites (1994). The first one uses the atmospheric concentrations and the flux at Bermuda. This relationship is given in equation 2.7. Bermuda was chosen for the Bloomington's flux calculations because both places had the similar tropospheric PCB residence times (Panshin and Hites,1994a).

$$F_{Bloomington} = F_{Bermuda} * (C_{Bloomington} / C_{Bermuda}) \quad (2.7)$$

where,

$F_{Bloomington}$: Flux in Bloomington, IN , $\mu g/m^2$-yr

$F_{Bermuda}$: Flux in Bermuda. 13 $\mu g/ m^2$-yr

$C_{Bloomington}$: Concentration in Bloomington, IN, 0.04-4.8 ng / m^3

$C_{Bermuda}$: Concentration in Bermuda, 0.38 ng / m^3

It is noteworthy to mention how the flux value used for $F_{bermuda}$ was determined. Panshin and Hites (1994a) used steady - state conditions in which the net PCB flux should be zero. The background PCB concentration was assumed as 0.3 ng/m^3 throughout the entire atmosphere, and the volume of atmosphere was $4 * 10^{18}$ m^3 at STP. Hence, the amount of PCB in air was calculated as $1.2 * 10^6$ kg. If the residence time of PCBs at atmosphere was 70 days and the earth's area was $5 * 10^{14}$ m^2, then the atmospheric PCB flux would be 13 $\mu g / m^2$-yr.

The measured $F_{Bloomington}$ values ranged from 1.5 to 160 $\mu g/ m^2$-yr. Because of temperature and PCB concentration changes, fluxes in Bloomington varied seasonally but those in Bermuda did not (Panshin and Hites, 1994a).

Panshin and Hites (1994b) also used a second approach to estimate the PCB flux from Bloomington to the atmosphere. This approach considers the PCB concentration gradient between the boundary layer (atmosphere from earth's surface to one kilometer) and the free troposphere (the next 9 km of the atmosphere). The flux equation is given as follows,

$$F = (C_B - C_T) / (r_a + r_b + r_c) \quad (2.8)$$

where,

F : Flux, ng/m^2-s.

C_B : The PCB concentration in the boundary layer, ng/m^3 (1.95 ng/m^3)

C_T : The PCB concentration in the free troposphere, ng/m^3 (0.8 ng/m^3)

r_a : The aerodynamic resistance, s/m (10 - 35 s/m)

r_b : The boundary layer resistance, s/m (10-20 s/m)

r_c : The canopy resistance, s/m. (200 - 625 s/m) (Inverse of the dep. veloc).

If values given by Panshin and Hites (1994b) are put into the above equation (2.8), the flux can be calculated as follows,

$$F = [1.95 - 0.8] / [10 + 10 + 200] * [\mu g / 1000 ng] * [86400 s/d * 365 d/yr]$$

$$F = 165 \mu g/ m^2\text{-yr}$$

Please note that, this value agrees well the one calculated using equation 2.7.

PCB deposition flux can also be estimated by using the deposition velocity and concentration. Table 2.12. summarizes some PCB dry deposition velocities found in the literature. These values vary a great deal possibly due to the spatial (urban and non-urban areas), temporal variations (winter and summer months), and micrometeorological conditions (such as wind velocity and direction). In general it is expected that dry

deposition velocity increases with the chlorination content of PCB congeners. Higher chlorinated PCBs are primarily associated with the particle phase and they deposit mainly by gravitational settling which is much bigger than diffusional settling. Even at the same sampling site, deposition velocities for a specific organochlorinated species varied one-to -two orders of magnitude (Bidleman et al., 1981). Tables 2.12, 2.13. and 2.14. summarize the dry deposition velocity ranges for the different types of gas and particles in order to provide insight about the gas and particle dry deposition phenomena.

Table 2.12. PCB Deposition Velocities

Value, cm/s	Date & Reference
0.91- aerosol[a]	1976 (McClure)
0.5 - aerosol	1981a (Doskey)
0.13± 0.04	1981 (Eisenreich)
0.18-total[a]	1982 (Atlas)
0.75-total[a]	1986 (Eisenreich)
0.16±0.13-total[a]	1988 (Swackhamer)
1.1-fine aerosol	1991 (Lee)
5.9-coarse aerosol	1991 (Lee)
0.39 to 0.88-total	1996 (Lee et al.)

[a] Values taken from Lee, 1991.

Table 2.13.. Deposition Velocity Range for Particles

Depositing particle	Deposition velocity, cm/s	Reference
Pollen	20	Sehmel, 1980
Rhodamine	<0.6 - 19	Sehmel, 1980
Potasium	0.6 - 13	Sehmel, 1980
Natural aerosol	0.8 - 7.6	Sehmel, 1980
PCB on coarse particle	4.8 - 7.3	Holsen et al. 1991

Table 2.14. Deposition Velocity Range for Gases

Depositing gas	Deposition velocity, cm/s	Reference
SO_2	0.1 - 1.0	Finlayson-Pitts, and Pitts, 1986
I_2	0.02 - 26.0	Zannetti, 1990
Cl_2	1.8 - 2.1	Zannetti, 1990
O_3	0.2 - 2.1	Zannetti, 1990
H_2S	0.015 - 0.38	Zannetti, 1990
CO_2	0.3	Zannetti, 1990
NO_2	0.3 - 1.9	Finlayson-Pitts, and Pitts, 1986
HNO_3	1.0 - 4.7	Finlayson-Pitts, and Pitts, 1986
NO_X	Minus - 0.5	Sehmel, 1980

The flux can be estimated with the following equation,

$$F = V_d * C \qquad (2.9)$$

where,

F : Dry deposition flux, ng/m^2-s.

V_d : PCB dry deposition velocity, m/s.

C : PCB concentration, ng/m^3.

The dry deposition flux of PCBs based on the measured Bloomington ambient air concentrations (0.65 - 2.53 ng/m^3) and reported dry deposition velocities [0.16 cm/s (Swackhamer et al., 1988) - 0.39 ~ 0.88 cm/s (Lee et al., 1996)] values can be calculated as follows:

$F = 0.16$ cm/s * 1m/100 cm * 0.65 ng/m^3 = 1.04 E-3 ng/m^2-s (32.8 $\mu g/m^2$-yr).

$F = 0.5$ cm/s * 1m/100 cm * 2.53 ng/m^3 = 12.65 E-3 ng/m^2-s (398.9 $\mu g/m^2$-yr).

The results indicate that this method agrees well with the previous methods.

Mass balance is another approach used to determine flux magnitude and direction. This approach generally uses the relative inputs and outputs of a chemical from a water body (assumed to be a lake). The contaminant(s) comes from river, groundwater, atmospheric deposition (wet and dry), sediment and benthic exchange. Contaminant may leave by

volatilization, river outflow, degradation (chemical or biological), sedimentation, and groundwater outflow (Baker et al., 1993; Strachan and Eisenreich, 1988; Jeremiason et al., 1994). Achman et al. (1993) and Hornbuckle et al. (1994) have simultaneously collected air and surface water samples from the Great Lakes to determine a concentration gradient so that a flux across the air-water would be determined. If only one flux value, net flux, is used rather than consideration of deposition and volatilization fluxes separately, this approach may cause underestimation of inputs from the atmosphere and overestimation from other inputs (Murphy, 1995). Therefore, a representative mass balance should consider all inputs and outputs separately in order to give a realistic value for each fraction.

Another method of dry deposition flux determination is the direct measurement with surrogate surfaces. This method might be better than the others because of control on the system in general including exposure times (meteorological variations), exposure locations (spatial differences), surface geometry, extraction methods (Davidson, 1985). To date different types of surrogate surfaces were used including bucket, filter paper, Teflon plates, petri dishes, and some kinds of greasy surfaces.

The drawbacks of these direct measurement studies are 1) extension to the natural surfaces is difficult and 2) no universally acceptable sampling and analyzing methods exist (Sehmel 1980; Davidson, 1985). Holsen et al. (1991) applied this method to determine the PCB fluxes in Chicago, IL. The PCB dry deposition flux was measured by using a smooth plate, including greased strips, with a sharp leading edge pointed into the

wind by a wind vane. The collection surface was designed based on wind tunnel studies in order to have minimum flow disruption and therefore, an estimation of the lower limit for dry deposition flux would be provided (Holsen et al., 1991). The deposition plate with greased strips has been successfully used as a surrogate surface to directly assess deposited material (Noll et al., 1990).

The average PCB dry deposition flux measured in Chicago, IL were 3800 ng/m^2-d (1387 μg/m^2-yr) in 1989 and 6000 ng/m^2-d (2190 μg/m^2-yr) in 1990 (Holsen et. al., 1991). These results are 3.5 to 67 times higher than the Bloomington, IN flux values which were calculated by using the indirect method even though both cities are considered urban areas. This difference can be attributed partly to particle deposition which was not taken into account in the Bloomington, IN flux calculation. The better and more realistic form of Equation 2.9 would be the one which considers each phase separately because each of them has different deposition characteristics. For example when particle diameter is bigger than 1 μm, the deposition phenomena is governed by gravitational settling whereas when particle diameter is smaller than 0.1 μm, the deposition phenomena is governed by Brownian motion. The modified new flux equation can be given as follows:

$$F = V_G * C_G + V_F * C_F + V_C * C_C \qquad (2.10)$$

where,

F : Dry deposition flux, ng/m^2-s (6040 ng/m^2-d).

V_G : Gas phase PCB dry deposition velocity, m/s (0.01 - 0.1 cm/s).

V_F : Fine particle phase PCB dry deposition velocity, m/s (0.1 - 0.5 cm/s).

V_C : Coarse particle phase PCB dry deposition velocity, m/s.

C_G : Gas phase PCB concentration, ng/m^3 (10.4 ng/m^3).

C_F : Fine particle phase PCB concentration, ng/m^3 (3.2 ng/m^3).

C_C : Coarse particle phase PCB concentration, ng/m^3 (0.9 ng/m^3).

The values inside the parentheses were taken from the study done by Holsen et al. (1991). In order to find the dry deposition velocity of coarse particles (V_C), Equation 2.10 was solved. Other parameters (F, C_G, C_F, C_C) were measured directly or obtained from literature i.e. V_G (Sehmel, G.A., 1984) and V_F (Davidson, 1985). Based on the calculations done by Holsen et al. (1991), V_C value fluctuated between 4.8 to 7.3 cm/s. Even though particulate PCB concentrations are very small compared to the total PCB concentrations, the flux associated with coarse particulates contributes the major portion of the total flux. This finding is because of their higher dry deposition velocities due to gravitational settling.

The above mentioned techniques are mainly applicable for particulate flux measurements. However, compounds like polychlorinated biphenyls (PCBs) and polycyclic aromatic hydrocarbons (PAHs) having both gas and particulate phases cannot be accurately measured with above mentioned surrogate surfaces. At the Illinois Institute of Technology (IIT), a new surrogate surface called water surface sampler (WSS) was developed. The new surrogate surface is water; thus, grease problems including analytical

difficulties and contamination were eliminated as well as the vapor phase is captured. The water surface plate (WSP) is put inside the water surface holder (WSH) at a height that allows the water on the WSP to be level with the top of the WSH. The water surface is continuously replenished with water to maintain constant water depth which carries captured contaminants (i.e. PCBs, PAHs) to the XAD-2 resin column. The retention time on the WSP is maintained as small as possible (2 - 4 minutes) in order to prevent any losses from deposited PCBs and PAHs. Detailed information about the WSS will be presented in Chapter III (Materials and Methods).

2.8.2. Wet Deposition. Wet deposition is another contaminant removal mechanism from the atmosphere. It has been evaluated better than dry deposition. Wet deposition is a combination of precipitation scavenging and surface deposition of fog and cloud droplets. Precipitation scavenging of the contaminants takes place either during droplet formation or as the rain drops go through the air column (Porter and Baker, 1996a). When a drop falls through the air , it interacts with aerosol particles and collects them (Seinfeld, 1986). Wet deposition also includes mass transfer between the rainfall and the contaminant in both the gas and particle phases due to their physical and chemical properties. Therefore, a single set of particle to gas partitioning coefficients is not enough to precisely model the concentrations of organic contaminants in wet precipitation (Poster and Baker, 1996b). These authors suggested that the equilibrium gas scavenging is not as important as particle scavenging for removal processes for PAHs during precipitation events. Poster and Baker (1996a) reported that PCBs and PAHs found on the filter

(associated with the nonfilterable particles) accounted for up to about 80% of the PCBs found in the rain and less than 9% were truly dissolved.

The equilibrium distribution of a contaminant between the rain drop and gas phase can be determined with Henry's law as follows:

$$RT/H = C_d/C_g \qquad (2.11)$$

where,

H : Henry's law constant, m^3/atm-mol.

R : Ideal gas constant, 8.21E-5 m^3/atm-mol-K.

T : Temperature, K.

C_d : Dissolved PCB and PAH concentration, ng/m^3.

C_g : Gaseous PCB and PAH concentration, ng/m^3.

The temperature dependence of H is a well known fact and if this phenomena is specifically addressed to PCBs (Poster and Baker, 1996), the following equation can be obtained:

$$\ln H = 18.58 - 7859 / T \qquad (2.12)$$

Poster and Baker (1996a) also reported that PCBs and PAHs are adsorbed differently to large and small particles. Their partition coefficients are not strongly correlated with hydrophobicity (Porter and Baker, 1996a).

Table 2.15. given below is the total PCB concentrations (dissolved + particulate) found in rain. All data is obtained from Poster and Baker's paper (1996a). The particle associated (non-filterable) PCBs ranged in their study between 7 to 50%.

Table 2.15. PCB Concentrations in Rain

PCB concentration, ng/L	Place	Date
0.85 - 2.2	Chesapeake Bay, MD	Late summer 1992
1.6	Chesapeake Bay, MD	1990 - 1991
3.5	Madison, WI	

In the literature, the rain PCB concentrations are higher than those calculated based on Henry's law indicating the rain drop is supersaturated. Thus, it can be concluded that precipitation scavenging of particle-associated PCBs is the main PCB removal mechanism from the atmosphere via wet deposition in spite of low particle concentration of the atmosphere (Murphy and Rzeszutko, 1977; Poster and Baker, 1996a).

Another type of wet deposition is snowfall. Franz (1994) found that snow, which accounts for 17% of annual precipitation in northern Minnesota, contributed 30 to 45%

of the annual loading of PCBs to this region. The concentration of PCBs in snow was higher than in the rain. It was reported that about 70% of the total PCB concentration was in the particle phase and more chlorinated congeners were dominant (Franz, 1994).

2.9. Models

Strachan and Eisenreich (1988) calculated that deposition was 90%, 63% and volatilization was 86%, 75% of the total inputs and outputs of the Lakes Superior and Huron, respectively. Moreover, Atlas et. al. (1986) reported that about 70% of the PCBs entering the oceans was due to air-water exchange. Even though quantification of PCB exchange is difficult, the estimated values indicate that air-water exchange of SOCs is a very important transfer mechanism. Some air - water fluxes of PCBs are given in Table 2.16.

Gas transfer magnitude is a function of concentrations in the atmosphere and water, chemical characteristics, season, and location (Achman et al., 1993; Hornbuckle et al., 1993 and 1994; Bidleman and McConnel, 1995). Estimation of direction and magnitude of the flux can be determined by either applying mass balance (Rate of change = inflow + resuspension + deposition +/- reaction - outflow - sedimentation - volatilization) or activity gradients measurements (with mass transfer calculations) (Strachan and Eisenreich, 1988; Hornbuckle et al, 1995; Murphy et al., 1981; Holsen et al, 1991).

Table 2.16. Estimated Air - Water Fluxes of PCBs

Location	PCB Flux, ng/m^2-day	Reference
Green Bay	-15 to -1300	Achman et. al., 1993
Lake Superior	-19 to -141	Baker and Eisenreich, 1990
Lake Superior	+40 to -110	Hornbuckle et al., 1994
Lake Superior	-63	Jeremiason et al., 1994
Siskiwit Lake	-23	Swackhamer et. al., 1986
Lake Michigan	-240	Strachan and Eisenreich, 1988
Lake Ontario	-81	Mackay, 1989
Ricer Elm, Sweden	-50	Larsson et. al., 1990
Chicago, IL	+2800 to +9700	Holsen et al., 1991
Bermuda	+35	Panshin and Hites, 1994a
Bloomington, IN	+145 to +450	Panshin and Hites, 1994b
Oceans	+0.6 to +10	Atlas et. al., 1986
Oceans	-12 to +35	Iwata et. al., 1993
Oceans	+160 to +450	GESAMP, 1989

Note: negative values refer to volatilization and positive values refer to water absorption.

Air-water exchange can be considered a diffusion phenomena. At calm or low wind speed conditions, a stagnant two-film model can be applied. On the other hand, the surface renewal model is applicable at higher turbulence where the parcels of air and water change rapidly (Schwarzenbach et al., 1993; Thibodeaux, 1979; Cussler, 1984).

The most commonly used model is the two-film theory proposed by Whitman (1923). The details of the theory can be found extensively in the literature (Liss and Slater, 1974, Thibodeaux, 1979, Cussler, 1984). This model assumes a stagnant layer between the air and liquid phases along the interface. Both bulk compartments are well mixed and offer no resistance to gas transfer. Under these conditions the rate of gas exchange or mass flux is written as follows:

$$\text{Flux} = {}^{2}k_{A1}(C_{A1} - C_{A1i}) = {}^{1}k_{A2}(C_{A2} - C_{A2i}) \qquad (2.13)$$

where ${}^{2}k_{A1}$ is the air phase individual mass transfer coefficient, ${}^{1}k_{A2}$ is the liquid phase individual mass transfer coefficient, C_{A1} ,C_{A1i} are the air phase bulk concentration and interface concentrations, and C_{A2}, C_{A2i} are the liquid phase bulk concentration and interface concentrations, respectively. Figure 2.4. shows a two-film model illustration. The transfer at the interface is assumed to be instantaneous and there is no resistance to transfer; therefore, Henry's Law is applicable:

$$C_{A1i} = HC_{A2i} / RT \qquad (2.14)$$

where H is called Henry's Law constant which defines the equilibrium distribution of a chemical between air and water (atm - m^3/mole). The Henry's Law constant influences both the concentration gradients and the magnitude of overall mass transfer coefficients. H is a function of temperature so the direction and magnitude of gas flux could be affected

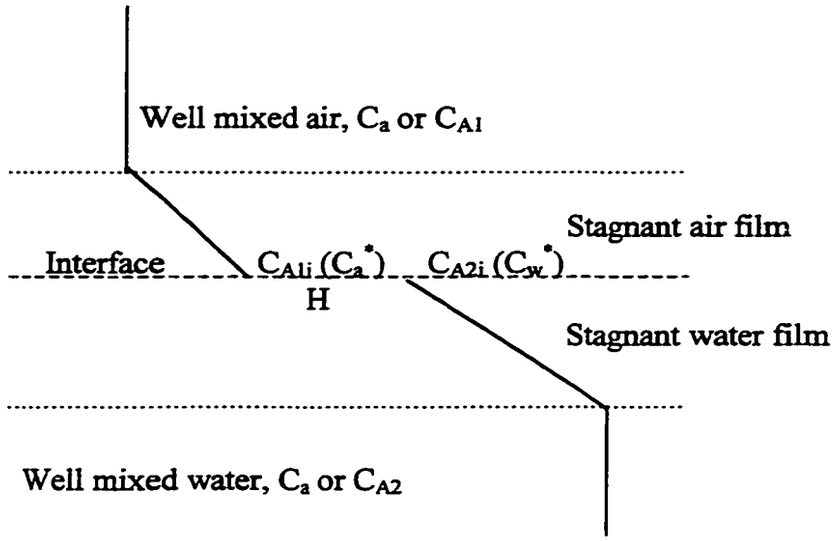

Figure 2.4 Stagnant Two-film Model Illustration

by the water temperature. This model incorporates unmeasurable parameters like the depth of the interfacial zones and interfacial concentrations. Thus, the flux can be calculated from the bulk concentrations using the overall mass transfer coefficient:

$$\text{Flux} = {}^2K_{A1}(C_a - C_a^*) = {}^1K_{A2}(C_w - C_w^*) \qquad (2.15)$$

$$C_w^* = C_aRT/H, \quad \text{and} \quad C_a^* = C_wH/RT \qquad (2.16)$$

where ${}^2K_{A1}$ (m/d) is the air phase overall mass transfer coefficient, ${}^1K_{A2}$ (m/d) is the liquid phase overall mass transfer coefficient. C_w^* (ng/m^3) is the hypothetical liquid phase concentration in equilibrium with the gas phase bulk concentration (or, the water concentration in equilibrium with the partial pressure of the gas in the atmosphere ,

$C_w^*=C_a/H$). Similarly, C_a^* is the hypothetical air phase concentration in equilibrium with the water phase bulk concentration. C_w (ng/m^3)and C_a (ng/m^3) are the bulk concentrations in water and air, respectively. R is the universal gas constant ($8.2*10^{-5}$ atm-m^3/mol-°K) and T is the absolute temperature (°K). The flux will have the unit of ng/m^2-d.

The overall resistance to mass transfer is the reciprocal of the overall mass transfer coefficient which is the sum of individual gas and water mass transfer coefficients:

$$1/{}^1K_{A2} = 1/{}^1k_{A2} + RT/({}^2k_{A1}H) \qquad (2.17)$$

$$1/{}^2K_{A1} = 1/{}^2k_{A1} + H/({}^1k_{A2}RT) \qquad (2.18)$$

Resistance in both phases occurs for PCBs, DDT and some PAHs. The resistance through the air film is about 20-30 % of the total resistance for PCB congeners (Hornbuckle et al., 1994). Water layer resistance dominates the mass transfer of PCBs in the air-water interface.

2.10 Mass Transfer Coefficients

Gas transfer can be measured directly in wind tunnel experiments and it has been determined that mass transfer is related to wind speed, waves, bubbles, and heat transfer (Liss and Slinn, 1983). Wind tunnels studies for the liquid phase controlled gases (O_2, and CO_2) exhibit low transfer rates at low wind speeds but transfer rate increased with the wind speed (Baker et. al., 1993; Liss and Slinn, 1983). Some researchers show

considerable correlation between k_w (water phase mass transfer coefficient) and wind speed in the laboratory; however, k_w cannot be described fully in the real environment due to complex relationships among wind speed, bubble formation, spray, waves and so on. There are not many reliable environmental data for k_w even though there are many published laboratory studies due to its real dependency on fetch, atmospheric stability, wind speed, pollutant characteristics (H, diffusivity, molecular weight) and surface microlayers (Mackay and Yeun, 1981).

There are some experimental methods to determine gas transfer rates. They are the direct flux method, oxygen balance approach, profile and eddy correlation technique, and natural and bomb produced ^{14}C methods (Liss and Slinn, 1983). All of these methods are good for the determinations of k_w except the eddy correlation technique. It is possible to run long term field experiments on gas transfer and mixing in the natural waters if a suitable tracer gas is used. SF_6 has been used because it is a good tracer of water controlled gas, has low detection limits, is chemically and biologically inert, and is not sorbed by aquatic particles.

The individual mass transfer coefficients (k_a and k_w) have been studied for different types of environments (evaporation pans, wind-water tunnel, circular wind-water tank, wind-wave tank) and compounds (O_2, CO_2, SF_6, H_2O) by many researchers. Their empirical formulae are represented in Tables 2.17 and 2.18 Mass transfer is wind speed dependent (Hoff et al., 1996); therefore, all k_a and k_w formulae given in these tables are function of wind speed. Mass transfer coefficients (k_a and k_w) calculated with these equations can be

converted for PCBs using the equations given under the Tables of 2.17. and 2.18. (Hornbuckle et al., 1994)

Hornbuckle et al. (1995) used the models developed by Schwarzenbach et al. (1993) and Wanninkof et al. (1991) to calculate the individual mass transfer coefficients for air-side (k_a) and water-side (k_w), respectively. Considering diffusivities and necessary correlations between reference compounds (H_2O and O_2) and PCBs, the individual mass transfer coefficients were calculated for PCB congeners. In another study Achman et al. (1993) used Liss and Merlivat's relationship in order to calculate the water-side individual mass transfer coefficient while Schwarzenbach's model was used for calculation of individual air-side mass transfer coefficient. Two-film theory was applied to calculate the overall mass transfer coefficient, K_{OL} (written in terms of water concentrations).

Achman et al. (1993) reported the value of K_{OL} between 0.02 and 0.31 m/day for the study done in Green Bay. Similarly, Doskey and Andren (1981) have reported K_{OL} values calculated based on two-film theory in their paper and the values ranging from 1.61 to 9.84 ± 5.04 E-4 m/d for Aroclor 1254. Atlas et al. (1982) calculated a K_{OL} value of 0.92 m/d considering $k_{w,\,O2}$ = 13-20 cm/h and $k_{a,H2O}$ = 1700-9300 cm/h. Baker and Eisenreich (1990) calculated K_{OL} values based on fugacities and they fluctuated from 0.05 to 0.08 m/d. Hornbuckle et al. (1994) has reported K_{OL} values for temperatures of 0 and 15 °C for 7 different congeners. These results indicated that when temperature increases K_{OL} also increases. When molecular weight increases for the PCB congeners, the K_{OL} value

Table 2.17. Some Empirical Relationships Between Air Phase Mass Transfer Coefficient (k_a) with Wind Speed [a, b]

No	Source	Data Type	k_a (H_2O) (cm/s)
1	Sverdrup et al. (1942)	Field	$k_a = 0.15u_{10}$
2	Penman (1948)	Evaporation pans	$k_a = 0.59+0.23u_{10}$
3	Rohwer (1931)	Evaporation pans	$k_a = 0.35+0.12u_{10}$
4	Liss (1973)	Wind-water tunnel	$k_a = 0.005+0.21u_{10}$
5	Munnich et al. (1978)	Circular wind-water tank	$k_a = 0.5+0.185u_{10}$
6	Mackay and Yeun (1983)	Wind-wave tank	$k_a = 0.065(6.1+0.63u_{10})^{0.5}u_{10}$
7	Schwarzenbach et al. (1993)	From Above Models	$k_a = 0.2u_{10}+0.3$
8	Thibodeaux (1979)	Forced and Natural Forces - Evaporation	$k_a=[(0.14Gr_{BI}^{1/3}+0.664Re^{0.5})D_{PCBI}Sc_{PCBI}^{1/3}] / (L)$ [c] $k_a =[(0.14Gr_{BI}^{1/3}+0.036Re^{0.8})D_{PCBI}Sc_{PCBI}^{1/3}]/(L)$ [d]
9	Yi (1997)	Thibodeaux and WSS	$k_a = k_a$ (obtained from Thibodeaux Model) / 0.54

Note: [a] All u_{10} values are in m/s.
[b] All relationships are taken from Schwarzenbach et al.(1993) except 8, 9.
[c, d] for laminar and turbulent regimes, respectively.

$$k_a(PCB) = k_a(H_2O) [D_{PCB, air} / D_{H2O, air}]^{0.61} \quad \text{(Hornbuckle et al., 1994)}$$

Table 2.18. Some Empirical Relationships Between Water Phase Mass Transfer Coefficient (k_w) with Wind Speed [a,b]

No	Source	Data Type	$k_w(O_2)$ or $k_w(CO_2)$ (cm/s)
1	Kanwisher (1963)	CO_2 , wind-water tunnel	$k_w(CO_2)=(4.1+0.417u_{10}^2)10^{-4}$
2	Banks (1975)	O_2 , lakes	If u_{10} <5.5 m/s
			$kw(O_2)=1.024^{(T-10\,C)}(4.2E\text{-}6\ u_{10}^{0.5})$
			If u_{10} >5.5 m/s
			$kw(O_2)=1.024^{(T-10\,C)}(0.32E\text{-}6\ u_{10}^2)$
3	Mackay and Yeun (1983)	O_2 , laboratory	$k_w(O_2)=1.75E\text{-}4(6.1+0.63u_{10})^{0.5}u_{10}$
4	Wanninkhof et al. (1987)	SF_6 , lakes	$k_w(SF_6)=(-8.9+5.8u_{10})10^{-4}$
5	Schwarzenbach et al (1993)		$k_w(O_2)= 4\ E\text{-}4 + 4E\text{-}5\ (u_{10})^2$

Note: [a] All u_{10} values are in m/s.
[b] All relationships are taken from Schwarzenbach et al.(1993) except IIT.

$$k_w(PCB) = k_w(CO_2)\ [\ Sc_{PCB,\ water} / Sc_{CO2,\ water}]^{-0.5}$$ (Hornbuckle et al., 1994)

decreases and therefore, overall resistance increases. Table 2.19. summarizes the mass transfer coefficients calculated at 15 °C for PCB homologs by Hornbuckle et al., 1995.

Table 2.19. Mass Transfer Coefficients for Water Temperature of 15 °C

PCB Homolog	k_w , m/d	k_a , m/d	K_{OL} , m/d
dichlorobiphenyl	0.206	334	0.181
trichlorobiphenyl	0.202	325	0.174
tetrachlorobiphenyl	0.197	316	0.154
pentachlorobiphenyl	0.192	308	0.122
hexachlorobiphenyl	0.187	302	0.093
heptachlorobiphenyl	0.185	295	0.056
octachlorobiphenyl	0.182	290	0.042
nonachlorobiphenyl	0.178	285	0.024

2.11. Summary of Literature Review

PCBs have been detected in almost all environmental matrixes (air, soil, water, biota and human tissue) and in many locations around the globe. The atmosphere serves as an important pathway for global transport of PCBs due to their physical and chemical characteristics (vapor pressure, Henry's law constant, solubility). Dry deposition becomes an important contamination source for the remote areas (i.e. Arctic) as well as other locations.

The concentration of PCBs in the air has been studied extensively. Even though PCBs exist mainly in the gas phase, they partition onto particles based on their vapor pressures and the atmospheric conditions. The Junge-Pankow model can be employed to predict the gas- particle partitioning.

The gas flux across a water surface is a function of Henry's law, the concentration gradient and overall mass transfer velocity (Hoff et al., 1996). Individual mass transfer coefficients have been studied extensively by many researchers and some empirical equations have been developed to estimate them. These equations will be used to estimate the overall gas mass transfer coefficients used in this study.

CHAPTER III

MATERIALS AND METHODS

A water surface sampler (WSS), which was constructed for this study, and greased strips on the knife-edge surrogate surfaces were used to determine the dry deposition fluxes for PCBs. Water evaporation experiments (to determine the k_a values - air side mass transfer coefficient) and O_2 transfer experiment (to determine the k_w - water side mass transfer coefficient) were done in the field. The ambient air concentrations for gas and particle phases were measured with high volume air sampler. The following sections of this chapter will explain the equipment and experiments employed during this study.

3.1. Sampling Program

Atmospheric samples were taken from June to October 1995. The sampling program was conducted in Chicago, IL which is large an urban industrialized area. Water surface samplers (WSSs), greased strips (plates) and a high-volume air sampler were used to collect the ambient air PCB samples.

3.1.1. Sampling Site. The sampling site is on the roof of a four-story building (~12 m height). This building is located on the Illinois Institute of Technology (IIT) campus, which is about 5.5 km south of Downtown Chicago, and 1.5 km west of Lake Michigan. It is in a mixed institutional, residential and commercial area on the south side of Chicago. Buildings around the sampling site are mainly low-rise and there are landscaped areas and big parking lots. The WSS sampler and meteorological tower on the

roof were out the roof wake boundary (Yi et al., 1997). This site was used for the Lake Michigan Urban Air Toxics Study (LMUATS) and it is being used in Lake Michigan Mass Budget/Mass Balance Study.

3.1.2. Sampling Duration. The dry deposition sampling duration was determined based on the likely detectable mass from the samplers. Greased strips on the deposition plates had a smaller area than the water surface sampler (WSS) (6 to 10 times smaller based on the number of strips used); thus, they required the largest sampling time. Daily samples were usually taken from 8:00 a.m. to 8:00 p.m. (day time). The sampling period depended on the weather conditions. When there was no rain, the sampling period was about five consecutive days (5x12 hours). When there was rain, sampling was postponed; however, total sampling time generally lasted 5 days.

Air samples were taken with a high-volume sampler. The overall average volume was about 150 m^3 and each sample was a two day composite (2x12 hours). Thirty-nine samples were taken during the sampling period. The limiting factor for the high -volume sampler was breakthrough and artifacts. PCBs and PAHs were sampled from the same filter and cartridge; and PAHs concentrations were much higher than the PCBs in the air. Therefore, the volume of air sampled was a compromise between PAH breakthrough and the detection limits for the PCBs.

The sampling information is summarized in the following table (Table 3.1.).

Table 3.1. Summary of Sampling Information (1995)

Sample No	Sampling Date	Sampling Time (min)	Avg. Wind Speed (m/s)	Avg. Temp. (°C)	Avg. RH (%)
1	6/29-7/6	3680	3.6	23.7	19.9
2	7/8-7/13	4020	3.0	26.9	51.9
3	7/14-7/21	3880	3.7	30.1	41.4
4	7/25-7/30	3750	2.9	29.1	21.8
5	8/5-8/12	4700	2.8	29.1	25.6
6	8/15-8/23	4305	2.8	27.3	20.5
7	8/24-8/31	4515	2.8	27.7	44.4
8	9/6-9/14	4920	3.6	19.3	52.0
9	9/15-9/25	4770	3.3	15.8	45.6
10	10/4-10/13	4615	3.2	20.6	40.3
11	10/15-10/23	3825	4.5	14.8	35.2

3.1.3. Sampling Method. In order to measure the dry deposition flux, samples were collected with greased surrogate surfaces (5 deposition plates with 16 to 25 strips) and two WSSs which were run simultaneously. These samples were taken during the day time (8:00 a.m.-8:00 p.m.) when there was no rain or threat of rain at the sampling site. Because of the small surface areas of greased strips and small concentrations of the PCBs in the ambient air, the sampling time for flux samplers was about 60 hours.

The collection of particle and vapor phases of PCBs in the ambient air was achieved with a high-volume sampler. These samples were obtained concurrently at the site while deposition samples were being taken. Sampling devices will be explained in detail in the following section (3.2.).

3.1.4. Meteorological Data. The temperature, wind speed, wind direction and relative humidity were obtained from a meteorological tower located on the top of the building located in the IIT's campus. The data collected from this sampler is automatically sent to Illinois State Water Survey (or now to Indiana University) with a modem. However, when this sampler malfunctioned, the meteorological data was obtained from Midway Airport measurements (the closest valid atmospheric data source).

3.2. Sampling Equipment and Supplies

3.2.1. High Volume Sampler. This sampler (Model PS-1, manufactured by Graseby General Metal Works, Cleves, OH) was used to collect suspended airborne particles and airborne vapors. Samples were taken by passing air through an 11 cm diameter glass fiber filter and then through a glass cartridge that contained polyurethane foam (PUF) and XAD-2 resin. The cartridge was about 5.6 cm in diameter and 10 cm in length. XAD-2 resin was placed between two PUFs in the cartridge. Average air volume was about 150 m^3.

Filters were used in both the WSS and high-volume sampler. The ones which were used in high volume air sampler had been weighed before and after sample collection. They were put in a desiccator for equilibration before weighing. Therefore, it was possible to determine the particle mass concentration. One potential disadvantage of this procedure is the loss of a small amount of PCBs from the particles on the filter.

Glass cartridges placed into the high volume sampler were used to hold the XAD-2 resin sandwiched between the two pieces of PUF. The purpose of the PUF and resin is to capture the vapor phase PCBs.

XAD-2 resin was also used in the WSS to sorb the dissolved PCBs from the water. Amberlite XAD-2 is produced as insoluble beads to adsorb soluble organic compounds from aqueous streams. It is a hydrophobic adsorbent made of polystyrene copolymers (SUPELCO). The amount and selectivity of soluble organic compounds by XAD-2 resin increases as the hydrophobicity of the organic molecule increases. The main characteristics of XAD-2 resin are given in Table 3.2.

Table 3.2. Typical Physical Properties of Amberlite XAD-2 Resin (SUPELCO).

Characteristics	Value or Explanation
Appearance	Hard, spherical opaque beads
Solids (%)	55
Porosity (mL pore/mL bead - dry basis)	0.42
Surface Area (m^2/g - dry basis)	300
Effective Size (mm)	0.4
Average Pore Diameter (A° - dry basis)	90
Bulk Density (g/L)	640

Field blanks were taken to determine the background mass of PCBs. A clean filter and a clean glass cartridge, which included PUF and resin, were carried to the sampling site. They will be described in more detail in the QA/QC section.

3.2.2. Knife-edge Deposition Plate. The knife-edge deposition plate is made from polyvinyl chloride and its design is similar to those used in wind tunnel studies (McCready, 1986). It was used widely with greased strips by researchers at IIT (Holsen et al., 1991, Holsen and Noll, 1992). It is about 21.6 cm long, 7.5 cm wide, and 0.55 cm thick with a sharp leading edge (<10°) that is pointed into the wind by a wind vane. Mylar strips (7.6 x 2.5 cm) placed on top of the plate were coated with approximately 3 - 4 mg of Apezion L grease (thickness ~ 5 μm). The collection area is 5.7 x 1.8 cm for the strips. Figure 3.1. shows a typical dry deposition plate with strips. PCB concentrations in the atmosphere are low; thus, five deposition plates each with up to five strips were used. One strip from each plate was weighed to determine the deposition mass.

The assumed theories behind this type of deposition sampler can be summarized as follows (Davidson, 1985, McCready, 1986 and Holsen et al. 1991):

1. Minimum deposition velocities are obtained on the smooth surrogate surfaces under atmospheric conditions. Therefore, all artifacts due to roughness are eliminated.

2. The plate provides a deposition environment which includes an aerodynamic boundary layer.

3. The greased surface (plates) can be used to directly assess deposited particles and does not allow particles to bounce.

4. Particles deposit on the surrogate plate due to interaction between particles and the turbulent motion of the atmosphere if the particles are in the inertial deposition range.

The atmospheric dry deposition flux for this surrogate surface can be calculated by using the following equation:

$$F = M/(A*t)$$

where:

F = particle dry deposition flux, ng/m^2-d

M = mass of PCBs associated with particles on the deposition plate, ng

A = greased collection area on the plate, m^2

t = exposure time, d

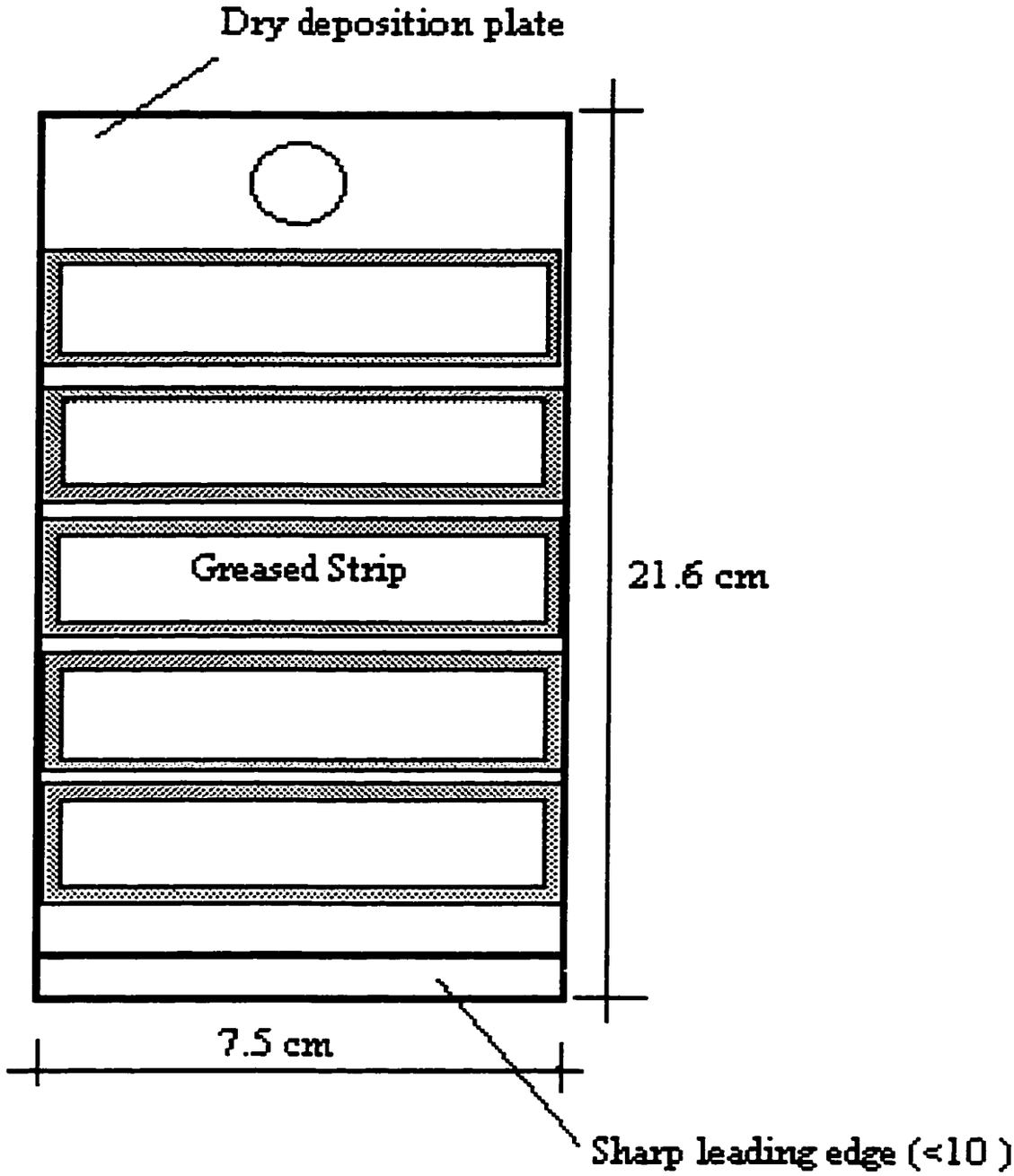

Figure 3.1. Top View of Deposition Plate

A summary of the preparation of Mylar strips for sampling is described below: Mylar, obtained from Graphic Arts Systems Cleveland, OH, were cut in strips (7.6 x 2.5 cm) and the area to be greased was marked with a sharp mechanical pen (5.7 x 1.8 cm). The strips were then cleaned several times with methanol and wiped with dust-free paper. This step was repeated with distilled water, and strips were then rinsed twice with DI water. Next, they were placed into the laminar-flow hood onto dust-free papers for drying. These Mylar strips were coated with 3 ~ 4 mg of Apezion type L grease (~5 μm in thickness). Prior to coating the grease was melted on a hot plate and then coated on the marked surface with a small paint brush. The Mylar strips were then put in a dust-free storage box for about 24 hours for equilibrium before weighing (ATI Cahn Balance, Model C-38). The ungreased areas are covered with PVC covers to prevent any deposition on them during field sampling.

Five deposition plates including 25 greased strips were prepared as blanks. These blanks were used for weight correction and background PCBs concentration determination. These plates were transported to the field and kept in an acrylic storage box during sampling.

3.2.3. Water Surface Sampler (WSS). Another surface used to measure the PCB dry deposition flux was a water surface. This new surrogate surface called water surface sampler (WSS) was developed by our group at the Illinois Institute of Technology (IIT) (Figure 3.2.). The water surface plate was put inside the water surface holder at a height that allows the water on the water surface plate to be level with the top of the water

surface holder. The WSS plate had a diameter of 15.5 inches (39.4 cm), thickness of 0.5 inch (1.27 cm) and water depth of 0.5 inch (1.27 cm). It was made of aluminum and coated after that. The WSS was continuously replenished with water to maintain a constant water depth. Water entered to WSS plate from its center and overflowed from the triangle weirs located at the sides. The purpose of the weirs were to prevent the water tension from causing the water level to be higher than the leading edge. The retention time on the WSS plate was maintained as small as possible (2-4 minutes) in order to prevent any evaporation loss from deposited PCBs and PAHs. The recycled water went through a filter and a resin (XAD-2) column before completing a cycle. All tubings andfittings used in this system were made of Teflon or stainless steel in order to minimize adsorption. A Prexplus aspirator bottle (4 L) was used as a reservoir. for the overflow water and this water was pumped to the WSP. The pump was a chemical-resistant adjustable liquid pump in which all wetted parts were Teflon.

The PCBs flux from this system can be calculated as follows:

$$F = M / (At)$$

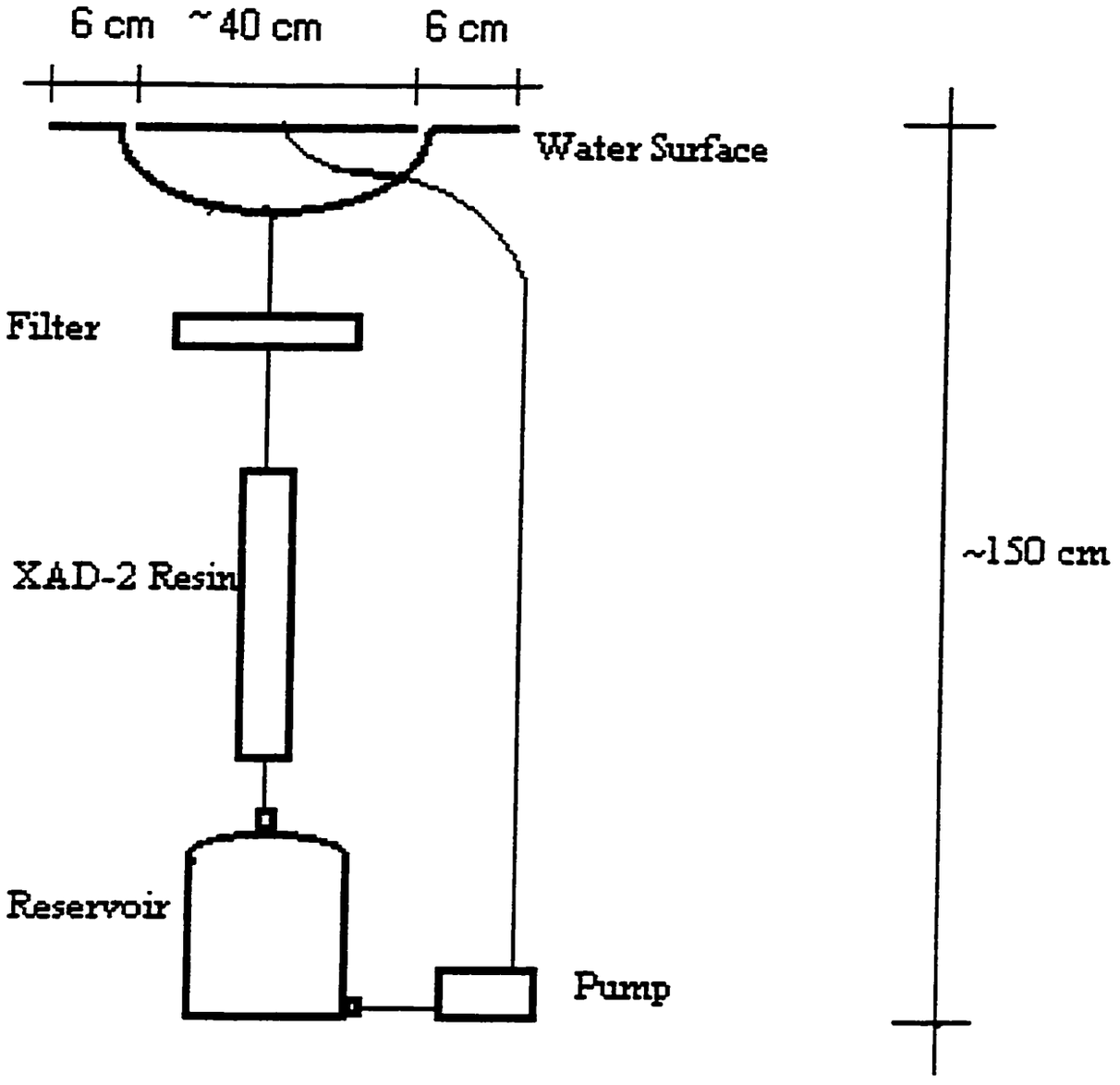

Figure 3.2. Schematic Layout of Water Surface Sampler (WSS)

where:

F = total dry deposition flux, ng/m^2-d

M = mass of PCBs collected in the resin or on the filter, ng

A = collection area on the WSS plate, m^2

t = exposure time, d

After each run, water surfaces were rinsed with DI water a couple times and wiped with clean paper (solvent washed) and this paper also analyzed with the sample. Before starting a new sample, the water surface was cleaned with distilled water and solvents (methanol, dichloromethane, hexane and acetone, respectively); then, a new filter and a resin column were put in the WSS.

Field blanks were taken by setting up the everything as in real sampling. However, in order to prevent any ambient air interaction with the WSS, its cover was closed. It stayed in this configuration for a real sample duration of approximately 5 days. Results will be discussed in the QA/QC section.

Two water surface samplers were run simultaneously. In terms of flux comparisons, they agreed well statistically as will be discussed later. A backup resin column was used to check whether there was a breakthrough or not. The results of these experiments showed no evidence of breakthrough from the resin column.

3.3. Mass Transfer Coefficient Determination Experiments

3.3.1. Water Evaporation Experiments (k_a determination). The purpose of this experiment was to measure the evaporation flux from the WSS to determine air side mass transfer coefficient (k_a) for this study. In these experiments the amount of evaporated water from the water surface was measured after every sample. Water evaporation volume from the water surface (WSS_1) was determined by measuring the volume of the water at the beginning and end of the each day. For the second water surface (WSS_2), the evaporation measurements were done at the end of the each run (once in every ~ 60 hours).

The individual air phase water MTC ($k_{a,\,H2O}$ (cm/s)) can be calculated using flux of evaporated water and the water concentration difference between stagnant layer and the ambient air which is relative humidity ($0 \leq RH \leq 1$). The representative equation can be given by:

$$k_{a,\,H2O} = \text{Flux} / (C_a^{*} - C_a) = \text{Flux} / (C_a^{sat} - RH\ C_a^{sat}) = \text{Flux} / C_a^{sat}\ (1\text{-}RH) \qquad (3.3.1.1.)$$

where C_a (mol/cm^3) is the water vapor concentration in the ambient air, C_a^{sat} (mol/cm^3) is the saturation water vapor concentration across air-water interface.

3.3.2. Oxygen Transfer Experiments (k_w determination). These experiments were conducted in the field to measure the oxygen transfer rates from the ambient air to the WSS. Since oxygen is water side controlled, these experiments effectively measure k_w for

this sampler. These experiments were not done simultaneously with PCB sampling because of contamination problems and sampling duration differences.

In these experiments some water was deoxygenated by purging it with nitrogen gas. This water was put into the WSS and it was started. Then, its dissolved oxygen (DO) concentration and temperature were measured. Every one minute these measurements were repeated until the DO value approached saturation. The wind speed values were also recorded simultaneously 2.5 m above the WSS. These experiments were done nine times. Three of them was conducted by closing the cover of water surface (imposing an effective wind speed equal to zero). Results were evaluated mathematically in order to get a relationship between oxygen transfer rate and meteorological conditions (especially wind speed) as will be discussed in the results and discussion section.

3.4. Cleaning Procedures

3.4.1. Glassware. Glassware was washed several times in hot water and with Alconox, rinsed a number of times with hot tap water, and distilled water. Then, the glassware was rinsed a couple times with methanol (MeOH), hexane (HEX) and acetone (ACE). They were placed in an oven at ~110 °C for at least 4 hours. When the glassware was removed from the oven, their openings were immediately covered with aluminum foil and they were stored. Prior to use, the insides of the glassware was rinsed twice with dichloromethane (DCM). Glassware exposure to the laboratory air was kept to a minimum at all times.

3.4.2. Na_2SO_4, NaCl, Glass Wool, Glass Beads, Vials. Na_2SO_4, NaCl, glass wool, glass beads, and vials were placed in a beaker and baked overnight in a muffle furnace at 450 °C. Then, they were stoppered and allowed to cool to 110 °C in an oven. After that, they were cooled to room temperature and stored until use.

3.4.3. Glass Fiber Filter. Glass fiber filters (GFFs) were used in the water surface sampler (WSS) and high-volume air sampler. The filters were wrapped loosely and put in a furnace whose temperature was over 450 °C overnight to combust any organic present on the filter. Filters were wrapped with clean aluminum foil in order to be prevent contamination.

3.4.4. Polyurethane Foam (PUF) and XAD-2 Resin. Cleaning of the PUF and XAD-2 resin was achieved by extracting them with DI water followed by methanol, dicholoromethane, and an acetone and hexane mixture, respectively. Each extraction step lasted about 24 hours. After extraction, resin was put in an oven at about 70 °C for drying (Amberlite XAD-2 resin has good thermal stability and may be used up to 200 ^{0}C (SUPELCO)). The cleaned cartridge was individually wrapped in hexane-rinsed aluminum foil and stored in a glass jar closed with a Teflon-lined cap. Cleaned resin and PUFs were stored in a glass jar with a Teflon-lined cap.

3.5. PCB Analysis

PCB congeners were adsorbed onto a matrix from the ambient air and they were removed from the adsorbent matrix into a solvent which was analyzed. The procedure used in this

study was a combination of the methods developed at University of Minnesota and Atmospheric Environment Service in Canada. The following subsections will explain the analysis steps in detail. QA/QC details will be explained in the following chapter.

3.5.1. Sample Extraction. A Soxhlet with a body capacity large enough to accommodate the sample (sample level was lower than the top loop of the siphon tube) was used. All glassware was rinsed twice with DCM. Glass beads were added to round bottom flask and a piece of clean glass wool was used to plug the bottom of Soxhlet to prevent any sample matrix or debris from entering siphon tube. Then, the Soxhlet was connected to the flask and the entire sample was added to the Soxhlet. Surrogate standards (Congener #14, 65, 166) and two cycles of extraction solvent were then put above the sample. The apparatus was placed on a heating mantle and connected to the condenser. Extraction continued for 24 hours and each cycle time was about 45 to 60 minutes. After 24 hours of extraction, the heat was turned off and Soxhlet was allowed to cool to room temperature. The sample was transferred into another bottle, the flask and Soxhlet were rinsed with that particular solvent (mixture) and added to the sample. Then, the bottle was closed tightly and stored in the freezer. If another solvent extraction step was needed (i.e. water sample), the next solvent (i.e. DCM) was added and extracted again for 24 hours.

If the sample matrix was used for water sampling (i.e. XAD-2 resin and GFF from WSS), the first 24 hour extraction was with MeOH, followed by a 24 hour DCM extraction. The

air sampling glass cartridge, including resin and PUF, and strips were extracted with 1:4 DCM:PE (20% v/v DCM in PE) for 24 hours

3.5.2. Back-Extraction of Water Samples. Water samples had two extracts, MeOH and DCM. After MeOH extraction, the MeOH fraction with 2 MeOH rinses and 2 DCM rinses of the bottle were added to a 2 L separatory funnel with Teflon stopcock. An equivalent amount of distilled water saturated with clean NaCl (as volume of MeOH fraction) and another equivalent volume of distilled water were added to the separatory funnel. This mixture was extracted 3 times with 50 mL DCM.

For each extraction, 50 mL DCM was added and funnel was stoppered. It was shaken once and inverted while holding the glass stopper in place and fumes were vented into the hood by opening the stopcock. The separatory funnel was shaken again once and fumes again vented. Then, it was vigorously shaken a couple times and fumes vented. The vigorous shaking was repeated twice while venting the built-up pressure. The separatory funnel was placed into a ring clamp on a ring stand and stopper was removed. The top of the separatory funnel was covered with aluminum foil and the funnel sat until all the DCM settled (~ 15 minutes). DCM was drained into a flask containing DCM from the Soxhlet extraction of the same water sample. These steps were repeated twice. After the last DCM extraction, the separatory funnel sat until the top MeOH/water mixture and DCM phases separated clearly (~ 1 hour) and the top MeOH/water mixture was discarded into a hazardous waste container (chlorinated waste because it contains some DCM). This step recovers nonpolar organics from the MeOH fraction.

After the DCM extraction, the DCM fraction was added with the two DCM rinses into the separatory funnel in order to remove any residual MeOH from the DCM fraction. This mixture was extracted with 250 mL of DI water and DCM was drained back into the bottle. DI water was discarded into a hazardous waste container. Again DCM was added to a separatory funnel and extracted twice with 100 mL DI water. After draining the funnel after the last extraction and discarding the water layer, DCM was poured back into the separatory funnel. Glass wool was plugged into a separation column, then, ~25 g clean anhydrous Na_2SO_4 was added. DCM from separation funnel was drained through the bed of Na_2SO_4 and into a bottle to remove any residual water from the DCM extract.

3.5.3. Concentration of Sample Extract. The goal in this step was to reduce the solvent amount and change it to hexane by the application of roto-evaporation apparatus and nitrogen gas purge.

The extract was placed into the flask of the rotovapor apparatus. This flask was put in a water bath, heated to ~ 30 °C and attached to the rotation unit of the condenser. This condenser was connected to a vacuum pump. The flask was slowly spun by the rotation unit and the vacuum pump was turned on. The extract was evaporated to approximately 5 mLs. Solvent was exchanged into hexane by adding 15 mL of hexane and then the extract was again concentrated to 5 mL. Again 15 mL of hexane was added and it was blown down to 2 mL using a gentle stream of nitrogen (~100 - 150 mL/min.). This

remaining solvent was hexane which was ready for the cleanup procedure which is described next.

3.5.4. Sample Clean-Up and Fractionation

3.5.4.1. Silicic Acid (SA) Preparation. Silicic acid-3% water was prepared by oven drying silicic acid at ~ 100 °C for several hours in a flask loosely covered with aluminum foil to eliminate moisture. After cooling, 3 g was weighed and 100 μL DI water was added and mixture shaken for deactivation. The 3% water mixture of silicic acid remained at room temperature for at least 1 hour before use (deactivated SA must be used within 12 hours).

3.5.4.2. Alumina (Al_2O_3) Preparation. Alumina-6% water was prepared by oven drying the alumina at about 450 °C for several hours. After cooling to room temperature, 120 μL of DI water was added to 2 g of Al_2O_3 . After mixing, it remained at room temperature until use.

3.5.4.3. Clean-up Column Preparation. The clean-up column, 1.5 cm i.d. x ~30 cm length with a Teflon stopcock, was rinsed twice with DCM before use. A clean glass wool plug was put at the bottom of the column using a glass rod. Then, the column was packed by adding 3 g of deactivated SA, 2 g of Alumina, and 1 cm Na_2SO_4, respectively. Figure 3.3. illustrates a typical packed column.

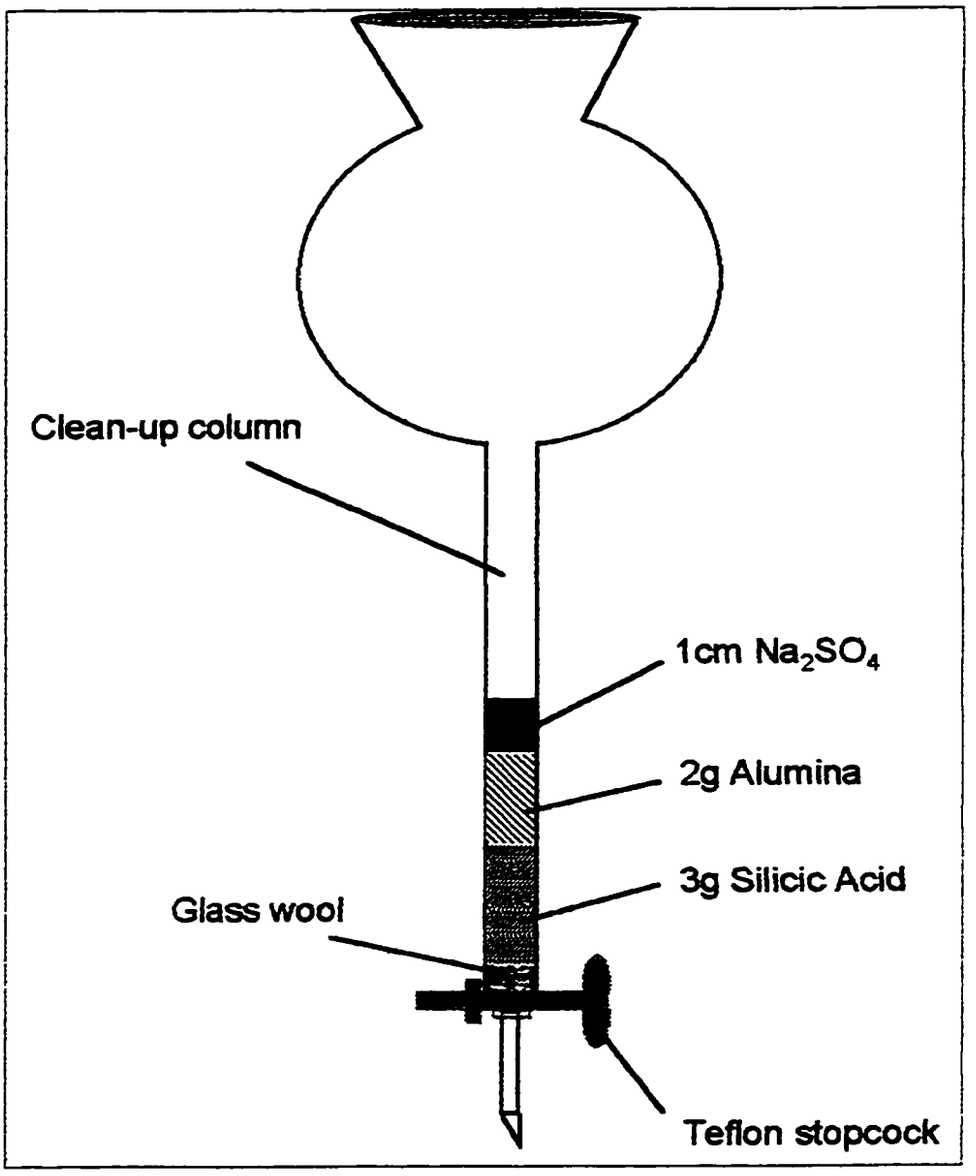

Figure 3.3 Typical Packed Clean-up Column

The packed column was then prewashed with 20 mL of DCM and then with 20 mL PE. Before the top of the column became dry, the sample was added.

In order to ensure that the sample stayed in the column and is not resuspended in the solvent, 2 mL of sample was poured into column and 1~2 mL of PE was added to push the sample through the column. After a few minutes the remaining sample was added. The fraction went through the column at a rate of about 2 drops per second. In order to collect the fraction containing the PCBs, 25 mL of PE was then added and collected.

3.5.5. Solvent Exchange and H_2SO_4 Cleaning. Before injecting the sample into the gas chromatograph (GC), the solvent had to be exchanged to hexane and cleaned with concentrated H_2SO_4.

3.5.5.1. Solvent Exchange. The fraction containing the PCBs was blown down by a gentle stream of high purity nitrogen gas to 5 mL. Fifteen mL of hexane were added and reduced again to 5 mL. This procedure was repeated one more time and finally the extract was reduced to 2 mL.

3.5.5.2. H_2SO_4 Cleaning. One mL of H_2SO_4 was added to the remaining ~ 2 mL extract. After mixing the liquid thoroughly, it was centrifuged for a few minutes. The top layer, the sample, was removed carefully with a pipette. Half a mL of hexane was added to the acid twice to rinse and remove the any residual PCBs and this hexane was added to the sample. It was very important not to collect any acid (the bottom layer which

was darker in color) because it could ruin the capillary column if injected to gas chromatograph (GC). This step removes all other soluble and probable problem causing organic compounds before GC analysis. After a final blow-down to 1 mL by N_2-gas the sample was ready for injection.

The final volume of deposition plate samples had grease in them. This grease could damage the GC capillary column and must be removed before injection. Therefore, the samples were put into the freezer where the grease precipitated and collected on the bottom of the vial. The top layer was quickly removed to another vial.

3.6. Gas Chromatography (GC)

Chromatography is one of the most extensively used methods to separate, isolate and identify related components in complex mixtures. A Hewlett Packard (HP) 5890 GC with electron capture detector (ECD) and HP 7673 auto sampler was used during this study.

Components are carried through the stationary phase by the flow of the mobile phase. The chromatographic separation is based upon the differences in the extent the PCBs partitioned between the mobile and stationary phases. A 25 m x 0.25 mm i.d. dimethyl polysiloxane capillary column with a 0.25 μm film thickness (DB-5) was used during the PCB analysis.

Analysis conditions were as follows: splitless injection of 1 μL sample under the 62-kPa hydrogen carrier gas flow; temperature program, injection at 80 °C, then temperature

increased 10 °C/min to 160 °C, then 2 °C/min to 250 °C followed by 5 °C/min to 280 °C/min and held for 2 minutes. Total run time was 61 minutes. The injector temperature was 240 °C and the ECD was held at 375 °C. Table 3.3. summarizes the operational parameters and conditions of the GC used in this study.

The ECD is placed at the end of the column to quantify the compounds that have been separated by passing through the column. The ECD detector identifies and measures PCB congeners in terms of their chlorine content. It is primarily used for the analysis of halogenated compounds due to its extreme sensitivity to these compounds (Rood, 1991). The ECD contains ^{63}Ni which is the source of β-particles which ionizes the carrier gas and forms electrons (Hinshaw and Ettre, 1994). When there is no organic matter, the chamber emission of electrons is constant and a standard current is formed (constant baseline). However, when organic matter is present a decrease in the current is noted due to the capture of electrons by the organic matter. The results are then described by a peak height or area representing the retention time of the mobile phase in the capillary column. The areas (in our case) of the peaks are compared with the ones generated by standards to determine concentration.

Table 3.3. Summary of the GC Conditions and Operational Parameters

No	Item	Condition / Parameter
1	GC Model	HP 5890
2	Auto Sampler Model	HP 7673A
3	Injector	Splitless
4	Injector Temperature	240 °C
5	GC Column Type	Capillary (DB-5)
6	GC Column Length/i.d./film thickness	25 m / 0.25 mm/ 0.25 μm
7	Detector Type	^{63}Ni ECD
8	Detector Temperature	375 °C
9	Carrier Gas	Hydrogen @ 2.36 mL/min
10	Make-up Gas	Argon/Methane (95/5 %) ~50 mL/min
11	Temperature Program	80 °C to 160 °C @ a rate of 10 °C/min, 160 °C to 250 °C @ a rate of 2 °C/min, 250 °C to 280 °C @ a rate of 5 °C/min, held @ 280 °C for 2 minutes.
12	Purge Time	0.80 min.
13	Sample Washed	Twice
14	Sample Pumps	6 times.
15	Solvent Washed	4 times
16	Injection Volume	1 μL (in general)

CHAPTER IV

QUALITY ASSURANCE/ QUALITY CONTROL (QA/QC)

This section presents the QA/QC plan used during this study. The details presented closely follow the USEPA's "Quality Assurance Plan Green Bay Mass Balance Study, 1988" (Swackhamer, 1988). Results reported as "Σ-PCBs " represents the summed contribution of 43 chromatographic PCB congener peaks which represent 50 individual or coeluting congeners after blank correction.

4.1. Sample Collection Procedures

Sample collection techniques differed based on the sample matrix (i.e. WSS and plates (greased strips), GFF, PUF and resin). However, the chosen procedure for each matrix was strictly followed during each sampling period. Sampling times, volumes, flow rates were controlled to collect sufficient quantities of PCBs on each matrix to avoid detection limit problems.

4.2. Sample Analytical Procedures

The methods used in the sample extraction and processing steps were developed based on the procedures of Dr. Tom Franz, Tom Harner and the available literature (Cotham and Bidleman, 1995; Falconer et al., 1995; Hornbuckle et al., 1994; Franz, 1994; Swackhamer, 1988; Alford-Stevens, 1986; Mullin et al., 1984). One of the goals of this project was to not split the sample for PCBs and PAHs analysis in order to keep concentrations as high as possible.

The chosen species and standard concentrations were also used by many other researchers (Franz, 1994; Hornbuckle et al., 1994; Swackhamer, 1988).

4.3. Analytical Standards

4.3.1. Calibration Standards. Calibration standard solution was prepared by Ultra Scientific. This solution contained all 50 targeted PCB congeners at known concentrations (either 20 or 30 ng/mL). PCB congeners and their concentrations in the calibration standard were chosen based on their presence in the ambient air. The standard was used to prepare calibration curves with 1/1, 1/2, and 1/40 dilution rates. The r^2 values of each congener in the calibration curve was above 99%. Table 4.1. shows the PCB congeners and their elution order numbers. In figures presented in this thesis the elution order numbers are called "congener order".

4.3.2. Surrogate Standards. Surrogate standards were used to monitor the analytical recoveries of the PCB congeners. The surrogate standards used were PCB #14 (3,5-dichlorobiphenyl), PCB #65 (2,3,5,6-tetrachlorobipheyl), and PCB #166 (2,3,4,4',5,6-hexachlorobiphenyl). As indicated in the QAPGBMBS (1988), the chosen concentrations were 22, 5, and 5 ng/mL for PCB 14, PCB 65, and PCB 166, respectively. This standard was added to each sample and blank prior to extraction.

It is important to note that both surrogate and internal standards are similar to the analyte of interest (PCB congeners) but they are not present in the environment.

Table 4.1. Congener Orders and Their Corresponding IUPAC PCB Numbers

Cong. Order	IUPAC No	Cong.Order	IUPAC No	Cong. Order	IUPAC No
1	8	16	60	30	126
2	18	17	101	31	187
3	15	18	99	32	128
4	16	19	97	33	185
5	31	20	81/87	34	171
6	28	21	77/110	35	156
7	33	22	82	36	180
8	22	23	149/123	37	200
9	52	24	118	38	169
10	49	25	114	39	198
11	47/48	26	105	40	207
12	44	27	141	41	205
13	42/37	28	137	42	206
14	74	29	138/163	43	209
15	66/95				

4.3.3. Internal Standards. The internal standard contained PCB congeners # 30 (2,4,6-trichlorobiphenyl) and #204 (2,2',3,4,4',5,6,6'-octachlorobipheyl). The internal standard was used for the volume correction of the sample. Fourteen μL containing PCB

#30 and PCB #204 at concentrations of 570 and 430 ng/mL, respectively were added to each sample. Therefore, the concentration in a 1 mL sample was 8 and 6 ng/mL for PCB congeners of # 30 and 204, respectively.

4.3.4. Performance Standards. A performance standard was the combination of calibration and surrogate standards. Relative proportions and concentrations of the congeners were observed every day before and during the sample runs. Instrument conditions (performance, reproducibility, sensitivity) were corrected daily as necessary.

In all cases the surrogate recovery efficiencies were in the acceptable range (between 50 and 120 %) as shown in Table 4.2. and Table 4.3. The values are similar to those published elsewhere (Franz, 1994, Swackhamer, 1988).

Accuracy is used to determine if a measured or computed value represents the true value of the analyte. The recovery of surrogate standards from a sample represents the extraction recovery of that sample. In this study, accuracy was assessed by evaluation of recoveries using surrogate spikes in each sample and matrix. It was suggested in QAPGBMBS (1988) that for a given set, the surrogate spike recoveries must be $\geq$50% and $\leq$120% in order to achieve acceptable accuracy. In all cases recoveries were in this range (Table 4.2 and 4.3).

Table 4.2. Summary of PCB Amounts in the Samples

	Amount (ng)	Surrogate Recovery
Samples (before blank correction)	WSS_{1F} (n=12) Total : 347.58 ± 526.62 ng	WSS_{1F} Recovery: 0.80 ± 0.21
	WSS_{1R} (n=11) Total : 755.13 ± 666.83 ng	WSS_{1R} Recovery: 0.89 ± 0.21
	Plate (n=12) Total : 119.74 ± 48.26 ng	Plate Recovery: 0.76 ± 0.06
	Air Filter (n=39) Total : 32.59 ± 37.64 ng	Air Filter Recovery: 0.75 ± 0.18
	Air PUF + Resin (n=39) Total : 246.24 ± 324.02 ng	Air PUF + Resin Recovery: 0.70 ± 0.16

where,

WSS_{1F} : Water surface sampler (1) filter,

WSS_{1R} : Water surface sampler (1) XAD-2 resin,

Air Filter : High-volume sampler filter,

Air PUF + Resin : High-volume sampler PUF and XAD-2 resin,

n : Number of sample or blank.

4.4. Identification and Quantitation

PCB congeners were identified by their retention times relative to the internal standard retention time. Peaks must have been within ±0.05 minutes of the retention time in the calibration standard in order to be considered a correct peak identification. Moreover, if any of the chromatographic peaks were contaminated, absent, out of calibration range or bigger than 25% of the total PCBs, they were not included in the sample results. When the detected amount was greater than the calibration range, the sample was diluted and rerun.

A HP Chemstation program was used to analyze the data. All baselines were reset by hand so that peak areas were accurately determined. The HP Chemstation was programmed to identify the congeners based on their retention time and correct them based on the internal standard (PCB # 30). However, the surrogate recovery correction could not be done automatically; thus, quantification was externally done using a spreadsheet (Excel for Windows).

It was experimentally determined that areas greater than approximately 100 were quantifiable. If peak areas were smaller than this value, the concentration was recorded as less than detection limit.

4.5. Limit of Detection (LOD)

The LOD was determined from the mean noise, in mass units, plus 3 standard deviations (3σ). The most dilute standard was injected 10 times and based on these results, mean noise and σ were determined.

Most congeners were observed in the samples. However, after blank correction, masses sometimes became zero. As will be discussed in the results section when a concentration exceeded the detection limit and but the flux was less than the detection limit or vise versa the 2/3 of the LOD was used for the missing value.

The lowest area that could be integrated was about 100. This value was determined by injecting the most diluted standard in which the PCB congener concentrations ranged between 0.5 to 0.75 ng/mL. However, GC was able to detect areas of 10 ~ 15 units without interfering with the background noise (> 5x noise). Therefore, the reported PCB congener values in this thesis were at least 8 ~ 10 times bigger than the minimum GC detection limit.

4.6. Blanks and Background Values

Field blanks were taken to determine the background contamination which is caused from the methods used. All blank materials were cleaned and prepared with the same procedures as the real samples. Field blanks were transported to the field in order to expose them to the same environment as the actual samples were exposed to before and after the sampling. After these blank samples were brought to the laboratory, they were

spiked with the surrogate standards and the other necessary steps for PCB analysis were performed. These blank values (Table 4.3) were subtracted from the corresponding real values. These results were used to calculate either concentrations or fluxes by considering air volumes or area and sampling times.

Table 4.3. Summary of PCB Amounts in the Blanks

	Amount (ng)	Surrogate Recovery
Matrix Blanks (This study)	WSS_{1F} (n=5) Total : 44.56 ± 22.16 ng	WSS_{1F} Recovery: 0.85 ± 0.06
	WSS_{1R} (n=5) Total : 68.06 ± 27.38 ng	WSS_{1R} Recovery: 0.85 ± 0.02
	Plate (n=3) Total : 32.95 ± 9.09 ng	Plate Recovery: 0.81 ± 0.02
	Air Filter (n=8) Total : 11.91 ± 9.30 ng	Air Filter Recovery: 0.77 ± 0.16
	Air PUF+Resin (n=5) Total : 16.65 ± 11.44 ng	Air PUF + Resin Recovery: 0.88 ± 0.08
Matrix Blanks (Franz, 1994)	Snow Filter (n=6) Total : 5.0 ± 2.8 ng	
	Air Filter (n=4) Total : 2.8 ± 1.3 ng	Air Filter (n=1) Recovery: 1.15
	Resin (n=5) Total : 8.0 ± 7.0 ng	Resin (n=2) Recovery: 1.02
	Air PUF (n=5) Total : 17 ± 13 ng	Air PUF Recovery: 1.02 ± 0.13

Particle PCB fluxes were measured with plates (greased strips) and the filter in the water surface sampler 1 (WSS_{1F}). Since PCBs are hydrophobic, they can have tendency to partition with the plates (greased strips). The grease (Apezoin-L) might have background PCBs in it. Therefore, the grease used for the strips was extracted and analyzed directly. The measured values (except one contaminated sample) were less than the plate field blanks (Myrczik, 1997). On the average, they were 57 to 85% of the field blank values. Even though there is small amount of PCB contamination (including preparation of the sample) in the grease, it is less than the field blanks (which were subtracted from the samples). Therefore, this background PCB value would not effect the reported values.

XAD-2 resin column was applied to sorb all the PCBs captured by WSS. Based on its properties and theoretical data, the breakthrough value was determined and then amount of XAD-2 resin was determined. In order to check the breakthrough, a second XAD-2 resin column was placed after the first (original) XAD-2 resin column. The average PCB amount detected from second XAD-2 column was about 31.6 ng which was less than the field blank value of the XAD-2 column (WSS_{1R}), 68.06 ng. Therefore, the assumption of no breakthrough from the column was a satisfactory assumption.

In all cases surrogate standard recoveries, which represent the accuracy, were in the acceptable range (between 50 and 120 % which was suggested by SWACKHAMER, 1988). Table 4.3. summarizes the results of the recoveries from matrix blanks and it also compares these results with Franz's results (1994). The results agree well although

Franz's standard deviations were slightly higher than this study's. The total PUF and resin blank value was 16.65 ng for this case. Franz has reported them separately and the total of them was 25 ng which was higher than our results. The mass observed from the blanks for filter was smaller for Franz's study. However, since the concentrations in our case were higher than theirs for the samples, the blanks did not cause any problem. Franz's results were chosen for the comparison because their research group at University of Minnesota has been performing PCB analysis for more than 15 years.

One reason for the high standard deviations seen in this study is the variety of wind directions seen during the sampling periods. If the wind blows from Gary, IN, which is a highly polluted area, the concentration of Σ-PCBs will be much bigger than when wind comes from the Lake Michigan and when wind comes from either downtown Chicago or the west or suburbs. Some literature values along with their lowest and highest values are presented in the Table 4.4. and based on these values the average and standard deviations were calculated. As this table shows the standard deviation in this study is smaller than the others.

4.7. Outliers

Traditionally, outliers for observations are determined by considering residuals (Kleinbaum et al., 1988). An outlier is any unusual observation appearing in the data. The presence of an outlier (extreme value) may affect the fitting model.

Table 4.4. Some Selected PCB Concentrations in Air and Their Fluctuation Range

Min Conc., ng/m^3	Max Conc., ng/m^3	Avg. ± SD ng/m^3	SD (%)	Reference
0.5	30	15.25 ± 20.86	136.8	Lee, 1991
0.3	9.9	5.1 ± 6.79	133.1	Cotham et al., 1992
0.09	14.2	7.15 ± 9.98	139.7	Simcik et al., 1997
<0.07	0.38	0.23 ± 0.22	97.4	Bidleman et al., 1987
0.65	2.53	1.59 ± 1.33	83.6	Panshin and Hites, 1994
1.04	3.00	2.09 ± 1.39	66.5	This study

The jackknife outlier test was applied to the data set in order to determine which values were outliers. The quantity of jackknife residual values and other used outlier tests used were calculated as follows (for more information please refer to Ch 12 of Kleinbaum et al., 1988):

$$r_{(-i)} = r_i \{[(n-k-1)-1]/[n-k-1)-r_i^2]\}^{1/2} = e_i / [S_{(-i)} (1-h_i)^{1/2}] \quad \text{(Jackknife)}$$

$$r_i = e_i / [S (1-h_i)^{1/2}] = z_i / (1-h_i)^{1/2} \quad \text{(Studentized)}$$

$$S^2 = [1/(n-k-1)] \Sigma e_i$$

$$e_i = y_i - y_{i,\,predicted}$$

$$Y_{i,\,predicted} = \beta_o + \beta_1 x + E_o$$

$$\beta_1 = [\Sigma x_i y_i - \Sigma x_i y_i /n] / [\Sigma x_i^2 - (\Sigma x_i)^2/n]$$

$\beta_o = y_{avg} - \beta_1 x_{avg}$

$h_i = 1/n + [(x-x_{avg.})^2 / (n-1)S^2_x]$ (Leverage)

$S_x = [1/ (n-1)]\Sigma (x-x_{avg})^2$

$z_i = e_i / S$ (Standardized)

$d_i = [(1/(k+1))*r_i^2 * (h_i/(1-h_i))] = \{e_i^2 h_i / [(k+1)S^2(1-h_i^2)]\}$ (Cook's Distance).

where ;

x_i : Independent variable,

y_i : Dependent variable,

n : Number of observations,

S_x^2 : Variance of the x values,

S^2 : Variance of the values,

$y_{i,\ predicted}$: Predicted y (dependent) value of the i^{th} sample,

β_o : Intercept of the $y_{i,\ predicted}$ equation,

β_1 : Slope of the $y_{i,\ predicted}$ equation,

E_o : Error (uncertainty).

Table 4.5. summarizes the above tests results for one sample (trichlorobiphenyls in plate samples).

Table 4.5. Comparison of Outlier Results (Plate sample for trichlorobiphenyls)

Conc. (ng/m^3)	Flux (ng/m^2-d)	Studentized r_i	Jackknife $r_{(-i)}$	Standardized z_i	Cook's distance d_i	Leverage h_i
0.001128	3.114078	No	No	No	No	No
0.00047	0.164583	No	No	No	No	No
0.000374	7.116865	No	No	No	No	No
0.012467	14.73365	No	No	No	Yes	Yes
0.005818	10.20579	No	No	No	No	No
0.000547	0.990589	No	No	No	No	No
0.003966	9.737447	No	No	No	No	No
0.007497	0.76458	No	No	No	No	No
0.002455	23.09458	Yes	Yes	Yes	Yes	Yes
0.003842	10.31156	No	No	No	No	No
0.002021	21.0487	Yes	Yes	Yes	No	No
0.000764	5.20049	No	No	No	No	No

If the regression assumptions are satisfied and approximately the same number of observations which were made at all predictor values, then the pattern in Standardized, Studentized and Jackknife residuals look very similar (Kleinbaum et al., 1988). Table 4.5 shows this relationship (these three test found the same outliers). Interestingly the Cook's Distance and Leverage test differed slightly from the other three tests. Since there is no

universally accepted "best" test to determine outliers the Jackknife test was used in this study.

Jackknife residuals, as seen in the above formulae, are closely related to standardized residuals. The Jackknife test may prevent an outlier from masking its own effect by considering a jackknifed residual variance estimate ($S_{(-i)}$) in which its contribution to S^2 is ignored.

The regression equation assumes that if the errors are independent and their variance is constant, their distribution will be normal. The approach used to the validity of the assumptions makes use of residuals (Box et al., 1978). A residual is the difference between an observed value of Y and the value of Y predicted from the regression equation. Therefore, a residual can be considered to be an observed error if the equation fits the data (Box et al., 1978; Kleinbaum et al., 1988).

A graphical technique may be used to examine the residuals. In this study, Jackknife residual values were plotted against the values of Y predicted. If there is a pattern in the plot, the regression equation should be checked.

Figure 4.1 shows no pattern in which the points form a horizontal band about the zero residual axis (Kleinbaum et al., 1988). This indicates that the variance of the errors is constant for all values. Therefore, it can be concluded the basic assumptions are true and this test is appropriate.

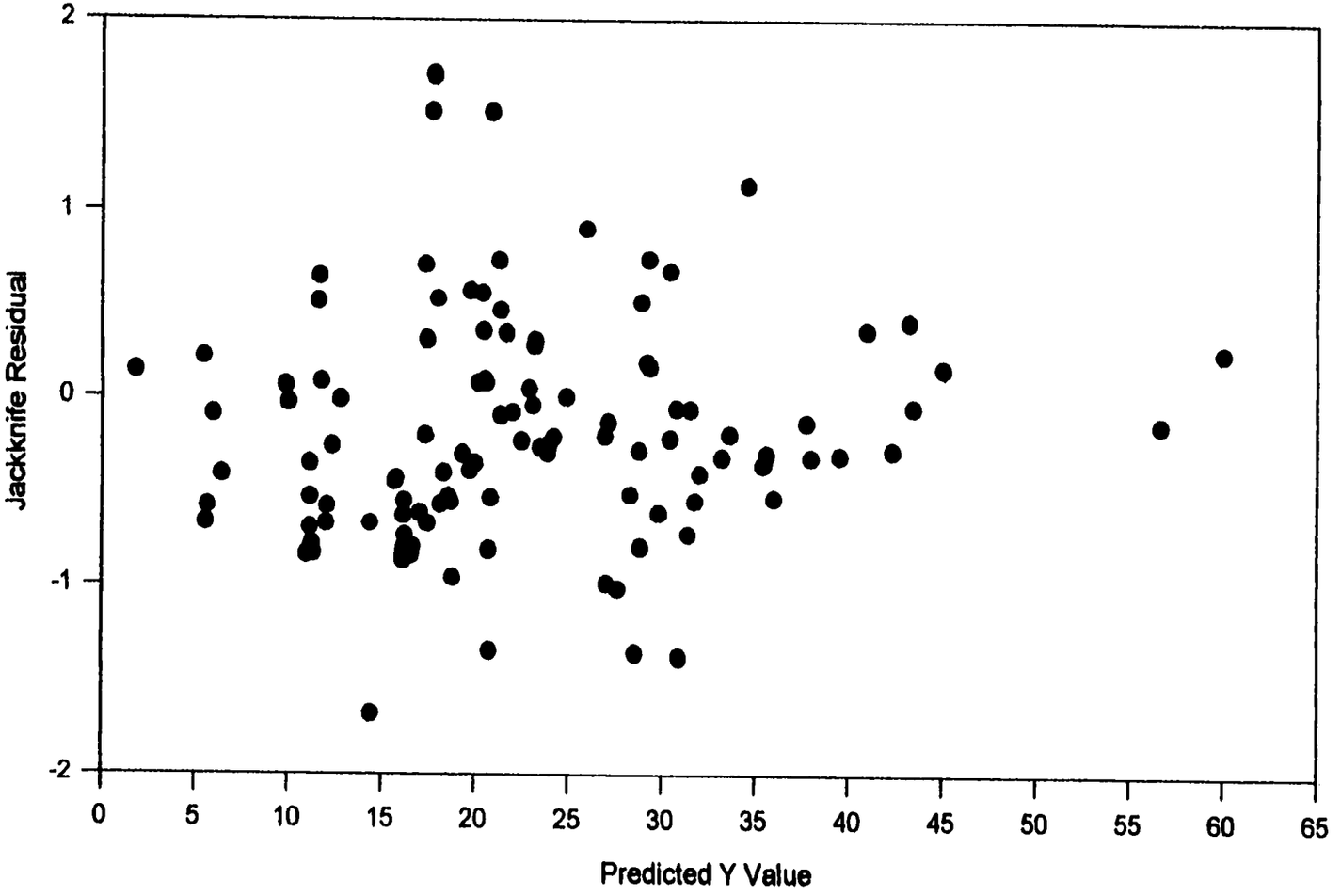

Figure 4.1. Residual Plot as a Function of Predicted Y Values

CHAPTER V

RESULTS AND DISCUSSION

This thesis is focused on the measurement of PCBs in the ambient air as well as PCBs deposited to two surrogate surfaces (i.e. greased strips (plates) and a water surface sampler (WSS)). The aim is to understand the specific collection surfaces characteristics and develop analytical methods for PCBs collected on these surfaces. The dry deposition velocities of particulate associated PCBs to the WSS and plates and mass transfer coefficients of gas phase PCBs at the air-water interface will be presented along with the flux and concentration values in this chapter.

5.1. Ambient Air PCB Concentration

Combined eleven ambient air samples were collected from June 1995 to October 1995 in Chicago, IL. Each one of the eleven samples consisted of 2 - 4 individual airborne samples (high volume samples) to match the flux sampling period. A modified high-volume sampler was employed to collect particulate and gas phase ambient PCBs in order to determine their concentrations and gas/particle phase distributions. The method used by this sampler was to pull air through a glass-fiber filter (GFF) followed by a cartridge containing XAD-2 resin sandwiched between two PUF pieces. The amount of PCBs collected on the GFF and PUF/XAD-2 cartridge are considered the particulate and vapor fraction, respectively. It is possible that a small amount of PCBs sorbed on the particulates may volatilize during sampling or some vapor phase PCBs may be sorbed by filter (Falconer et al., 1995; Hart and Pankow, 1994; Pankow and Bidleman, 1991). The

average air volume sampled with the high-volume sampler was about 150 m^3 (at a rate of ~0.1 m^3/minute) per sample.

In this thesis, Σ-PCBs (total PCBs) refer to the summed contribution of 43 chromatographic PCB congener peaks which represent 50 individual or coeluting congeners. Moreover, Σ-PCBs represent the combination of vapor and particulate phase blank corrected concentrations. The mean concentrations for Σ-PCBs detected in this work ranged between 1.04 ng/m^3 and 3.00 ng/m^3 (Table 5.1.) The average Σ-PCB concentration was 1.91 ng/m^3 and this concentration is comparable to those reported previously (Table 2.5. and 2.6.). The mean Σ-PCB concentration agreed well with the latest measurements from Chicago, IL by Cotham et al. (1995) and Simcik et al. (1997). However, this concentration is higher than those measured in the non-urban areas (Basu et al., 1993; Sweet and Basu, 1993). The vapor pressure of the lower molecular weight (MW) PCB congeners are in the μg/m^3 to mg/m^3 range (Mackay et al., 1992; TPFP, 1993). However, atmospheric concentrations (pg /m^3 or ng/m^3) are much smaller than these theoretically suggested levels.

Chicago air contained both low MW and high MW congeners but PCBs with lower and middle molecular weights predominated (Figure 5.1). The congeners patterns were not similar to the distribution found in commercial PCB mixtures (Aroclors). This was expected because PCB congeners have a wide range of physical and chemical

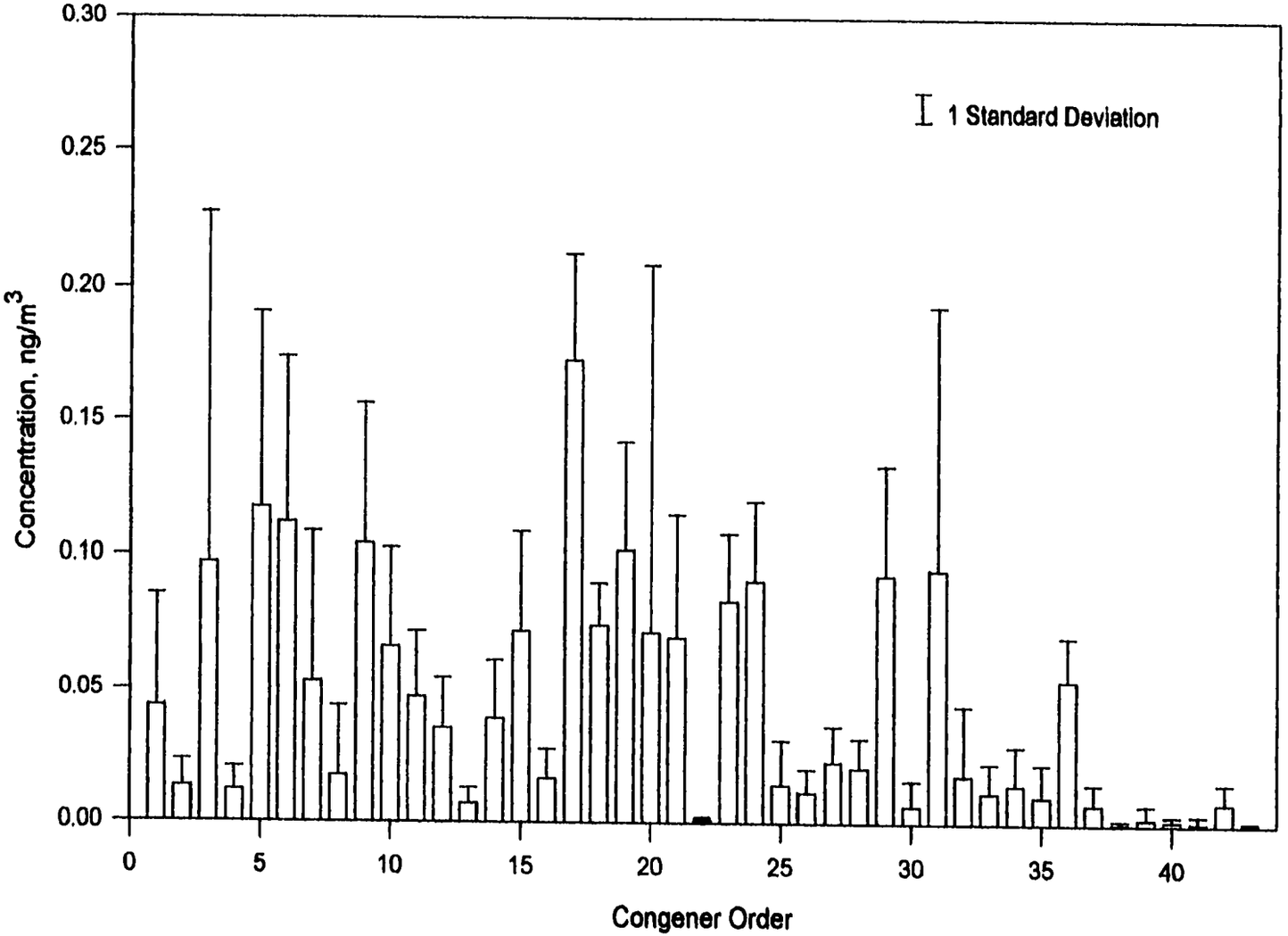

Figure 5.1. Average Congener Distribution in the Total PCB Concentration

characteristics. Therefore, congeners act differently under different atmospheric conditions and have different characteristics. Therefore, congeners act differently under different atmospheric conditions and have different transport and partitioning properties. Thus, the atmospheric fate and residence times of the congeners and as a result their concentrations in the ambient air are not the same.

Table 5.1. Ambient Air PCB Concentrations (ng/m^3) in Chicago, IL

Sample No	Sampling Date (1995)	Particle PCB Concentration	Vapor PCB Concentration	Total PCB Concentration
1	6/29-7/6	0.15	2.28	2.43
2	7/8-7/13	0.03	1.08	1.11
3	7/14-7/21	0.03	1.22	1.24
4	7/25-7/30	0.07	1.86	1.93
5	8/5-8/12	0.11	0.93	1.04
6	8/15-8/23	0.17	1.15	1.32
7	8/24-8/31	0.03	1.88	1.91
8	9/6-9/14	0.03	1.57	1.60
9	9/15-9/25	0.07	1.33	1.40
10	10/4-10/13	0.09	2.92	3.00
11	10/15-10/23	0.04	1.34	1.38

The average individual congener concentrations ranged between 0.3 pg/m^3 and 173 pg/m^3 (Figure 5.1). PCB 169 has the lowest and PCB 101 has the highest average concentration of the congeners measured. While PCB 101 was the most abundant congener, it accounts for only 9 % of the Σ-PCB concentration. It is not like polycyclic hydrocarbons (PAHs) whose most abundant compound, phenanthrene, can be more than 30% of Σ-PAHs (Cotham and Bidleman, 1995; Odabasi et al., 1997). The concentration of PAH samples

taken simultaneously with PCB samples using the same equipment ranged about 150 to 850 ng/m^3 with an average of 420 ng/m^3.

PCBs are semivolatile organic compounds; therefore, they evaporate into the atmosphere from soil, water or other sorbents when conditions are suitable. In general, when the temperature increases, the amount of PCBs present in the ambient air increases (Simcik et al., 1997; Kaupp et al., 1996; Sweet and Basu, 1993; Manchester-Neesvig and Andren, 1989). Figure 5.2. illustrates how the Σ-PCB concentration and ambient air temperature change with time (sample number) during this study. Even though samples were taken over a 5 month period, no temporal trend was observed between Σ-PCBs and temperature. The likely reason for this lack of correlation is both the long sampling time which masked the diurnal temperature variation and changes in the wind directions. For each sample period winds were observed from all directions (i.e. Lake Michigan; Gary, IN; Downtown Chicago; West Suburbs). Since the PCB concentration in the air is different for each direction, large fluctuations were not observed. Other researchers have indicated that the seasonal variations in PCB concentrations were also not observed in their studies even though their sampling times were less than those in this study (Hornbuckle et al., 1993 and 1994; Sugita et al., 1994, Ngabe, 1992).

In this study, atmospheric PCBs were dominated by tri-, tetra-, and pentachlorinated homologs (Figure 5.3). This result agrees well with the previously reported literature; however, other studies suggested that the dominant homolog pattern should also include

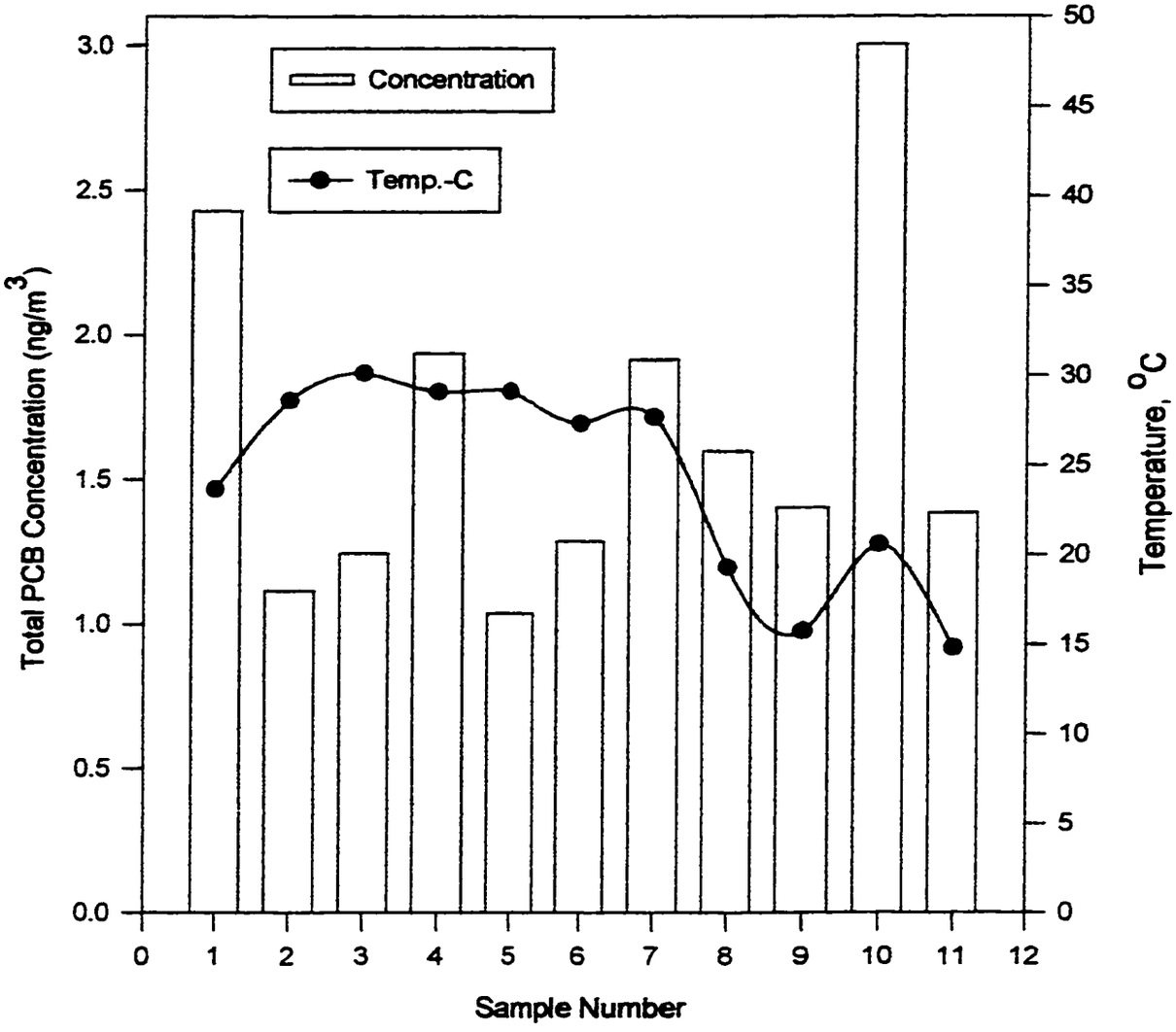

Figure 5.2. Total PCB Concentration of Each Sample

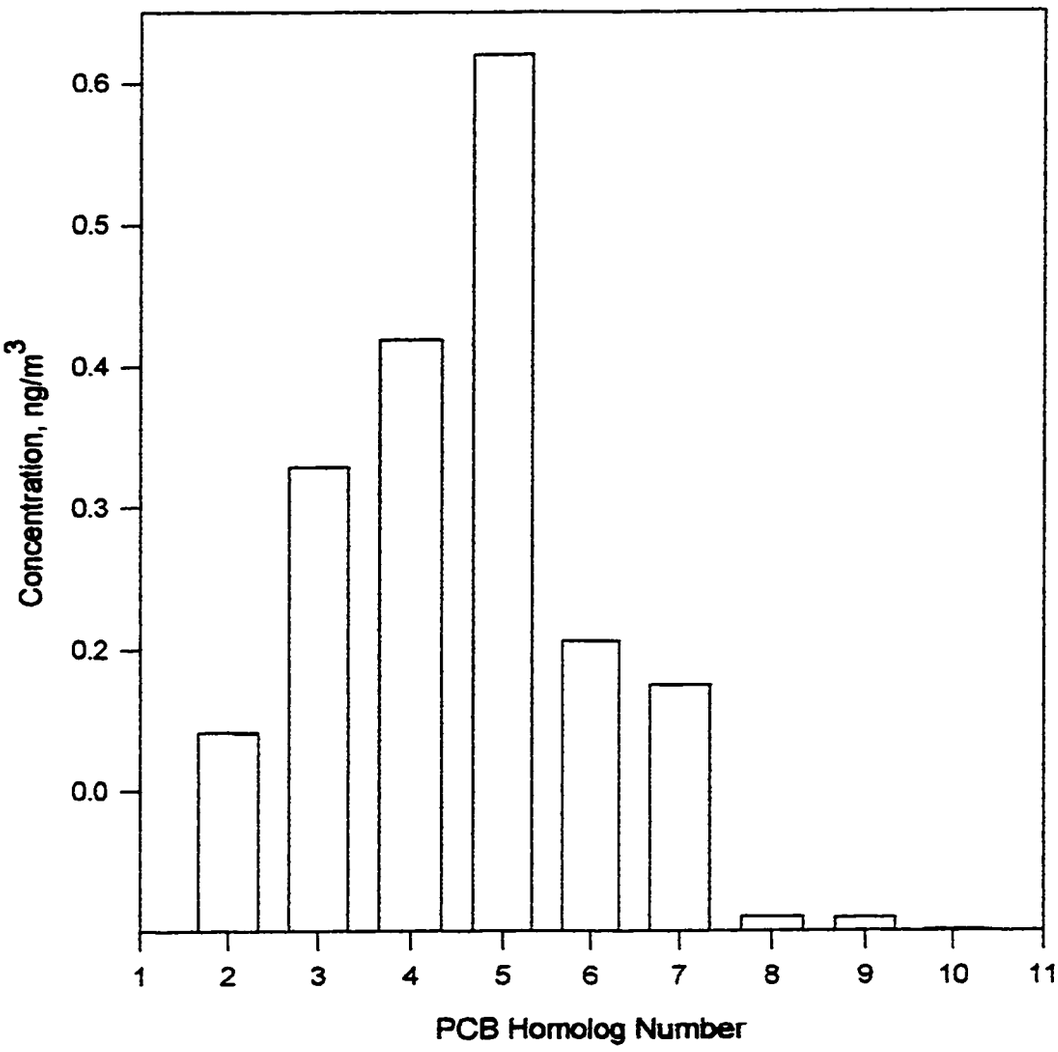

Figure 5.3. Overall Average Concentration of Each PCB Homolog

the dichlorinated homolog (Murphy and Rzeszutko, 1977; Manchester-Neesvig and Andren, 1989; Hermanson and Hites, 1989; Hornbuckle et al., 1993; Franz, 1994). One reason for having a smaller dichlorinated homolog concentration is only two congeners in dichlorinated homolog were analyzed for in this study.

5.2. Gas/Particle Partitioning of PCBs

PCBs in the air are mainly in the vapor phase (Murphy and Rzeszutko, 1977; Hermanson and Hites, 1989; Sweet and Basu, 1993; Simcik et al., 1997). However, when PCBs enter the atmosphere from incinerators, degassing from landfills containing PCB contaminated materials or soil and air/water exchange, they are distributed between the vapor and particulate phase based on their amount, vapor pressure, ambient air temperature, and amount and characteristics of particulate matter present in the air (Cotham and Bidleman, 1992; Falconer et al., 1995; Hoff et al., 1996). In this study, the overall average concentrations of particulate and vapor phase PCBs were approximately 0.09 and 1.82 ng/m^3, respectively. The average vapor phase concentration is 95% of the Σ-PCB concentration. This finding agrees well with the previously reported values (57 - 100% for gas phase). Figure 5.4 shows the particulate and vapor phase PCB concentration distribution over the sampling period.

The distribution in the vapor and particulate phase was calculated and results are presented in Figure 5.5 which indicates that the less chlorinated PCB congeners (di-, tri-, tetrachlorinated homologs) are mostly in the vapor phase. This finding is reasonable

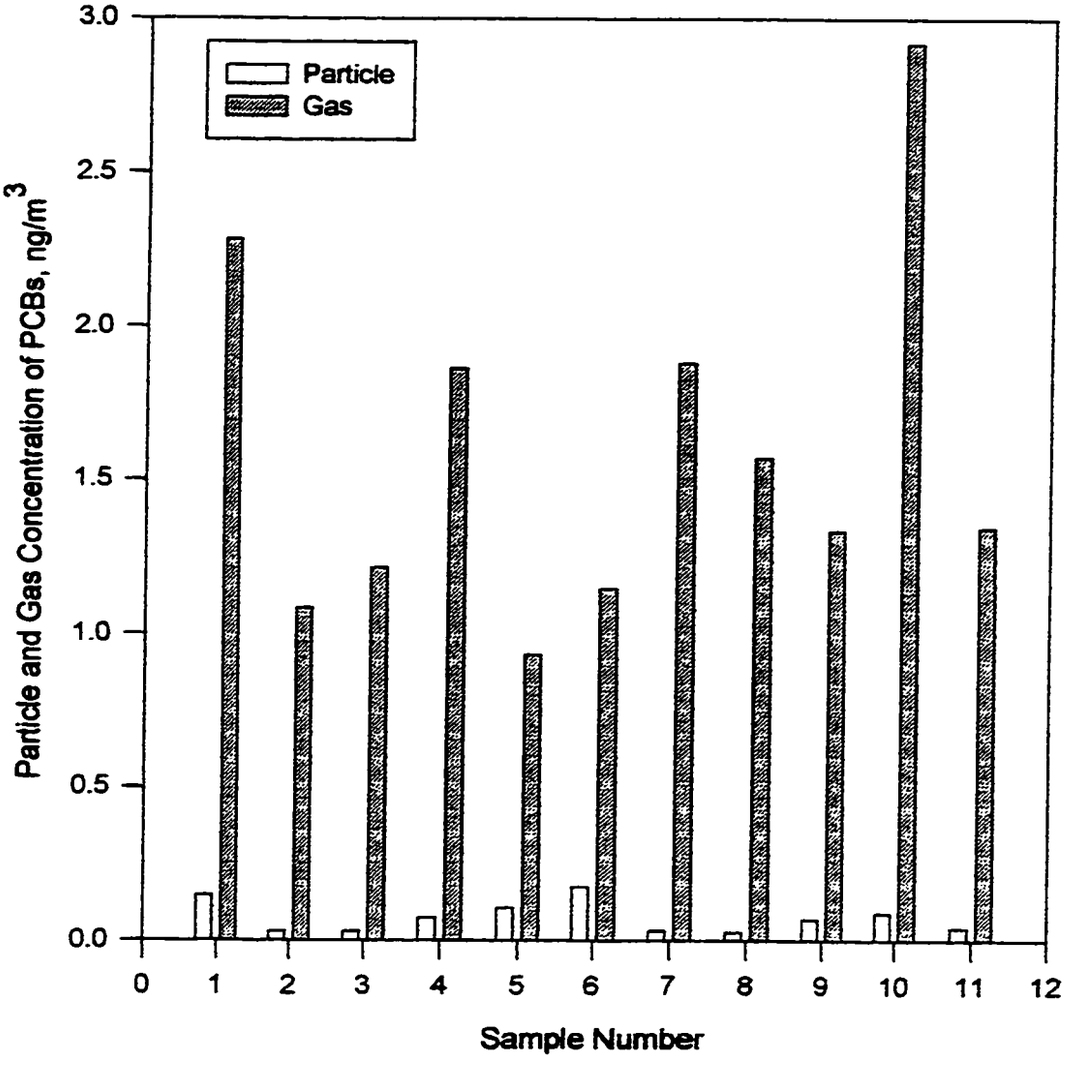

Figure 5.4. Particle and Gas Phase Concentrations of Each Sample

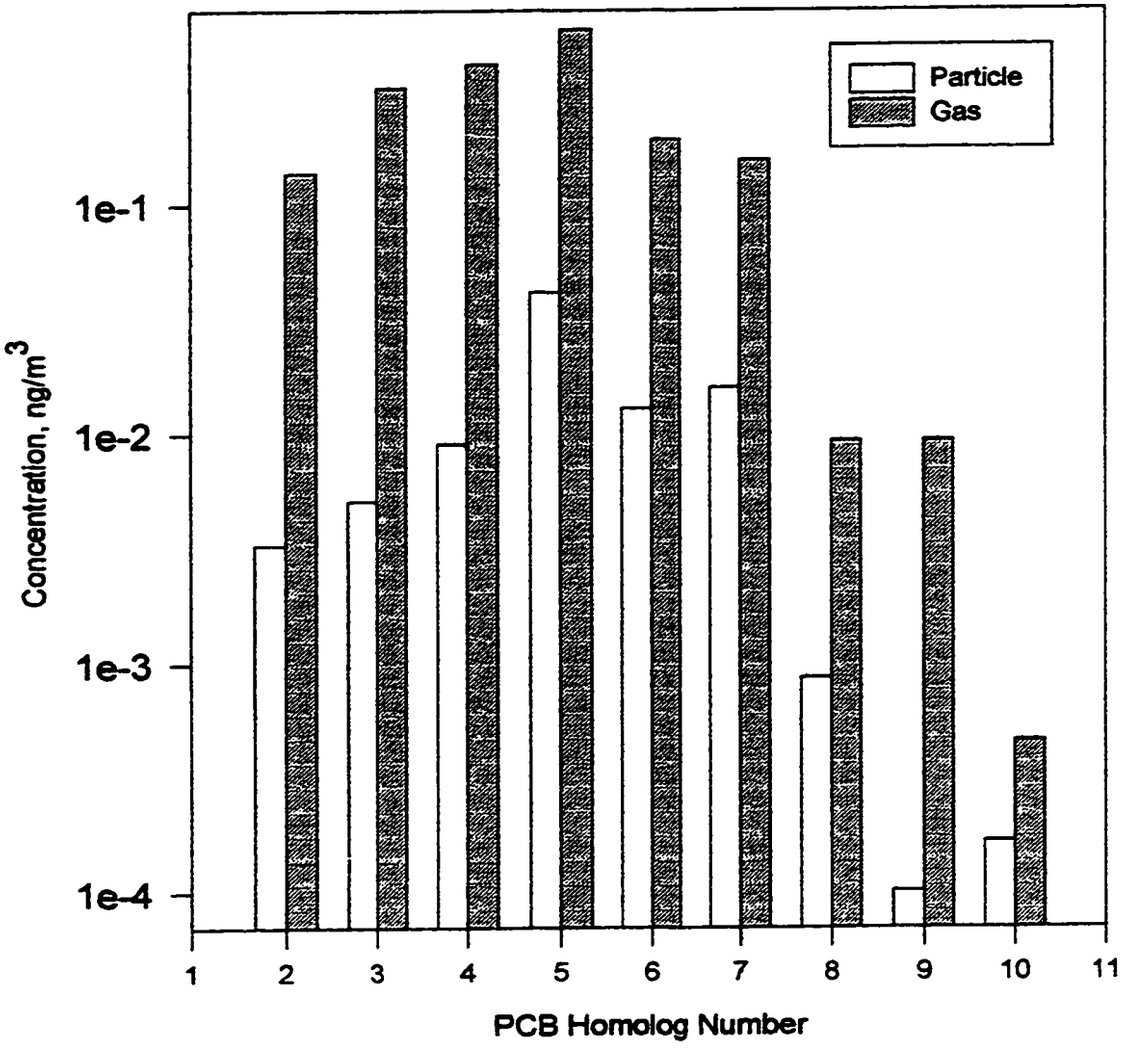

Figure 5.5. Overall Average PCB Homolog Concentrations

because lower MW PCB congeners tend to stay in the vapor phase due to their high vapor pressures.

As the number of chlorine atoms on a congener increases, its vapor pressure decreases and its tendency to partition with the particulate matter increases. In this study, the gas phase ranged between 56% and 100% for individual PCB congeners. The particulate phase percentage generally increased with increasing PCB molecular weight (Figure 5.6.) which is similar to the theoretical expectation, yet sampling artifacts, ambient air concentrations and atmospheric conditions might effect this relationship.

The distribution between the gas and particulate phase can be represented by K_p ($[C_p/TSP]/C_g$) which refers to gas/particle partition coefficient and were C_p is the contaminant concentration associated with aerosols (ng/ m^3), C_g is the gas-phase contaminant concentration (ng/m^3) and TSP is the total suspended particle concentration ($\mu g/m^3$) (Pankow, 1994; Pankow et al., 1993; Pankow and Bidleman, 1991; Cotham and Bidleman, 1995).

K_p is related to the subcooled liquid phase vapor pressures (p_L°) of the PCBs at the sampling ambient air temperature by

$$\log K_p = \log [(C_p/TSP)/C_g] = b_r - m_r \log p_L^\circ \quad \text{(Falconer et al., 1995)} \quad (5.1)$$

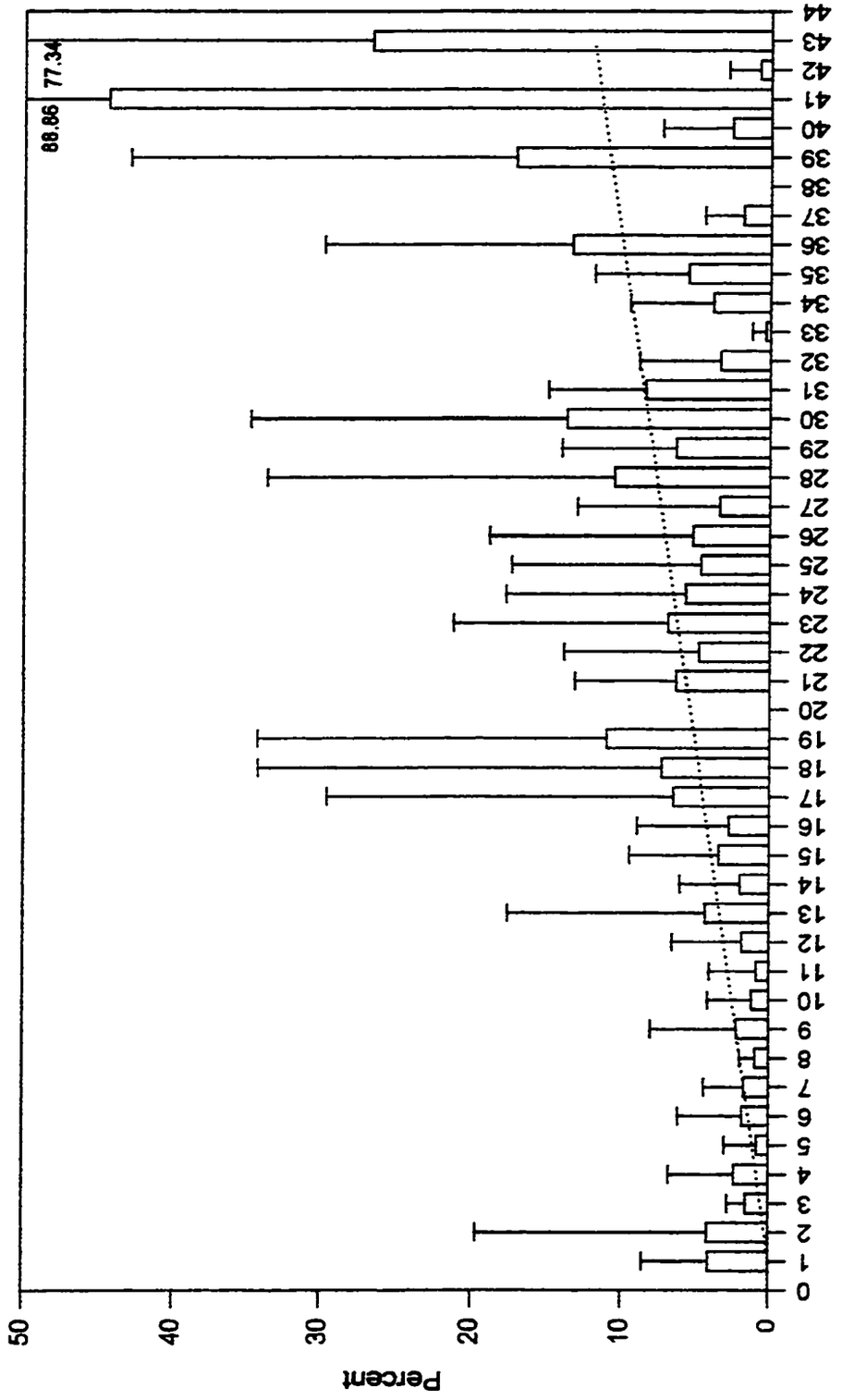

Figure 5.6. Average Particle Percentages of Each Congener

where m_r and b_r are the slope and intercept of the linear regression of log K_p and log p_L° and p_L° is the subcooled liquid vapor pressure. The p_L° value was calculated by

$$p_L^\circ = m_L/T + b_L \qquad (5.2)$$

where m_L and b_L are the slope and intercept, respectively and T is temperature with the unit of °K. Falconer and Bidleman (1995) summarized m_L and b_L values for 180 PCB congeners.

Typical plots of log K_p versus log p°_L obtained from this study are shown for Σ-PCBs for different sampling days in Figure 5.7. Air samples based on the wind direction were categorized as "lake" and "land". The average ± 1 standard deviation values of the slopes were -0.24 ± 0.45 and -0.47 ± 0.36 and similarly the intercepts were -4.08 ± 1.49 and -3.98 ± 1.07 for land and lake samples, respectively. The average slope for the lake samples is closer to the theoretically suggested value, m_r = -1. Reasons for this observation of a larger lake slope can be due to more time for equilibrium over the lake and the presence of fresh (unequilibrated) PCB sources in Chicago. The relative humidity may or may not be a reason for this slope difference. Cotham and Bidleman (1992) found no significant effect of RH in the 30 - 95% range at 20 °C but about a substantial reduction in K_p was observed at 95% RH and 30 °C.

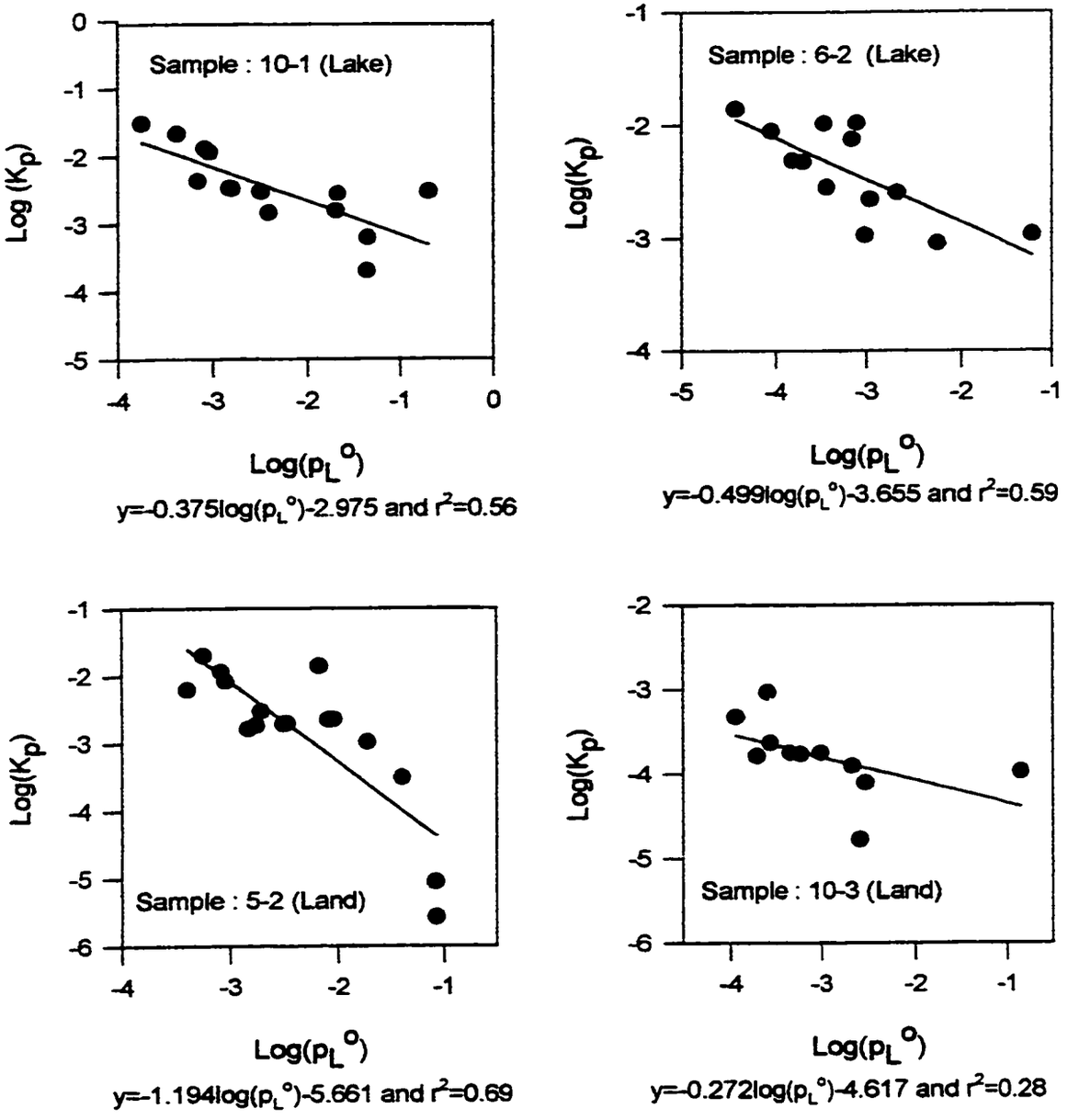

Figure 5.7. Log K_p vs Log p_L^o for Some Lake and Land Samples

It should be noted that field investigations of gas/particle distribution are complicated by artifacts (Falconer et al., 1995; Hart and Pankow, 1994). Cotham and Bidleman (1995) stated that event-to-event changes in the regression parameters were large in Chicago even over a short period (~ 2 weeks). Possible reasons for these slopes to be different from -1 could be (Pankow and Bidleman, 1991; Hart and Pankow, 1994; Cotham and Bidleman, 1995; Hoff et al., 1996): 1) sorption equilibrium is not always attained in the atmosphere, 2) Σ-PCB airborne concentration changes over the sampling period, 3) fluctuations in the TSP amount and characteristics in the atmosphere, 4) filtration artifacts (see Section 2.7), and 5) variability in c, the thermodynamic quantity, among PCB congeners.

If vapor pressure alone controlled partitioning, a plot of log Kp vs. log p_L° would show that all congeners fall on the same line. In other words, when there is no sampling artifacts and c is constant, the theoretical slope is equal to -1 and intercept of equation 5.1. (b_r) is a function of the specific surface area of the particles, the number of sorption sites per unit area, and absorption characteristics such as p_L°, the weight fraction of the aerosol that consists of absorbing liquid film and the activity coefficient of the solute in the film (Cotham and Bidleman, 1995; Falconer et al., 1995). Since in this study the gas/particle distribution is not at equilibrium ($m_r \neq -1$), b_r depends on not only on the specific surface area of the particle but also on m_r (Hart and Pankow, 1994; Pankow and Bidleman, 1991; Cotham and Bidleman, 1995). Even though the slopes from lake and land samples were not equal to -1, their intercept values were very close to each other which suggests that the characteristics of the particles did not change with wind direction.

In order to explain the gas/particle partitioning better, absorption phenomena were incorporated into a model by Pankow (Falconer et al., 1995). This model considers organic matter partitioning with the water film on the particle. In this case b_r becomes a function of the organic film, activity coefficient of solute in the water film and the sorbate p_L° (Falconer et al., 1995). The model suggests that sampling artifacts may be minimized by decreasing the sampling time because the atmospheric changes (temperature, RH) and concentration changes of PCBs and TSP values will be reduced.

More volatile PCBs, which have higher p_L°, come to sorptive equilibrium faster than the less volatile ones (Rounds and Pankow, 1990) due to their higher diffusivities and their higher concentrations. Therefore, the lower MW PCBs (more volatile) found on the PUF/XAD-2 represents the average of various air masses which were sampled by the PUF/XAD-2. On the other hand, because of the fast attainment of equilibrium, the PCB amount on the filter reflects the latest air parcel sampled (Baker et al., 1993). Since equilibrium between particles and higher MW PCBs (less volatile) is not as fast as lower MW PCBs, particles on the filter may reflect amounts of higher MW PCBs better in terms of longer time (lag phase). Therefore, the slopes (m_r) obtained from the field samples can fluctuate from unity in either a positive or negative direction (Pankow and Bidleman, 1990). In general, negative slopes are common (Vardar et al., 1997; Falconer et al., 1995; Cotham and Bidleman, 1995). This conclusion confirms our results because they averaged between -0.24 and -0.47 for land and lake samples, respectively.

In this study, PAHs samples were also obtained simultaneously with the PCB samples. The regression results between log K_p and Log p_L° indicated PAHs have different slopes (-0.49 ~ -0.97) and intercepts (-4.44 ~ -6.58) than PCBs (Vardar et al., 1997). This suggests that PCBs and PAHs are adsorbed on particles to a different extent due to particle properties (size, surface area available, organic content, water content, etc.) because the environmental and sampling conditions were identical for both PAHs and PCBs.

The values of c=17.2 Pa-cm and θ=1.1 e-5 cm^2/cm^3 were used in the Junge-Pankow model calculations since Chicago is an urban area. Different behaviors for PCBs and PAHs were seen by the application of this model (Vardar et al., 1997). For example, Cotham and Bidleman (1995) reported that PAHs were adsorbed to a greater extent than PCBs in their Chicago data. However, both PCB and PAH particle phase concentrations were underestimated (measured ϕ / modeled ϕ >1, where $\phi = C_p/[C_p+C_g]$) for lower MW compounds yet they were overestimated for the higher MW compounds (measured ϕ / modeled ϕ <1) (Figure 5.8.). The ratio (measured ϕ / modeled ϕ) for PCB homologs ranged between 19 and <0.01 (Figure 5.9.). The overall measured to modeled ratio of ϕ is about 3.8, which considers all ratio values individually (not the averages of the congeners). This is a reasonable value because 1) modeled values (from Junge - Pankow

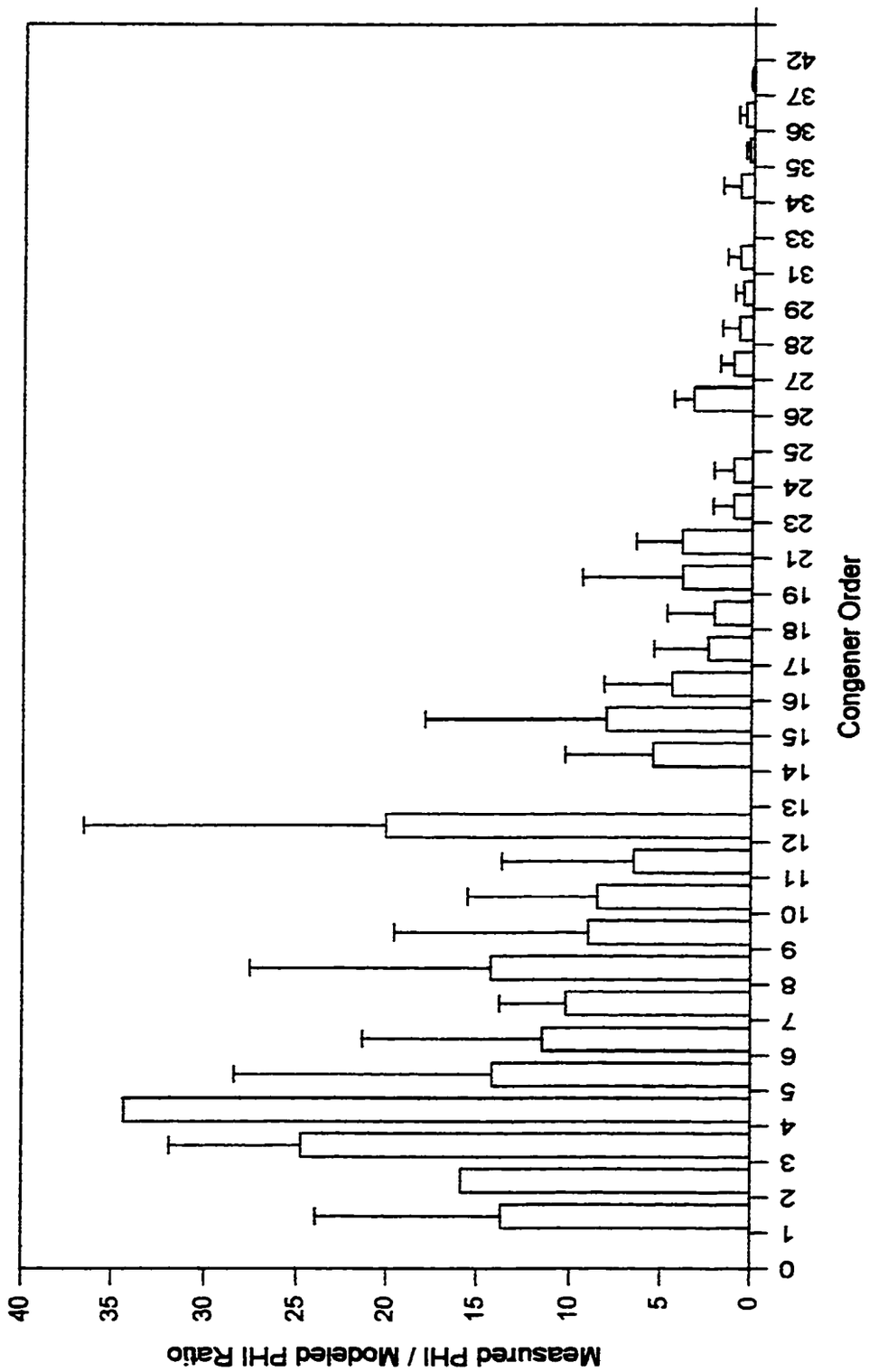

Figure 5.8. Measured / Modeled PHI ($\hat{\Phi}$) Values for All Congeners

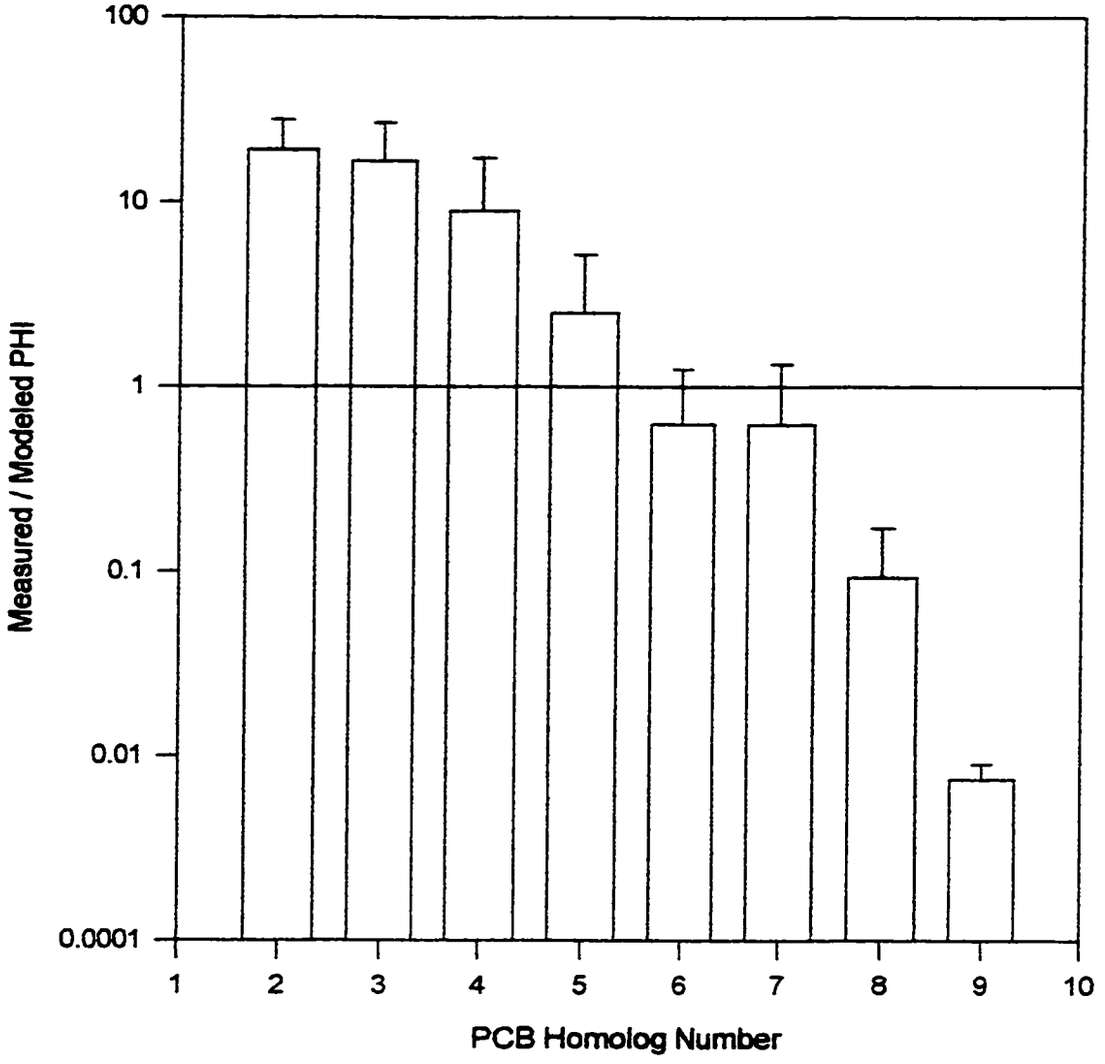

Figure 5.9. Measured/Modeled PHI (Φ) Values for PCB Homologs

model, 1987) assume constant values for c and θ, 2) high-volume sampling artifacts can cause some fluctuations, 3) p_L° values may change slightly from one study to another, 4) c which represents the difference of the enthalpy of desorption of the compound from particulate matter and vaporization of the pure compound (Pankow, 1987; Falconer et al., 1995; Cotham , 1990) is expected to be a function of compound class and as a result it should be constant within that class. However, it was stated that c might not be constant during the sampling for a specific compound due to sampling and meteorological conditions (Falconer et al., 1995), 5) θ used in the calculations was 1.1 E-5 cm^2/cm^3 which is for urban air (Cotham, 1990; Cotham and Bidleman, 1992). This value was suggested based on a typical size distribution of accumulation mode aerosols which fluctuates between samples. For example, Chicago is considered as an urban site; however, the ambient air characteristics can change a great deal based on the wind directions (over Lake Michigan may be nonurban, over Gary, IN may be highly-polluted), and 6) the model is not able to consider humidity (Cotham and Bidleman, 1995).

It should be emphasized that even though there are some deficiencies with the Junge-Pankow model, this model predicts the gas/particle partitioning of organic compounds reasonably well and therefore, it has been used widely (Falconer and Bidleman, 1994; Falconer et al., 1995; Cotham and Bidleman, 1992 and 1995; Foreman and Bidleman, 1990; Pankow, 1987; Vardar et al., 1997). Figure 5.10. illustrates the modeled and measured ϕ values against Log p_L° values for all congeners available. As seen from this

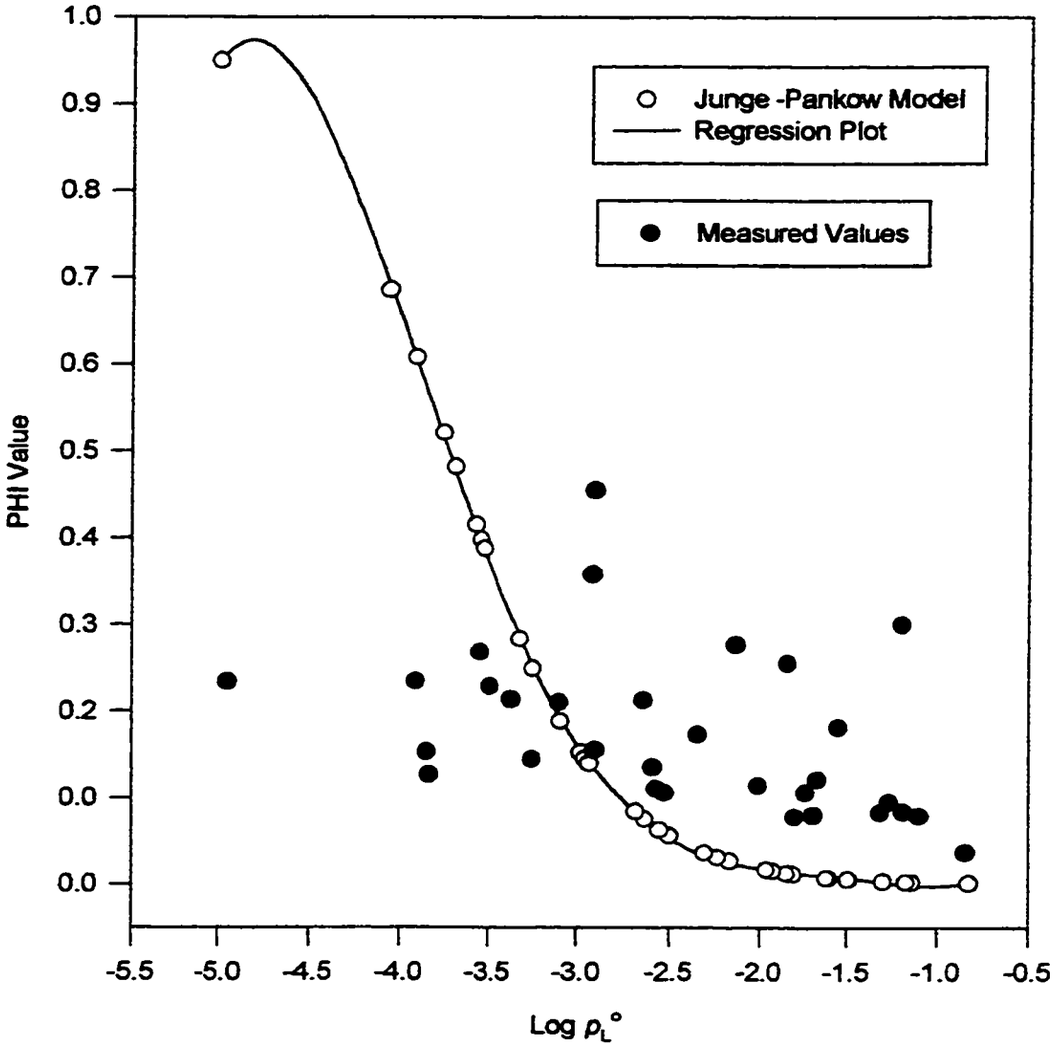

Figure 5.10. Comparison of Average Measured and Modeled (Junge-Pankow) PHI (Φ) Values

figure the Junge-Pankow model overestimates the lower MW PCBs while underestimating the higher MW PCBs. In the model calculations, the overall average temperature value was used.

In this study single GFF was used in the high-volume sampler. However, it is believed that the GFF in the high-volume sampler adsorbs both particulates and gases (Hart et al., 1992; Pankow and Bidleman, 1991). Therefore, some researchers use two GFFs at the same time. PCBs on the front filter (FF) are assumed to be particulate and gaseous PCBs adsorbed to the GFF and particles; on the other hand, the back filter (BF) is assumed to adsorb only gases equal to the amount adsorbed on the FF. Therefore, not using two GFFs in the sampler could bias the particulate sample high and the calculation of ϕ based on measurements would be overestimated. Thus the ratio between measured ϕ / modeled would increase as was found in this study. This suggests that if two filters had been used in this study, the agreement between the measured and modeled ϕ values would have been better because the ratio between measured ϕ / modeled ϕ would become closer to unity. Moreover, overestimation of the particle phase concentration (C_p) increases the Log K_p value because K_p is equal to $(C_p/TSP)/C_g$. As a result of this increase, the slope (m_r) in equation 5.1 becomes steeper.

Efforts on understanding a contaminant's distribution in the atmosphere based on the concentration, liquid phase subcooled vapor pressure, season, source, and particle characteristics can be used to calculate the annual deposition loadings (Pankow, 1987; Pankow et al., 1994; Hart et al., 1992; Foreman and Bidleman, 1990; Hoff et al., 1996;

Hornbuckle et al., 1994; Baker and Eisenreich, 1990). Another important application of gas/particle distribution is related to health concerns because some precautions can be taken if the phase in which the contaminant mainly exists is known. For example, highly toxic mono- and non-ortho PCBs are associated mostly with particles (Falconer et al., 1995). Therefore, simple filtration could be enough to prevent harm from these pollutants.

5.3. Atmospheric Dry Deposition Fluxes of PCBs

This section is focused on the determination and interpretation of the dry deposition of PCBs fluxes to two surrogate surfaces (greased strips and water surface). To date there is no acceptable collection and analytical method for dry deposition even though more than 50% of Lakes Superior, Michigan and Huron's current PCB loadings are believed to be coming from atmospheric deposition (Murphy et al., 1995; Achman et al., 1993; Baker et al., 1993). Therefore, our aim is to improve specific collection and analysis methods for PCBs present in the environment to quantify and characterize them. The abbreviations used frequently in this section are given below:

WSS_1 : Water surface sampler 1 ,

WSS_2 : Water surface sampler 2,

WSS_A : Average of the water surface samplers,

WSS_{1R} : Water surface sampler 1 resin,

WSS_{1F} : Water surface sampler 1 filter,

Plate : Greased strips on the plates,

WSS_{A-P} : Average water surface sampler [(WSS_1 + WSS_2)/2] minus plate,

5.3.1. Overall Fluxes. Total PCB fluxes were measured with two water surface samplers (WSSs) (water surfaces 1 and 2 (WSS_1 and WSS_2)). Unlike WSS_1, WSS_2 did not contain a filter in the water recirculation line, it contained only XAD-2 resin. The water surface sampler used in this study was different from the ones previously used at IIT. The new WSS was made of aluminum rather than acrylic. In addition, one of the new WSSs had a filter to collect particle phase PCBs separately and both samplers contained a XAD-2 resin column to collect all of the PCBs contained in the water. In order to operate the filter and column appropriately, the WSS was run under pressure which was also different than the previous version.

Two WSSs were run simultaneously under the same conditions and their collection surfaces were exactly the same. Using a paired the t-test for a total number of 43 pairs of congeners only one congener was rejected (~98% of them accepted). Therefore, both WSS_1 and WSS_2 fluxes were statistically the same. Moreover, their correlation to each other is above 90%. This close agreement confirms that the sampling and analysis methods were consistent and capable of collecting the targeted PCBs.

The average Σ-PCB flux values ranged between 210 and 2340 ng/m^2-d and averaged 1170 ng/m^2-d for WSS_1 samples. The flux values for the WSS_2 varied from 150 to 3010

ng/m^2-d and averaged about 1150 ng/m^2-d (Figure 5.11). The average of the two WSSs is referred to as WSS_A ([WSS_1+WSS_s]/2). When there was no data for either WSS, the remaining value was used. The flux values for WSS_A varied between 170 and 2560 ng/m^2-d and with the average of about 1200 ng/m^2-d for the 11 samples (Figure 5.12).

The eleven PCB flux measurements together with average ambient air temperatures are shown on Figure 5.12. The overall PCB fluxes were not well correlated with temperature. However, PAH samples, collected simultaneously with the same WSSs, showed better temporal variations but not at the theoretically expected level (Tasdemir et al., 1997).

The interest in atmospheric deposition by the scientific community has increased a great deal over the past decade but as mentioned earlier there is no generally accepted collection method (sampling technique). There are many different reported flux values for PCBs in the literature. The differences are due to different sampling locations and different sampling/calculation technique. The reported flux values fluctuated between -1300 (Achman et al., 1993) and +9700 ng/m^2-d (Holsen et al., 1991) (Table 2.16). The negative flux value refers to volatilization and positive value refers to deposition.

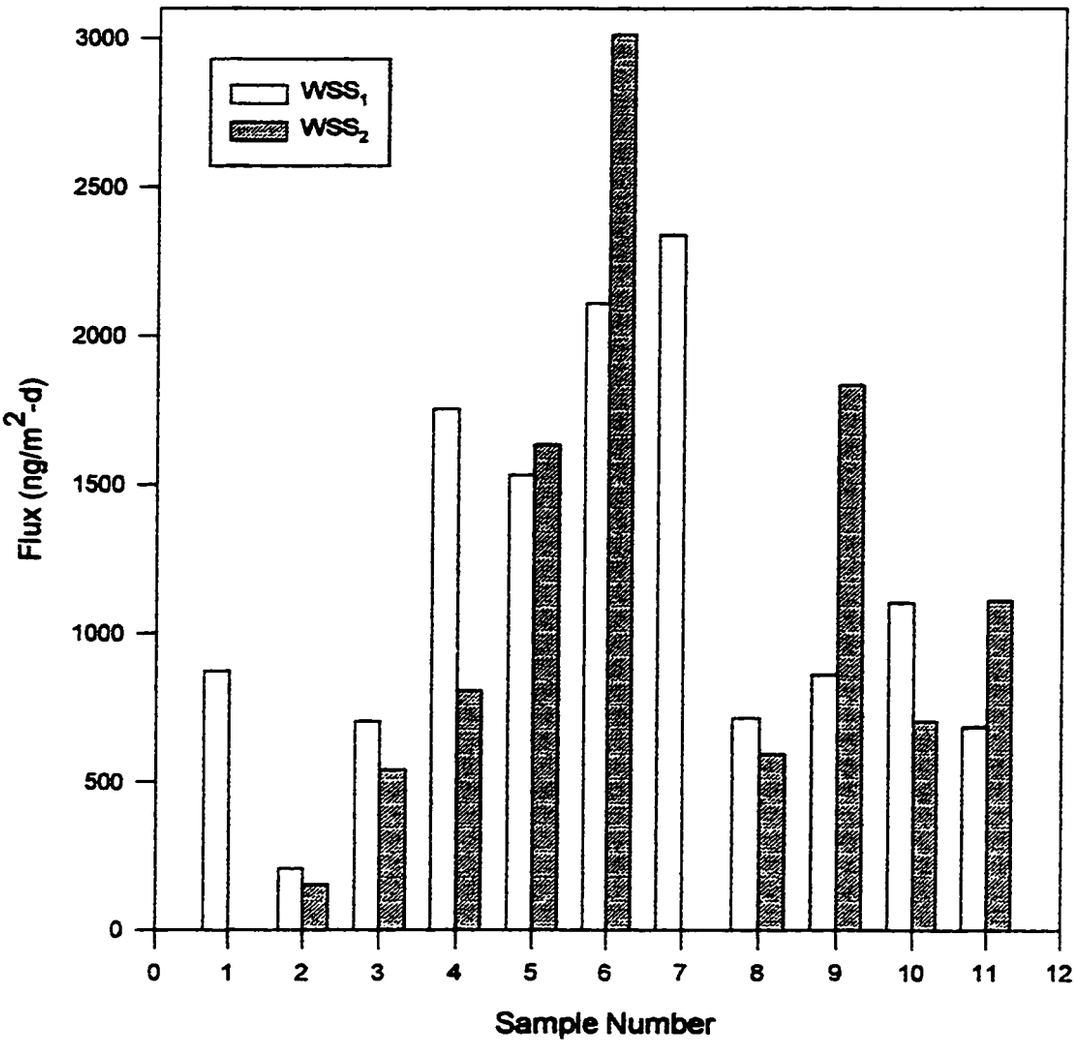

Figure 5.11. WSS_1 and WSS_2 Fluxes of Each Sample

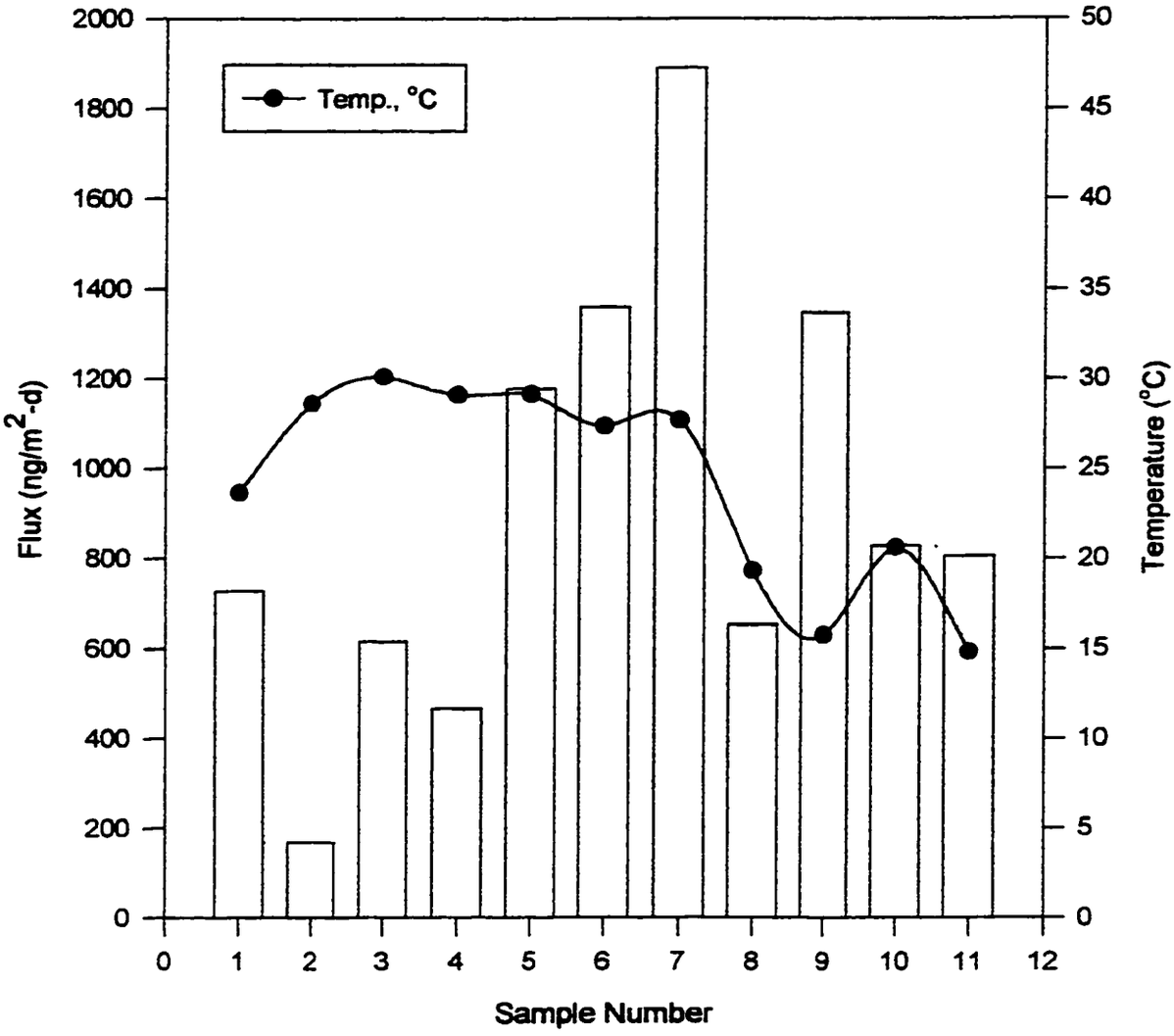

Figure 5.12. Total Flux Values (WSS_A) of Each Sample

The average overall flux value (~1200 ng/m^2-d) for WSS_A is comparable to those reported for urban areas (Holsen et al., 1991 and Panshin and Hites, 1994b).

In this study, direct flux measurements were made rather than calculated from measured concentrations and dry deposition velocities. Some researchers measured air and water PCB concentrations simultaneously in the Great Lakes (Achman et al. (1993), Hornbuckle et al. (1994)) and flux calculations were based on concentration gradients and overall MTC. In this study, the PCB concentration in the water was always very low due to the use of XAD-2 resin and therefore, the maximum PCB transfer from atmosphere to the water was observed. However, in natural water bodies due to background water concentrations, the magnitude and even direction of flux changes. In this study the maximum flux from air to clean water was determined with minimal volatilization interference.

The congener with the highest average flux was PCB 138/163. It accounted for approximately 12 % of Σ-PCB flux. Of the congeners measured the lowest flux was accounted for by PCB 207 (< 1%). Figure 5.13 shows the distribution of the targeted 50 PCB congeners with one standard deviation. The fluxes were higher for the mid-range molecular weight (MW) PCB congeners. The pentachlorinated homolog accounted for the highest portion of the flux (Figure 5.14).

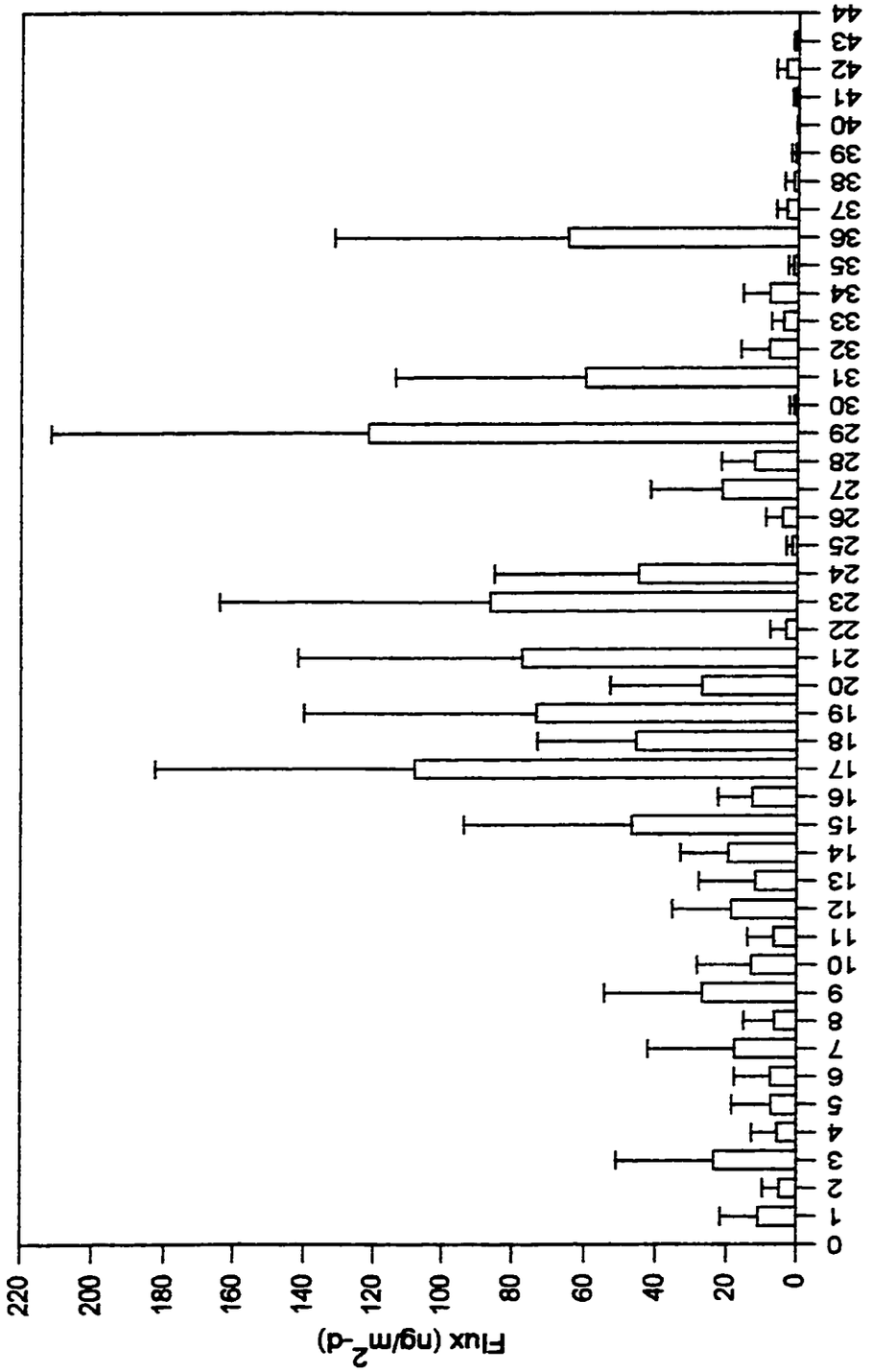

Figure 5.13. Average Overall (WSS_A) Flux for Each Congener

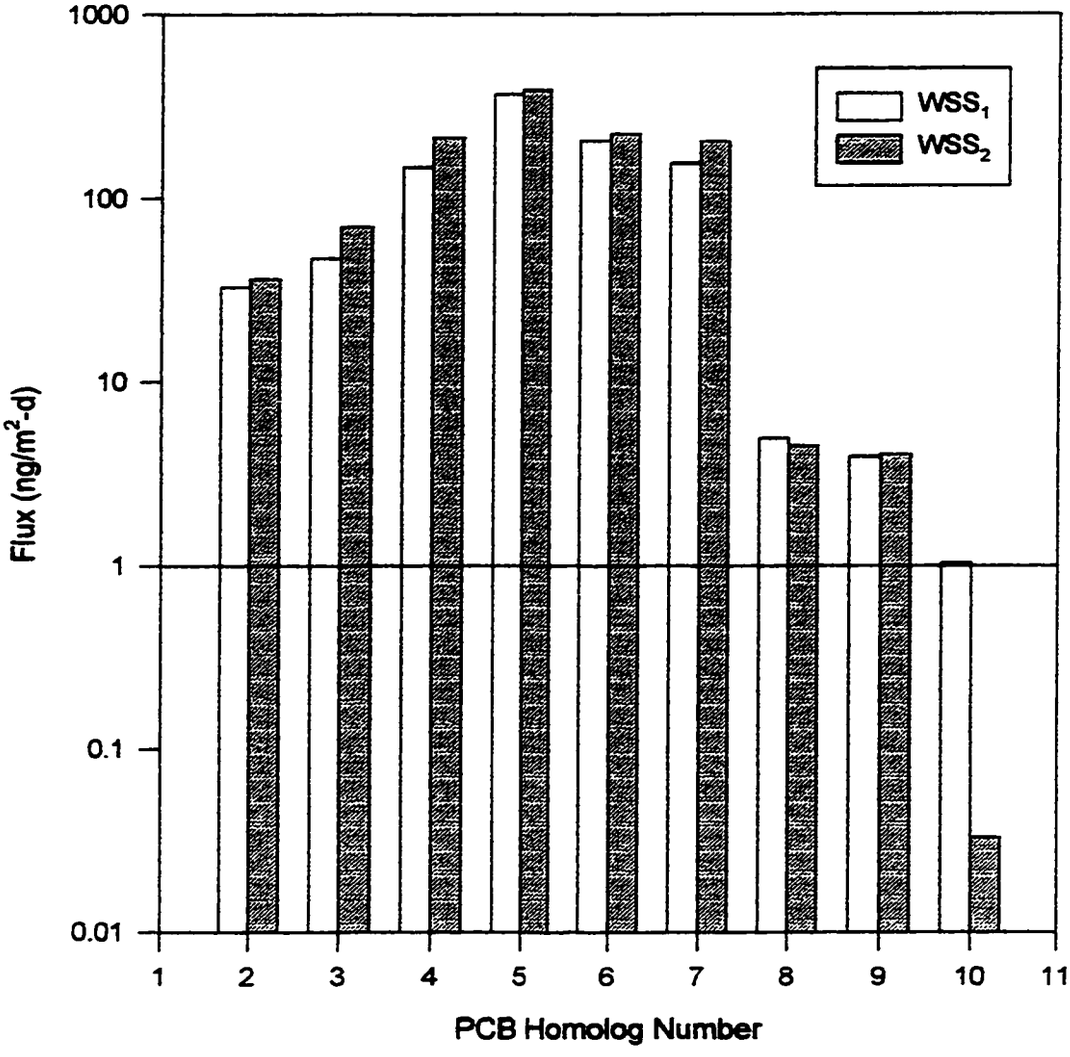

Figure 5.14. Flux Values of Homologs for WSS_1 and WSS_2

As mentioned in the previous section, PAH samples were collected simultaneously with the PCB samples. The reported overall average PAH flux obtained from WSS_1 was about 332,500 ng/m^2-d for 13 PAH species (Tasdemir et al., 1997). Based on the sampling location a big fluctuation in the flux values can be observed. For instance, Eisenreich et al. (1981) reported a value of 5384 ng/m^2-d for total (gas + particle) PAH flux in Great Lakes region whereas Sheu et al. (1996) have reported about 200 times bigger values (1,217,000 ng/m^2-d) only for particle phase PAH fluxes in a traffic intersection in Taiwan.

It should be noted that the experiments done under controlled conditions or in the laboratory may not necessarily reflect the real life phenomena. Therefore, the accuracy of extrapolating these types of measurements to the real water bodies (lakes, oceans) is open to discussion. Atmospheric deposition is quite complex and is a function of wind, waves, bubbles, heat transfer, fetch distances, atmospheric stability as well as surface and compound characteristics (Liss, 1983; Mackay and Yeun, 1983; Bidleman and McConnell, 1995). Thus, deposition values may fluctuate a great deal between laboratory and the real environment as well as between two different environments.

5.3.2. Particle Phase Fluxes. The average overall particle PCB flux values ranged between 105 and 390 ng/m^2-d and averaged about 240 ng/m^2-d for plate samples. The particle PCB flux values for WSS_{1F} ranged from 65 to 510 ng/m^2-d and averaged about 260 ng/m^2-d. Each PCB congener flux from the plate samples were compared with the WSS_{1F} using a paired t-test. More than 75% of the congeners were accepted as

statistically not different ($H_o : \mu_1 = \mu_2$). There was no pattern for the rejected congeners. However, the average overall flux was slightly higher from the WSS_{1F} than from the plate samples (Figure 5.1). The particle flux values of the eleven samples were not correlated with average ambient air temperatures (Figure 5.15). As explained earlier, this lack of correlation is probably due to the long sampling time (> 5 days).

PCB 101 had the highest overall average flux for the plate samples and it accounted for approximately 15 % of Σ-PCB flux. PCB 180 had the highest flux for the WSS_{1F} flux samples and it accounted for approximately 11% of Σ-PCB flux. The lowest flux belonged to PCB 207 in WSS_{1F} samples while in the plate samples 11 congeners were under the detection limit including PCB 207. Figure 5.16. shows the average flux of the targeted 50 PCB congeners (including one standard deviation). The flux in both cases reached the highest value for the mid-range MW PCB congeners. The pentachlorinated homologs accounted for the highest percentage of the flux for both the WSS_{1F} and plate samples (Figure 5.17).

Low MW PCBs were detected in the particle PCB fluxes (Figure 5.16.). Theoretically, the lower MW PCBs would not be on the particles, they should be in the gas phase. The possible explanations for finding them in the plate samples (greased strips) could be 1) some gas phase PCBs may be captured by grease, 2) some gas phase PCBs may be associated with particles and then deposited on the plates (greased strips). On the other

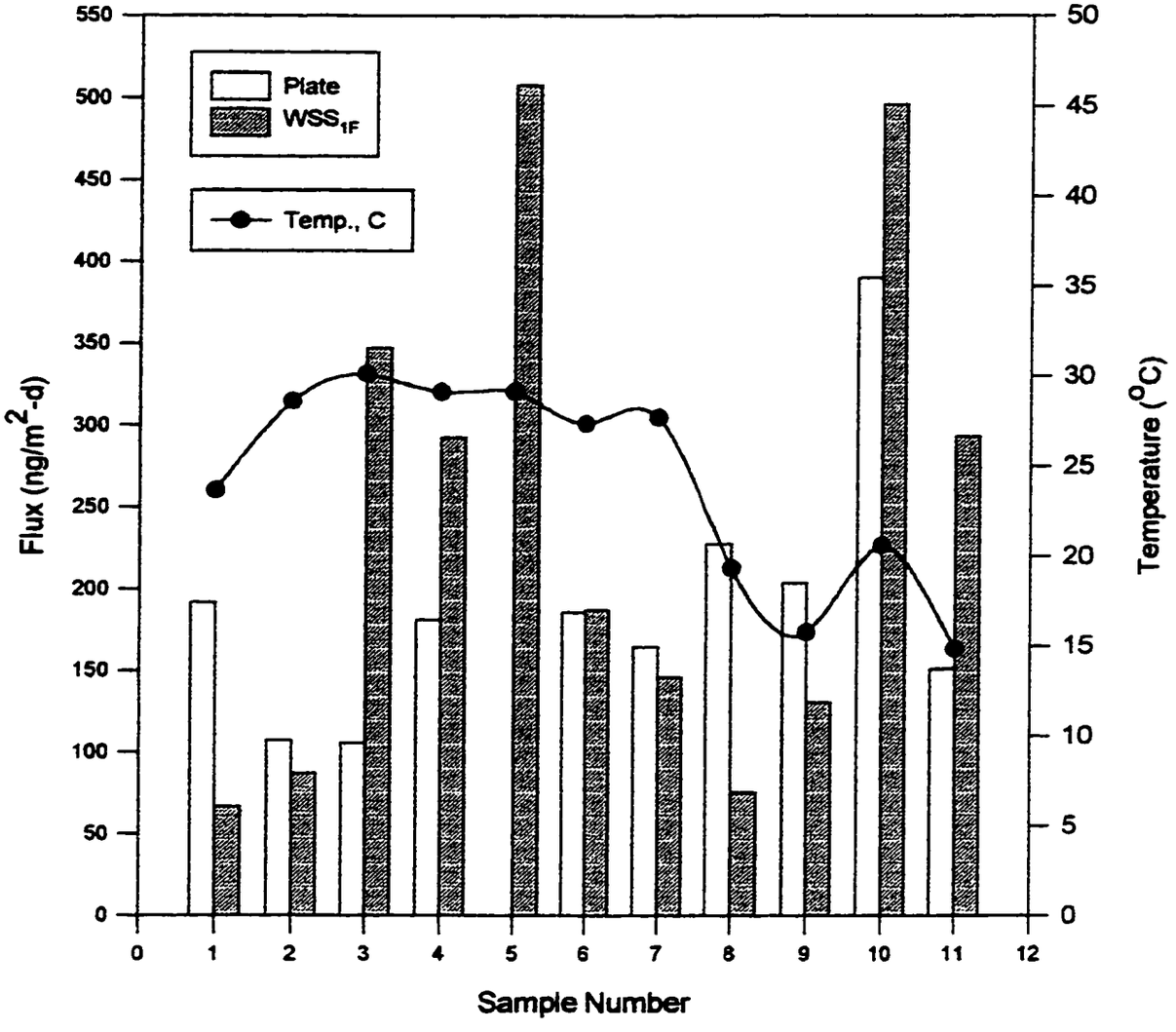

Figure 5.15. Particulate Flux Values (Plate and WSS_{1F}) of Each Sample

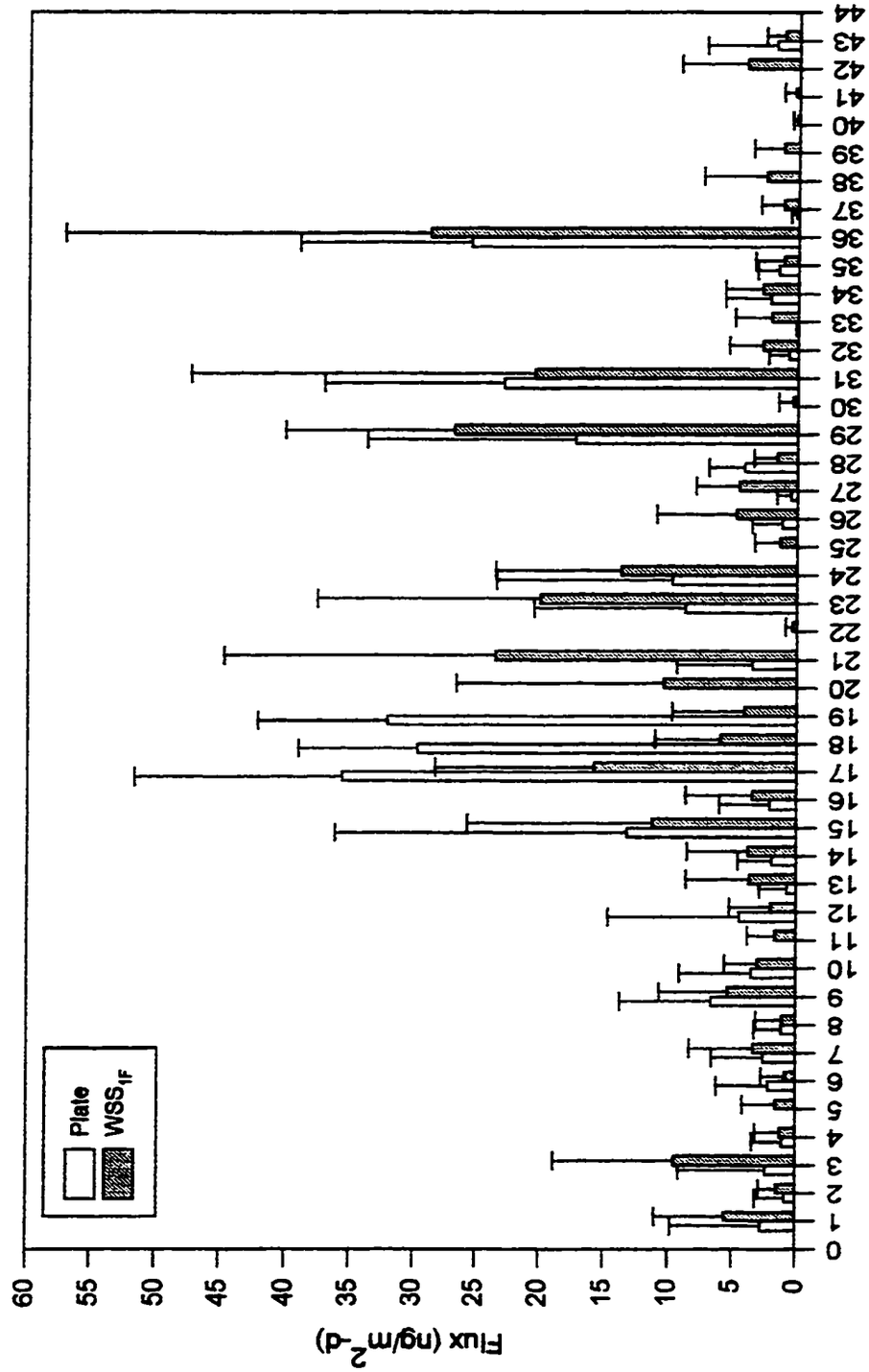

Figure 5.16. Particulate Fluxes (Plate and WSS_{1F}) of Each Congener

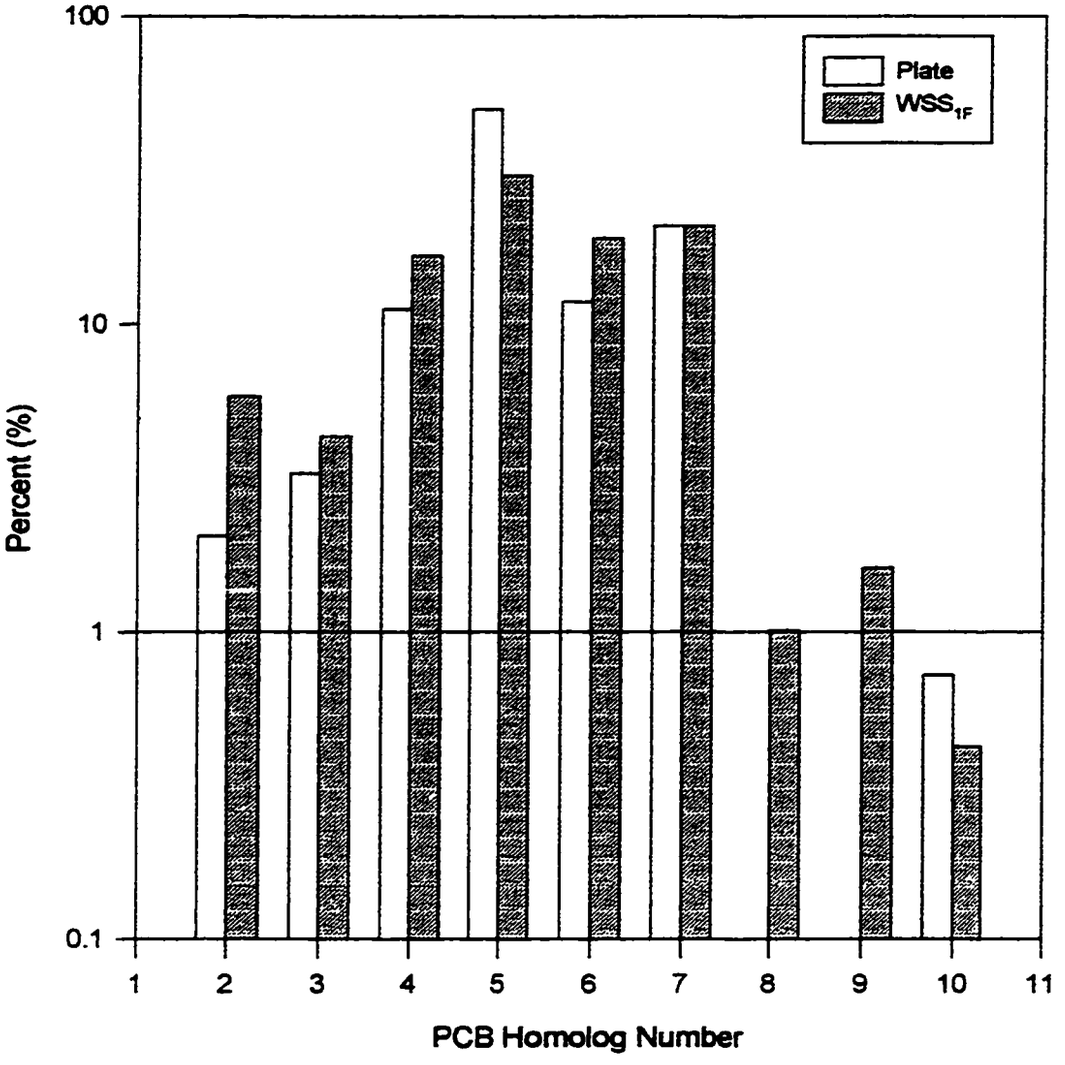

Figure 5.17. Percentages of Homologs in Particulate Fluxes

hand, there could be some PCB losses from the plates. The possible reasons for this loss could be 1) evaporation of PCBs from deposited particles, 2) evaporation of PCBs from plates (greased strips). This equilibrium loss may be minimized by decreasing the sampling time. To test this Myrczik (1997) performed some experiments. Rather than using same plates for 5 days (long term samples), he replaced some of the plates with the new ones after every sampling day (short term sample). Myrczik (1997) reported that short term sample fluxes were statistically the same. Even though the long and short term fluxes are not statistically different, the real difference may be explained by the evaporation/equilibrium losses from the plates and particles on the plates.

The possible artifacts in WSS_{1F} samples can be summarized as follows 1) partitioning of gas phase (dissolved) PCBs on the filter and 2) partitioning of gas phase PCBs onto particles on the filter. A possible reason for the underestimation of particulate PCB fluxes on the WSS_{1F} samples would be dissolution of PCBs associated with particles on the filter. Unlike plate samples, there should not be any evaporation losses from WSS_{1F} because the filter was in a totally closed holder and always under water.

WSS_{1F} and plate fluxes indicated that they were statistically the same for 75% of the congeners. The most problem causing congeners might be the lower MW PCBs (as mentioned above paragraphs). However, the results indicated that their flux values were little higher in WSS_{1F} samples but this difference was not substantial. Overall these agreements may suggest that either of them can be used for PCB particulate phase flux

collection. However, the WSS_{1F} detected more congeners (in terms of the number) in the samples and this is due to its bigger surface area. For example, some higher MW PCB homologs were not observed. If the surface area of plates is increased, this difference can be handled. It should be stressed that the work needed for cleaning and sample preparation with plates are very difficult job. Moreover, some background PCB level exists in the grease (plate samples). Therefore, it might be better to use WSS_{1F} for the sampling. Another reason for WSS_{1F} choice can be the collection surfaces for the PCB fluxes. Since WSS is used to collect total PCB flux, it can be possible to collect the particulate phase flux by application of WSS_{1F} and gas phase flux simultaneously from same surface (in terms of type, area and other characteristics) and under the same atmospheric conditions (because temperature and wind effects may be different for grease and water surfaces); thus these results (gas and particulate fluxes of PCBs) would be more consistent to each other.

The reported overall average particle PAH flux obtained from plates was about 144,000 ng/m^2-d for 13 PAHs during this study (Tasdemir et al., 1997; Odabasi, personal communication). In the literature, particle phase PAH fluxes were reported between 423 and 1,217,000 ng/m^2-d (McVeety et al., 1988 and Sheu et al., 1996). Since PAHs are the products of incomplete combustion of fossil fuels and other organic matter, the flux value is directly related to the sampling site and therefore, very large fluctuations in the reported values can be seen. For example, a flux of 1,217,000 ng/m^2-d was measured in a traffic intersection (in Taiwan) where the PAH flux was expected to be very high (Sheu et al.,

1996). The most abundant PAH species was phenanthrene and it accounted for about 30% of the total particle PAH flux (Tasdemir et al., 1997).

As mentioned earlier, PCB dry deposition fluxes were measured by two different surfaces, WSS and plates (greased strips). If there was no PCB gas phase dry deposition into the WSS, the ratio of the WSS PCB fluxes to the plates should be unity. As seen from Figure 5.18, the WSS fluxes were always higher than the plate fluxes. This difference between these two surfaces was caused by PCB gas phase dry deposition into the WSS. Namely, while the WSS collects both particle and gas phase PCB dry deposition, the plates (greased strips) measures only the particle phase. Therefore, the gas phase PCB dry deposition flux would be equal to the difference between WSS flux (gas and particle) and plate flux (particle). As Yi (1995) has determined the WSS and plates have different deposition properties for the gas phase but similar deposition properties for the particle phase. This was confirmed to be true in this study also because based on the t-test between WSS_{1F} and plate flux values, more than 75% of the congeners were not statistically different.

5.3.3. Gas Phase Fluxes. The WSSs were used to collect both gas and particle phase PCB fluxes. Gas flux values were calculated based on the difference between overall WSS_A flux (including gas and particle) and particle flux obtained from plate samples. This flux is abbreviated as WSS_A-P. The gas flux values averaged 460 and 490 ng/m^2-d for WSS_{A-P} and WSS_{1R}, respectively. The gas phase PCB fluxes were not correlated with temperature (Figure 5.19). As explained earlier, the long sampling time (> 5 days) is probably the main reason for this.

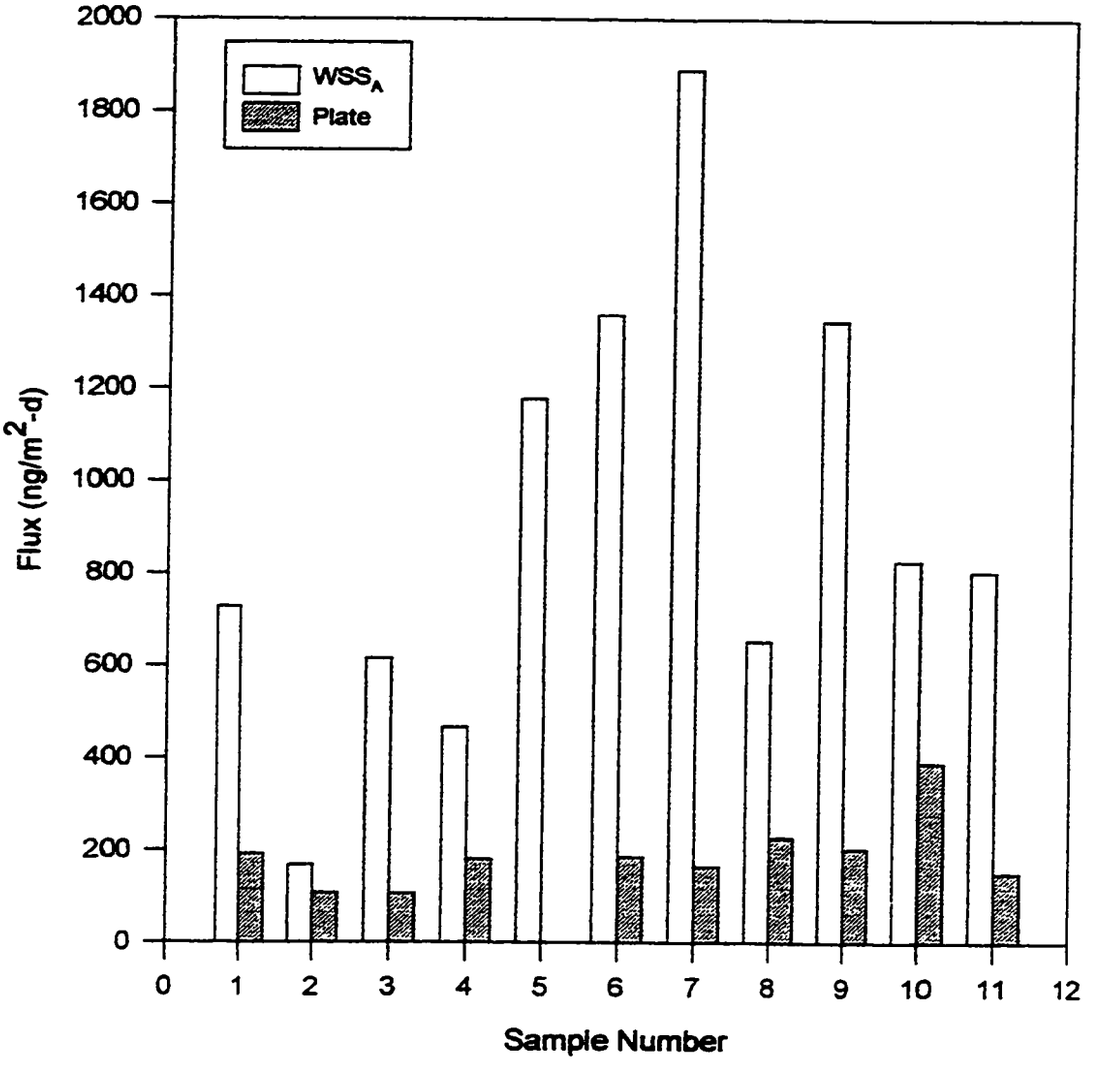

Figure 5.18. Total Flux (WSS_A) versus Particulate Flux (Plate) Comparison

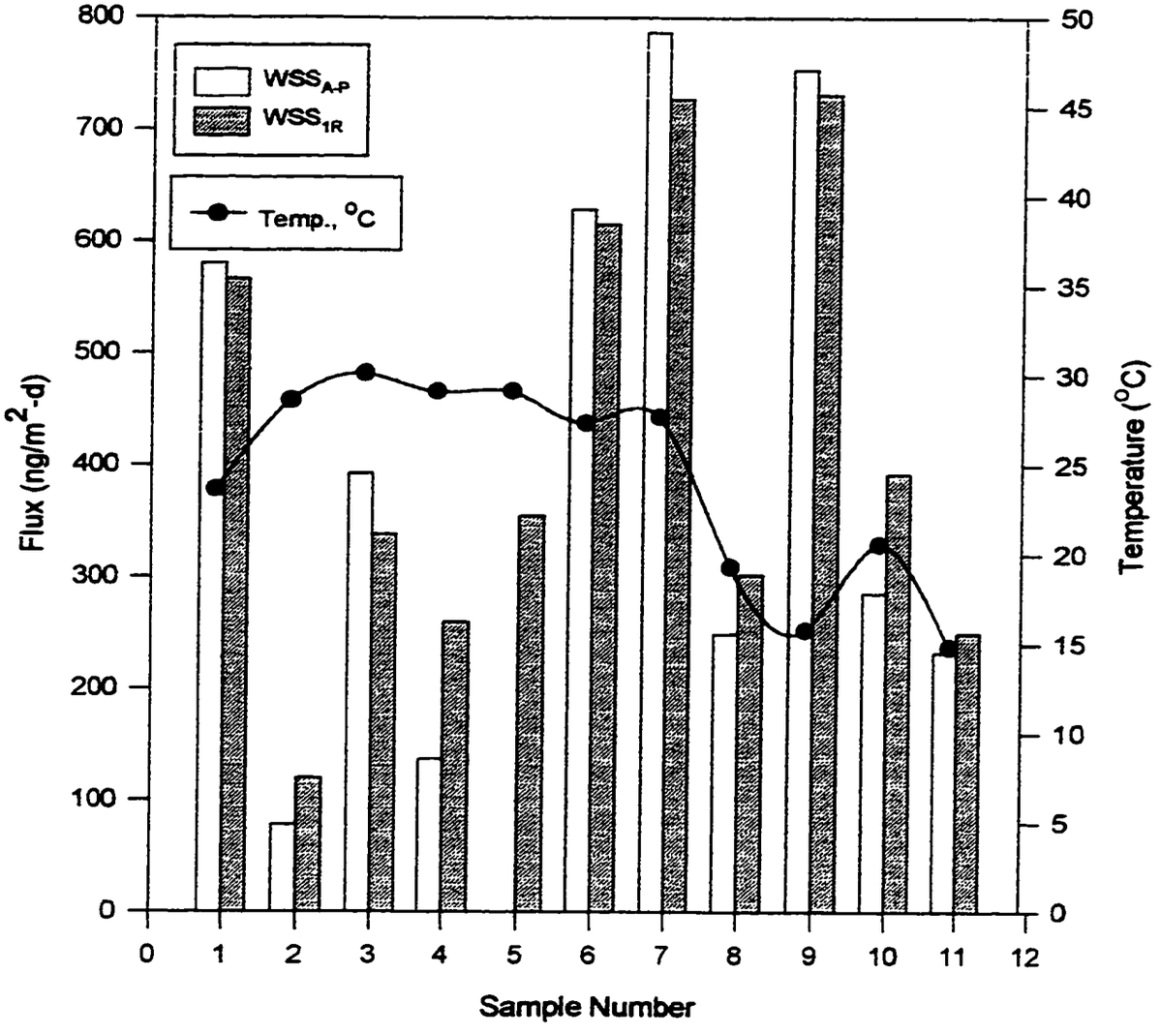

Figure 5.19. Gas Fluxes (WSS_{A-P} and WSS_{1R}) of Each Sample

In this study, the gas phase fluxes were also determined by the direct measurement of WSS_{1R}. The WSS_1 contains a filter and XAD-2 resin column. Since the filter collected the particle phase PCBs, the remaining flux captured by the XAD-2 resin can be considered as the gas phase flux. Figure 5.20. shows the average measured flux of the targeted 50 PCB congeners. The WSS_{1R} overall (gas) flux value is about 490 ng/m^2-d and it agreed well with WSS_{A-P}. This is due to the good agreement between particulate fluxes (WSS_{1F} and plate) because gas phase fluxes are simply the difference between particle phase fluxes and total fluxes. The gas flux reached the highest values for the mid-range MW PCB congeners. The pentachlorinated homolog accounted for the highest percentage of fluxes (Figure 5.21).

.

The PAH flux samples were collected simultaneously using the same collectors in this study. The overall average gas PAH flux value was about 163,400 ng/m^2-d (Odabasi, personal communication). This flux is much bigger than the gas phase PCB flux due to high gas phase PAH concentrations in the ambient air. PCBs and PAHs behave similarly in the air due to their physical similarities.

In general, the gas phase PCB fluxes were larger than particle phase PCB fluxes (Figure 5.22). This is reasonable because the concentration of PCBs in the air is mostly in the gas phase (~ 95% for this study) and deposition flux is proportional to the concentration (Flux = Concentration x Mass transfer coefficient (MTC)). The average ratio between gas and particle phase PCB concentration was 19. However, the flux ratio between the gas and particle phase was only about 2 based on the overall average flux values. This

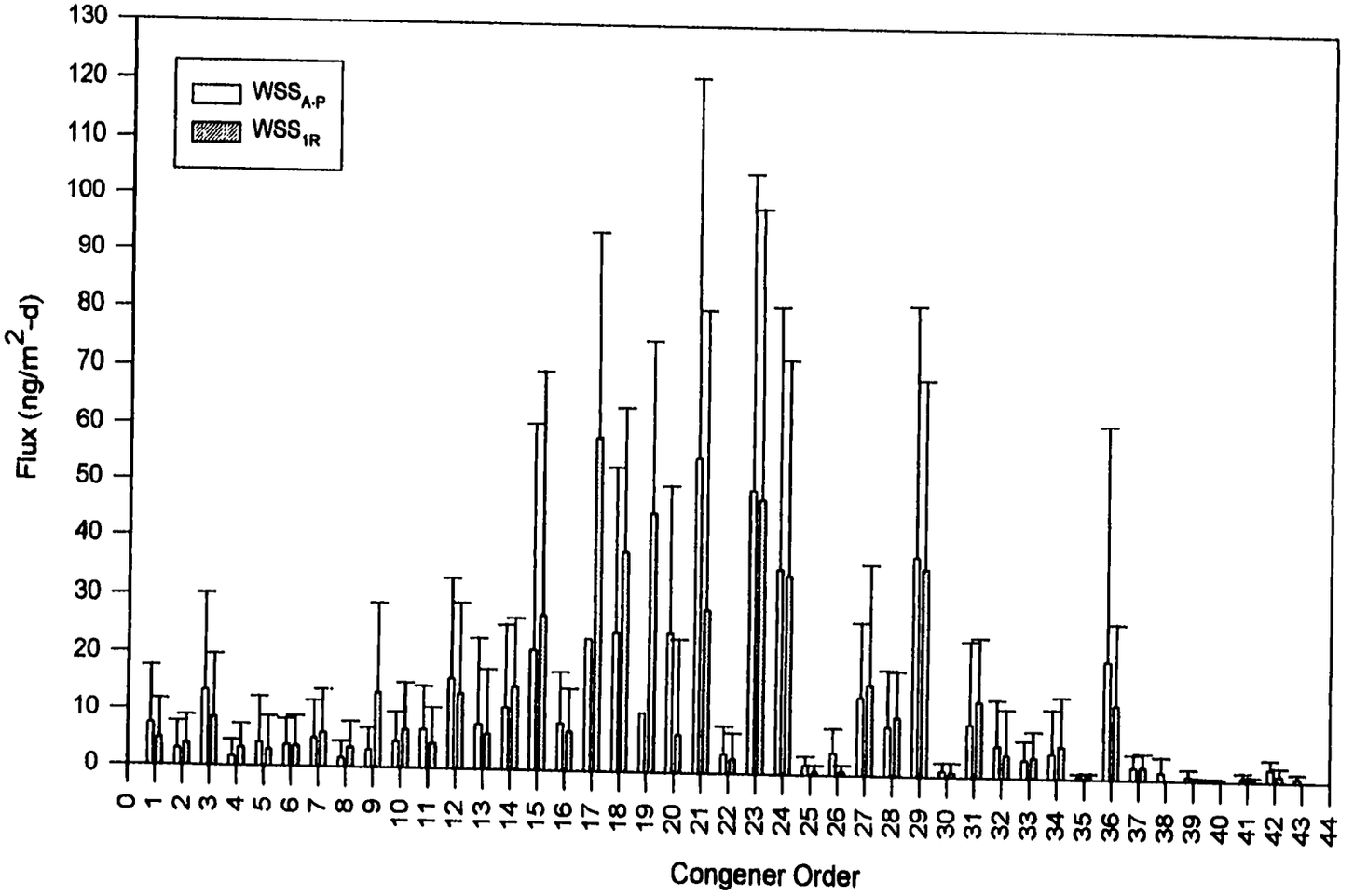

Figure 5.20. Gas Flux Values (WSS_{1R} and WSS_{A-P}) of Each Congener

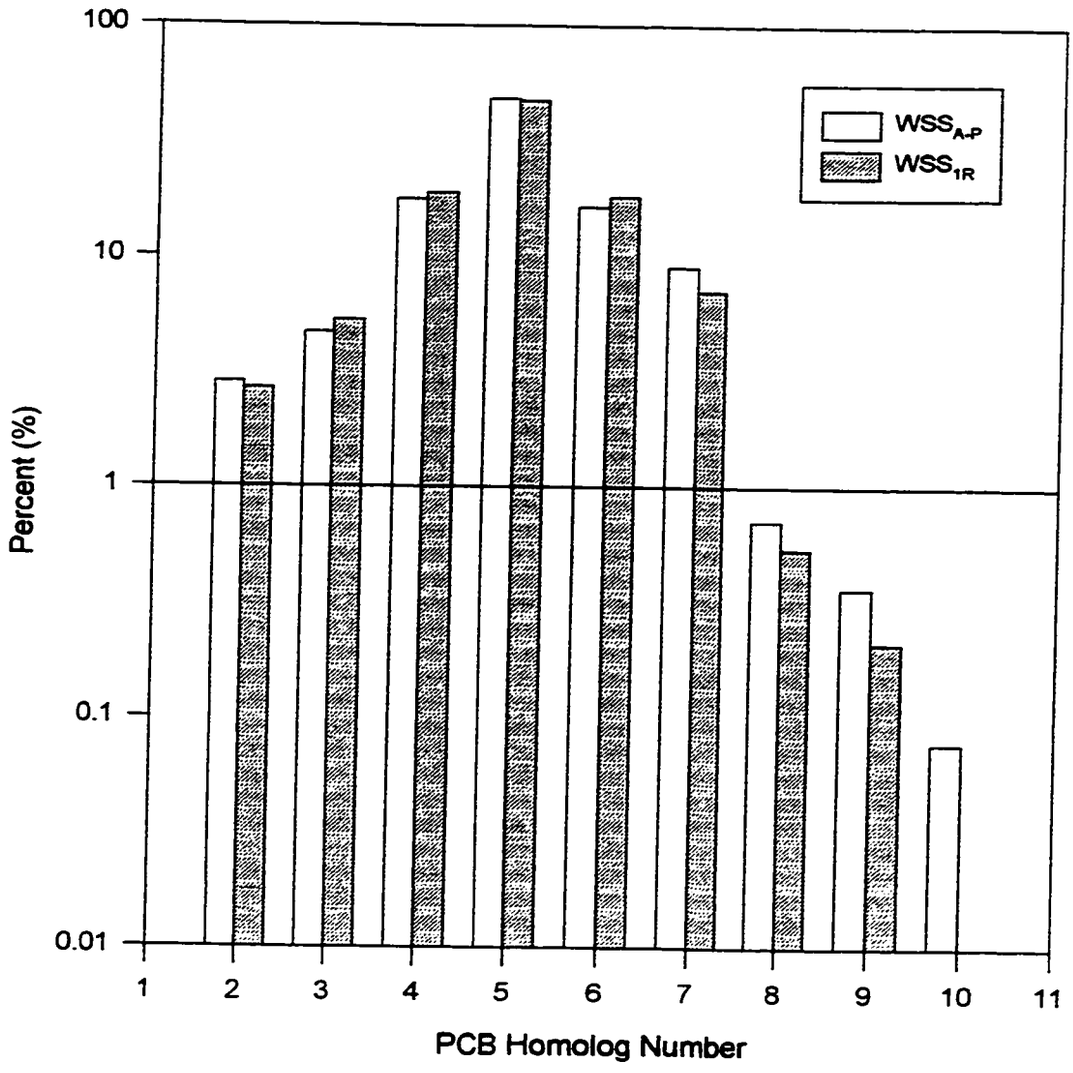

Figure 5.21. Percentages of Homologs for Gas Phase PCB Fluxes

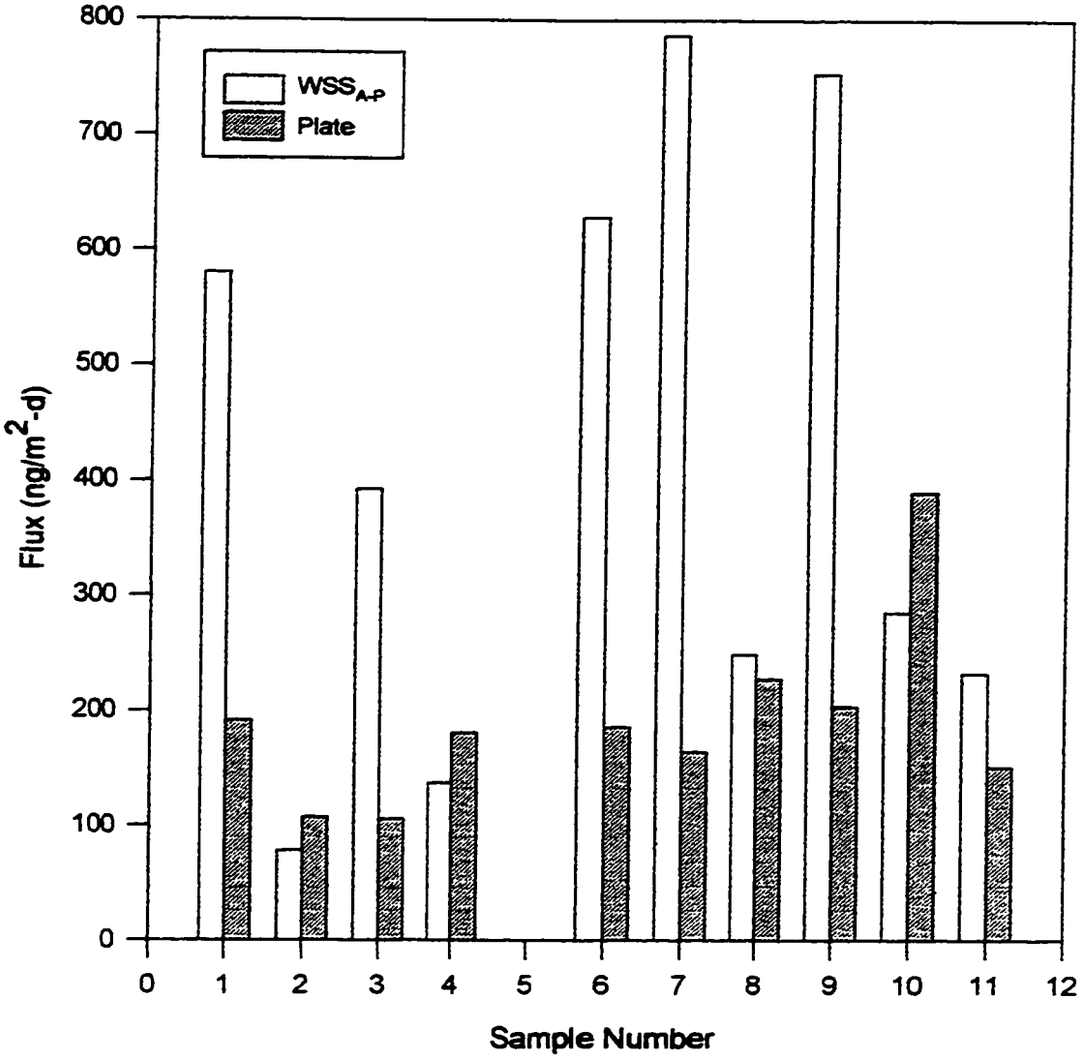

Figure 5.22. Comparison of Gas (WSS_{A-P}) & Particle (Plate) Fluxes

difference between the ratios can be explained by the differences in the deposition phenomena affecting the particles and gases. For example the MTC, or dry deposition velocity, for particles is about 8 times bigger than those calculated for the gas phase. The ratio between gas and particle PAH flux (~1.1) was smaller than the ratio found for PCBs. This finding suggests that PCBs exist more in the gas phase than in the particle phase in the ambient air than do PAHs (in terms of percentage). However, it should be noted that the average PAH concentration is in general a couple of orders of magnitude bigger than the PCB concentrations in the atmosphere (Odabasi et al., 1997; Cotham and Bidleman, 1995; Hoff et al., 1996).

5.4. Dry Deposition Velocities of PCBs

The dry deposition velocity can be calculated as follows:

$$V_d = F / C \qquad (5.3)$$

V_d : Dry deposition velocity, length/time,

F : Dry deposition flux, mass/(area x time),

C : Concentration, mass/volume.

The dry deposition velocity in combination with a measured concentration can be used to estimate fluxes into water bodies because the direct flux measurements are expensive, appropriate for a single time period (when samples are collected), and depends

intensively on qualified labor. Therefore, environmentally representative and accurate dry deposition velocities could lead to better estimates of dry deposition fluxes to natural bodies. Data used to obtain deposition velocities should be obtained under the different meteorological conditions (ambient air temperature, wind speed and direction, stability, relative humidity), collection surface properties (for example for water; temperature, characteristics, other compounds and so on) and the physical and chemical characteristics and amount of contaminant. Then, based on these different scenarios, a reasonable flux estimate can be made.

During the analysis some unexpectedly high dry deposition velocities were found. The reasons for these physically impossible values could be 1) contamination during the analysis, 2) coelution with another compound at the same retention time, 3) incorrect GC baselines (however, baselines were checked at least twice for each congener in all samples), or 4) some other unknown phenomena. These high numbers accounted for less than 4% of the total results and they randomly occurred (no pattern is observed). Therefore, it was decided to remove them from the rest of data. The criteria used for this purpose was five times higher dry deposition velocity values which were expected based on the typical PCB MMD values in Chicago reported by Holsen et al. (1991). Thus, the threshold for the physically impossible particulate PCB dry deposition velocity values was determined to be 25 cm/s. On the other hand, gas phase PCBs have significantly smaller deposition velocity values so the threshold value for the physically impossible PCB gas phase dry deposition was chosen to be 5 cm/s.

Regression tests were applied between average dry deposition of each sample and corresponding temperatures (°C), wind speeds as u_{10} (m/s). However, very poor regressions were observed from temperature and u_{10} applications to the dry deposition velocities. This lack of correlation observed from all phases (overall, gas and particle dry deposition).

As mentioned in the LOD section (in Chapter IV), LOD was calculated from the mean noise, in mass units, plus 3 standard deviations (3σ). In some instances there was a mass but it was not detected due to blank correction. In this study, the 2/3 of LOD value was used when a datum is missing (i.e. when either a flux or concentration was measured but the corresponding flux or concentration value was under the detection limit). During the V_d (= Flux / Conc.) calculations if both concentration and flux values were missing, they were not replaced with 2/3 LOD. The effect of this replacement on the V_d values will be discussed in detail in the following sections. In all cases the dry deposition velocity became smaller and in some cases the number of data points increased over 25% from the original (blank corrected) numbers.

5.4.1. Overall Dry Deposition Velocities. The overall dry deposition velocity was calculated using both the Σ-PCB concentration and total flux values (both gas and particulate phases). In other words, the dry deposition velocity was calculated by $V_{d,\ overall} = F_{total} / C_{total}$. No outlier test was performed; however, physically impossible values ($V_d >$ 10 cm/s) were removed (2.7% of the total number of values). Since this overall dry

deposition velocity is a combination of gas and particulate phase, this threshold V_d of 10 cm/s is very conservative and minimized data loss.

The average overall dry deposition velocity was calculated to be 1.1 ± 1.3 cm/s. This result is comparable to previously reported ones. For example, Holsen et al. (1991) reported a narrower range for the overall PCB dry deposition velocities (0.4 ~ 0.6 cm/s). Table 2.12 shows the some other available literature values. Using LOD values, the overall dry deposition velocity decreased to 0.8 ± 0.9 cm/s (The number of data points increased by about 10%). Figure 5.23 shows the average dry deposition velocity variations for each congener before and after LOD application.

5.4.2. Particle Phase Dry Deposition Velocities. Particle dry deposition velocities were obtained from the measured particle PCB fluxes and concentrations ($V_{d,particle}= F_{particle}/C_{particle}$). Particle depositional flux values were obtained from WSS_{1F} and plates while concentrations were obtained from filter of the high-volume air sampler. The calculated dry deposition velocities for particle PCBs were 5.2 ± 3.8 cm/s (range : 0.4 - 9.7) and 6.5 ± 5.0 cm/s (range : 1.4 - 10.5) for WSS_{1F} and plate samples, respectively. These two average dry deposition velocities are comparable to each other. Figure 5.24. illustrates the particle dry deposition variation during the sampling period and Figure 5.25. shows the deposition velocity variation for each congener. The variation in the dry deposition velocities is probably a direct function of meteorological conditions.

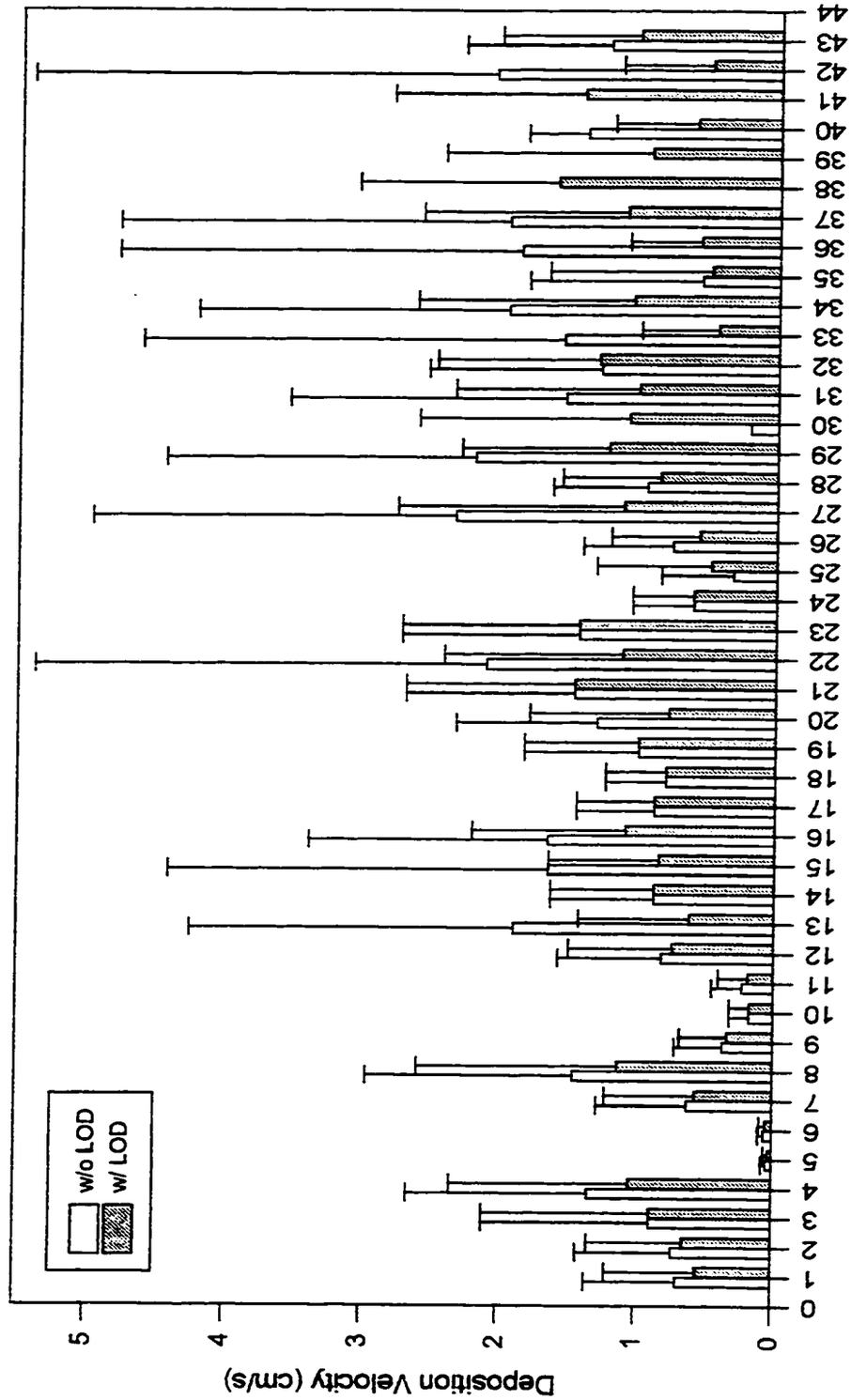

Figure 5.23. Overall Dry Deposition Velocities with and without LOD from WSS_{A-P}

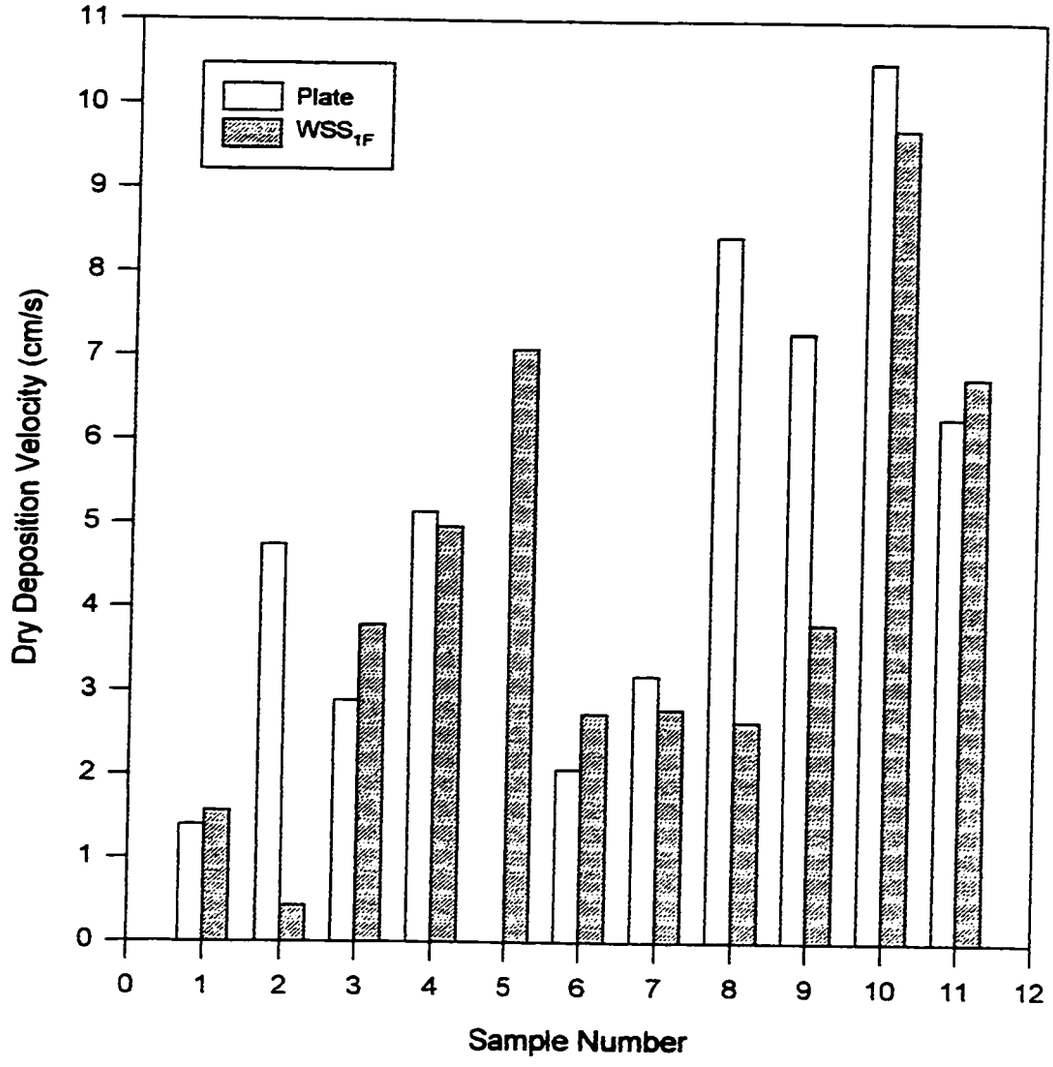

Figure 5.24. Particulate (WSS_{1F} and Plate) Dry Deposition Velocities

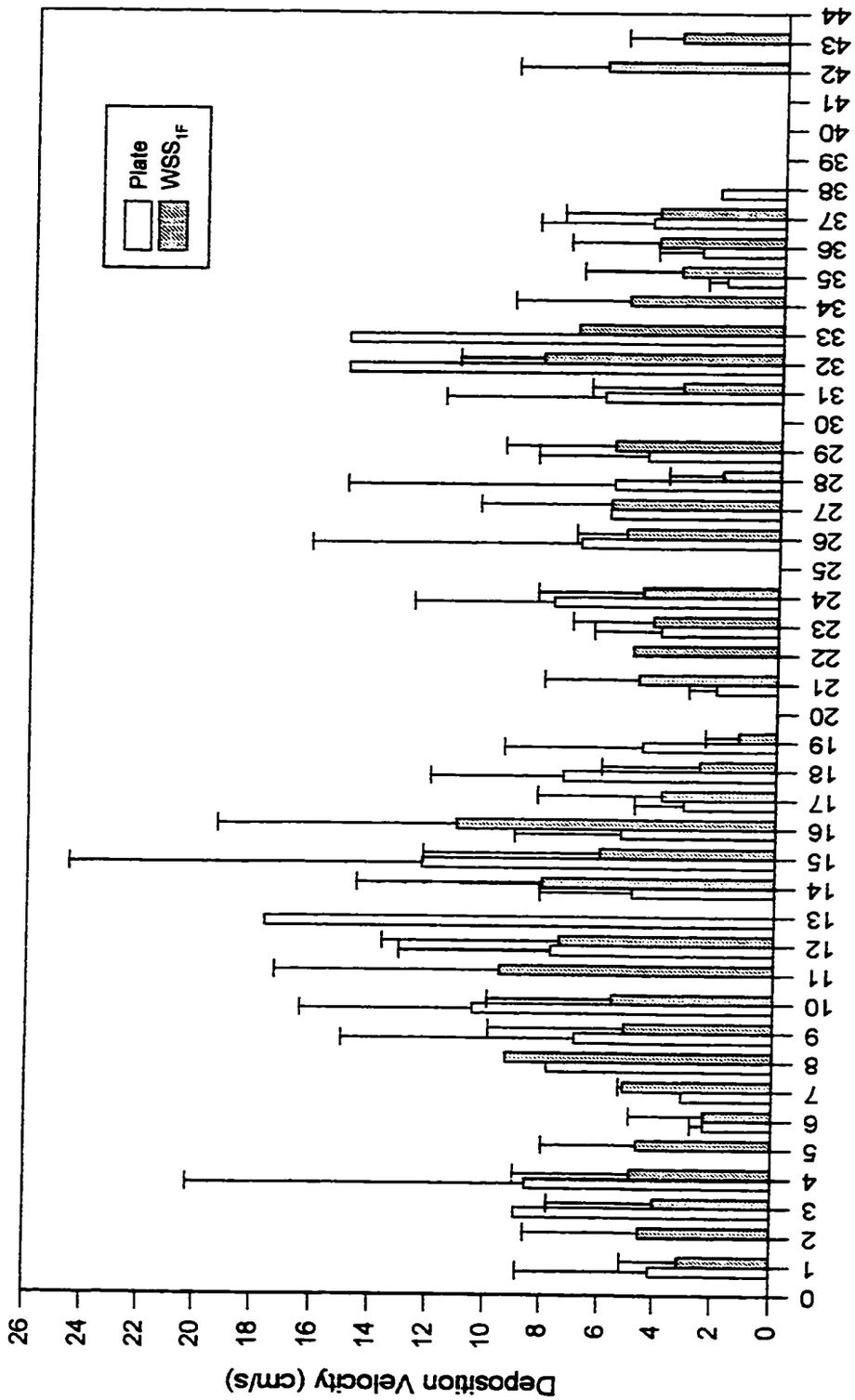

Figure 5.25. Particle (Plate and WSS$_{1F}$) Deposition Velocities of Each Congener

However, because of long sampling times these effects were masked. By using a large enough collection area, daily (or even shorter) samples may eliminate this masking problem.

The previously reported particle phase PCB dry deposition velocities were comparable to the value obtained from this study. For example, McClure (1976), Doskey (1981a) and Holsen et al. (1991) have published dry deposition values for particle phase PCBs of 0.91, 0.5 and 4.8 ~ 7.3 cm/s, respectively. Different experimental conditions and collector surfaces could be the reasons for the differences of these values. The work done by Holsen et al. (1991) was done with a technique very similar to this study and the results agree well. Another comparison can be done with the PAHs because PAHs are semivolatile organic compounds like PCBs and they were sampled simultaneously with PCBs in this study. The dry deposition velocity for particle PAH phase was about 6.7 ± 2.8 cm/s (average ± standard deviation) which agree well reasonably with the PCB results (Odabasi, personal communication). Figure 5.26 illustrates the variation in particle phase dry deposition of the PCB homologs.

When 2/3 LOD values were used for under detection limit values, the dry deposition velocities were calculated to be 4.5 ± 4.3 cm/s for WSS_{IF} and 4.8 ± 4.9 cm/s for plate samples. The increase in the data points amounted to more than 25% for both plate and WSS_{IF}. Figure 5.27 and 5.28 shows the particle dry deposition velocity variations for each congener with and without LOD application.

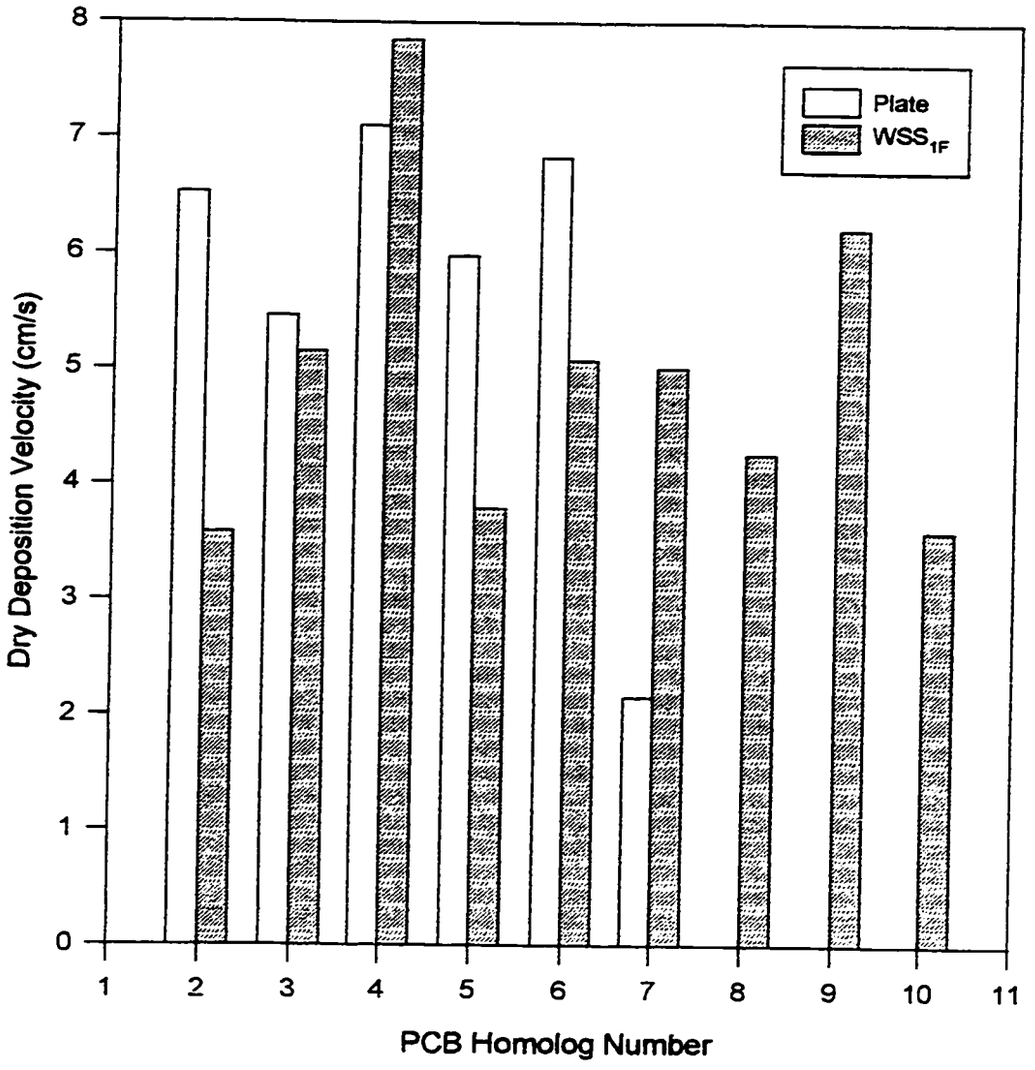

Figure 5.26. Particulate Dry Deposition Velocities for PCB Homologs

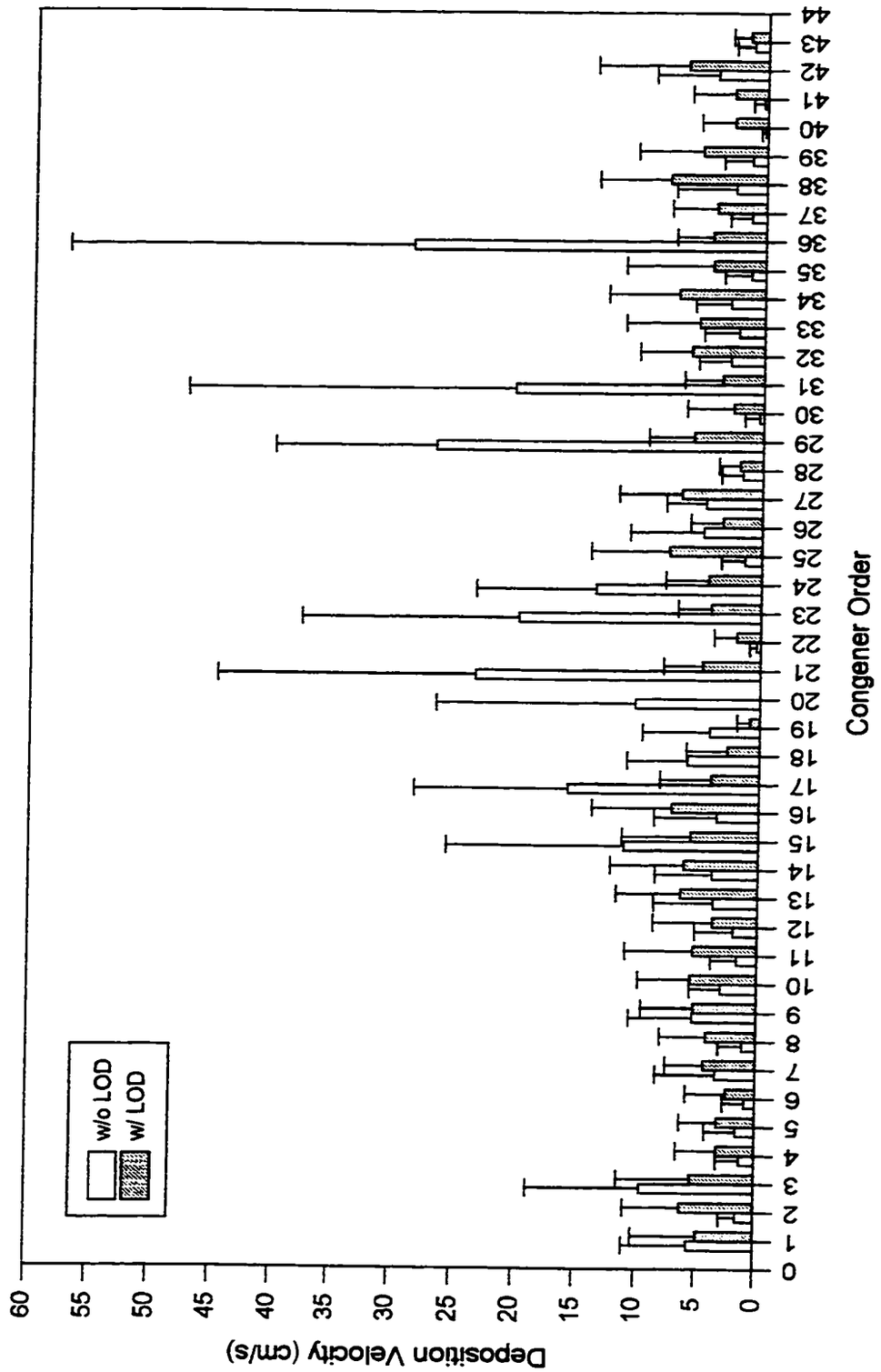

Figure 5.27. Particle Dry Deposition Velocities with and without LODs from WSS_{1F} Samples

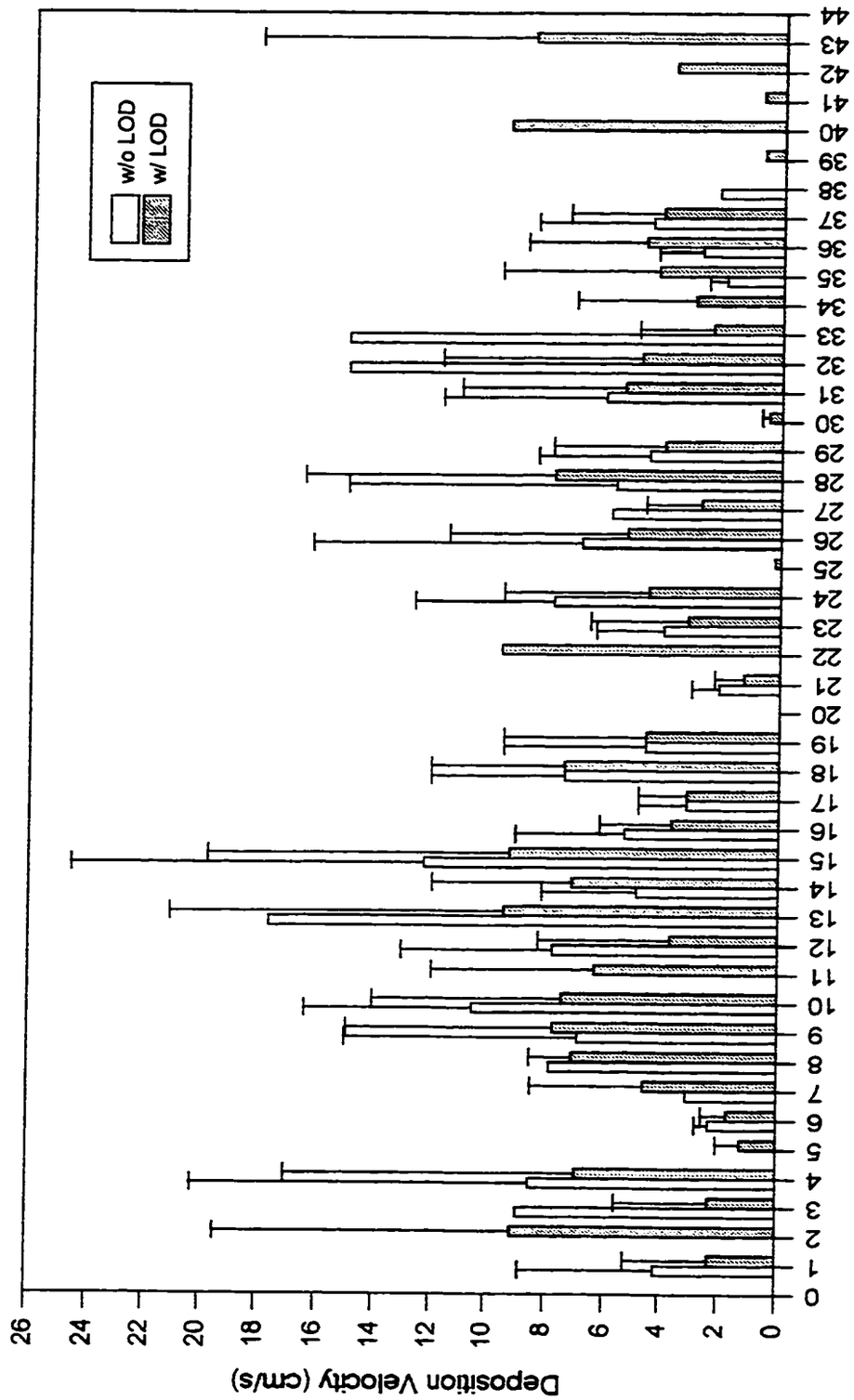

Figure 5.28. Particle Deposition Velocities with and without LODs from Plate Samples

In general, the result of this study suggest that PCBs have higher particle dry deposition velocities than is normally expected. Possible reasons might be: 1) Although the particle size distribution is one of the most important features controlling PCBs deposition velocities, only a little data exists on particle size distributions of PCBs (Baker et al., 1993). Chen et al. (1996) reported that the particle size distribution of PCBs had a bimodal size distribution and PCBs existed mainly in the coarse mode (d_p>2.5 μm) in the urban area. This conclusion supports the results obtained by Holsen et al. (1991) who studied PCB size distribution on coarse particles and based on their calculations, the coarse particles were an important contributor to the dry deposition burden. The calculated MMD (mass median diameter) of coarse particles associated with PCBs was about 25 μm. 2) Coarse particles are dominant in heavily populated cities and therefore, more chance for partitioning between coarse particles and PCBs is possible (Hoff et al., 1996). Similar to the findings of Holsen and Hoff, Sweet et al. (1993) stated that at City of Green Bay up to 50% of the particulate PCBs were associated with large particles (d_p = 2~10 μm). If this is the case for urban areas, then high dry deposition velocities for the particulate phase PCBs should be expected 3) Another explanation for PCBs and coarse particle partitioning in the urban areas can be explained by examining PAH behavior. PAH partitioning in the urban air would not be in equilibrium due to many local PAH sources. However, they are expected to be closer to the equilibrium with particles in the rural areas. PAHs in the rural samples showed higher association with the coarse particles than urban samples (Allen et al., 1996). Rural data indicate that at equilibrium more than 50% of PAHs would be attached with coarse rural particles (Allen et al., 1996). This tendency to associate with larger particles could be due to mechanical processes such as

atmospheric turbulence and dispersion (Baek et al., 1991). Since there are no point sources for PCBs to the atmosphere, they are theoretically in a steady state everywhere (like PAHs in the rural area). Thus, it is expected that PCBs will have high particle dry deposition velocities due to their association with coarse particles.

5.4.3. Gas Phase Dry Deposition Velocities. The gas phase overall PCB mass transfer coefficient (the gas phase PCB dry deposition velocity) was calculated by dividing the PCB gas flux by the ambient gas phase PCB concentration. The average overall mass transfer coefficient (MTC) for PCBs was calculated to be 0.68 ± 0.64 cm/s and 0.54 ± 0.51 cm/s for WSS_{A-P} (average water surface flux minus greased strip flux on the plates) and WSS_{1R}, respectively. Figure 5.29 shows the overall MTC during the sampling period and Figure 5.30 illustrates the average MTC values of each congener. The difference in MTCs was probably due to changes in meteorological conditions including temperature and wind speed. Figure 5.31 shows that the MTCs of PCB homologs and there is no trend between chlorine number and MTC.

When 2/3 LOD values were replaced for the values under detection limit values, the dry deposition velocities for gas phase were calculated to be 0.39 ± 0.48 cm/s for WSS_{1R} and 0.50 ± 0.64 cm/s for WSS_{A-P} samples. The number of data points increased about 35% in both cases. The gas dry deposition velocity variations for each congener before and after LOD application are shown in Figures 5.32 and 5.33.

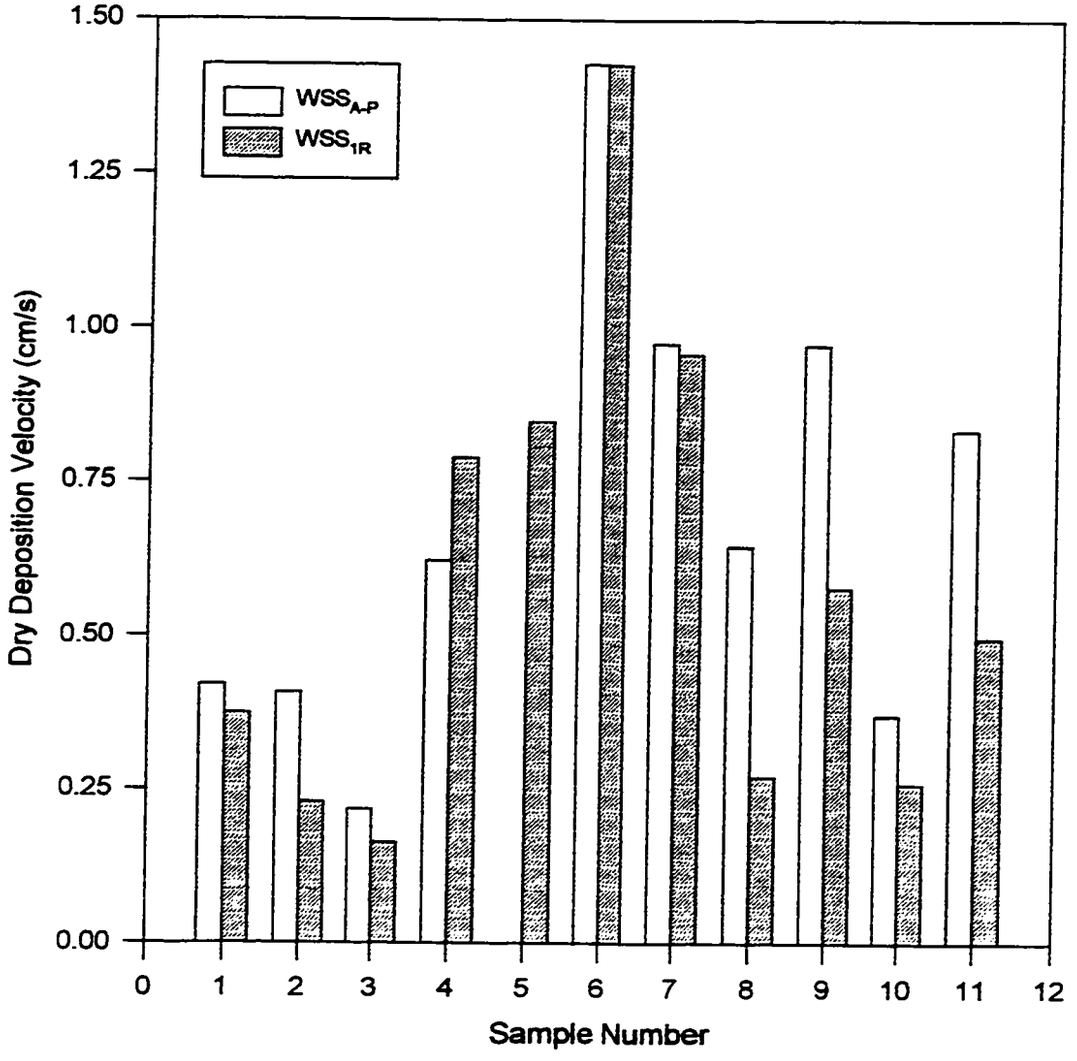

Figure 5.29. Gas (WSS_{A-P} and WSS_{1R}) Dry Deposition Velocities

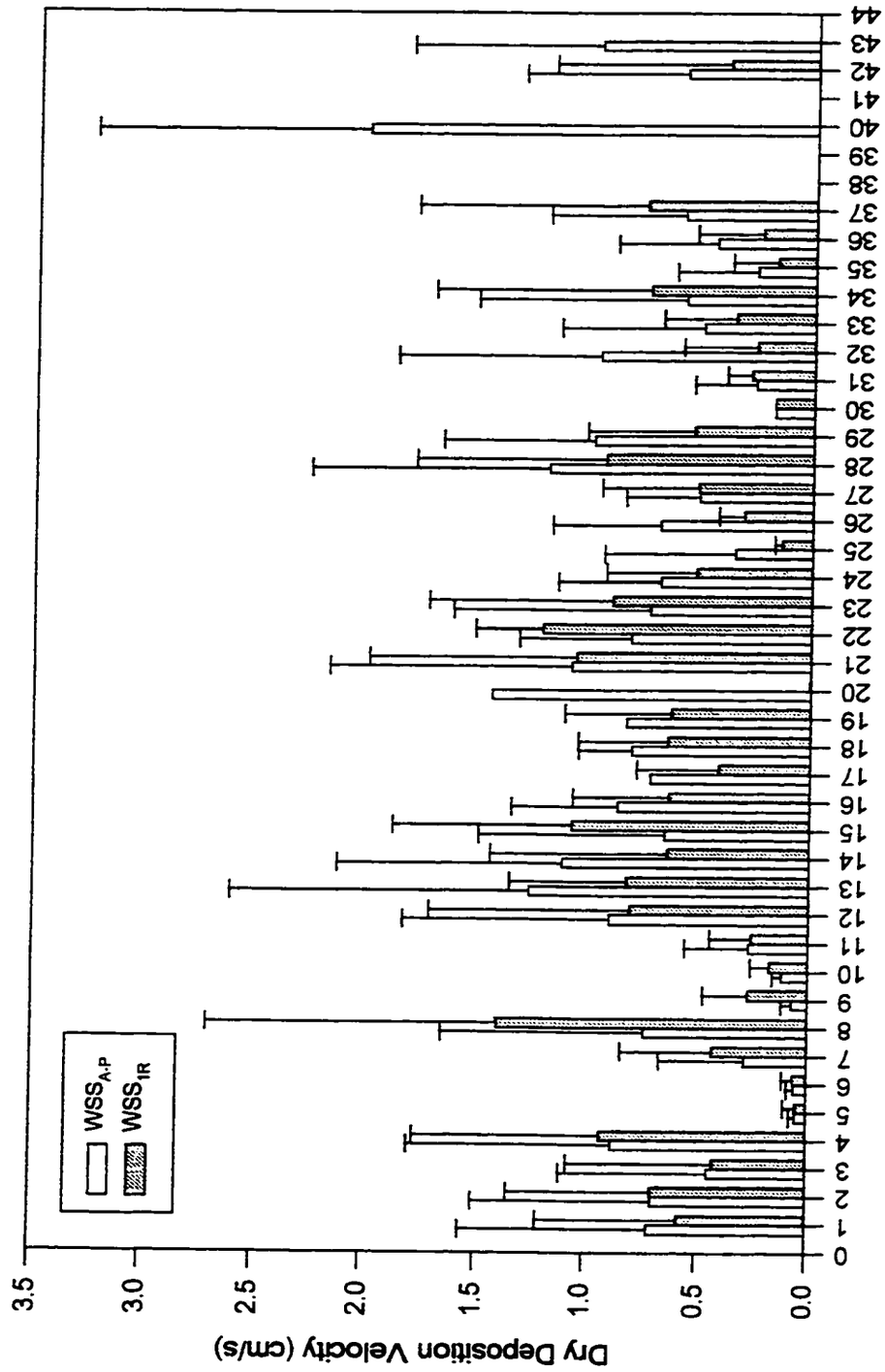

Figure 5.30. Gas (WSS$_{A-P}$ and WSS$_{IR}$) Dry Deposition Velocity of Each PCB Congener

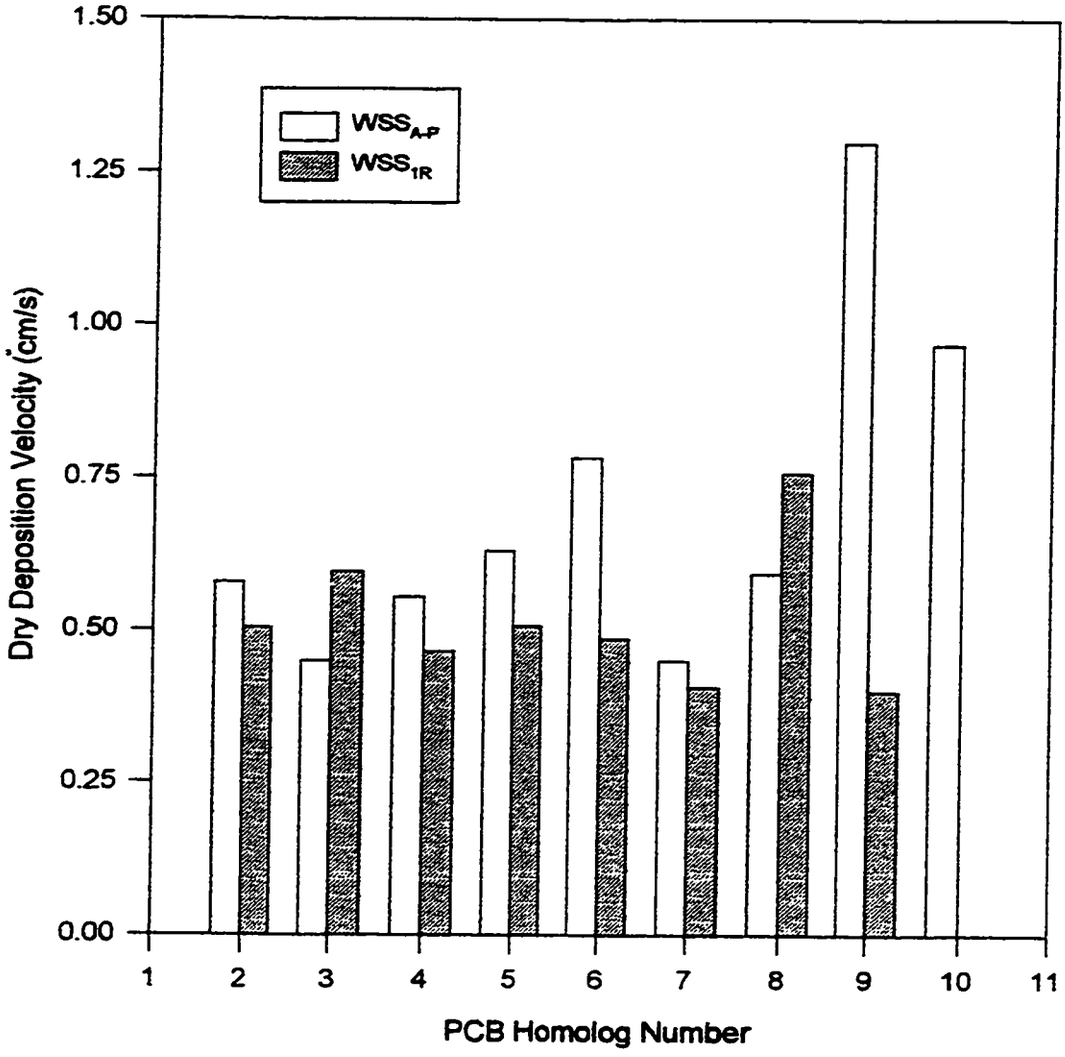

Figure 5.31. Gas Dry Deposition Velocities for PCB Homologs

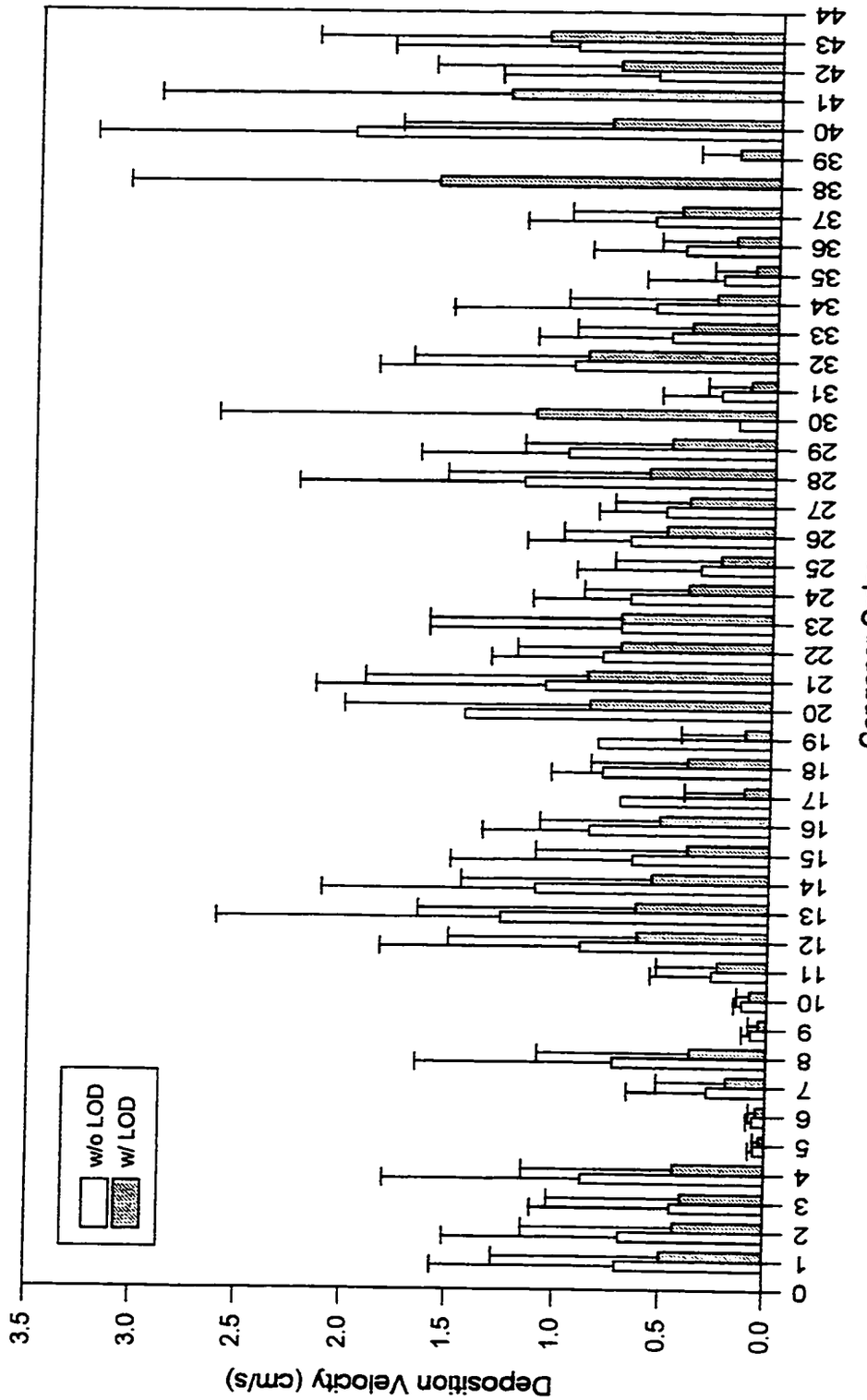

Figure 5.32. Gas Phase Dry Deposition Velocities with and without LODs from WSS_{A-P} Samples

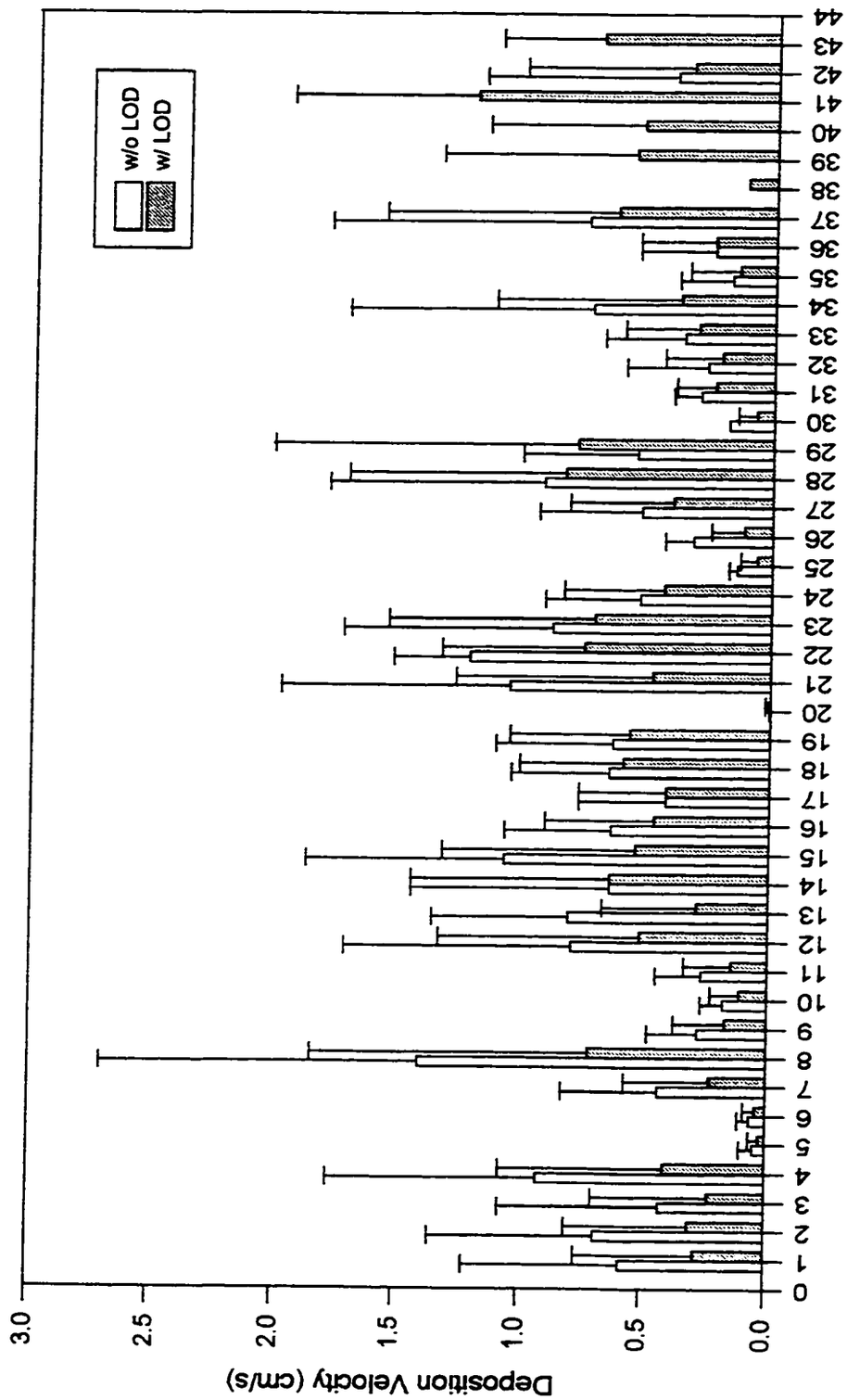

Figure 5.33. Gas Phase Dry Deposition Velocities with and without LODs from WSS_{1R} Samples

PAH MTC values obtained during this sampling program averaged about 0.7 ± 0.5 cm/s for WSS_{A-P} (average ± standard deviation) which is little higher but comparable to the PCB results (Odabasi, personal communication).

There is a distinct difference between particle and gas phase dry deposition velocities (Figure 5.34). The approximate ratio between particle and gas phase dry deposition velocities is about 10. This dissimilarity comes from the different deposition characteristics of gas and particle phases. In fact, this difference is not specific for PCBs but for almost all other species. Because gravitational settling becomes important for particles larger than one micron whereas the deposition of very small particles is controlled by Brownian movement and maybe their chemical interactions with the surface.

5.5. Two-film Theory and Models for Approximations of Mass Transfer Coefficients

The two-film gas exchange model will be used to calculate the overall mass transfer coefficients across the air-water interface of the WSS. The basis of the model is molecular diffusion between the phases (air and water film). The rate of PCB exchange across the air-water interface is mainly limited by the water film yet the air film also shows some resistance to this transfer.

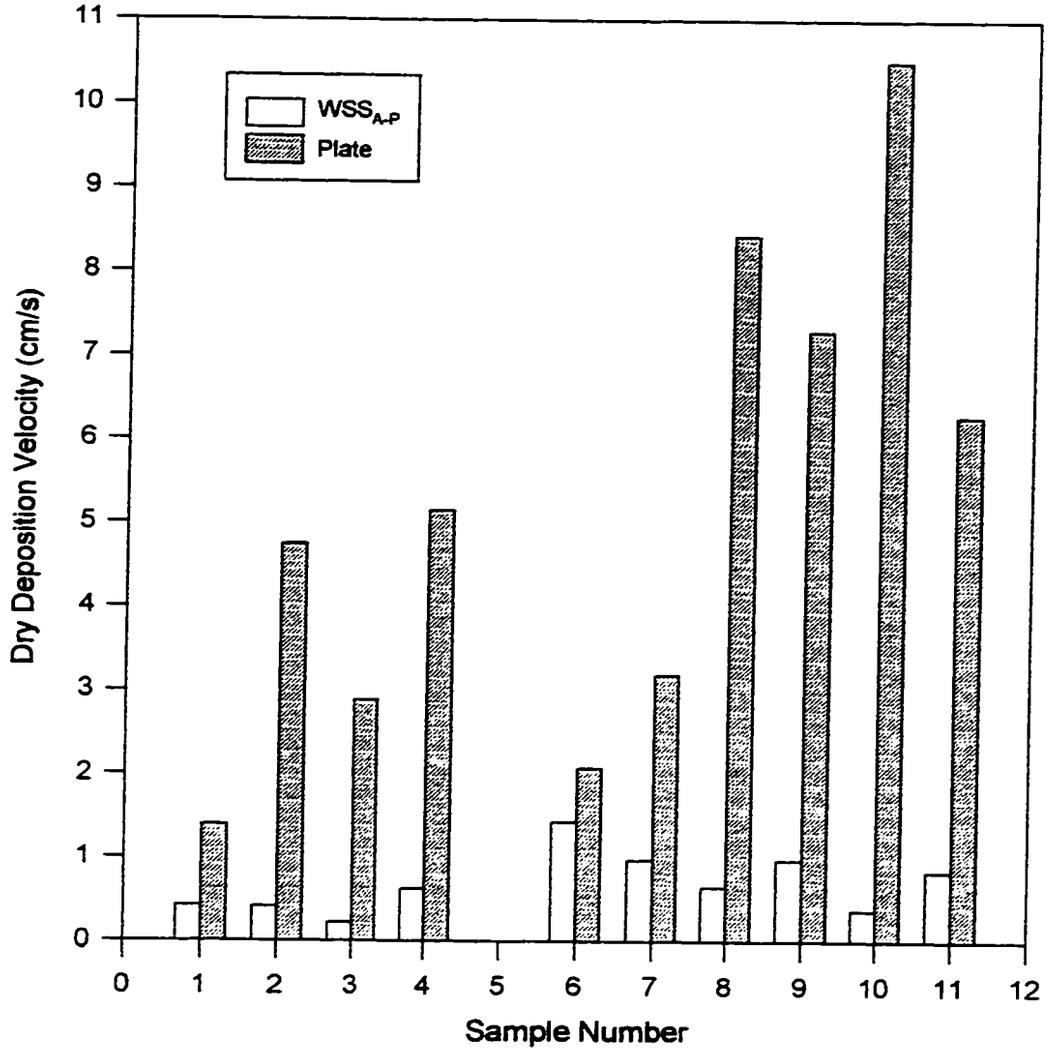

Figure 5.34. Gas (WSS_{A-P}) and Particulate (Plate) Dry Deposition Velocities for Each Sample

The PCB flux for the air-water interface can be calculated from the MTCs across the air and water films and the PCB concentration in the bulk air and water phases. The equations to explain this phenomena in general are as follows:

$$\text{Flux} = {}^{2}K_{A1} (C_a - C_a^{*}) \tag{5.4}$$

$$\text{Flux} = {}^{1}K_{A2} (C_w - C_w^{*}) \tag{5.5}$$

where,

$$1/{}^{2}K_{A1} = (1/{}^{2}k_{A1}) + (H/{}^{1}k_{A2}RT) \tag{5.6}$$

$$1/{}^{1}K_{A2} = (1/{}^{1}k_{A2}) + (RT/{}^{2}k_{A1}H) \tag{5.7}$$

$$C_a^{*} = C_w H/RT \tag{5.8}$$

$$C_w^{*} = C_a RT/H \tag{5.9}$$

${}^{2}K_{A1}$ (cm/s) is the overall air phase MTC across the air-water interface, ${}^{1}K_{A2}$ (cm/s) is the overall water phase MTC across the air-water interface, ${}^{2}k_{A1}$ (cm/s) is the individual air phase MTC, ${}^{2}k_{A1}$ (cm/s) is the individual water phase MTC, C_a (ng/m^3) is the gas phase PCB concentration in the ambient air, C_w (ng/m^3) is the PCB concentration in the water, C_a^{*} (ng/m^3) is the air concentration in equilibrium with the dissolved PCB concentration

in the water, C_w^* (ng/m^3) is the water concentration in equilibrium with the partial pressure of the PCB in the atmosphere, H (atm-L/mol) is the Henry's Law Constant which defines the equilibrium distribution of the PCBs in the air and water, R (0.08208 atm-L/mol-°K) is the ideal gas law constant, T (°K) is the absolute ambient air temperature. H can be calculated by the chemical's saturation vapor pressure, p^o (atm), divided by that compound's water solubility, S ($mole/m^3$) when low concentrations and ambient temperatures exist. The Henry's constant is a function of temperature and in this case the formulae suggested by ten Hulscher et al. (1992) was used to correct Henry's law constants for water temperature.

$$\log H_T = \log H_{298} + 8.76 - (2611/T) \text{ (ten Hulscher et al., 1992)} \qquad (5.10)$$

Henry's law constants decreased by a factor of about 2.5 for each 10 °C decrease in water temperature (Achman et al., 1993). Therefore, temperature decrease has a direct effect on the exchange process which occurs across the air and water interface. In water systems (including WSS), the net direction and magnitude of flux (either volatilization or absorption) would change with changing water temperature. H controls not only the equilibrium water concentration of PCBs ($C_w^* = C_a/H$) but also the magnitude of the individual gas film MTC (Hk_a/RT).

The overall MTC was calculated by using the gas phase concentrations obtained from high volume sampler and the gas phase dry deposition flux, WSS_{A-P} (average WSS flux minus plate (greased strip) flux) and WSS_{1R}. The PCB concentration in the water (C_w)

was assumed to be zero because the XAD-2 resin would remove all PCBs from the inflowing water. The temperature, wind speed, ambient PCB concentration and gas phase dry deposition flux were used to calculate the individual water phase MTC and overall PCB MTC.

Table 5.2 . lists the parameters used to calculate the MTC which includes concentrations of Σ-PCBs in the ambient air (gas phase), ambient air temperature, water temperature on the WSS, and wind speed.

Table 5.2. Summary of Variables Used in the MTC Calculations

Sample No	PCB Gas Phase Conc. (ng/m^3)	Air Temp. (^oC)	Water Temp. (^oC)	Wind Speed (m/s)
1	2.28	23.7	22.5	3.6
2	1.08	28.6	27.5	2.6
3	1.22	30.1	29.0	3.7
4	1.86	29.1	25.7	2.9
5	0.93	29.1	27.8	2.8
6	1.15	27.3	26.0	2.8
7	1.88	27.7	26.8	2.8
8	1.57	19.3	18.0	3.6
9	1.33	15.8	15.2	3.3
10	2.92	20.6	20.5	3.2
11	1.34	14.8	14.7	4.5

In this study, the water surface was used as dry deposition collection surface for the gas phase of PCBs; however, the incoming water to the WSS was clean and therefore, only absorption will be observed (at the maximum rate because $C_w = 0$ so that ΔC can be at its

maximum). Mass transfer between air and water depends on wind speed, temperature of air and water, concentrations of air and water, water characteristics (presence of other interfering chemicals) and characteristics of the compound (physical and chemical) as well as location (Liss, 1983; Bidleman and McConnell, 1995). In this study, PCB congeners were employed to calculate the magnitude of their transfer rates to the water surface.

Since the incoming water was PCB free (QA/QC Chapter), this water should have been stayed there as short as possible in order not to loss any deposited PCBs due to volatilization. With the pump at its highest rate, the retention time of water on the WSS was about 3 minutes. This 3 minutes was a reasonable time to minimize evaporative PCB losses. Therefore, it was checked whether in this 3 minute retention time PCBs can reach their equilibrium with the atmosphere because if this was the case, the background concentration assumption, C_w was negligible, would not be held. Based on the considerations of obtained flux, collection area (WSS area), collection time (3 minutes), ambient air concentrations, dimensionless Henry's Law Constants, and volume of the water on which the collection occurred, the average retention time needed for the equilibrium was calculated to be about 43 minutes. Since this value is much higher than real retention time (3 minutes) on the WSS, the assumption of the C_w was negligible during the sampling is satisfied.

As mentioned above, the model used most often for describing the exchange of contaminants at the interface of the air and water is the stagnant two-film model

developed by Whitman (1923). The rate of this interface phenomena is calculated by using an accurate H, individual water phase MTC (k_w), individual air phase MTC (k_a) and bulk air (vapor phase) and water concentrations as well as other environmental parameters (temperatures of air and water, wind speed). If the corrections are made for molecular diffusivities, the MTCs for other compounds (water, carbon dioxide, sulfur hexa fluoride, oxygen) can be used to calculate PCB MTC because the movement across the stagnant films is due to molecular diffusion. Many researchers have developed relationships between the individual MTCs (k_a and k_w) and wind speed. In the following subsections, the determination of these individual MTCs in this study and their calculations with the available models will be discussed.

5.5.1. Individual Air Phase Mass Transfer Coefficient (k_a). Conceptually there are two films that exist between the bulk air and bulk water phases and in this section the air phase film will be discussed. The available models were given in Table 2.17. In this study individual PCB gas phase MTCs ($k_{a,PCB}$) for the WSS were correlated with the water MTC ($k_{a,\ H2O}$). One of the model used in this study is an empirical equation provided by Thibodeaux (1979) based on measurements of water evaporation. This empirical equation includes both natural and forced evaporation. The individual PCB air phase MTC across the air film can be calculated as follows (Thibodeaux, 1979; Yi et al., 1995):

$$^2k_{PCB1} = {}^2k_{PCB1N} + {}^2k_{PCB1F} = [(0.14Gr_{B1}{}^{1/3}+0.664Re_L{}^{0.5})D_{PCB1}Sc_{PCB1}{}^{1/3}] / (L) \quad (5.11)$$

for laminar flow, and

$$^{2}k_{PCB1} = {}^{2}k_{PCB1N} + {}^{2}k_{PCB1F} = [(0.14Gr_{B1}{}^{1/3}+0.036Re_{T}{}^{0.8})D_{PCB1}Sc_{PCB1}{}^{1/3}] / (L) \quad (5.12)$$

for turbulent flow

where :

$$Gr_{B1} = (g\zeta_{B1}L^{3}(y_{Bi} - y_{B}))/\nu^{2} \quad (5.13)$$

$$Sc_{PCB1} = \nu / D_{PCB1} \quad (5.14)$$

$$Re_{T} = u_{10} L_{T} / \nu , \qquad Re_{L} = u_{10} L_{L} / \nu \quad (5.15)$$

$$\zeta = -1 / [y_{Bi} + M_{1} / (M_{B} - M_{1})] \quad (5.16)$$

Gr_{B1} (unitless) is the Grashof number, Sc (unitless) is the Schmidt number, L (m) is the total length of a deposition surface, g (9.8 m/s^2) is gravitational acceleration, ζ_{B1} (unitless) is the concentration coefficient of volume expansion, y_B (unitless) is the water vapor concentration (i-interface), ν (m^2/s) is the kinematic viscosity of air, D_{PCB1} (m^2/s) is the diffusion coefficient of PCB in the air, u_{10} (m/s) is the wind speed at 10 m above the water surface, y_B (unitless) is the water vapor concentration (i-in the interface)

($RHxP_s/P_T$), M_I (28.9 g/mol) is the molecular weight of air, M_B (18 g/mol) is the molecular weight of water.

To apply these equations the water surface area was divided into nine segments (seven of them have 5 cm width and two of them have 2 cm width). Then, individual PCB air phase MTCs were calculated over each segment based on turbulent or laminar flow regimes based on the Reynolds numbers. The critical Reynolds number (between turbulent and laminar flow) for the flat plates varies in the literature. Thibodeaux (1979) and Reist (1993) reported critical Reynolds numbers (ranging from 80,000 to 100,000) and Yi (1995) applied those Reynolds numbers to the WSS in his study and he determined that the critical Reynolds number was about 95,000. Based on the turbulent or laminar flow conditions, different theoretical equations were used to calculate the individual air phase MTC. For example, if Reynolds number is higher than critical value ($Re > 95,000$), the flow regime is turbulent (Eqn. 5.5.1.1) whereas when Reynolds number is less than 95,000 ($Re < 95,000$), then flow is in the laminar flow regime (Eqn. 5.5.1.2). Based on the length of each segment (L: the length of deposition surface) and above given relationships (equations 5.5.1.1 and 5.5.1.2), the individual air phase MTCs were calculated. These different areas for each segment was multiplied by the corresponding MTC and added together. Then, this sum was divided by the total area of nine segments in order to calculate the area weighted average individual air phase MTC. This calculation is shown as follows:

$$\text{Area weighted average } k_a = (\Sigma (k_a)_i \times (\text{Area})_i) / (\Sigma \text{ Area}) \qquad (5.17)$$

where i: segment number, $(\text{Area})_i$ is the area of i^{th} segment. This k_a value was calculated for each sample. u_{10} and k_a were correlated to each other and the relationship between u_{10} and k_a values for the WSS is shown in Figure 5.35.

This empirical model which is the sum of natural and forced evaporation has some improvements over other models (Table 2.17.). While other models are related only to wind speed, this empirical model contains both wind speed, relative humidity and temperature effects which is directly related to diffusivity and Schmidt number (Sc).

As an alternative to using Thibodeaux model evaporation fluxes from the WSSs were measured to determine air side individual mass transfer coefficient (k_a) (water evaporation has only air side resistance). The amount of evaporated water from the water surface was determined by measuring its volume (details were given in the Materials and Methods Chapter). The individual air phase water MTC ($k_{a,\,H2O}$ (cm/s)) was calculated using the flux of evaporated water and the water concentration difference between the stagnant layer and the ambient air (relative humidity ($0 \leq RH \leq 1$)). The equation used for $k_{a,\,H2O}$ is given by:

$$k_{a,\,H2O} = \text{Flux} / (C_a^{*} - C_a) = \text{Flux} / (C_a^{sat} - RH\, C_a^{sat}) = \text{Flux} / C_a^{sat} (1-RH) \qquad (5.18)$$

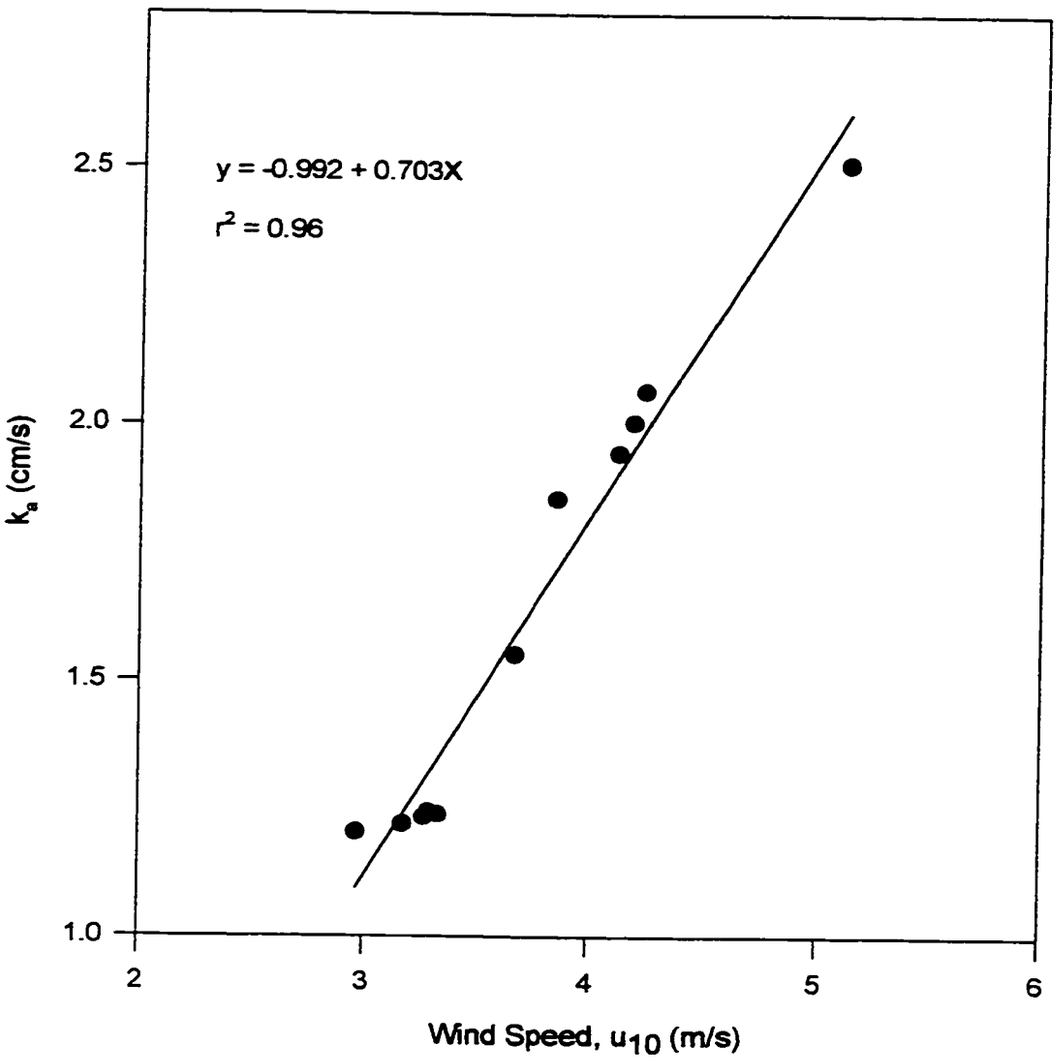

Figure 5.35. The Variation of k_a with Wind Speed (Thibodeaux Model)

where C_a (mol/cm^3) is the water vapor concentration in the ambient air, C_a^{sat} (mol/cm^3) is the saturation water vapor concentration across the air-water interface. The results from the above equation is direct a reflection of the characteristics of the WSSs and the meteorological conditions (temperature, wind speed, RH, wind direction) over the sampling period. Since it has been proven by many researchers (Table 2.17) that k_a is directly related to the wind speed, the calculated k_a values from this study were correlated to u_{10} (m/s) and corrected to 20 °C. The proposed new equation is then:

$$k_{a,\,H2O} = 0.815 + 0.649\ u_{10} \quad (r^2 = 0.33) \tag{5.19}$$

This formula is specific for the WSS and it is based on the field measurements rather than laboratory studies in which the flow pattern over the surface is typically laminar.

The correlation coefficient (r = 0.57) value shows some scatter in this linear relationship (Figure 5.36). The possible reasons for this scattered data could be: 1) the wind speed was averaged for the 5 day (minimum) sampling period for each sample. Therefore, rather than only wind speed , other parameters become important on this relationship. It was reported that if 15 minute periods were considered rather than 24 hours averages, the percent in daily fluxes integrated using wind speeds would increase 13 - 37% for PAHs (Gustafson and Dickhut, 1997). 2) The average wind speeds did not fluctuate much in the samples. This narrow range of wind speeds masked the correlation between wind speed and $k_{a,\,H2O}$ values, other less significant parameters (like temperature and RH) become important in this correlation and therefore, the correlation between k_a and wind speed

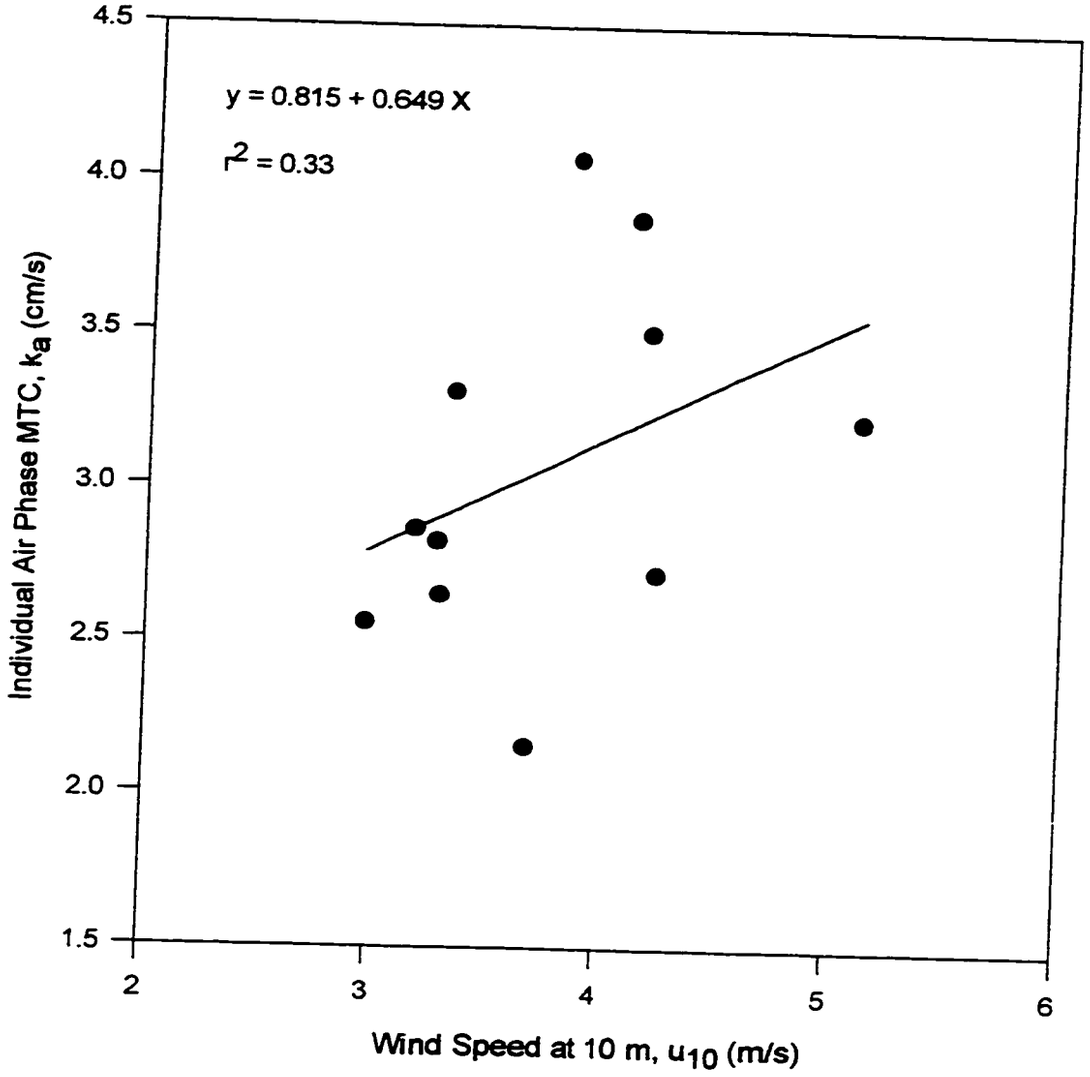

Figure 5.36. The Variation of k_a with Wind Speed (Evaporation Experiment)

(u_{10}) decreases and 3) the k_a values obtained from evaporation flux were correlated only with wind speed. In fact, this relationship also depends on ambient air temperature and relative humidity (RH).

The WSS was also used to perform an oxygen experiment in order to determine $k_{w,\,O2}$ values and their relationship with wind speed. Some very windy and some calm days were sampled. The results will be discussed in detail in the following section. Briefly, the results showed that the correlation between $k_{w,\,O2}$ and u_{10} (m/s) was over 90%. This suggests that only a small portion of this correlation was related with other parameters (meteorological (temperature, RH) or operational) due to short sampling periods (less than 30 minutes with ~8 seconds wind speed readings).

Wind speeds are important in the MTC calculations because it was shown that MTCs were linearly correlated with the wind speeds (as shown in Table 2.17). The wind speeds were measured at about 2.5 m above the water surface during the sampling period. These wind speeds were corrected to 10 m for use in the individual air phase MTC model equations by means of the following correlation (Yi, 1995; Achman et al., 1993; Schwarzenbach et al., 1992):

$$u_z = [(\ln z + 8.1) / 10.4]\, u_{10} \qquad (5.20)$$

$$\text{then,} \qquad u_{10} = u_z / [(\ln z + 8.1) / 10.4] \qquad (5.21)$$

where u_{10} (m/s) is the wind speed at 10 m above the water surface, u_z (m/s) is the wind speed measured at distance z (m) from the water surface, and a boundary roughness height of 0.03 cm is assumed. The influence of wind speed on the calculated flux is high for example when wind speed increased from 1 m/s to 4 m/s, the volatilization flux increased from 90 ng/m^2-d to 800 ng/m^2-d (Achman et al., 1993). This is an expected result as predicted by the formula in Table 2.17. When wind speed increases both k_a and k_w increases (resistance decreases) and as a result of this, the flux increases.

Diffusion coefficient conversion from one temperature to another one was performed by considering a known diffusion coefficient and the temperature as follows (Thibodeaux, 1979, Schwarzaenbach et al., 1993):

$$D_{a,\,H2O}\,(@T_2) = D_{a,\,H2O}\,(@T_1)\,[T_2 / T_1]^{1.75} \quad \text{(in the air phase)} \qquad (5.22)$$

where,

$D_{a,\,H2O}$: Diffusivity coefficient of H_2O in the air, cm^2/s,

T_1 ,T_2 : Reference and targeted temperatures, °K.

The vapor pressure of water was calculated in inHg by (Thibodeaux, 1979),

$$P_s = 0.0295\,[\exp(21.66-(5431.3/T))]RH \qquad (5.22)$$

where,

T : Temperature, °K,

RH : Relative humidity, percent.

The molecular diffusivities for PCBs were calculated by using the Fuller Equation for air phase diffusion (Thibodeaux, 1979 and Schwarzenbach et al., 1993) as follows;

$$D_{a,PCB} = 10^{-3} \{[T^{1.75} (m_{Air}^{-1} + m^{-1})]^{1/2} \} / \{P [V_{air}^{1/3} + V_{PCB}^{1/3}]^2\} \text{ (Fuller Eqn.)} \quad (5.23)$$

where,

$D_{a, PCB}$: PCB diffusivity coefficient in the air, cm^2/s,

m_{Air} : Average molecular mass of air, 28.9 g/mol,

m : Molecular mass of PCB congener, g/mol,

P : 1 atm,

V_{air} : Average molar volume of gas in air, 20 cm^3/mol,

V_{PCB} : Average molar volume of PCB congener, cm^3/mol,

Individual water mass transfer coefficient (MTC) in the air ($k_{a, H2O}$) was correlated with PCB mass transfer coefficient ($k_{a, PCB}$) using the air phase diffusivities of water and PCBs ($D_{a,PCB}$, $D_{a, H2O}$). The relationship between these two MTC can be expressed as follows:

$$k_{a, PCB} = k_{a, H2O} [D_{a,PCB} / D_{a, H2O}]^{0.61} \quad (5.24)$$

The expected exponent in two-film theory is equal to one. However, in this equation it is equal to 0.61 due to experimental data (Hornbuckle et al., 1994).

The proposed model (Eqn.'s 5.11. and 5.12) for this study was used by Yi (1995) for SO_2. His results showed that measured and modeled values were in agreement. In this study, the above model (Eqn.'s 5.11 and 5.12) gave some of the highest predicted k_a values for the PCB congeners. Table 5.3. summarizes the calculated $k_{a,PCB}$ values for all of the available models. The models were calculated for each sample separately and the average of all samples is presented in Table 5.3.

The overall average $k_{a,PCB}$ values changed between 0.18 cm/s (from Sverdrup model (1942)) and 1.08 cm/s (from evaporation experiment study-this study) for PCB # 8. In general, when the molecular weight of the PCB congener increases, the calculated $k_{a,PCB}$ values decreases. This change was about 17% for all models. This change is reasonable because 1)when the molecular weight of the PCB congeners decreases their tendency to be in the air increases due to their higher vapor pressure values and 2) diffusivities decreases as MW increases. Therefore, air side resistance (resistance = $1/k_{a,PCB}$) will decrease. Based on the models developed (modified) in this study, the percentage of air side resistance in total resistance increased from the lightest to heaviest congeners.

Table 5.3. Calculated $k_{a,\ PCB}$ (cm/s) Values From Available Models

Congener	Evaporation (this study)	Thibodeaux	Yi	Schwarzenbach	Sverdrup	Penman	Rohwer	Liss	Munnich	Mackay and Yuen
8	1.26	0.64	1.18	0.41	0.22	0.56	0.31	0.31	0.46	0.28
18	1.22	0.62	1.15	0.40	0.21	0.55	0.30	0.30	0.45	0.27
15	1.26	0.64	1.18	0.41	0.22	0.56	0.31	0.31	0.46	0.28
16	1.22	0.62	1.15	0.40	0.21	0.55	0.30	0.30	0.45	0.27
31	1.22	0.62	1.15	0.40	0.21	0.55	0.30	0.30	0.45	0.27
28	1.22	0.62	1.15	0.40	0.21	0.55	0.30	0.30	0.45	0.27
33	1.22	0.62	1.15	0.40	0.21	0.55	0.30	0.30	0.45	0.27
22	1.22	0.62	1.15	0.40	0.21	0.55	0.30	0.30	0.45	0.27
52	1.19	0.60	1.12	0.39	0.21	0.53	0.29	0.29	0.44	0.26
49	1.19	0.60	1.12	0.39	0.21	0.53	0.29	0.29	0.44	0.26
47/48	1.19	0.60	1.12	0.39	0.21	0.53	0.29	0.29	0.44	0.26
44	1.19	0.60	1.12	0.39	0.21	0.53	0.29	0.29	0.44	0.26
42/37	1.19	0.60	1.12	0.39	0.21	0.53	0.29	0.29	0.44	0.26
74	1.19	0.60	1.12	0.39	0.21	0.53	0.29	0.29	0.44	0.26
66/95	1.16	0.59	1.09	0.38	0.20	0.52	0.29	0.28	0.43	0.25
60	1.19	0.60	1.12	0.39	0.21	0.53	0.29	0.29	0.44	0.26
101	1.16	0.59	1.09	0.38	0.20	0.52	0.29	0.28	0.43	0.25
99	1.16	0.59	1.09	0.38	0.20	0.52	0.29	0.28	0.43	0.25
97	1.16	0.59	1.09	0.38	0.20	0.52	0.29	0.28	0.43	0.25
81/87	1.16	0.59	1.09	0.38	0.20	0.52	0.29	0.28	0.43	0.25
77/110	1.16	0.59	1.09	0.38	0.20	0.52	0.29	0.28	0.43	0.25
82	1.16	0.59	1.09	0.38	0.20	0.52	0.29	0.28	0.43	0.25
149/123	1.14	0.58	1.07	0.37	0.20	0.51	0.28	0.28	0.42	0.25
118	1.16	0.59	1.09	0.38	0.20	0.52	0.29	0.28	0.43	0.25
114	1.16	0.59	1.09	0.38	0.20	0.52	0.29	0.28	0.43	0.25
105	1.16	0.59	1.09	0.38	0.20	0.52	0.29	0.28	0.43	0.25
141	1.14	0.58	1.07	0.37	0.20	0.51	0.28	0.28	0.42	0.25
137	1.14	0.58	1.07	0.37	0.20	0.51	0.28	0.28	0.42	0.25
138/163	1.14	0.58	1.07	0.37	0.20	0.51	0.28	0.28	0.42	0.25
126	1.16	0.59	1.09	0.38	0.20	0.52	0.29	0.28	0.43	0.25
187	1.11	0.56	1.04	0.36	0.19	0.50	0.27	0.27	0.41	0.24
128	1.14	0.58	1.07	0.37	0.20	0.51	0.28	0.28	0.42	0.25
185	1.11	0.56	1.04	0.36	0.19	0.50	0.27	0.27	0.41	0.24
171	1.11	0.56	1.04	0.36	0.19	0.50	0.27	0.27	0.41	0.24
156	1.14	0.58	1.07	0.37	0.20	0.51	0.28	0.28	0.42	0.25
180	1.11	0.56	1.04	0.36	0.19	0.50	0.27	0.27	0.41	0.24
200	1.09	0.55	1.02	0.35	0.19	0.49	0.27	0.27	0.40	0.24
169	1.14	0.58	1.07	0.37	0.20	0.51	0.28	0.28	0.42	0.25
199	1.09	0.55	1.02	0.35	0.19	0.49	0.27	0.27	0.40	0.24
207	1.07	0.54	1.00	0.35	0.19	0.48	0.26	0.26	0.39	0.23
205	1.09	0.55	1.02	0.35	0.19	0.49	0.27	0.27	0.40	0.24
206	1.07	0.54	1.00	0.35	0.19	0.48	0.26	0.26	0.39	0.23
209	1.05	0.53	0.99	0.34	0.18	0.47	0.26	0.26	0.39	0.23

5.5.2. Individual Water Phase Mass Transfer Coefficient (k_w). The WSS used in this study is not an exact representation of the lakes or wind tunnel studies used to develop the other available models. In order to determine the specific mass transfer conditions in the WSS, oxygen transfer experiments were performed. In these experiments oxygen free distilled water was added into the WSS and dissolved oxygen (DO) was monitored with time. Oxygen was used because its mass transfer is controlled by water phase resistance. Measured wind speeds were corrected to u_{10} by applying the equations (Eqn. 5.20 and 5.21) given in section 5.5.1.

The amount of oxygen transferred into the WSS water was measured by a DO meter. The individual water phase MTC ($k_{w, O2}$) was determined using the measured oxygen transfer (flux) and the saturation concentration. The oxygen flux was calculated by:

$$F = [(C_i - C_e)\, V] / [A\, t] \qquad (5.25)$$

where C_i (mg/L) and C_e (mg/L) are the water DO concentrations at the beginning and at the end of the interval, respectively. V (L) is the volume of water, A (m^2) is the collection area, and t (minute) is the sampling time

The equation used for $k_{w, O2}$ calculation is:

$$k_{w, O2} = \text{Flux} / (C_a^{sat} - C) \qquad (5.26)$$

where C (mg/L) is the average DO concentration in the water for that calculation period, C_a^{sat} (mg/L) is the saturation DO saturation concentration in water. The results from above equation are a direct reflection of the characteristics of the WSS under the different wind speeds. It has been shown by many researchers (Table 2.18) that k_w is proportional to wind speed. Based on WSS oxygen experiments, the relationship between u_{10} (m/s) and k_w (cm/s) is given in Figure 5.37. The obtained regression equation is as follows:

$$k_{w,O2} = 4.794x10^{-4} + 5.377x10^{-5}\, u_{10} + 6.229x10^{-5}\, u_{10}^2 \quad (r^2 = 0.91) \qquad (5.27)$$

Another method used to calculate the individual water-side MTC is the oxygen absorption method for well mixed environments. The equation is given as follows:

$$\ln[(C_{w,O2}^{sat} - C_w)/(C_w - C_w^{initial})] = -k_{abs.}t \qquad (5.28)$$

where $C_{w,O2}^{sat}$ (mg/L) is the oxygen saturation concentration in water, C_w (mg/L) is the dissolved oxygen concentration at time t, $C_w^{initial}$ (mg/L) is the initial dissolved oxygen concentration, $k_{abs.}$(1/second) is the absorption coefficient and t (second) is the time. Since $k_{abs.}$ has a unit of "1/time", it was converted $k_{w,O2}$,"length/time", by multiplying by V/A, where V (cm^3) is the volume of water in the system and A (cm^2) is the surface area. Then, $k_{w,O2}$ is correlated with u_{10} (m/s). The relationship obtained is as follows:

$$k_{w,O2} = 4.350x10^{-4} + 1.318x10^{-4}\, u_{10} + 5.538x10^{-5}\, u_{10}^2 \quad (r^2 = 0.88) \qquad (5.29)$$

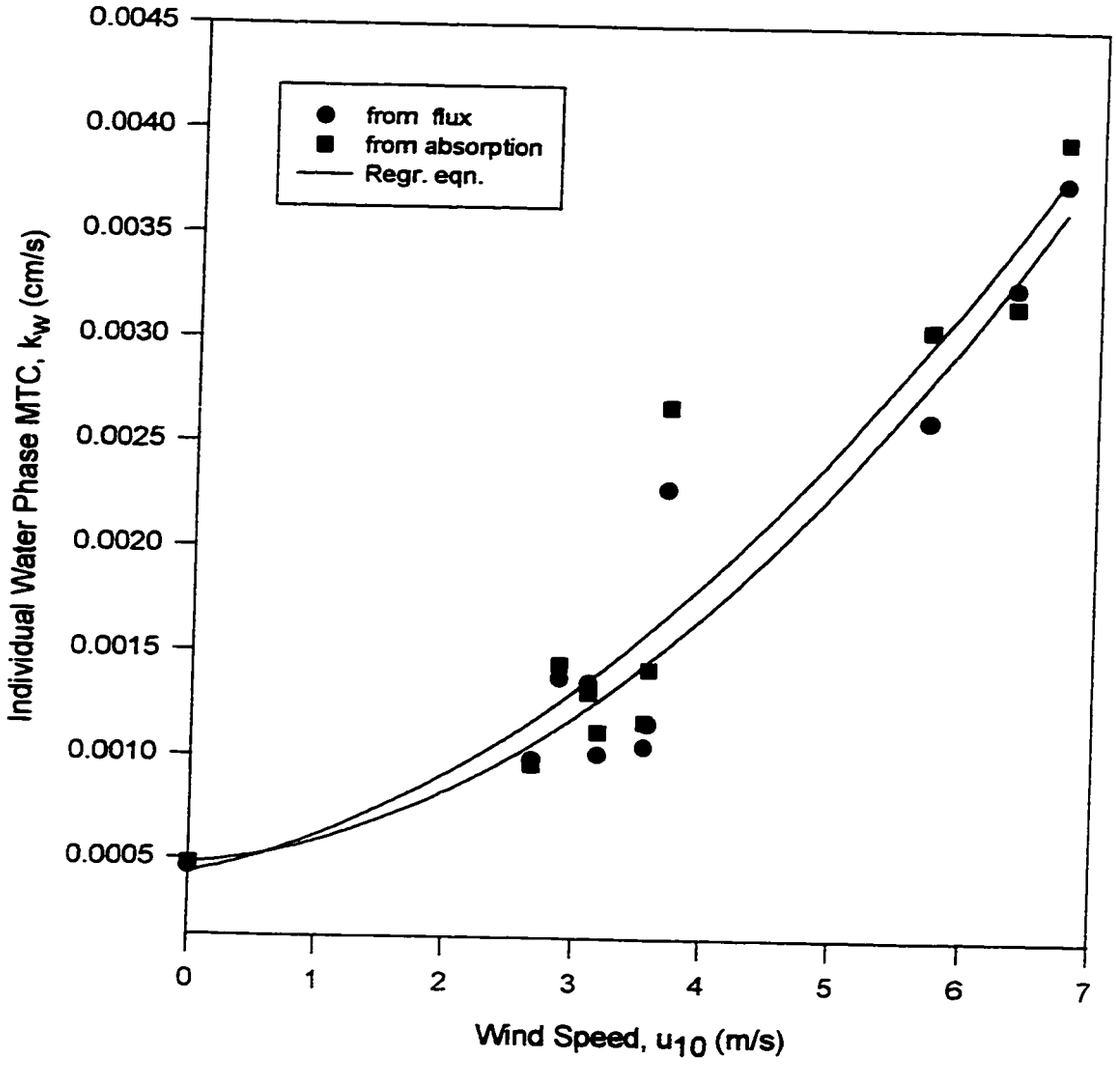

Figure 5.37. The Variation of k_w with Wind Speed (Oxygen Experiment)

In a manner similar to the individual air phase MTC, a relationship has been proposed to relate water side MTCs between oxygen and PCBs. It is based on experiments with SF_6 whose volatilization was correlated with wind speed in the lakes (Hornbuckle et al., 1994).

$$k_{w,PCB} = k_{w,CO2} [Sc_{PCB} / Sc_{CO2}]^{-0.5} \qquad (5.30)$$

In this correlation Sc represents the Schmidt number. The PCB congener molecular diffusivities were calculated using the Wilke-Chang equation. In all calculations temperature correction was done for viscosities and diffusivities. When temperature increased, both the k_w and k_a values increased.

Diffusion coefficient conversion from one temperature to another one was done by considering a known diffusion coefficient and the temperatures of the water phase. The following relationship was used :

$$D_{w,O2} (@T_2) = D_{w,O2} (@T_1)[(T_2\ \mu_1)/(T_1\ \mu_2)] \quad \text{(in the water phase)} \qquad (5.31)$$

where,

$D_{w,O2}$: Diffusivity coefficient of O2 in the water, cm^2/s,

T_1 ,T_2 : Reference and targeted temperatures, ^oK,

μ_1, μ_2 : Dynamic viscosities, Ns/m^2.

The molecular diffusivity values for PCBs were calculated by Wilke-Chang Equation for the water phase diffusion (Thibodeaux, 1979 and Schwarzenbach et al., 1993) as follows:

$$D_{w,\,PCB} = 7.4\ 10^{-8}\ [(\psi_2\ M_2)^{1/2}\ T) / (\mu_2\ V_{PCB}^{0.6}]\ \text{(Wilke-Chang Eqn)} \qquad (5.32)$$

where,

$D_{w,\,PCB}$: PCB diffusivity coefficient in the water, cm^2/s,

m : Molecular mass of PCB congener, g/mol,

V_{PCB} : Average molar volume of PCB congener, cm^3/mol,

ψ_2 : 2.6 for water,

M_2 : Molecular weight of water, 18 g/mol,

μ_2 : Dynamic viscosity, centipoise (poise = g/cm/s).

Table 5.4. summarizes the calculated $k_{w,\,PCB}$ values for all the available models. The whole sample set was used to calculate the individual water side MTC and their averages for each model are presented in Table 5.4. The overall average $k_{w,PCB}$ values varied between 6.19 E-6 cm/s (from Banks model (1975) for u_{10} <5.5 m/s) to 0.001054 cm/s (from Mackay and Yuen model (1983). In general, when the molecular weight of the PCB congeners increase, the calculated $k_{w,PCB}$ values decrease. This change was calculated to be about 20% for all models. Based on the models used in this study, the percentage of water side resistance in the total resistance decreased from the lightest to heaviest congeners.

Table 5.4. Calculated $k_{w, PCB}$ (cm/s) Values for Available Models

Congener	O2 Exp. (this study)	Absorption	Schwarzenbach	Mackay and Yuen	Banks	Wanninkhof	Kanwisher	Liss & Merlivat
8	0.00094	0.00102	0.00058	0.00114	6.68E-06	0.00068	0.00062	0.00025
18	0.00091	0.00100	0.00056	0.00111	6.51E-06	0.00066	0.00061	0.00024
15	0.00094	0.00102	0.00058	0.00114	6.68E-06	0.00068	0.00062	0.00025
16	0.00091	0.00100	0.00056	0.00111	6.51E-06	0.00066	0.00061	0.00024
31	0.00091	0.00100	0.00056	0.00111	6.51E-06	0.00066	0.00061	0.00024
28	0.00091	0.00100	0.00056	0.00111	6.51E-06	0.00066	0.00061	0.00024
33	0.00091	0.00100	0.00056	0.00111	6.51E-06	0.00066	0.00061	0.00024
22	0.00091	0.00100	0.00056	0.00111	6.51E-06	0.00066	0.00061	0.00024
52	0.00089	0.00097	0.00055	0.00108	6.35E-06	0.00064	0.00059	0.00023
49	0.00089	0.00097	0.00055	0.00108	6.35E-06	0.00064	0.00059	0.00023
47/48	0.00089	0.00097	0.00055	0.00108	6.35E-06	0.00064	0.00059	0.00023
44	0.00089	0.00097	0.00055	0.00108	6.35E-06	0.00064	0.00059	0.00023
42/37	0.00089	0.00097	0.00055	0.00108	6.35E-06	0.00064	0.00059	0.00023
74	0.00089	0.00097	0.00055	0.00108	6.35E-06	0.00064	0.00059	0.00023
66/95	0.00087	0.00095	0.00054	0.00106	6.21E-06	0.00063	0.00058	0.00023
60	0.00089	0.00097	0.00055	0.00108	6.35E-06	0.00064	0.00059	0.00023
101	0.00087	0.00095	0.00054	0.00106	6.21E-06	0.00063	0.00058	0.00023
99	0.00087	0.00095	0.00054	0.00106	6.21E-06	0.00063	0.00058	0.00023
97	0.00087	0.00095	0.00054	0.00106	6.21E-06	0.00063	0.00058	0.00023
81/87	0.00087	0.00095	0.00054	0.00106	6.21E-06	0.00063	0.00058	0.00023
77/110	0.00087	0.00095	0.00054	0.00106	6.21E-06	0.00063	0.00058	0.00023
82	0.00087	0.00095	0.00054	0.00106	6.21E-06	0.00063	0.00058	0.00023
149/123	0.00085	0.00093	0.00053	0.00103	6.08E-06	0.00062	0.00057	0.00022
118	0.00087	0.00095	0.00054	0.00106	6.21E-06	0.00063	0.00058	0.00023
114	0.00087	0.00095	0.00054	0.00106	6.21E-06	0.00063	0.00058	0.00023
105	0.00087	0.00095	0.00054	0.00106	6.21E-06	0.00063	0.00058	0.00023
141	0.00085	0.00093	0.00053	0.00103	6.08E-06	0.00062	0.00057	0.00022
137	0.00085	0.00093	0.00053	0.00103	6.08E-06	0.00062	0.00057	0.00022
138/163	0.00085	0.00093	0.00053	0.00103	6.08E-06	0.00062	0.00057	0.00022
126	0.00087	0.00095	0.00054	0.00106	6.21E-06	0.00063	0.00058	0.00023
187	0.00083	0.00091	0.00052	0.00101	5.96E-06	0.00060	0.00055	0.00022
128	0.00085	0.00093	0.00053	0.00103	6.08E-06	0.00062	0.00057	0.00022
185	0.00083	0.00091	0.00052	0.00101	5.96E-06	0.00060	0.00055	0.00022
171	0.00083	0.00091	0.00052	0.00101	5.96E-06	0.00060	0.00055	0.00022
156	0.00085	0.00093	0.00053	0.00103	6.08E-06	0.00062	0.00057	0.00022
180	0.00083	0.00091	0.00052	0.00101	5.96E-06	0.00060	0.00055	0.00022
200	0.00082	0.00090	0.00051	0.00100	5.85E-06	0.00059	0.00054	0.00022
169	0.00085	0.00093	0.00053	0.00103	6.08E-06	0.00062	0.00057	0.00022
199	0.00082	0.00090	0.00051	0.00100	5.85E-06	0.00059	0.00054	0.00022
207	0.00081	0.00088	0.00050	0.00098	5.75E-06	0.00058	0.00054	0.00021
205	0.00082	0.00090	0.00051	0.00100	5.85E-06	0.00059	0.00054	0.00022
206	0.00081	0.00088	0.00050	0.00098	5.75E-06	0.00058	0.00054	0.00021
209	0.00079	0.00087	0.00049	0.00096	5.66E-06	0.00057	0.00053	0.00021

The models (presented in Table 2.18) were developed based on data obtained from either wind-water tunnels or lakes. These individual MTCs (k_a and k_w) are used to calculate the overall MTC ($^2K_{Al}$) to compare to the ones found in these experiments. Table 5.5. summarizes these by with congener number. The $^2K_{Al}$ value was calculated based on the models developed/modified in this study. In general, the measured overall MTCs are bigger than the modeled overall MTCs. The overall average differences between measured and modeled overall MTC ranged from 37.4% to -8.4% using the Mackay and Yuen model for k_w which has given the highest value and evaporation model for k_a (Table 5.5).

This agreement is good considering 1) there are many sampling uncertainties, 2) individual MTCs were related only to wind speed in the models, 3) there are probably some deficiencies in the equations used in the calculations. For example, water phase PCB diffusivities were calculated with Wilke-Chang Equation. This equation is thought to estimate a diffusivity with ± 10% (Schwarzenbach et al., 1993). Probably the Fuller Equation has a similar uncertainty range for air side diffusivity calculations, 4) the individual MTCs were not directly calculated. They were related with either water or oxygen individual MTCs which may not be representative of PCBs in the air-water interface, 5) the conversion exponent values may change from sampler to sampler and 6) the wind speed effects may be masked due to the long sampling periods (~ 5 days). As shown in the oxygen experiment results, the correlation between individual MTCs and wind speed increases when sampling time decreases.

Table 5.5. Overall Measured and Modeled MTCs (cm/s)

Congener	WSS_{A-P}	WSS_{A-P} w/LOD	WSS_{1R}	WSS_{1R} w/LOD	Regression	Model O_2 Exp.	Model Absorption	Model Mackay and Yuen
8	0.707	0.497	0.584	0.278	0.016	0.104	0.112	0.123
18	0.693	0.435	0.694	0.304	0.011	0.093	0.101	0.110
15	0.450	0.400	0.424	0.222	0.077	0.091	0.099	0.109
16	0.872	0.440	0.928	0.408	0.105	0.114	0.124	0.136
31	0.049	0.024	0.051	0.026	0.071	0.114	0.124	0.136
28	0.059	0.041	0.063	0.042	0.092	0.114	0.124	0.136
33	0.288	0.194	0.432	0.223	0.037	0.132	0.143	0.156
22	0.734	0.371	1.405	0.727	0.119	0.155	0.168	0.183
52	0.071	0.037	0.274	0.166		0.112	0.121	0.132
49	0.118	0.080	0.174	0.112	0.085	0.107	0.116	0.127
47/48	0.271	0.245	0.261	0.146	5.949	0.116	0.126	0.138
44	0.892	0.626	0.802	0.514	0.435	0.170	0.184	0.200
42/37	1.264	0.634	0.815	0.282	0.923	0.203	0.218	0.236
74	1.109	0.559	0.642	0.642	0.313	0.203	0.218	0.236
66/95	0.653	0.396	1.066	0.536		0.170	0.183	0.199
60	0.860	0.525	0.637	0.459	0.030	0.239	0.257	0.277
101	0.717	0.121	0.415	0.415		0.217	0.233	0.253
99	0.799	0.400	0.645	0.586	1.098	0.242	0.260	0.281
97	0.823	0.121	0.631	0.562	0.804	0.251	0.269	0.290
81/87	1.441	0.866	0.004	0.010		0.299	0.319	0.343
77/110	1.073	0.877	1.052	0.471		0.299	0.319	0.343
82	0.806	0.723	1.210	0.758	0.100	0.299	0.319	0.343
149/123	0.724	0.724	0.890	0.713	0.097	0.366	0.388	0.415
118	0.679	0.409	0.525	0.430	0.099	0.397	0.421	0.448
114	0.352	0.254	0.138	0.060		0.341	0.362	0.388
105	0.684	0.511	0.313	0.112	0.512	0.529	0.554	0.584
141	0.519	0.408	0.523	0.396	0.443	0.273	0.292	0.314
137	1.185	0.599	0.928	0.844	0.490	0.449	0.473	0.501
138/163	0.983	0.495	0.542	0.795		0.645	0.670	0.698
126	0.178	1.139	0.178	0.068				
187	0.264	0.116	0.287	0.230	0.045	0.551	0.576	0.604
128	0.958	0.900	0.262	0.208		0.689	0.713	0.740
185	0.505	0.410	0.359	0.300	4.741	0.620	0.644	0.672
171	0.582	0.297	0.738	0.375	0.026	0.638	0.662	0.690
156	0.264	0.104	0.173	0.145	0.046	0.651	0.676	0.704
180	0.448	0.204	0.240	0.240	0.317	0.739	0.761	0.785
200	0.593	0.468	0.757	0.634	0.182	0.626	0.650	0.676
169		1.607		0.114		0.676	0.700	0.728
199		0.194		0.563		0.725	0.746	0.770
207	2.008	0.807		0.531		0.788	0.806	0.827
205		1.282		1.209		0.821	0.839	0.859
206	0.590	0.771	0.400	0.332		0.865	0.880	0.896
209	0.968	1.107		0.704		0.882	0.894	0.908
Average	0.681	0.498	0.538	0.393	0.617	0.384	0.401	0.421
Diff. (%)	37.4	14.5	20.8	-8.4	31	-9.8	-5.2	0.0

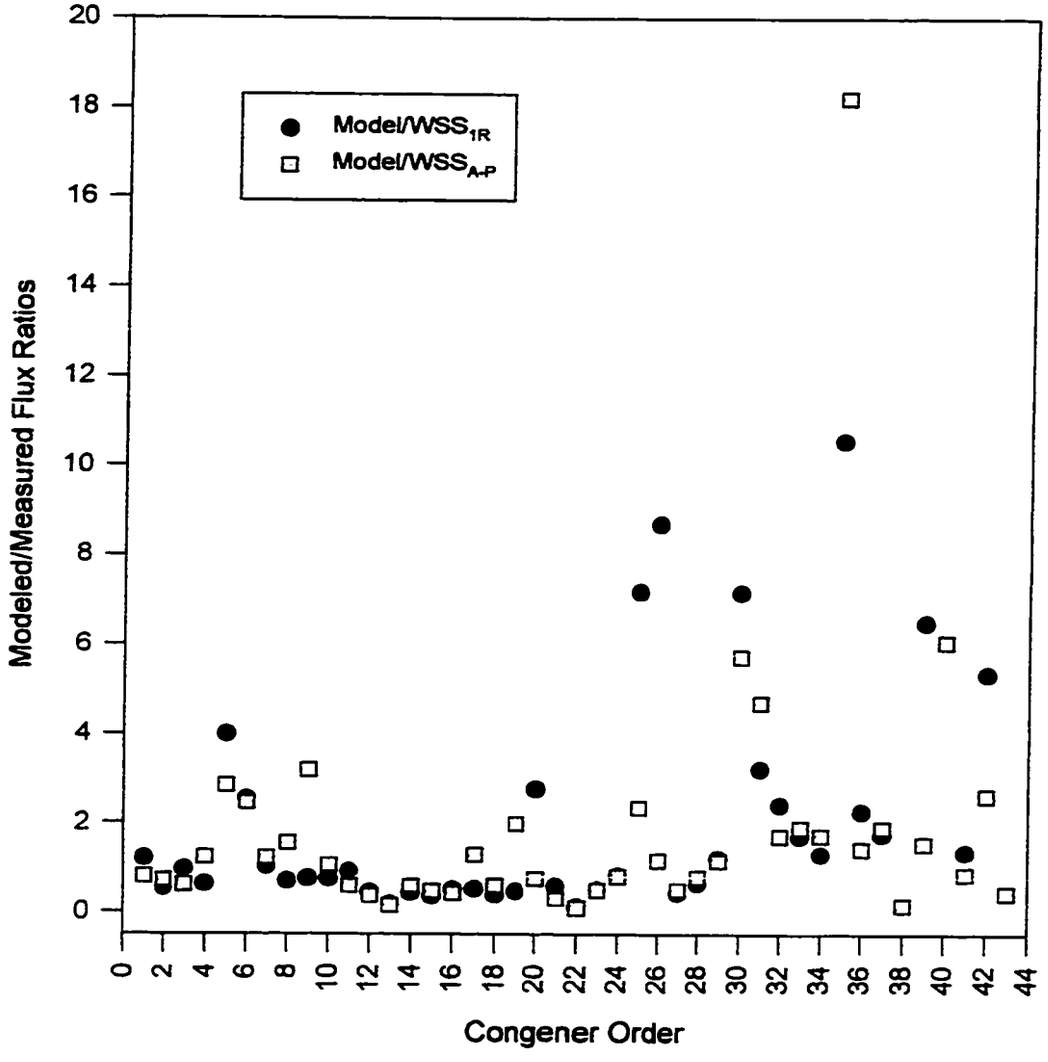

Figure 5.38. Modeled and Measured Flux Ratios of Each Congener

In order to minimize the masking effects from long sampling periods, the measured hourly wind speeds and temperatures were used to calculate the individual MTCs. Hourly fluxes were estimated using the measured concentrations and MTCs. Table 5.6. summarizes the overall average measured and modeled (calculated) flux values. The sum of the overall average calculated flux value of the 11 samples is about 404 ± 360 ng/m^2-d. It is 81 to 88% of the measured flux values of WSS_{1R} and $WSS_{A\text{-}P}$, respectively. This is much better agreement than the comparison between overall MTCs. The regression analysis of congeners between WSS_{1R} and this modeled flux is y = 1.973 + 1.023x and r^2 = 0.50. Interestingly, if calculations were performed for daily rather than 5 days, the average overall calculated flux value increases to 426 ± 600 ng/m^2-d. Figure 5.38. shows the ratios of the measured and modeled values. The agreement between measured and modeled values increases to 86 - 93%. This result clearly shows the importance of short term calculations to compare to measured values.

5.6. Regression Analysis Between Flux and Concentrations

Holsen et al. (1991) proposed a dry deposition flux calculation based on individual gas and particulate concentrations and dry deposition velocities for gas and particulate phases. The modified flux calculation based on these compartments can be given as follows:

$$F = C_g V_{d,g} + C_p V_{d,p} \qquad (5.33)$$

Table 5.6. Summary of Overall Average of the Measured and Modeled Fluxes

No	Congener	WSS1R	WSS	Model (Daily)	Model (>5 days)
1	8	4.793	7.278	5.753	5.846
2	18	3.889	2.935	2.082	2.037
3	15	8.495	13.346	8.117	7.188
4	16	3.196	1.637	1.994	1.970
5	31	2.968	4.177	11.848	11.822
6	28	3.650	3.773	9.257	8.893
7	33	6.050	5.040	6.130	5.709
8	22	3.458	1.542	2.374	2.110
9	52	13.317	3.127	9.929	9.554
10	49	6.654	4.699	4.910	4.757
11	47/48	4.383	6.790	3.942	3.977
12	44	13.308	15.933	5.755	5.579
13	42/37	6.184	7.803	1.067	1.091
14	74	14.800	10.956	6.327	6.480
15	66/95	27.169	21.209	9.756	9.542
16	60	6.800	8.199	3.392	3.144
17	101	58.327	23.398	29.829	28.801
18	99	38.287	24.469	14.379	13.903
19	97	44.915	10.382	20.480	19.455
20	81/87	6.563	24.424	18.132	15.228
21	77/110	28.583	54.812	16.403	14.910
22	82	2.410	3.194	0.282	0.272
23	149/123	47.529	49.299	23.768	22.614
24	118	34.639	35.776	28.340	26.889
25	114	0.485	1.486	3.475	3.175
26	105	0.507	3.815	4.405	4.236
27	141	15.972	13.691	6.802	6.272
28	137	10.210	8.477	6.490	6.879
29	138/163	36.212	38.126	43.482	43.738
30	126	0.737	0.921	5.271	4.797
31	187	13.251	9.085	42.646	37.913
32	128	3.885	5.490	9.360	8.733
33	185	3.418	3.058	5.789	5.580
34	171	5.599	4.248	7.258	6.511
35	156	0.516	0.299	5.444	4.773
36	180	13.007	20.798	29.424	27.552
37	200	2.198	2.028	3.822	3.704
38	169	0.000	1.350	0.204	0.167
39	198 or 199	0.158	0.670	1.025	0.976
40	207	0.000	0.153	0.929	1.009
41	205	0.315	0.500	0.422	0.345
42	206	1.048	2.138	5.592	5.357
43	209	0.000	0.617	0.261	0.305
Min		0.000	0.153	0.204	0.167
Max		58.327	54.812	43.482	43.738
Sum		497.885	461.150	426.348	403.793

where F (ng/m^2-d) is the total flux, C_g (ng/m^3) and C_p (ng/m^3) are the concentrations of gas and particulate phase, respectively, and $V_{d,g}$ (cm/s) and $V_{d,p}$ (cm/s) are the dry deposition velocities for gas and particulate phase, respectively.

Since in this study F, C_p and C_g values were measured, $V_{d,g}$ and $V_{d,p}$ values can be estimated by applying the regression between F values and C_p and C_g values. In the regression analysis each PCB congener was considered separately by using the 11 sample values for that congener. The regression was applied when all three (F, C_p and C_g) values exist. In the regression calculations, 95% confidence level was chosen and the intercept was zero. The calculated values of $V_{d,g}$ and $V_{d,p}$ are given in Figure 5.39. The average values of $V_{d,g}$ and $V_{d,p}$ were 0.63 and 7.93 cm/s, respectively. These values were comparable to the ones calculated during this study. For example overall average gas phase MTC values were calculated to be 0.68 cm/s and 0.54 cm/s for WSS_{A-P} and WSS_{1R}, respectively and particle phase dry deposition velocities were 5.2 WSS_{1F} and 6.5 cm/s for particles.

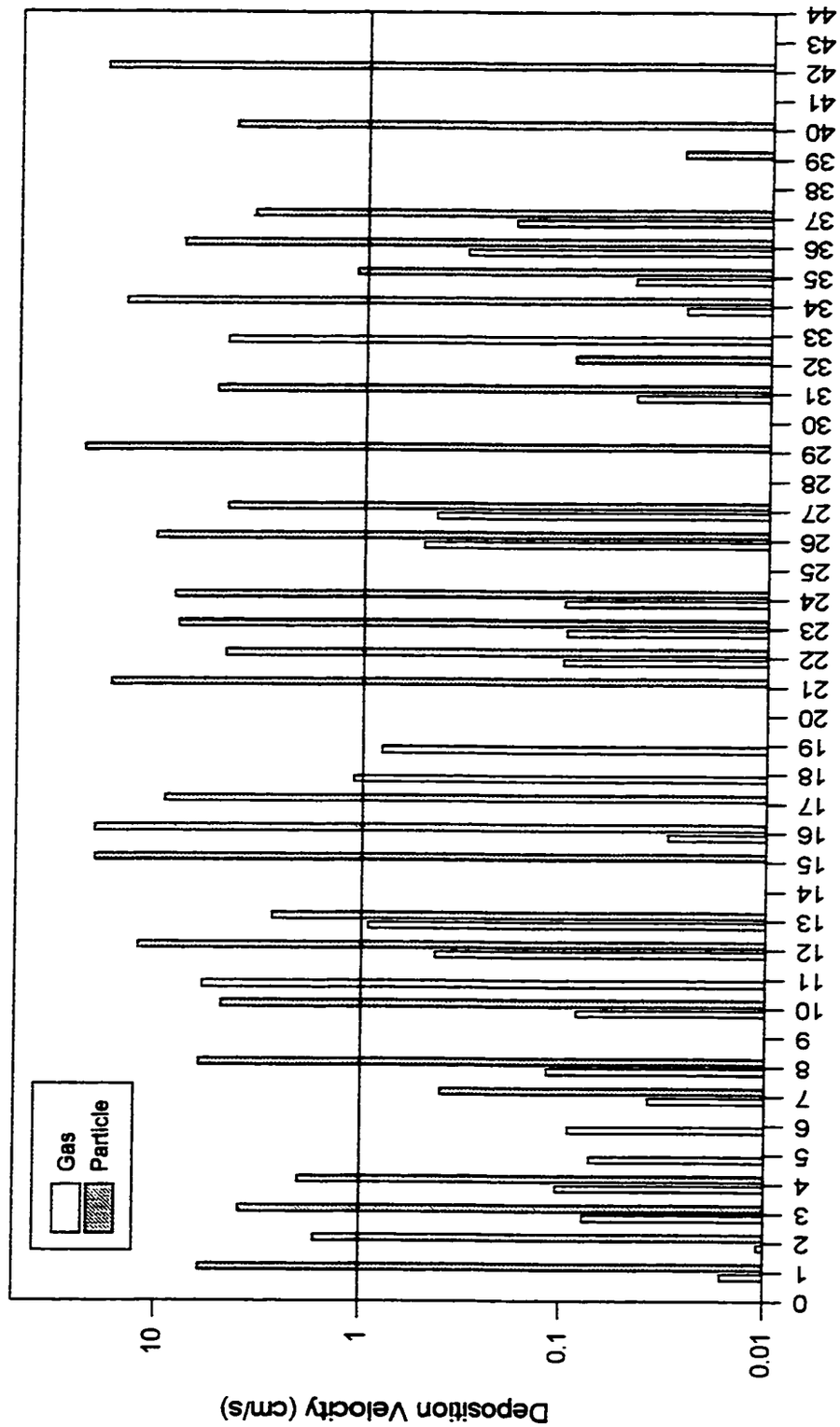

Figure 5.39. Dry Deposition Velocities of Particulate and Gas Phase PCBs (from regression analysis)

CHAPTER VI

CONCLUSIONS

This study focused on the determination of the concentration of PCBs in the ambient air as well as on their deposition to surrogate surfaces (plates (greased strips) and water surface). Therefore, specific collection surfaces and analysis methods were used. The main conclusions from this study can be summarized as follows:

1) This study provided a comprehensive measurement of a large number of individual PCB congeners in the atmosphere by using a high-volume air sampler, WSS and plates (greased strips).

2) Concentrations (Σ-PCB concentration : 1.9 ng/m^3) and their distributions between the gas (95%) and particle (5%) were comparable to those observed in previous studies. The percent of particulate associated PCBs increased with increasing PCB molecular weight.

3) The PCB gas/particle partitioning of PCBs in urban South Chicago atmosphere was non-ideal. This could be due to changes in aerosol characteristics and atmospheric concentrations due to changing meteorological conditions. The Junge-Pankow model underestimates the amount of particle phase with lower MW PCBs while overestimating with the higher MW PCBs.

4) This was the first time the dry deposition flux of PCBs has been directly measured into a water surface under conditions of no volatilization (only particle deposition and absorption). Therefore, the results (1200 ng/m^2-d) were higher than the ones found in lake environments (-1300 to -23 ng/m^2-d). This study has important applications for mass balance studies in terms of giving direct input of dry deposition and absorption values.

5) Modified water surface samplers (WSS) were developed to measure the dry deposition of PCBs. The fluxes measured with the two WSSs were statistically the same. The PCB fluxes measured with the WSS (1200 ng/m^2-d) were higher than the fluxes measured with the plates (240 ng/m^2-d). This is because unlike the plates, the WSS captures both particle and gas phase PCBs.

6) The gas phase flux was determined by subtracting the plate fluxes (particle) from the WSS fluxes (particle + gas). The gas phase fluxes were bigger than the particle fluxes. This is reasonable because the average overall gas phase PCB concentration was about 19 times bigger than the particle phase. However, the flux ratio between gas and particle phase was only about 2. This difference between ratios can be explained by the differences in the deposition phenomena affecting the particles and gases.

7) The dry deposition velocity of PCBs associated with particulates was about 8 times bigger than the ones for the gas phase. This is because the particle phase dry deposition is controlled by gravitational settling whereas the gas phase dry deposition is governed by Brownian motion and their interactions with the surface.

8) The organic chemical exchange model applied here between the air and water interface was the modified two-film theory and this model was the best estimate of PCB flux to the WSS in this study. The overall mass transfer coefficients (MTC) calculated based on the available individual MTC models were slightly smaller than the measured ones (Table 5.5).

9) The accuracy of extrapolating these types of measurements to the real water bodies is open to debate because deposition phenomena is very complex in terms of the effects of wind, waves, bubbles, heat transfer, fetch distances as well as surface and compound characteristics. Thus, deposition values fluctuate a great deal not only from natural to laboratory studies but also among the natural water and terrestrial areas.

CHAPTER VII

FUTURE WORK

1) In order to see the effects of meteorological data and minimize artifacts, the sampling time should be reduced maybe by increasing the collection areas (WSS and specially plates) and collection amounts (high-volume sampler).

2) Alternate sites can be tried (or other chemical species such as mercury, PCDD/F).

3) Particle size distribution of PCBs needs to be determined because different size particles partition and deposit differently in the ambient air.

4) Two filters can be used to measure the gas adsorption onto the filter.

5) Models for PCB fate and transport should be developed to understand their fate.

6) PCB behavior in the water column (partitioning with the particles, sedimentation, evaporation) should be studied.

7) Surrogate standards should be added before sample collection. It would yield information about the efficiency of the collection process. Supercritical fluid extraction (SFE) could be investigated for use in PCB extractions in order to shorten the extraction times and minimize solvent use.

APPENDIX

Table A1. Some Characteristics of the Congeners Used in This Study

Order	Congener	MW (g/mol)	MV (cm3/mol)	log H atm m^3/mol	H atmL/mol
1	8	223.1	226.4	-3.64	0.229087
2	18	257.54	247.3	-3.6	0.251189
3	15	223.1	226.4	-3.58	0.263027
4	16	257.54	247.3	-3.7	0.199526
5	31	257.54	247.3	-3.7	0.199526
6	28	257.54	247.3	-3.7	0.199526
7	33	257.54	247.3	-3.77	0.169824
8	22	257.54	247.3	-3.85	0.141254
9	52	291.99	268.2	-3.7	0.199526
10	49	291.99	268.2	-3.68	0.20893
11	47/48	291.99	268.2	-3.72	0.190546
12	44	291.99	268.2	-3.91	0.123027
13	42/37	291.99	268.2	-4	0.1
14	74	291.99	268.2	-4	0.1
15	66/95	326.43	289.1	-3.92	0.120226
16	60	291.99	268.2	-4.09	0.081283
17	101	326.43	289.1	-4.05	0.089125
18	99	326.43	289.1	-4.11	0.077625
19	97	326.43	289.1	-4.13	0.074131
20	81/87	326.43	289.1	-4.23	0.058884
21	77/110	326.43	289.1	-4.23	0.058884
22	82	326.43	289.1	-4.23	0.058884
23	149/123	360.88	310	-4.37	0.042658
24	118	326.43	289.1	-4.41	0.038905
25	114	326.43	289.1	-4.31	0.048978
26	105	326.43	289.1	-4.62	0.023988
27	141	360.88	310	-4.19	0.064565
28	137	360.88	310	-4.51	0.030903
29	138/163	360.88	310	-4.82	0.015136
30	126	326.43	289.1		1000
31	187	395.32	330.9	-4.69	0.020417
32	128	360.88	310	-4.89	0.012882
33	185	395.32	330.9	-4.8	0.015849
34	171	395.32	330.9	-4.83	0.014791
35	156	360.88	310	-4.83	0.014791
36	180	395.32	330.9	-5	0.01
37	200	429.77	351.8	-4.83	0.014791
38	169	360.88	310	-4.87	0.01349
39	199	429.77	351.8	-5	0.01
40	207	462.21	372.7	-5.15	0.007079
41	205	429.77	351.8	-5.19	0.006457
42	206	462.21	372.7	-5.33	0.004677
43	209	498.66	393.6	-5.42	0.003802

Note: Above values were obtained Hornbuckle (1996) and Mackay et al. (1992)

Table A2. Amount (ng) of PCB Congeners in the PUF+Resin Blanks (High-volume)

Order	Congener	Blank 1	Blank 2	Blank 3	Blank 4	Blank 5	Average	Std. Deviation
1	8	1.12	0.42	0.47	0.98	1.62	0.92	0.50
2	18	0.32	0.08	0.05	0.09	ND	0.11	0.13
3	15	1.44	0.50	0.44	1.01	1.54	0.99	0.51
4	16	0.24	0.04	0.09	0.18	0.42	0.19	0.15
5	31	0.78	0.17	0.46	0.65	ND	0.41	0.33
6	28	1.16	0.25	0.35	0.57	1.75	0.82	0.63
7	33	0.49	0.12	0.22	0.34	0.14	0.26	0.16
8	22	0.13	ND	0.04	0.03	ND	0.04	0.05
9	52	1.47	0.41	0.53	0.91	0.82	0.83	0.41
10	49	0.56	0.15	0.20	0.34	0.36	0.32	0.16
11	47/48	0.02	ND	0.03	ND	0.19	0.05	0.08
12	44	0.75	0.06	0.22	0.37	0.43	0.37	0.26
13	42/37	ND	ND	0.01	ND	0.09	0.02	0.04
14	74	0.38	0.07	0.15	0.21	0.54	0.27	0.19
15	66/95	1.80	0.39	0.58	1.03	3.19	1.40	1.14
16	60	0.39	ND	0.09	0.33	0.09	0.18	0.17
17	101	2.78	0.67	0.78	1.44	1.95	1.52	0.87
18	99	1.06	0.29	0.31	0.58	0.06	0.46	0.38
19	97	2.86	0.64	0.64	1.39	1.95	1.50	0.94
20	81/87	ND	ND	ND	ND	ND	ND	ND
21	77/110	2.49	0.80	0.59	0.97	0.52	1.08	0.81
22	82	ND	ND	ND	0.10	0.10	0.04	0.06
23	149/123	1.60	0.36	0.35	0.75	1.47	0.91	0.60
24	118	1.69	0.46	0.44	0.81	1.43	0.97	0.57
25	114	ND	ND	ND	ND	ND	ND	ND
26	105	ND	ND	ND	ND	ND	ND	ND
27	141	0.23	0.04	0.06	0.12	ND	0.09	0.09
28	137	0.52	0.08	0.08	0.18	0.38	0.25	0.20
29	138/163	1.31	0.42	0.29	0.65	0.72	0.68	0.39
30	126	ND	ND	ND	ND	ND	ND	ND
31	187	1.87	0.28	0.31	0.71	0.99	0.83	0.65
32	128	ND	ND	ND	ND	ND	ND	ND
33	185	0.08	ND	ND	ND	ND	0.02	0.03
34	171	0.32	ND	0.03	0.04	0.03	0.09	0.13
35	156	0.15	0.04	0.04	0.09	ND	0.06	0.06
36	180	1.75	0.47	0.31	0.82	1.07	0.89	0.57
37	200	0.14	ND	ND	ND	0.15	0.06	0.08
38	169	ND	ND	ND	ND	ND	ND	ND
39	198 or 199	ND	ND	ND	ND	0.08	0.02	0.03
40	207	ND	ND	0.06	ND	ND	0.01	0.03
41	205	ND	ND	ND	ND	ND	ND	ND
42	206	0.09	ND	ND	ND	ND	0.02	0.04
43	209	ND	ND	ND	ND	ND	ND	ND
Max		2.86	0.80	0.78	1.44	3.19	1.52	1.14
Sum		30.02	7.21	8.20	15.72	22.08	16.65	11.44

Table A3. Amount (ng) of PCB Congeners in the Filter Blank (High-volume)

Order	Congener	Blank 1	Blank 2	Blank 3	Blank 4	Blank 5	Blank 6	Blank 7	Blank 8	Avg	St. Dev.
1	8	1.55	0.82	0.35	0.49	0.44	0.15	0.62	0.57	0.62	0.42
2	18	0.29	0.08	0.04	0.11	0.20	ND	0.64	0.04	0.18	0.21
3	15	0.91	1.20	1.86	1.18	0.76	1.81	0.95	1.02	1.21	0.41
4	16	0.10	0.34	0.14	0.31	0.05	0.47	0.25	0.31	0.25	0.14
5	31	0.38	0.18	0.21	0.58	0.31	0.50	0.35	0.60	0.39	0.16
6	28	1.33	0.39	0.11	0.37	0.36	0.12	0.32	0.20	0.40	0.39
7	33	0.08	0.48	0.19	0.13	0.24	0.34	0.12	0.31	0.24	0.13
8	22	0.05	0.03	ND	ND	ND	0.21	0.05	ND	0.04	0.07
9	52	0.28	0.58	0.28	1.86	0.98	0.59	0.25	0.67	0.69	0.54
10	49	0.33	0.28	0.11	0.25	0.09	0.12	0.10	0.19	0.19	0.09
11	47/48	ND	0.03	ND	ND	ND	ND	ND	ND	ND	0.01
12	44	0.27	0.34	0.12	0.23	0.32	0.19	0.69	0.27	0.31	0.17
13	42/37	ND	ND	ND	ND	0.02	ND	ND	ND	ND	0.01
14	74	0.15	0.05	0.09	0.23	0.10	0.19	0.09	0.06	0.12	0.07
15	66/95	0.39	2.15	0.97	1.10	0.88	0.71	0.24	0.57	0.88	0.59
16	60	0.15	0.21	ND	0.09	0.10	0.07	ND	0.08	0.09	0.07
17	101	1.63	1.51	1.27	0.92	0.59	0.66	0.48	0.81	0.98	0.44
18	99	0.29	0.22	0.26	0.24	0.22	0.21	0.33	1.39	0.39	0.40
19	97	2.18	2.35	1.43	0.46	0.38	0.51	0.18	0.25	0.97	0.89
20	81/87	ND	ND	ND	ND	ND	ND	0.30	ND	0.04	0.11
21	77/110	2.18	3.78	2.06	1.80	ND	ND	0.25	ND	1.26	1.41
22	82	0.01	ND	ND	ND	ND	ND	ND	ND	ND	ND
23	149/123	1.03	1.29	0.24	0.31	0.28	0.29	0.22	0.16	0.48	0.43
24	118	0.66	0.46	0.50	1.54	0.50	0.30	0.68	0.10	0.59	0.43
25	114	ND	ND	ND	ND	ND	ND	ND	ND	ND	ND
26	105	0.15	ND	ND	ND	ND	ND	ND	0.23	0.05	0.09
27	141	0.08	0.20	ND	0.03	ND	ND	ND	0.08	0.05	0.07
28	137	0.14	0.28	ND	0.02	ND	0.01	ND	0.17	0.08	0.11
29	138/163	0.52	1.09	0.19	0.91	0.03	0.07	0.25	0.37	0.43	0.39
30	126	ND	ND	ND	ND	ND	ND	ND	ND	ND	ND
31	187	0.60	0.76	0.21	0.15	0.39	ND	0.11	1.39	0.45	0.46
32	128	ND	ND	ND	ND	ND	ND	0.25	ND	0.03	0.09
33	185	ND	ND	ND	ND	ND	ND	ND	ND	ND	ND
34	171	ND	0.10	ND	ND	ND	ND	ND	ND	0.01	0.03
35	156	0.06	0.10	0.05	0.09	ND	ND	ND	0.04	0.04	0.04
36	180	1.14	1.01	0.27	0.21	0.29	0.26	0.29	0.11	0.45	0.40
37	200	ND	0.03	ND	ND	ND	ND	ND	ND	ND	0.01
38	169	ND	ND	ND	ND	ND	ND	ND	ND	ND	ND
39	198 or 199	ND	ND	ND	ND	ND	ND	ND	ND	ND	ND
40	207	ND	ND	0.01	0.01	ND	ND	ND	ND	ND	0.01
41	205	ND	ND	ND	0.02	ND	ND	ND	0.03	0.01	0.01
42	206	ND	ND	ND	ND	ND	ND	ND	ND	ND	ND
43	209	ND	ND	ND	ND	ND	ND	ND	ND	ND	ND
Max		2.18	3.78	2.06	1.86	0.98	1.81	0.95	1.39	1.26	1.41
Sum		16.93	20.35	10.96	13.66	7.53	7.80	8.02	9.99	11.91	9.30

Table A4. Amount (ng) of PCB Congeners in the WSS_{1F} Blank

Order	Congener	Blank 1	Blank 2	Blank 3	Blank 4	Blank 5	Average	Std. Deviation
1	8	1.56	ND	0.71	1.22	2.18	1.13	0.83
2	18	0.17	ND	ND	0.01	0.38	0.11	0.17
3	15	2.19	0.65	0.85	1.96	4.93	2.11	1.71
4	16	0.58	0.04	0.24	0.20	0.96	0.41	0.37
5	31	1.64	1.40	0.97	1.11	3.54	1.73	1.04
6	28	1.83	1.58	1.24	1.04	2.89	1.72	0.72
7	33	0.69	0.10	0.15	0.51	1.61	0.61	0.61
8	22	0.21	ND	ND	ND	0.41	0.12	0.18
9	52	2.22	1.76	1.38	1.62	4.23	2.24	1.15
10	49	0.53	0.52	0.46	0.46	1.49	0.69	0.45
11	47/48	0.22	0.02	ND	ND	0.05	0.06	0.09
12	44	0.69	ND	0.60	0.57	1.89	0.75	0.69
13	42/37	ND	ND	ND	ND	0.04	0.01	0.02
14	74	0.85	0.82	0.71	0.43	1.37	0.84	0.34
15	66/95	3.09	1.74	1.48	1.78	5.67	2.75	1.75
16	60	0.62	ND	ND	0.21	0.82	0.33	0.37
17	101	4.20	5.66	4.67	2.75	6.99	4.85	1.59
18	99	1.70	2.77	2.08	1.18	2.55	2.06	0.64
19	97	4.17	5.01	4.20	2.72	6.70	4.56	1.45
20	81/87	ND	ND	ND	ND	ND	ND	ND
21	77/110	1.25	0.99	1.84	0.85	2.33	1.45	0.62
22	82	ND	0.09	ND	0.17	0.39	0.13	0.16
23	149/123	2.15	2.32	1.80	1.25	4.08	2.32	1.07
24	118	2.65	3.74	3.03	1.70	4.82	3.19	1.18
25	114	ND	0.11	ND	ND	ND	0.02	0.05
26	105	0.51	ND	ND	ND	ND	0.10	0.23
27	141	0.45	0.31	0.47	0.16	0.67	0.41	0.19
28	137	0.70	1.14	0.90	0.34	1.15	0.85	0.34
29	138/163	2.68	2.54	2.11	1.13	3.90	2.47	1.00
30	126	ND	ND	ND	ND	ND	ND	ND
31	187	3.38	3.52	2.00	1.02	3.63	2.71	1.15
32	128	ND	0.12	ND	0.16	0.71	0.20	0.29
33	185	ND	0.05	ND	ND	0.07	0.02	0.03
34	171	0.24	ND	0.13	ND	0.47	0.17	0.20
35	156	0.20	ND	0.33	0.24	0.43	0.24	0.16
36	180	3.43	3.84	2.65	1.56	3.49	2.99	0.91
37	200	0.02	0.03	0.04	ND	0.08	0.04	0.03
38	169	ND	ND	ND	ND	ND	ND	ND
39	198 or 199	ND	0.23	ND	ND	ND	0.05	0.10
40	207	ND	ND	ND	ND	0.62	0.12	0.28
41	205	ND	ND	ND	ND	ND	ND	ND
42	206	ND	0.01	ND	ND	ND	ND	0.01
43	209	ND	ND	ND	ND	ND	ND	ND
Max		4.20	5.66	4.67	2.75	6.99	4.85	1.75
Sum		44.82	41.12	35.05	26.33	75.50	44.56	22.16

Table A5. Amount (ng) of PCB Congeners in the WSS_{1R} Blank

Order	Congener	Blank 1	Blank 2	Blank 3	Blank 4	Average	Std. Deviation
1	8	0.69	0.68	3.10	1.21	1.42	1.15
2	18	0.16	0.15	0.52	0.05	0.22	0.20
3	15	ND	0.79	4.12	1.88	1.70	1.79
4	16	0.21	0.04	0.70	0.28	0.31	0.28
5	31	ND	ND	3.59	2.06	1.41	1.75
6	28	1.64	1.52	4.37	2.79	2.58	1.33
7	33	0.40	0.16	2.01	0.73	0.82	0.82
8	22	ND	0.04	0.53	ND	0.14	0.26
9	52	1.65	2.88	5.46	3.42	3.35	1.59
10	49	0.62	1.21	1.93	0.90	1.16	0.56
11	47/48	0.27	0.46	0.41	0.03	0.29	0.19
12	44	ND	0.87	2.99	0.58	1.11	1.31
13	42/37	ND	ND	0.20	ND	0.05	0.10
14	74	1.28	1.12	1.83	1.13	1.34	0.34
15	66/95	2.55	1.23	6.59	3.25	3.41	2.28
16	60	0.10	ND	0.96	0.41	0.37	0.43
17	101	8.02	8.91	9.23	6.84	8.25	1.07
18	99	3.39	3.38	3.81	2.74	3.33	0.44
19	97	6.44	6.50	8.35	6.09	6.84	1.02
20	81/87	ND	ND	ND	ND	ND	ND
21	77/110	1.06	1.17	9.28	3.69	3.80	3.85
22	82	ND	ND	0.14	ND	0.04	0.07
23	149/123	3.65	3.54	5.45	3.12	3.94	1.03
24	118	5.93	5.18	6.17	4.02	5.33	0.97
25	114	ND	ND	ND	ND	ND	ND
26	105	0.20	ND	1.97	0.71	0.72	0.88
27	141	1.10	1.10	0.99	0.58	0.94	0.25
28	137	1.43	1.33	1.64	1.14	1.38	0.21
29	138/163	5.04	3.55	4.70	2.87	4.04	1.01
30	126	0.57	ND	ND	ND	0.14	0.29
31	187	4.59	3.92	4.37	3.69	4.14	0.41
32	128	ND	0.13	ND	ND	0.03	0.07
33	185	0.17	0.06	0.15	0.09	0.12	0.05
34	171	ND	0.62	0.69	0.39	0.42	0.31
35	156	0.59	0.46	0.44	0.33	0.45	0.11
36	180	4.79	3.68	4.35	3.54	4.09	0.58
37	200	0.31	0.10	0.20	0.12	0.18	0.10
38	169	ND	ND	ND	ND	ND	ND
39	198/199	ND	ND	ND	ND	ND	ND
40	207	0.06	ND	0.19	0.07	0.08	0.08
41	205	ND	ND	ND	ND	ND	ND
42	206	0.33	0.05	ND	ND	0.09	0.16
43	209	0.09	ND	ND	ND	0.02	0.05
Max		8.02	8.91	9.28	6.84	8.25	3.85
Sum		57.31	54.78	101.43	58.71	**68.06**	**27.38**

Table A6. Amount (ng) of PCB Congeners in the Plate Blanks

Order	Congener	Blank 1	Blank 2	Blank 3	Average	Std. Deviation
1	8	1.84	1.18	1.04	1.35	0.43
2	18	0.55	0.42	0.30	0.42	0.13
3	15	3.09	2.26	2.60	2.65	0.42
4	16	0.59	0.34	0.36	0.43	0.14
5	31	1.45	0.73	1.24	1.14	0.37
6	28	1.39	0.85	1.18	1.14	0.27
7	33	0.93	0.35	0.56	0.61	0.29
8	22	ND	ND	ND	ND	ND
9	52	2.92	1.80	1.95	2.23	0.61
10	49	0.73	0.38	0.51	0.54	0.18
11	47/48	0.37	ND	ND	0.12	0.21
12	44	0.96	0.62	0.58	0.72	0.21
13	42/37	ND	ND	ND	ND	ND
14	74	0.58	0.47	0.50	0.51	0.06
15	66/95	2.64	1.69	2.10	2.14	0.48
16	60	0.60	0.40	0.21	0.40	0.20
17	101	3.91	3.26	3.50	3.56	0.33
18	99	1.83	1.26	ND	1.03	0.93
19	97	3.29	2.36	2.65	2.77	0.48
20	81/87	ND	ND	ND	ND	ND
21	77/110	3.68	2.78	3.65	3.37	0.51
22	82	0.06	ND	ND	0.02	0.03
23	149/123	2.20	1.30	1.54	1.68	0.46
24	118	2.09	1.70	2.38	2.06	0.34
25	114	ND	ND	ND	ND	ND
26	105	0.07	ND	0.37	0.15	0.20
27	141	0.25	0.05	0.12	0.14	0.10
28	137	0.41	0.20	0.27	0.29	0.11
29	138/163	1.64	0.76	1.32	1.24	0.45
30	126	ND	ND	ND	ND	ND
31	183	ND	ND	ND	ND	ND
32	128	ND	ND	ND	ND	ND
33	185	ND	ND	ND	ND	ND
34	171	0.02	ND	ND	0.01	0.01
35	156	0.24	0.09	0.09	0.14	0.09
36	180	1.97	1.26	1.29	1.51	0.40
37	200	ND	ND	ND	ND	ND
38	169	ND	ND	ND	ND	ND
39	198 or 199	ND	ND	ND	ND	ND
40	207	0.93	0.52	ND	0.48	0.47
41	205	ND	ND	ND	ND	ND
42	206	ND	ND	ND	ND	ND
43	209	0.35	ND	ND	0.12	0.20
Max		3.91	3.26	3.65	3.56	0.93
Sum		41.57	27.00	30.29	32.95	9.10

Table A7. Overall Average Concentrations (C) and Standard Deviations (SD) (ng/m^3)

Congener	Order	PSF-C	PSF-SD	PSP-C	PSP-SD	Total-C	Total-SD
8	1	0.002	0.002	0.042	0.043	0.043	0.042
18	2	0.001	0.002	0.013	0.010	0.013	0.010
15	3	0.002	0.002	0.096	0.129	0.097	0.130
16	4	0.000	0.000	0.012	0.009	0.012	0.009
31	5	0.001	0.002	0.117	0.074	0.118	0.073
28	6	0.002	0.003	0.110	0.061	0.112	0.062
33	7	0.001	0.002	0.052	0.054	0.053	0.056
22	8	0.000	0.000	0.017	0.026	0.017	0.027
52	9	0.002	0.003	0.102	0.052	0.104	0.052
49	10	0.001	0.001	0.065	0.036	0.066	0.037
47/48	11	0.000	0.001	0.047	0.025	0.047	0.025
44	12	0.001	0.001	0.035	0.019	0.036	0.019
42/37	13	0.000	0.001	0.007	0.006	0.007	0.006
74	14	0.001	0.001	0.038	0.022	0.039	0.022
66/95	15	0.002	0.002	0.069	0.036	0.072	0.037
60	16	0.000	0.001	0.016	0.011	0.016	0.012
101	17	0.011	0.009	0.161	0.038	0.173	0.040
99	18	0.005	0.004	0.069	0.013	0.074	0.016
97	19	0.011	0.009	0.091	0.037	0.102	0.040
81/87	20	0.000	0.000	0.072	0.138	0.072	0.138
77/110	21	0.004	0.003	0.065	0.046	0.070	0.046
82	22	0.000	0.000	0.001	0.001	0.001	0.001
149/123	23	0.006	0.004	0.077	0.025	0.083	0.025
118	24	0.005	0.004	0.086	0.030	0.091	0.030
114	25	0.001	0.002	0.013	0.017	0.014	0.017
105	26	0.001	0.001	0.011	0.008	0.011	0.009
141	27	0.001	0.001	0.022	0.014	0.023	0.014
137	28	0.002	0.003	0.018	0.011	0.020	0.012
138/163	29	0.006	0.003	0.087	0.039	0.093	0.041
126	30	0.001	0.002	0.006	0.009	0.006	0.009
187	31	0.008	0.006	0.087	0.099	0.095	0.098
128	32	0.001	0.001	0.017	0.027	0.018	0.027
185	33	0.000	0.000	0.011	0.011	0.011	0.011
171	34	0.001	0.001	0.014	0.015	0.014	0.015
156	35	0.001	0.001	0.009	0.012	0.010	0.012
180	36	0.007	0.003	0.044	0.017	0.054	0.016
200	37	0.000	0.000	0.007	0.008	0.007	0.008
169	38	0.000	0.000	0.000	0.001	0.000	0.001
198 or 199	39	0.000	0.001	0.002	0.004	0.002	0.005
207	40	0.000	0.000	0.002	0.002	0.002	0.002
205	41	0.000	0.001	0.000	0.001	0.001	0.003
206	42	0.000	0.000	0.008	0.008	0.008	0.007
209	43	0.000	0.000	0.000	0.001	0.001	0.001
Sum		0.089	0.083	1.816	1.248	1.908	1.262

Table A8. Overall Average of Gas Fluxes (F: ng/m^2-d) and Their Std. Dev.(SD)

Congener	Order	WSS_{1R}-F	WSS_{1R}-SD	WSS_{A-P}-F	WSS_{A-P}-SD
8	1	4.793	7.120	7.278	10.372
18	2	3.889	5.018	2.935	4.803
15	3	8.495	11.280	13.346	16.971
16	4	3.196	4.233	1.637	2.950
31	5	2.968	5.882	4.177	8.284
28	6	3.650	5.264	3.773	4.641
33	7	6.050	7.761	5.040	6.794
22	8	3.458	4.587	1.542	3.092
52	9	13.317	15.701	3.127	3.806
49	10	6.654	8.464	4.699	5.197
47/48	11	4.383	6.416	6.790	7.834
44	12	13.308	15.903	15.933	17.492
42/37	13	6.184	11.542	7.803	15.392
74	14	14.800	11.872	10.956	14.593
66/95	15	27.169	42.617	21.209	39.536
60	16	6.800	7.708	8.199	9.348
101	17	58.327	35.727	23.398	
99	18	38.287	25.571	24.469	28.607
97	19	44.915	30.366	10.382	
81/87	20	6.563	17.031	24.424	25.518
77/110	21	28.583	52.000	54.812	66.377
82	22	2.410	4.628	3.194	5.038
149/123	23	47.529	50.887	49.299	55.517
118	24	34.639	37.654	35.776	45.533
114	25	0.485	1.133	1.486	1.625
105	26	0.507	1.201	3.815	4.319
141	27	15.972	20.819	13.691	13.084
137	28	10.210	8.278	8.477	10.164
138/163	29	36.212	33.020	38.126	43.740
126	30	0.737	1.671	0.921	1.541
187	31	13.251	11.318	9.085	14.837
128	32	3.885	8.078	5.490	8.252
185	33	3.418	4.659	3.058	3.445
171	34	5.599	8.795	4.248	7.823
156	35	0.516	0.565	0.299	0.644
180	36	13.007	14.245	20.798	40.970
200	37	2.198	2.373	2.028	2.261
169	38	0.000	0.000	1.350	2.619
198 or 199	39	0.158	0.364	0.670	1.312
207	40	0.000	0.000	0.153	0.265
205	41	0.315	0.463	0.500	1.021
206	42	1.048	1.399	2.138	1.637
209	43	0.000	0.000	0.617	0.792
Sum		497.885	543.616	461.150	558.048

Table A9. Overall Average Particulate Fluxes (F: ng/m^2-d) and Their Std. Dev. (SD)

Congener	Order	Plate-F	Plate-SD	WSS_{1F}-F	WSS_{1F}-SD
8	1	2.670	7.149	5.559	5.462
18	2	0.832	2.259	1.458	1.363
15	3	2.303	6.908	9.591	9.277
16	4	1.040	2.347	1.213	1.918
31	5	0.000	0.000	1.537	2.645
28	6	2.093	4.165	0.813	1.830
33	7	2.515	4.095	3.281	5.136
22	8	1.102	2.085	1.092	1.983
52	9	6.650	7.084	5.351	5.361
49	10	3.448	5.720	2.943	2.672
47/48	11	0.000	0.000	1.607	2.189
44	12	4.447	10.218	1.936	3.296
42/37	13	0.711	2.132	3.636	5.052
74	14	1.886	2.689	3.723	4.897
66/95	15	13.192	22.989	11.245	14.443
60	16	2.016	4.073	3.402	5.318
101	17	35.631	16.038	15.815	12.502
99	18	29.736	9.291	5.980	5.093
97	19	32.156	10.025	4.081	5.716
81/87	20	0.000	0.000	10.405	16.192
77/110	21	3.433	5.961	23.493	21.262
82	22	0.000	0.000	0.320	0.548
149/123	23	8.767	11.717	19.979	17.616
118	24	9.809	13.585	13.685	9.811
114	25	0.000	0.000	1.339	1.931
105	26	1.140	2.344	4.798	6.197
141	27	0.510	1.080	4.584	3.416
137	28	4.110	2.880	1.571	1.792
138/163	29	17.322	16.416	26.821	13.323
126	30	0.000	0.000	0.341	1.131
187	31	22.862	14.269	20.516	26.881
128	32	0.719	1.515	2.707	2.680
185	33	0.032	0.103	2.033	2.905
171	34	2.107	3.624	2.746	2.985
156	35	1.529	1.644	1.134	2.174
180	36	25.533	13.511	28.825	28.297
200	37	0.172	0.384	1.169	1.756
169	38	0.000	0.000	2.454	5.036
198 or 199	39	0.000	0.000	1.179	2.304
207	40	0.000	0.000	0.142	0.332
205	41	0.000	0.000	0.273	0.906
206	42	0.000	0.000	4.041	5.242
209	43	1.755	5.549	1.104	1.430
Sum		242.226	213.849	259.923	272.298

Table A10. Overall Average of Dry Deposition Velocities (cm/s) for Gas Phases

Congener	Order	WSS_{iR}-V_d	WSS_{1R}-SD	WSS_{A-P}-Vd	WSS_{A-P}-SD
8	1	0.584	0.631	0.707	0.861
18	2	0.694	0.657	0.693	0.819
15	3	0.424	0.650	0.450	0.658
16	4	0.928	0.849	0.872	0.928
31	5	0.051	0.054	0.049	0.029
28	6	0.063	0.049	0.059	0.030
33	7	0.432	0.403	0.288	0.379
22	8	1.405	1.302	0.734	0.923
52	9	0.274	0.204	0.071	0.048
49	10	0.174	0.089	0.118	0.042
47/48	11	0.261	0.188	0.271	0.290
44	12	0.802	0.912	0.892	0.936
42/37	13	0.815	0.538	1.264	1.342
74	14	0.642	0.800	1.109	1.007
66/95	15	1.066	0.809	0.653	0.844
60	16	0.637	0.429	0.860	0.490
101	17	0.415	0.361	0.717	
99	18	0.645	0.398	0.799	0.240
97	19	0.631	0.472	0.823	
81/87	20	0.004		1.441	
77/110	21	1.052	0.930	1.073	1.083
82	22	1.210	0.309	0.806	0.516
149/123	23	0.890	0.836	0.724	0.894
118	24	0.525	0.397	0.679	0.461
114	25	0.138	0.034	0.352	0.581
105	26	0.313	0.115	0.684	0.484
141	27	0.523	0.425	0.519	0.320
137	28	0.928	0.863	1.185	1.064
138/163	29	0.542	0.472	0.983	0.690
126	30	0.178		0.178	
187	31	0.287	0.111	0.264	0.281
128	32	0.262	0.332	0.958	0.918
185	33	0.359	0.325	0.505	0.633
171	34	0.738	0.975	0.582	0.941
156	35	0.173	0.207	0.264	0.365
180	36	0.240	0.301	0.448	0.439
200	37	0.757	1.039	0.593	0.600
169	38				
198 or 199	39				
207	40			2.008	1.227
205	41				
206	42	0.400	0.776	0.590	0.730
209	43			0.968	0.861
Average		0.538	0.507	0.681	0.638

Table A11. Overall Average of Dry Deposition Velocities (cm/s) for Particulate Phase

Congener	Order	Plate-V_d	Plate-SD	WSS_{1F}-V_d	WSS_{1F}-SD
8	1	4.148	4.676	3.146	2.057
18	2			4.527	4.051
15	3	8.912		4.018	3.775
16	4	8.536	11.749	4.893	4.078
31	5			4.657	3.359
28	6	2.323	0.451	2.322	2.616
33	7	3.106		5.177	0.160
22	8	7.878		9.311	
52	9	6.942	8.082	5.186	4.741
49	10	10.519	5.935	5.624	4.354
47/48	11			9.564	7.746
44	12	7.771	5.315	7.490	6.180
42/37	13	17.656			
74	14	4.925	3.257	8.105	6.456
66/95	15	12.313	12.239	6.120	6.165
60	16	5.366	3.693	11.121	8.191
101	17	3.159	1.720	3.906	4.374
99	18	7.420	4.640	2.622	3.463
97	19	4.590	4.891	1.286	1.120
81/87	20				
77/110	21	2.074	0.942	4.755	3.343
82	22			4.986	
149/123	23	3.979	2.418	4.272	2.888
118	24	7.810	4.889	4.656	3.704
114	25				
105	26	6.912	9.347	5.281	1.802
141	27	5.903		5.873	4.564
137	28	5.758	9.288	1.970	1.825
138/163	29	4.541	3.870	5.758	3.812
126	30				
187	31	6.142	5.560	3.371	3.252
128	32	15.069		8.287	2.953
185	33			7.117	
171	34	1.734	0.739	5.279	4.021
156	35	2.891	1.620	3.475	3.471
180	36	4.738	4.113	4.263	3.158
200	37			4.258	3.391
169	38				
198 or 199	39				
207	40				
205	41				
206	42			6.216	3.060
209	43			3.591	1.879
Average		6.540	4.974	5.214	3.750

Table A12. Slopes and Intercept Values of Log $K_p = b_r - m_r \text{Log } p_L^o$

Sample No	Slope (m_r)	Intercept (b_r)	r^2	Wind Direction
S1-2	0.041067	-2.783136	0.004484	Lake/Land
S4-1	-0.105324	-2.66784	0.025414	Lake/Land
S4-2	0.176328	-1.857585	0.093779	Lake/Land
S9-3	0.201914	-2.251248	0.140179	Lake/Land
S9-4	-0.095628	-2.990649	0.013325	Lake/Land
S11-2	0.033318	-3.28133	0.004215	Lake/Land
Average	0.041946	-2.638631	0.046899	

Sample No	Slope	Intercept	r^2	Wind Direction
S1-1	0.317448	-2.1775	0.307798	Land
S3-1	-0.013548	-4.080429	0.00119	Land
S5-3	0.028255	-2.318579	0.002277	Land
S5-4	-1.193791	-5.660844	0.686988	Land
S7-3	-0.140083	-3.638378	0.018816	Land
S10-2	-0.720749	-6.847833	0.135974	Land
S10-3	-0.271697	-4.61729	0.281617	Land
S10-4	-0.118612	-3.493603	0.134511	Land
S11-3	-0.066946	-3.838645	0.016166	Land
Average	-0.242191	-4.074789	0.176149	

Sample No	Slope	Intercept	r^2	Wind Direction
S4-3	-1.193316	-5.75046	0.72847	Lake
S5-2	-0.638447	-4.823555	0.410852	Lake
S6-1	-0.252411	-2.71082	0.407194	Lake
S6-2	-0.499019	-3.655243	0.591366	Lake
S7-1	-0.226353	-4.316715	0.082241	Lake
S7-2	-0.119817	-2.974754	0.090784	Lake
S10-1	-0.375468	-3.607097	0.564254	Lake
Average	-0.472119	-3.976949	0.410737	

Table A13. Summary of All Dry Deposition Velocities (cm/s) From All Cases

Sample Name	w/o Jackknife	w/ Jackknife w/o LOD	w/ Jackknife w/ LOD
Overall	2.55 ± 5.14	1.11 ± 1.32	0.82 ± 0.90
Plate	7.28 ± 5.61	6.54 ± 4.97	4.79 ± 4.87
WSS_{IF}	5.48 ± 4.10	5.21 ± 3.75	4.52 ± 4.34
WSS_{IR}	0.64 ± 0.64	0.54 ± 0.51	0.39 ± 0.48
WSS_{A-P}	0.74 ± 0.72	0.68 ± 0.64	0.50 ± 0.64

BIBLIOGRAPHY

Achman, D. R., Hornbuckle, K. C., and Eisenreich, S. J., "Volatilization of Polychlorinated Biphenyls from Green Bay, Lake Michgan," Environmental Science and Technology, Vol. 27, No. 1, pp. 75-87, 1993.

Alcock, R. E., Halsall, C. J., Harris, C. A., Johnston, A. E., Lead, W. A., Sanders, G., and Jones, K. C., "Contamination of Environmental Samples Prepared for PCB Analysis," Environmental Science and Technology, Vol. 28, No. 11, pp. 1838-1842, 1994.

Alcock, R. E.,Johnston, A. E., McGrath, S. P., Berrow, M. L., and Jones, K. C., "Long - Term Changes in the Polychlorinated Biphenyl Content of United Kingdom Soils," Environmental Science and Technology, Vol. 27, No. 9, pp 1918-1923, 1993.

Alford-Stevens, A. L., "Analyzing PCBs: Basic Information about PCBs and How They are identified and Measured,", Environmental Science and Technology, Vol. 20, No. 12, pp. 1194-1199, 1986.

Allen, J. O., Dookeran, N. M., Smith, K.A., Sarofim, A.F., Taghizadeh, K., and Lafleur,, A.L., "Measurement of PAHs Associated with Size-Segregated Atmospheric Aerosols in Massachusetts," Environ. Science Technol., Vol. 30, No. 3, pp. 1023-1031, 1996.

Baek, S.O., Goldstone, M.E.,Kirk, P.W.W., Lester, J.N. and Perry, R., "Phase Distribution and Particle Size Dependency of {Ahs in the Urban Atmosphere,' Chemosphere, pp. 503-520, 1991.

Baker, J. E., and Eisenreich, S. J., "Concentrations and Fluxes of Polycyclic Aromatic Hydrocarbons and Polychlorinated Biphenyls across the Air - Water Interface of Lake Superior," Environmental Science and Technology, Vol. 26 , No 7, pp. 1375 - 1382, 1992.

Baker, J. E., Eisenreich, S. J. and Eadie, B. J., "Sediment Trap Fluxes and Benthic Recycling of Organic Carbon, PAHs, Polychlorobiphenyl Congeners in Lake Superior," Environmental Science and Technology, Vol. 25, No. 3, pp 500-509, 1991.

Baker, J.E., T. M. Church, S. J. Eisenreich, W. F. Fitzgerald, J. R. Scudlark, Relative Atmospheric Loadings of Toxic Contaminants and Nitrogen to the Great Lakes Report, 1993

Bidleman, T.F. and E.J. Christensen,"Atmospheric Removal Processes for High Molecular Weight Organochlorines," 1979, J. Geophysics Res., Vol. 84, pp. 7857-7862.

Bidleman, T.F., E.J. Christensen, and H.W. Harder, "Aerial Deposition of Organochlorines in Urban and Coastal South Carolina," in Atmospheric Pollutants in Natural Waters by S. J. Eisenreich, Ann Arbor Science Publisher, Inc., 1981.

Bidleman, T.F., Wideqvist, U., Jansson, B. and Soderlund, R, "Organochlorine Pesticides and Polychlorinated Biphenyls in the Atmosphere of Southern Sweden," Atm. Environ., Vol. 21, pp. 641-654, 1987.

Brunner, S., Hornung, E., Santl, H., Wolff, E., Piringer, O.G., Altschuh, J., Bruggeman, R., "Henry's Law Constants for Polychlorinated Biphenyls: Experimental Determination and Structure-property Relationships," Environ. Sci. Technol., Vol. 24, No. 11, pp. 1751-1754, 1990.

Carter, D. S., And Hites, R. A., "Fate and Transport of Detroit River Derived Pollutants Throughout Lake Erie," Environmental Science and Technology, Vol. 26, No 7, pp. 1333 - 1341, 1992.

Chen, S-J, Hsieh, L-T., and Hwang, P-S., "Concentration, Phase Distribution, and Size Distribution of Atmospheric Polychlorinated Biphenyls Measured in Southern Taiwan," Environ. Int., Vol. 22, No. 4, pp. 411-423, 1996.

Colombo, J. C., Bilos, C., Campanaro, M., Presa, M. J. R., and Catoggio, J. A., "Bioaccumulation of Polychlorinated Biphenyls and Chlorinated Pesticides by the Asitatic Clam *Corbicula fluminea*: Its Use as Sentinel Organism in the Rio de La Plata Estuary, Argentina," Environmental Science and Technology, Vol. 29, No. 4, pp 914 - 927, 1995.

Cotham W.E. and Bidleman, T.F. "Laboratory Investigations of the Partitioning of Organochlorine Compounds between the Gas and Atmospheric Aerosols on Glass Fiber Filters," Environ. Sci. Technology, Vol. 26, No. 3, pp. 469- 477, 1992.

Cotham, W. E., and Bidleman, T. F., "Polycyclic Aromatic Hydrocarbons and Polychlorinated Biphenyls in Air at an Urban and a Rural Site near Lake Michigan," Environmental Science and Technology, Vol. 29, No 11, pp. 2782 - 2789, 1995.

Davidson, C. I., Lindberg, S. E., Schmidt, J.A., Cartwright, L. G., and Landis, L.R.., "Dry Deposition of Sulfate Onto Surrogate Surfaces," J. of Geophysical Research, Vol. .90, No. D1, pp. 2123-2130, 1992.

Dickhut, R.M., and Gustafson, K.E., "Gaseous Exchange of PAHs Across the Air-Water Interface of Southern Chesapeake Bay," Environ. Science and Technology, Vol. 31, No. 6, pp. 1623-1629, 1997.

Doskey, P. V. and Andren, A. W., "Concentrations of Airborne PCBs Over Lake Michigan," J. Great Lakes Res. 7 (1), pp. 15-20, 1981.

Doskey, P.V. and A.W.Andren, "Modeling the Flux of Atmospheric PCBs Across the Air/Water Interface," Environ. Sci. Techno. ,Vol. 15, pp.705-711, 1981a.

Dunnivant, F. M., Eizerman, A. W., Jurs, P. C., and Hasan, M. N., "Quantitative Structutre-Property Relationships for Aqueous Solubilities and Henry's Law Constants of PCBs," Environmental Science and Technology, Vol. 26, No. 8, pp 1567 - 1573, 1992.

Eisenreich, S.J. Atmospheric Pollutants in Natural Water, Ann Arbor Science Publisher, Inc., 1981.

Eisenreich, S.J., Looney, B.B. and Thornton, L.D., "Airborne Organic Contaminants in the Great Lakes Ecosystem", Environ. Sci. Technol., 15, 30-38, 1981.

Eitzer, B. D., and Hites, R. A., "Atmospheric Transport and Deposition of Polychlorinated Dibenzo-p-dioxins and Dibenzofurans," Environ. Sci. and Techno.,Vol. 23 , No 11, pp. 1396 - 1401, 1989.

Eitzer, B. D., and Hites, R. A., "Polychlorinated Dibenzo-p-dioxins and Dibenzofurans in the Ambient Atmosphere of Bloomington, Indiana," Environ. Sci. and Techno.. Vol. 23 , No 11, pp. 1389 - 1395, 1989.

Falconer, R.L., Bidleman, T.F., Cotham, W.E., "Preferential Sorption of Non- and Mono-ortho-polychlorinated Bipheyls to Urban Aerosols," Environ. Sci. Technology, Vol. 29, No. 6, pp. 1666-1673, 1995.

Fangmark, I., Stromberg, B., Berge, N., and Rappe, C., "Influence of Postcombustion Temperature Profiles on the Formation of PCDDs, PCDFs, PCBzs, and PCBs in a Pilot Incinerator," Environmental Science and Technology, Vol. 28, No. 4, pp 624 - 629, 1994.

Fendinger, N. J., Glotfelty, D. E., and Freeman, H. P., "Comparison of Two Experimental Techniques for Determining Air / Water Henry's Law Constants," Environmental Science and Technology, Vol. 23 , No 12, pp. 1528-1531, 1989.

Finlayson-Pitts, B. J., Pitts J.N., Atmospheric Chemistry: Fundamentals and Experimental Techniques, John Wiley & Sons, 1986.

Foreman, W. T., and Bidleman, T. F., "Semivolatile Organic Compounds in the Ambient Air of Denver, Colorado," Atmospheric Environment, Vol. 24A, No. 9, pp. 2405 - 2416, 1990.

Formica, S. J., Baron, J. A., Thibodeaux, L. J., and Valsaraj, K. T., "PCB Transport into Lake Sediments. Conceptual Model and Laboratory Simulation," Environmental Science and Technology, Vol. 22, No.12, pp 1435 - 1440, 1988.

Franz, T.P., "Deposition Of Semivolatile Organic Chemicals By Snow," Ph.D. Thesis of University Of Minnesota, December 1994.

Gilbertson, M., "Background to the Regulation of PCBs in Canada, Task Force on PCBs," Report to Environ. Comittee of Environment Canada and Health and Welfare, Toronto, Canada, 1976.

Haneef, S. J., Johnson, J. B., Dickson, C, Thompson G. E., and Wood, G. C., " Effect of Dry Deposition of NO_x and SO_2 Gaseous Pollutants on the Degradation of Calcareous Building Stones," Atmospheric Environment, Vol. 26A, No. 16, pp. 2963-2974, 1992.

Harner, T., Mackay, D., and Jones, K. C.,"Model of the Long-term Exchange of PCBs Between Soil and the Atmosphere in the Southern U.K.," Environmental Science and Technology, Vol. 29, No. 5, pp 1200 - 1209, 1995.

Hart, K. M., and Pankow, J. F. " High-Volume Air Sampler for Particle and Gas Sampling. 2. Use of Backup Filters to Correct for the Adsorption of Gas-Phase PAHs to the Front Filter," Environmental Science and Technology, Vol. 28, No. 4, pp. 655 - 661, 1994.

Hart, K. M., Isabelle, L. M., and Pankow, J. F. " High-Volume Air Sampler for Particle and Gas Sampling. 1. Design and Gas Sampling Performance," Environmental Science and Technology, Vol. 26, No. 5, pp. 1048 -1052, 1992.

Hawker, D. W., "Vapor Pressures and Henry's Law Constants of Polychlorinated Biphenyls," Environmental Science and Technology, Vol. 23, No 10, pp. 1250 - 1253, 1989.

Hawker, D.W., Connell, D.W., "Octanol-Water Partition Coefficients of Polychlorinated Biphenyl Congeners," Environ. Sci. Technol. 1988, 22, 382-387.

Hawthorne, S. B., Miller, D. J., Langenfeld, J. J. and Kriger, M. S.,"PM-10 High-Volume Collection and Quantitation of Semi- and Nonvolatile Phenols, Methoxylated Phenols, Alkanes, and PAHs from Winter Urban Air and Their Relationship to Wood Smoke Emissions," Environmental Science and Technology, Vol. 26, No. 11, pp 2251 - 2262, 1992.

Hermanson, M. H., and Hites, R. A., "Long - Term Measurements of Atmospheric Polychlorinated Biphenyls in the Vicinity of Superfund Dumps," Environmental Science and Technology, Vol. 23, No 10, pp. 1253 - 1258, 1989.

Hinshaw,J.V. and Ettre, L.S. Introduction to Open-Tubular Column Gas Chromatograph ADVANSTAR Communications, Cleveland, OH, 1994.

Hoff, R. M., Muir, D. C. G., and Grift, N. P., "Annual Cycle of Polychlorinated Biphenyls and Organohalogen Pesticides in Air in Southern Ontario. 1. Air Concentration Data," Environmental Science and Technology, Vol. 26 , No 2, pp. 266 - 275, 1992.

Hoff, R. M., Muir, D. C. G., and Grift, N. P., "Annual Cycle of Polychlorinated Biphenyls and Organohalogen Pesticides in Air in Southern Ontario. 1. Air Concentration Data," Environmental Science and Technology, Vol. 26 , No 2, pp. 276 - 283, 1992.

Holsen, T. M., Noll, K. E., Liu, S-P, and Lee, W-J., "Dry Deposition of Polychlorinated Biphenyls in Urban Areas," Environmental Science and Technology, Vol. 25, No 6, pp. 1075 - 1081, 1991.

Holsen, T.M. and Noll, K.E. "Dry Deposition of Atmospheric Particles: Application of Current Models to Ambient Data," Environmental Science and Technology, Vol. 27, 1327-1333, 1992.

Holsen, T.M., Noll, K.E., Fang, G-C., Lee, W-J., and Lin J-M., "Dry Deposition and Particle Size Distributions Measured during the Lake Michigan Urban Air Toxics Study," Environmental Science and Technology Vol. 27, No. 7, pp. 1327-1333, 1993.

Holsen, T.M., Noll, K.E., Liu, S. and Lee, W., "Dry Deposition of Polychlorinated Bipheyls in Urban Areas," Environ. Sci. Technology, Vol. 25, No. 6, pp. 1075-1081, 1991.

Hornbuckle, K. C., Achman, D. R., and Eisenreich, S.J., "Over - Water and Over - Land Polychlorinated Bipheyls in Green Bay, Lake Michigan," Environmental Science and Technology, Vol. 27, No 1, pp. 87 - 98, 1993.

Hornbuckle, K. C., Jeremiason, J. D., Sweet, C. W., and Eisenreich, S. J., "Seasonal Variations in Air - Water Exchange of Polychlorinated Biphenyls in Lake Superior," Environmental Science and Technology, Vol. 28 , No 8, pp. 1491 - 1501, 1994.

Hornbuckle, K. C., Sweet, C. W., Pearson, R. F., Swackhamer, D. L., and Eisenreich, S. J., "Assessing Annual Water - Air Fluxes of Polychlorinated Biphenyls in lake Michigan," Environmental Science and Technology, Vol. 29, No 4, pp. 869 - 877, 1995.

Hornbuckle, K.C., Jeremiason, J.D., Sweet, C.W., and Eisenreich, S.J., "Seasonal Variations in Air-Water Exchange of Polychlorinated Biphenyls in Lake Superior," Environ. Sci. Technol., V 28, No 8, pp 1491-1501, 1994.

Jeremiason, J. D., Hornbuckle, K. C., and Eisenreich S. J., "PCBs in Lake Superior, 1978 1992: Decreases in water Concentrations Reflect Loss by Volatilization," Environmental Science and Technology, Vol. 20 , No 5, pp. 903 - 914, 1994.

Kaupp, H., and Umlauf, G., "Atmospheric Gas-Particle Partitioning of Organic Compounds: Comparison of Sampling Methods," Atmospheric Environment, Vol. 26A, No. 13, pp. 2259 - 2267, 1992.

Kaupp, H., Doerr, G., Hippelein, M., McLachlan, M.S., and Hutzinger, O., "Baseline Contamination Assessment For A New Resource Recovery Facility In Germany. Part IV: Atmospheric Concentrations Of Polychlorinated Biphenyls and Hexachlorobenzene," Chemosphere, Vol. 32, No. 10, pp. 2029-2042, 1996.

Keller, C. D., and Bidleman, T. F.,"Collection of Airborne PAHs and Other Organics with a Glass Fiber Filter-PUF System," Atmospheric Environment, Vol. 18, No. 4, pp. 837 - 845, 1984.

Kleinbaum, D.G., L.L. Kupper, K.E. Muller, Applied Regression Analysis and Other Multivariable Methods, PWS-Kent Publishing Co., 1988.

Koester, C. J., and Hites, R. A., "Wet and Dry Deposition of Chlorinated Dioxins and Furans," Environmental Science and Technology, Vol. 26 , No 7, pp. 1375 - 1382, 1992.

Krieger, M. S. and Hites, R. A, "Diffusion Denuderfor the Collection of Semivolatile Organic Compounds," Environmental Science and Technology, Vol. 26, No. 8, pp. 1551 - 1555, 1992.

Krieger, M. S. and Hites, R. A, "Measurement of PCBs and PAHs in Air with a Diffusion Denuder," Environmental Science and Technology, Vol. 28, No. 6, pp. 1129 - 1133, 1994.

Lane, D. A., Johnson, N. D., Barton, S. C., Thomas, G. H. S., and Schroeder, W. H., "Development and Evaluation of a Novel Gas and particle Sampler for emivolatile Chlorinated Organic Compounds in Ambient Air," Environmental Science and Technology, Vol. 22 , No 8, pp. 941 - 947, 1988.

Lane, D. A., Schroeder, W. H., and Johnson, N. D., "On the Spatial and Temporal Variations in Atmospheric Concentrations of Hexachlorobenzene and Hexachlorocyclohexane Isomers at Several Locations in the Province of Ontario, Canada," Atmospheric Environment, Vol. 26A, No. 1, pp. 31 - 42, 1992.

Larsen, B. R. "HRGC Separation of PCB Congeners," J. High Resol. Chromatogr., Vol. 18, pp. 141- 151, March 1995.

Larsen, B., Bowadt, S., and Facchetti, S., "Seperation of Toxic Congeners from PCB Mixtures on Two Selected Coupled Narrow-bore Columns," International Journal of Environmental Analytical Chemistry, Vol. 47, No.3, pp. 147-166, 1992.

Lead, W. A., Steinnes, E. and Jones, K. C., " Atmospheric Deposition of PCBs to Moss (*Hylocomium splendens*) in Norway between 1977 and 1990," Environmental Science and Technology, Vol. 30, No. 2, pp. 524 - 530, 1996.

Lee, D. S., and Longhurst, J. W. S., "A Comparison Between Wet and Bulk Deposition at an Urban Site in the U.K.," Water, Air and Soil pollution, Vol. 64, pp. 635-648, 1992.

Lee, W-J, "The Determination Of Dry Deposition Velocities For Gases And Particles," Ph.D. Thesis of Illinois Institute of Technology, June 1991.

Lee, W-J., Lin Lewis, S-. J., Chen, Y-Y., Wang, Y-F., Sheu, H-L., Su, C-C, and Fan, Y-C., "Polychlorinated Biphenyls in the Ambient Air of Petroleum Refinery, Urban and Rural Areas," Fourth Int. Conf. On Atmospheric Science and Applications To Air Quality, July 1996.

Li, A., and Andren, A. W., "Solubility of Polychlorinated Biphenyls in Water/Alcohol Mixtures. 1. Experimental Data," Environmental Science and Technology, Vol. 28 , No 1, pp. 47 - 52, 1994.

Lin, J. J., Noll, K.E., and Holsen T.M., "Dry Deposition Velocities as a Function of Particle Size in the Ambient Atmosphere," Aerosol Science and Technology Vol.20, pp. 239-252, 1994.

Lindfors V, Joffre S. M., and Damski, J., "Meteorological Variability of the Wet and Dry Deposition of Sulfur and Nitrogen Compounds Over the Baltic Sea," Water, Air and Soil Pollution, Vol. 66, pp. 1-28, 1993.

Liss, P. S. and P. G. Slater, "Flux of Gases Across the Air-Sea Interface," 1974, Nature, Vol. 247, pp. 181-184.

Liss, P.S. and W.G.N Slinn, :Air-Sea Exchange of Gases and Particles," NATO ASI Series#108, D. Reidel: Dordrecht: New York, 1983.

Little, J. C., "Applying the Two - Resistance Theory to Contaminant Volatilization in Showers," Environmental Science and Technology, Vol. 26, No 7, pp. 1341 - 1349, 1995.

Liu, S-P, "Atmospheric PArticle-Bound PCB Concentration And Dry Deposition In Urban Areas," M.S. Thesis of Illinois Institute of Technology, May 1990.

Mackay, D. and A.T.K. Yuen, "Transfer Rates of Gaseous Pollutants and Between The Atmosphere and Natural Waters," in Atmospheric Pollutants in Natural Waters by S. J. Eisenreich, Ann Arbor Science Publisher, Inc., 1981.

Mackay, D., Shiu, W.Y., and Ma, K.C., Illustrated Handbook of Physical-Chemical Properties and Environmental Fate for Organic Chemicals, Volume 1, Lewis Publishers, Inc., Michigan, 1992.

Manahan, S.E. Environmental Chemistry, Lewis Publishers Inc., 1991.

Manahan, S.E., Hazardous Waste Chemistry Toxicology and Treatment, Lewis Publishers, Inc., 1990.

Manchester - Neesvig, J. B., and Andren, A. W., "Seasonal Variation in the Atmospheric Concentration of Polychlorinated Biphenyl Congeners," Environmental Science and Technology, Vol. 23, No 9, pp. 1138 - 1148, 1989.

McDow, S. R., and Huntzicker, J.J., "Vapor Adsorption Artifact in the Sampling of Organic Aerosol: Face Velocity Effects," Atmospheric Environment, Vol. 24A, No. 10, pp. 2563 - 2571, 1990.

Mullin, M. D., Pochini, C. M., McCrindle, S., Romkes, M., Safe, S., and Safe, L.M., "High-Resolution PCB Analysis: Synthesis and Chromatographic properties of All 209 PCB Congeners," Environmental Science and Technology, Vol. 18, No. 6, pp 468-476, 1984.

Murphy, T. J., Comment on "Seasonal Variations in Air - Water Exchange of Polychlorinated Biphenyls in Lake Superior," Environmental Science and Technology, Vol. 29, No 38, pp. 846 - 847, 1995.

Murphy, T.J. and C.P. Rzeszutko, "Precipitation Inputs of PCBs to Lake Michigan," J. Great Lakes Res., Vol. 3, pp. 305-312, 1977.

Murphy, T.J., A. Schinsky, G. Paolucci, and C. P. Rzeszutko "Inputs of PCBs from the Atmosphere to Lakes Huron and Michigan," in Atmospheric Pollutants in Natural Waters by S. J. Eisenreich, Ann Arbor Science Publisher, Inc., 1981.

Myrczik, P, "Comparison of Long and Short-term Dry Deposition Measurements of Polychlorinated Biphenyls," Special Study of Illinois Institute of Technology, February 1997.

Neilson, A.H., Organic Chemicals in the Aquatic Environment: Distribution, Persistence and Toxicity, CRC Press, Inc., 1994.

Noll, K. E., Po-Fat, Y., and Fang, K.Y.P, "Atmospheric Coarse Particulate Concentrations and Dry Deposition Fluxes for Ten Metals in Two Urban Environments," Atmospheric Environment, Vol. 24A, No. 4, pp. 903-908, 1990.

Odabasi, M., Tasdemir, Y, Vardar, N., Sofuoglu, A., and Holsen, T.M., "Polycyclic Aromatic Hydrocarbons and Polychlorinated Biphenyls in the Ambient Air of Chicago," Proceedings of Symp. On Air Quality Management, Istanbul, Turkey, September 1997.

Odum, J.R., Yu, J. and Kamens, R. M.,"Modeling the Mass Transfer of Semivolatile Organics in Combustion Aerosols," Environmental Science and Technology, Vol. 28, No. 13, pp 2278 - 2285, 1994.

Ong, V., S., and Hites, R., "Determination of Pesticides and Polychlorinated Biphenyls in Water: A Low-Solvent Method," Environmental Science and Technology, Vol. 29, No. 5, pp 1259-1266, 1995.

Pankow, J. F., "Review and Comparative Analysis of the Theories on Partitioning Between the Gas and Aerosol particulate Phases in the Atmosphere," Atmospheric Environment, Vol. 21, No. 11, pp. 2275 - 2283, 1987.

Pankow, J. F., and Bidleman, T. F., "Effects of Temperature, TSP and percent Non-Exchangeable Material in Determining the Gas-Particle Partitioning of Organic Compounds," Atmospheric Environment, Vol. 25A, No. 10, pp. 2241 - 2249, 1991.

Pankow, J. F., Isabelle, L. M., Buchholz, D. A., Luo, W., and Reeves, B. D.," Gas/Particle Partitioning of PAHs and Alkanes to Environmental Tobacco Smoke," Environmental Science and Technology, Vol. 28, No. 2, pp. 363 - 365, 1994.

Pankow, J. F., Storey, J. E., and Yamasaki, H., "Effects of Relative Humidity on Gas/Particle Partitioning of Semivolatile Organic Compounds to Urban Particulate Matter," Environmental Science and Technology, Vol. 27, No. 10, pp. 2220 - 2226, 1993.

Panshin, S.Y. and Hites, R.A., "Atmospheric Concentrations of Polychlorinated Biphenyls at Bermuda," Environ. Sci. Technol., 1994a,Vol. 28, pp.2001-2007..

Panshin, S.Y. and Hites, R.A., "Atmospheric Concentrations of Polychlorinated Biphenyls at Bloomington, IN," Environ. Sci. Technol.,Vol. 28, pp. 2008-2013, 1994b.

Patton, G.W., Walla, M.D. and Bidleman T.F., "Airborne Organochlorine Compounds in the Atmosphere of Northern Ellesmere Island, Canada," J. Geophy. Res., Vol. 96D, pp. 10867-10879, 1989.

Peters, K. and Eiden, R., "Modeling the Dry Deposition Velocity of Aerosol Particles to a Spruce Forest," Atmospheric Environment, Vol. 26A, No. 16, pp. 2555 - 2564, 1992.

Picer, M., and Picer, N., "Levels of Some High Molecular Chlorinated Hydrocarbons in Sediment Samples from the Eastern Adriatic Coastal Waters," Water, Air, and Soil Pollution, Vol. 68, pp. 435 - 447, 1993.

Poster, D. L., and Baker, J.E., "Influence of Submicron Particles on Hydrophobic organic Contaminants in Precipitation.1. Concentrations and Distributions of Polycyclic Aromatic Hydrocarbons and Polychlorinated Biphenyls in Rainwater," Environ. Sci. Technology, Vol. 30, No. 1, pp. 341-348, 1996(a).

Poster, D. L., and Baker, J.E., "Influence of Submicron Particles on Hydrophobic organic Contaminants in Precipitation.2. Scavenging of Polycyclic Aromatic Hydrocarbons by Rain," Environ. Sci. Technology, Vol. 30, No. 1, pp. 349-354, 1996(b).

Potter, D. W., and Pawlioszyn, J., "Rapid Determination of Polyaromatic Hydrocarbons and Polychlorinated Biphenyls in Water Using Solid-phase Microextraction and GC/Ms," Environmental Science and Technology, Vol. 28, No. 2, pp 298-305, 1994.

Rapaport, R. A., and Eisenreich S. J., "Historical Atmospheric Inputs of High Molecular Weight Chlorinated Hydrocarbons to Eastern North America," Environmental Science and Technology, Vol. 22 , No 8, pp. 931 - 941, 1988.

Reist, P.C., Aerosol Science and Technology, Second Edition, John Wiley and Sons, Inc., New York, 1993.

Rickman, W.S., CRC Handbook of Incineration of Hazardous Wastes, CRC Press Inc., 1991

Riederer, M., "Estimating Partitioning and Transport of Organic Chemicals in the Foliage Atmosphere System: Discussion of Fugacity - Based Model," Environmental Science and Technology, Vol. 28 , No 8, pp. 1491 - 1501, 1994.

Ritts, D. and Williamson, R., "The Atmospheric Deposition of PCBs into San Francisco Bay," Air & Waste Management Association - 85th Annual Meeting and Exhibition, 1992.

Rojas, C. M., Van Grieken, R. E., and Laane, R. W., "Comparison of Three Dry Deposition Models Applied to Field Measurements in the Southern Bight of the North Sea," Atmospheric Environment, Vol. 27A, No. 6, pp. 363 - 370, 1993.

Rood, D., A practical Guide to the Care, Maintenance, and Troubleshooting of Capillary Gas Chromatographic Systems, Huthig Buch Verlag GmbH, Heidelberg 1991.

Rubel, G. O., "Partitioning of Partially Soluble Volatiles Between the Vapor and Liquid Aerosol Phase," Atmospheric Environment, Vol. 25A, No. 5/6, pp. 1009 - 1012, 1991.

Sanders, G., Jones, K. C., Hamilton-Taylor, J., and Dorr, H., " Historical Inputs of Polychlorinated Biphenyls and Other Organochlorines to a Dated Lacustrine Sediment Core in Rural England," Environmental Science and Technology, Vol. 26, No. 9, pp 1815 - 1821, 1992.

Sawyer, C.N., McCarty, P.L., Parkin, G.F, Chemistry for Environmental Engineering, McGraw-Hill, Inc., 1994.

Schantz, M., M., Parris, R., M., Kurz, J., Ballschmiter, K., and Wise, S., A., " Comparision of Methods for the Gas-Chromatographic Determination of PCB Congeners and Chlorinated Pesticides in Marine Refernce Materials," Fresenius' Journal of Analytical Chemistry, Vol. 346, pp. 766-778, 1993.

Schulz, D. E., Petrick, G., and Duinker, J. C., "Complete Characterization of PCB Congeners in Commercial Aroclor and Clophen Mixtures by Multidimensional Gas Chromatography-ECD," Environmental Science and Technology, Vol. 23, No. 7, pp 852 - 859, 1989.

Sedlak, D. L., Andren, A. W., "The Effects of Sorption on the Oxidation of Polychlorinated Biphenyls (PCBs) by Hydroxyl Radical," Water Res. , Vol. 28, No. 5, pp. 1207 - 1215, 1994.

Sehmel, G. A., "Particle and Gas Dry Deposition: A Review," Atmospheric Environment, Vol. 14, pp. 983 - 1011, 1980.

Seinfeld, J.H., Atmospheric Chemistry and Physics of Air Pollution, John Wiley and Sons, New York, 1986.

Simcik, M.F., Zhang, H., Eisenreich, S.J. and Franz, T.P. "Urban Contamination of the Chicago/Lake Michigan Atmosphere by PCBs and PAHs During AEOLOS," Submitted to Environ. Science and Techno., 1997.

Slinn, S. A., and Slinn, G. N., "Predictions for Particle Deposition on Natural Waters," Atmospheric Environment, Vol. 14, pp. 1013 - 1016, 1980.

Stow, C. A., and Carpenter, S. R., "PCB Accumulation in Lake Michigan Coho and Chinook Salmon: Individual-Based Models Using Allometric Relationships," Environmental Science and Technology, Vol. 28, No. 8, pp 1543 - 1549, 1994.

Sugita, K., Asada, S., Yokochi, T., Okazawa, T., Ono, M., and Goto, S., "Survey of Polychlorinated Dibenzo-p-dioxins, Polychlorinated Dibenzofurans, and Polychlorinated Biphenyls in Urban Air," Chlorinated Dioxins and Related Compounds, Elseveir Science Publishing, New York, 1994.

(SUPELCO)"Adsorption on Media," pp. 262 - 265.

Swackhamer, D., L., " Quality Assurance plan Green Bay Mass Balance Study: I. PCBs and Dieldrin," US EPA Great Lakes National Program Office, 1988.

Swain, R. W., "Toxic Substances in the Ecosystem," in A.D. Misener and G.Daniel, eds., Decisions for the Great Lakes (Hiram, Ohio: Great Lakes Tomorrow, and Hammond, Ind.: Purdue Univ.), Calument, 1982.

Sweet, C.W., and Basu, I., "Distribution of PCBs, , Pesticides and PAHs in Air and Precipitation Samples from Lake Superior and Lake Ontario" OME 36th Conference of the International Association for great Lakes Research, pp. 145, De Pere WI, June 1993.

Sweet, C.W., and Basu, I., "Measurements of Airborne PCBs Near Green Bay," OME 36th Conference of the International Association for great Lakes Research, pp. 65, De Pere WI, June 1993.

Sweet, C.W., Murphy, T.J., Bannach, J.H., Kelsey, C.A., and Hong, J., "Atmospheric Deposition of PCBs into Green Bay," J. Great Lakes Res., 19(1), pp. 109-128, 1993.

Tasdemir, Y., Odabasi, M., Vardar, N., Sofuoglu, A., Noll, K.E., and Holsen, T.M., "Development and Evaluation of a Water Surface Sampler to Investigate the Deposition of Semivolatile Organic Compounds (SOCs)," Proceedings of Symp. On Air Quality Management, Istanbul, Turkey, September 1997.

(TPFP) Department of Health and Human Services, Toxicological Profile for Selected PCBs (Aroclor-1260, 1254, 1248, 1242, 1232, 1221, and 1016), 1993.

Thibodeaux, L.J., Chemodynamics: Environmental Movement of Chamicals in Air, Water, and Soil, John Wiley and Sons, New York, 1979.

Thomas, D. R., Carswell, K. S., and Georgiou, G., "Mineralization of Biphenyl and PCBs by the White Rot Fungus *Phanerochaete chrysosporium*," Biotechnology and Bioengineering, Vol. 40, pp 1395 - 1402, 1992.

Turrio-Baldassarri, L, Carere, A., di Domenico, A., Fuselli, S., Iacovella, N., and Rodriguez, F., "PCDD, PCDF, and PCB Contamination of Air and Inhalable Particulate in Rome," J. Anal. Chem., Vol. 348, pp. 144-147, 1994.

Vandenberg, J. J., and Knoerr, K. R., "Comparison of Surrogate Surface Techniques for Estimation of Sulfate Dry Deposition," Atmospheric Environment, Vol. 19, No. 4, pp. 627-635, 1985.

Vardar, N., Tasdemir, Y., Odabasi, M., Sofuoglu, A., Noll, K.E., and Holsen, T.M., "Gas-Partitioning of Polycyclic Aromatic Hydrocarbons (PAHs) and Polychlorinated Biphenyls (PCBs) in an Urban Atmosphere," Proceedings of Symp. On Air Quality Management, Istanbul, Turkey, September 1997.

Watanabe, S., Laovakul, W., Boonyathumanondh, R., Tabucanon, M.S., and Ohgaki, S., "Concentration and Composition of PCB Congeners in the Air Around Stored Used Capacitors Containing PCB Insulator Oil in a Suburb of Bangkok, Thailand," Environ. Pollut., Vol. 92, No. 3, pp. 289-297, 1996.

Webb, R. G., and McCall, A. C., " Quantitative PCB Standards for Electron Capture Gas Chromatography," Journal of Chromatographic Science, Vol 11, pp 366-373, 1973.

Welsch-Pausch, K., Mclachlan, M., and Umlauf, G., "Determination of the Principal Pathways of Polychlorinated Dibenzo-p-dioxins and Dibenzofurans to Lolium Multiflorum (Welsh Ray Grass)," Environmental Science and Technology, Vol. 29, No. 4, pp 1090-1098, 1995.

Whitman, W. G. , "The Two Film Theory Of Gas Absorption," Chem. Metal. Eng.,Vol. 29, pp. 146-148, 1923.

Wilke, C. R., and Chang, P., "Correlation of Diffusion Coefficients in Dilute Solutions," A. I. Ch. E. Journal, Vol. 1, No. 2, pp. 264 - 270, 1955.

Williams, R. M., "A Model for the Dry Deposition of Particles to Natural Water Surfaces," Atmospheric Environment, Vol. 16, No. 8, pp. 1933 - 193.8, 1982.

Wirth, E. F., Chandler, G. T., DiPinto, L. M., and Bidleman, T. F.,"Assay of PCB Bioaccumulation from Sediments by Marine Benthic Copepods Using a Novel Microextraction Technique," Environmental Science and Technology, Vol. 28, 1609 - 1614, 1994.

Yi, S-M, "Development And Evaluation Of A Water Surface To Measure Dry Deposition," Ph.D. Thesis of Illinois Institute Of Technology, December 1995.

Yi, S-M, Holsen, T.M., Zhu, X., and Noll, K.E., "Sulfate Dry Deposition Measured with a Water Surface Sampler: A Comparison to Modeled Results," submitted for publishing.

Zannetti, P. Air Pollution Modeling: Theories, Computational Methods and Available Software, Van Reinhold, 1990.

Zhang, X., and McMurry, P. H., "Theoretical Analysis of Evaporative Losses of Adsorbed or Absorbed ,Species during Atmospheric Aerosol Sampling," Environmental Science and Technology, Vol. 25, No. 3, pp. 456 - 459, 1991.